

---

---

# **STEM CELL DERIVED CARDIOMYOCYTES**

## **AS MODELS OF PHARMACOLOGY,**

## **PHYSIOLOGY, AND TOXICOLOGY**

---

A thesis submitted for the degree of Doctor of Philosophy

by

Benjamin Arthur Llewellyn Finnin, B Form Sc B Pharm Sc (Hons)

Department of Drug Discovery Biology  
Faculty of Pharmacy and Pharmaceutical Sciences  
Monash University

**Notice 1**

Under the Copyright Act 1968, this thesis must be used only under the normal conditions of scholarly fair dealing. In particular no results or conclusions should be extracted from it, nor should it be copied or closely paraphrased in whole or in part without the written consent of the author. Proper written acknowledgement should be made for any assistance obtained from this thesis.

# Erratum

Page 2: Line 4, “lead” should be replaced with “led”.

Page 11: It should be noted that while hESC can now be passaged enzymatically, manual dissection is still preferred as it is tidier and leads to better quality cells for long term passage.

Page 26: Post-conditioning (also known as ischemic post-conditioning) refers to the use of treatments following ischemic insult to reduce damage caused by reperfusion injury. This is in contrast to pre-conditioning referring to the use of treatments prior to ischemic insult.

Page 35: The systematic IUPAC name of the chemicals listed is included below

Atenolol - (*RS*)-2-{4-[2-Hydroxy-3-(propan-2-ylamino)propoxy]phenyl}acetamide  
Propranolol - (*RS*)-1-(1-methylethylamino)-3-(1-naphthyloxy)propan-2-ol  
ICI 118551 - 3-(isopropylamino)-1-[(7-methyl-4-indanyl)oxy]butan-2-ol  
DPCPX - 8-cyclopentyl-1,3-dipropyl-7*H*-purine-2,6-dione  
ZM 241385 - 4-(2-(7-amino-2-(furan-2-yl)-[1,2,4]triazolo[1,5-a][1,3,5]triazin-5-ylamino)ethyl)phenol  
MRS 1523 - 3-Propyl-6-ethyl-5-[(ethylthio)carbonyl]-2 phenyl-4-propyl-3-pyridine carboxylate  
Isoprenaline - (*RS*)-4-[1-hydroxy-2-(isopropylamino)ethyl]benzene-1,2-diol  
Salbutamol - (*RS*)-4-[2-(*tert*-butylamino)-1-hydroxyethyl]-2-(hydroxymethyl)phenol  
Forskolin - (3*R*, 4*aR*, 5*S*, 6*S*, 6*aS*, 10*S*, 10*aR*, 10*bS*)- 6, 10, 10*b*- trihydroxy- 3, 4*a*, 7, 7, 10*a*- pentamethyl- 1- oxo- 3- vinyldodecahydro- 1*H*- benzo[*f*] chromen- 5- yl acetate  
Ouabain - 1 $\beta$ ,3 $\beta$ ,5 $\beta$ ,11 $\alpha$ ,14,19-Hexahydroxycard-20(22)-enolide 3-(6-deoxy- $\alpha$ -L-mannopyranoside)  
NECA - 1-(6-Amino-9*H*-purin-9-yl)-1-deoxy-N -ethyl- $\beta$ -D-ribofuranuronamide  
CPA - 2*R*,3*R*,4*S*,5*R*)-2-[6-(cyclopentylamino)purin-9-yl]-5-(hydroxymethyl)oxolane-3,4-diol  
IB-MECA - 1-Deoxy-1-[6-[(3-iodophenyl)methyl ]amino]-9*H*-purin-9-yl]-N-methyl- $\beta$ -D-ribofuranuronamide

Page 37: Line 15, “BD FACS Canto II” should be replaced with “BD FACS Canto II flow cytometer”.

Page 38: Line 8, “1:1 mix of PBS and filtered conditioned media” with “1:1 mix of filtered conditioned growth media and 10% FBS in PBS.”

Page 40: Line 7 insert “To detect cells expressing c-kit (CD117) a mouse monoclonal antibody conjugated to Phycoerythrin (PE) was obtained from Beckman Coulter.

Page 47: Line 8, “FACS” should be replaced with “Flow Cytometry”.

Page 48: Figure 3.1, graph in the middle of the page should be labeled C, Image bottom left should be labeled D and Image bottom right should be labeled E. Figure legend, “FACS” should be replaced with “Flow Cytometry”.

Page 52: Line 17, “FACS” should be replaced with “Flow Cytometry”. Line 20, “2 and 6 days” should be replaced with “4 and 6 days”.

Page 56: Figure legend, “FACS sorted” should be replaced with “analysed using flow cytometry”.

Page 61: Line 11, “crucial” should be replaced with “is crucial”.

Page 62: Line 8, “FACS sorted” should be replaced with “FACS”.

Page 73: Line 2, “FACS sorted” should be replaced with “FACS”.

Page 74: Line 17, “FACS sorted” should be replaced with “sorted using FACS”.

Page 81: Line 1, “FACS sorted” should be replaced with “sorted using FACS”.

Page 98: Line 7, insert “There was heterogeneity in both short-term and long-term cultures, however, the results represent multiple differentiations across many months from different passage number ES cells thus reflecting inherent heterogeneity. It is possible that some of the results in this chapter may have been attributable to “primary-myocardial-like” cells, however investigating this was outside the scope of these studies.”

Page 99: Title: “PPONTANEOUSLY” should be replaced with “SPONTANEOUSLY”.

Page 103: Line 9, “FACS sorting” should be replaced with “FACS enriched”.

Page 113: Line 7, “Figure 1 B” should be replaced with “Figure 2 B”. Line 10, “Figure 1 C” should be replaced with “Figure 2 C”.

Page 124: Line 4, insert “It is possible that some of the results in this chapter may have been attributable to “primary-myocardial-like” cells that had not fully differentiated into pacemaker or Hispurkinje cells.”

Page 131: The image on the bottom left should be labeled “E”.

Page 137: Line 6, replace “{Sartipy:2011ek, Mandenius:2011ds, Cohen:2011ik}” with “(Sartipy & Björquist 2011; Mandenius et al 2011; Cohen et al 2011)”.

Page 139: Line 5, “hESC cell line” should be replaced with “hESC line”  
The reference for the cell line is;  
Elliott, D. A. *et al.* NKX2-5eGFP/w hESCs for isolation of human cardiac progenitors and cardiomyocytes. *Nat. Meth.* **8**, 1037–1040 (2011).

Page 141: Figure legend, “Adult heart tissue” should be replaced with “adult heart tissue (E)”.

Page 142: Figure legend, “differentiation time point)” should be replaced with “differentiation time point)(A). “Day 97” should be replaced with “Day 97 (B).

Page 143: Line 12, “add to the that the” should be replaced with “add to that the”. Line 18, “Figure 6.5 C” should be replaced with “Figure 6.6 C”.

Page 144: Line 3, “Figure 6.4 A” should be replaced with “Figure 6.5 A”. Line 4 “Figure 6.4 B” should be replaced with “Figure 6.5 D”, “Figure 6.6” should be replaced with “Figure 6.7”. Line 11, “Figure 6.5 D” should be replaced with “Figure 6.6 D”.

Page 148: Line 5, “Sustained exposure” should be replaced with “Sustained exposure over 5 days”. Line 10, “Figure 6.6” should be replaced with “Figure 6.7”.

Page 157: Line 10, “is one of their key strengths” should be replaced with “is their key strength”.

Page 158: Line 16 “Loss” should be replaced with “loss”.

Page 178, Line 5 replace “Maltsev et al...*Mechanisms of*” with “Maltsev, V. A., Rohwedel, J., Hescheler, J. & Wobus, A. M. Embryonic stem cells differentiate in vitro into cardiomyocytes representing sinusnodal, atrial and ventricular cell types. *Mech. Dev.* **44**, 41–50 (1993).”

Page 178, Line 9 insert “Mandenius, C.-F. et al. Cardiotoxicity testing using pluripotent stem cell-derived human cardiomyocytes and state-of-the-art bioanalytics: a review. *J. Appl. Toxicol.* **31**, 191–205 (2011).”

Page 181, Line 22 insert “Sartipy, P. & Björquist, P. Concise Review: Human Pluripotent Stem Cell-Based Models for Cardiac and Hepatic Toxicity Assessment. *Stem Cells* **29**, 744–748 (2011).”

# Responses to examiners comments

*If this were an oral examination, I would have asked for further clarification on the heterogeneity associated with the EBs, particularly in short-term versus the long-term (>90 days) cultures and how this would have affected data interpretation. Additional discussion in Chapter 4 would have been welcome. Also in Chapter 4, some of the results may have been attributable to “primary-myocardial-like” cells. According to the work of Moorman and colleagues, pacemaker like cells may originate from primary myocardium; however, the relative immaturity and the time dependence of ESC-CMs formation, and the effects of CPA may be explained by this possible alternative explanation.*

Added as addendum to Chapter 4

There was heterogeneity in both short-term and long-term cultures, however, the results represent multiple differentiations across many months from different passage number ES cells thus reflecting inherent heterogeneity.

It is possible that some of the results in this chapter may have been attributable to “primary-myocardial-like” cells.

*Chapter 5 is overall very solid and has already been vetted for publication; however, the possibility of early primary myocardial like cells that had not fully differentiated into pacemaker or Hispurkinje cells may be part of the interpretation.*

Added as addendum to Chapter 5

While it is possible that the results in this chapter may have been attributable to “primary-myocardial-like” cells that had not fully differentiated, this seems less likely than the hypothesis that the cells characterized at a late stage of differentiation had developed phenotypes representative of different parts of the conductive system. Identifying if these cells were mature or early myocardial-like is difficult to prove as early myocardial like cells have similar protein expression patterns and rely on similar functional pathways for spontaneous calcium flux (Boheler 2002). The functional changes and cKit expression characterized in this chapter support a development between days 13 and 20. The most logical interpretation of this development is maturation, leading to spontaneous calcium fluxes which correlate with the calcium currents identified in published electrophysiology studies for cells from the conduction system.

*Also at the very end of Chapter 5, the Candidate refers to the “mature phenotype”. This I would argue is an absolute misnomer. Perhaps relative to day 20 ESCCMs, these cells seem mature based on the reliance on SR calcium and HCN channels, but relative to an adult heart, these cells remain very immature with regards to function and contractile strength. Numerous other “maturation” deficits have been described, and I think it unfortunate that other authors like to use “mature cardiomyocytes” as jargon to improve their chances of publication when the evidence argues against this statement.*

While in this context “mature phenotype” could be considered a misnomer it is commonly used in this context in the literature.

*In Chapter 6, some of the data with human ESC-CMs argue that the mixed EB system is required to identify potential toxicity, and in fact the Candidate suggests that endothelial-like cells play a major role. This point has not however been fully validated or clarified.*

While experimental evidence would suggest a role for endothelial cells in the cardiotoxicity of trastuzumab, definitive experiments to validate this hypothesis would have required further experiments that were not possible due to time constraints. This does not take away from the evidence that the heterogeneity of the mixed EB system may prove more useful for toxicity studies than highly purified systems.

*Second, I was surprised by the lack on comment or experimental data in Chapter 4 and the effects that Iso or adenosine or other pro-arrhythmic drugs may have had on the generation of arrhythmic waveforms. In many of the drug screening protocols, this is a major limitation and one that can have obvious catastrophic effects when administered to patients.*

The information regarding pro-arrhythmic drugs would certainly be interesting, however given limits of time and resources this was considered outside the scope of this thesis.

*While I realize that the videomorphometry (or object tracking) may work best in 2D, the rates of contraction as well as the contraction amplitude could have been addressed in this thesis. These findings would have increased the impact of the current study if described in explicit detail, and it is my feeling that inclusion of this data could provide the detail that may be currently lacking for publication.*

Many of the results discussed in Chapter 4 used object tracking as a form of videomorphometry, however the difficulties associated with using this technique with 3D cultures limited the interpretation of results that could be achieved with this methodology.

*Third, Chapter 6 is by far the weakest of the chapters in this thesis. It is my impression that the writing of this chapter was rushed, and as a consequence, the Results section is much more difficult to follow. It reads more like a list of experimental findings, but the Candidate often failed to refer to the graphs, and other components of the chapter. See specific comments below. Other weaknesses included the inability of the Candidate to master the hESC differentiation protocol – while minor, this is important if he chooses to continue along this research stream. While the model employed is laudable, the purity of CMs and relative proportion of CMs vs non- CMs is lacking. It is also very easy to state that some research efforts are “difficult” and that nothing is “standardized”, but I would argue that as part of the training, the Candidate should make these statements and then define how he/she would define these parameters. In Science, many aspects are poorly defined or mis-defined and need to be dealt addressed. (see attached pages) Also in Chapter 6, the Candidate has failed to consistently refer to the data presented in the figures. Chapter 6 has nine figures and often four or so panels within each figure, yet the written results are only ~3.5-~4 pages long (excluding figures) and the Candidate fails to refer to the subpanels consistently. He skips from Figure 6.1 to Figure 6.3, then back to Figure 6.2 and then on to Figure 6.6 and back to Figure 6.5C. While Figures 6.7 and 6.8 contain valuable information, the Candidate failed to note these in the text and provide adequate explanation throughout the Results section. Overall, the results provided in Chapter 6 are not as detailed or as eloquently presented as in the other chapters, even though valuable information is provided. Regrettably this is considered unacceptable, and it is not consistent with the high quality of the rest of the thesis. Technically, this chapter should be edited, and mostly what it needs is editing, addition of information referring to the figures, and a few minor corrections.*

**In the words of the examiner “The data are present, the presentation and interpretation, while minimal, is adequate, and the Discussion is acceptable – but not the Candidate’s best work.”**

*It would also have been useful if the Candidate had further discussed the finding that apoptosis often causes cells to detach from the plate or substrate, and consequently, the supernatant should also be retained, centrifuged and cells assessed for apoptosis. Quantitative assessments should always take this into account.*

The ELISA assay used to quantify Troponin released into the supernatant in Chapter 6, as a measure of cardiomyocyte death, included a lysis buffer, which would have included any cells detached from the plate/substrate.

*Misusage of terms:*

*Finally, I noted throughout the early chapters of this thesis, only once in Chapter 5 and not very much Chapter 6 or the Conclusions, the misuse of the term FACS, FACS sorting, and Flow cytometry. Regrettably, this is a common mistake in the literature and not one that would necessarily be known by the Candidate. I do, however, believe it important to learn now the proper terminology as misused jargon can lead to confusion in publications. The proper term should be fluorescence-°C-based flow cytometry. From Wikipedia, Fluorescence-activated cell sorting (FACS) is a specialized type of flow cytometry. It provides a method for sorting a heterogeneous mixture of biological cells into two or more containers, one cell at a time, based upon the specific light scattering and fluorescent characteristics of each cell. The use of FACS sorting or FACS sorted is therefore redundant and these terms should be corrected. At other times, flow cytometry and not FACS should be employed. Most of these errors have been noted on post-°C-it notes affixed to the thesis.*

As acknowledged the wider use of the term FACS is common in the literature, however usage of terms FACS and flow cytometry have been clarified in the erratum.

*Other typographical errors (spelling, capitalization, etc) have also been noted, and in one chapter I suggest that you define all of the chemical names. Some of these are defined elsewhere, but I think that an erratum could deal with all of the noted errors/typos etc, although you might consider adding a page of abbreviations dealing with the drugs employed in your studies.*

While this may improve the readability of the thesis all abbreviations are defined.

The following examiner comments have all been addressed in the erratum;

*Page 26, the term “post-°C-conditioning” should be defined -°C- erratum*

*Page 38, the buffer mentioned here vs in Chapter 5 did not fully correspond. Please clarify*

*Page 40 and elsewhere, when performing flow cytometry it is best to give the antibody information in detail (company, Cat or clone Number) and also clarify whether the antibodies were purchased conjugated to a fluorophore or whether you did it with a kit yourself Figure 3.1: Failed to label sections C, D and E*

*Page 52 – data presented do not support the findings that 2 days of decreased oxygen improved numbers of ESC-°C-CMs when compared with data presented in Fig 3.3. Please clarify, as improvements seem to have been seen at day 3 of low oxygen tension*

*Page 99: Title: misspelled SPONTANEOUSLY AS PPONTANEOUSLY*

*Page 113, I believe that you mean to refer to Table A, B and C as no Figure 1 is given. Please correct accordingly*

*Page 131: “E” is missing from the Figure*

*Page 137: 3 references failed to format, two of which are absent from the final reference list*

*Page 141: Figure legend fails to refer to Figure 6.1E*

*Page 178: Reference by Maltsev et al is incomplete*

---

## Table of Contents

<b>SUMMARY .....</b>	<b>VI</b>
<b>LIST OF FIGURES .....</b>	<b>VI</b>
<b>LIST OF TABLES .....</b>	<b>IX</b>
<b>LIST OF SUPPLEMENTARY VIDEOS.....</b>	<b>IX</b>
<b>DECLARATION.....</b>	<b>X</b>
<b>ACKNOWLEDGEMENTS .....</b>	<b>XI</b>
<b>COMMUNICATIONS.....</b>	<b>IXII</b>
<b>PUBLICATIONS .....</b>	<b>XIII</b>
<b>ABBREVIATIONS.....</b>	<b>XIV</b>
<b>CHAPTER 1 – GENERAL INTRODUCTION .....</b>	<b>1</b>
<b>1.1 TARGET DISCOVERY – ID AND VALIDATION.....</b>	<b>2</b>
<b>1.2 DRUG DISCOVERY.....</b>	<b>3</b>
<b>1.2.1 Hit to Lead.....</b>	<b>3</b>
<b>1.2.2 Lead Optimisation.....</b>	<b>4</b>
<b>1.3 PRECLINICAL TESTING.....</b>	<b>4</b>
<b>1.3.1 In Vitro models.....</b>	<b>6</b>
<b>1.3.2 Animal models .....</b>	<b>7</b>
<b>1.3.3 Model deficiencies .....</b>	<b>8</b>
<b>1.4 STEM CELL DERIVED MODELS.....</b>	<b>10</b>
<b>1.4.1 Embryonic Stem cells.....</b>	<b>10</b>
<b>1.4.2 Cardiac Differentiation.....</b>	<b>13</b>
<b>1.5 HEART PHYSIOLOGY .....</b>	<b>17</b>
<b>1.5.1 Cardiac development and Physiology .....</b>	<b>17</b>
<b>1.5.2 Heart Structure .....</b>	<b>18</b>
<b>1.6 HEART CELLULAR PHYSIOLOGY .....</b>	<b>20</b>
<b>1.6.1 Myocytes.....</b>	<b>20</b>
<b>1.6.2 Pacemakers.....</b>	<b>21</b>
<b>1.7 MODEL RECEPTOR TARGETS AND DRUGS .....</b>	<b>23</b>
<b>1.7.1 Adrenergic receptors.....</b>	<b>23</b>
<b>1.7.3 Doxorubicin .....</b>	<b>27</b>
<b>1.7.4 Monoclonal antibodies and Trastuzumab .....</b>	<b>28</b>
<b>1.8 STEM CELL MODELS IN DRUG DISCOVERY - WORK TO DATE .....</b>	<b>29</b>
<b>1.9 AIMS.....</b>	<b>31</b>
<b>CHAPTER 2 - MATERIALS AND METHODS .....</b>	<b>32</b>

---

<b>2.1 MOUSE ESC LINES.....</b>	<b>33</b>
<b>2.3 CARDIAC DIFFERENTIATION OF MOUSE ESCS .....</b>	<b>33</b>
<b>2.4 MOUSE ESC-DERIVED EMBRYOID BODY CONTRACTILITY STUDIES.....</b>	<b>34</b>
<b>2.5 DATA ANALYSIS.....</b>	<b>35</b>
<b>2.6 IMMUNOLABELLING OF MESC-DERIVED EMBRYOID BODIES.....</b>	<b>36</b>
<b>2.7 FLUORESCENCE ACTIVATED CELL SORTING .....</b>	<b>37</b>
2.7.1 Cell digestion .....	37
2.7.2 Analysis .....	37
2.7.3 Sorting.....	38
<b>2.8 MOUSE Nkx2.5-eGFP<sup>+</sup> CALCIUM IMAGING .....</b>	<b>38</b>
2.8.1 Post Calcium Imaging Analysis Mouse Nkx2.5-eGFP <sup>+</sup> Cells .....	39
2.8.2 Post calcium imaging immunocytochemistry of Mouse Nkx2.5-eGFP <sup>+</sup> cells .....	39
2.8.3 Post calcium imaging TO-PRO®-3 cell death assay.....	40
<b>2.9 HYDROETHIDINE (HE) REACTIVE OXYGEN IMAGING.....</b>	<b>40</b>
<b>2.10 HUMAN EMBRYOID BODY TOXICITY STUDIES .....</b>	<b>41</b>
2.10.1 Troponin ELISA .....	41
2.10.2 TBARS assay for lipid peroxidation.....	42
2.10.3 TO-PRO®-3 cell death assay – Acute and chronic chemical toxicity.....	42
2.10.4 CaspGLOW red assay .....	43
<b>2.11 DRUGS AND CHEMICALS .....</b>	<b>43</b>
<b>CHAPTER 3 - METHOD DEVELOPMENT .....</b>	<b>45</b>
<b>3.1 FOREWORD .....</b>	<b>46</b>
<b>3.2 EMBRYONIC STEM CELL CULTURE .....</b>	<b>46</b>
3.3.1 Results and Discussion – EB differentiation .....	50
3.3.2 Maximising cardiomyocyte yield.....	50
3.3.3 Effect of oxygen tension on cardiogenesis.....	52
<b>TABLE 3.1 .....</b>	<b>55</b>
3.4.1 Results and discussion .....	57
3.5.1 Stability and reactive oxygen species .....	61
<b>CHAPTER 4 - STEM CELL DERIVED CARDIOMYOCYTES AS MODELS OF ORGANOTYPIC PHARMACOLOGY: ADRENOCEPTOR AND ADENOSINE RECEPTOR SIGNALING .....</b>	<b>71</b>
<b>4.1 INTRODUCTION .....</b>	<b>72</b>
<b>4.2 METHODS.....</b>	<b>73</b>
4.2.1 cAMP AlphaScreen assays .....	73
4.2.2 Statistical Analysis.....	73

---

<b>4.3 RESULTS.....</b>	<b>74</b>
4.3.1 Effects of Isoprenaline, a $\beta$ -adrenoceptor agonist.....	74
4.3.2 $\beta$ -adrenoceptor subtype identification .....	75
4.3.3 Acute $\beta$ -adrenoceptor desensitisation. ....	76
Figure 4.3 - Effects of.....	79
4.3.4 Effects of NECA, a non-selective adenosine receptor agonist.....	80
4.3.5 Effects of CPA, a selective adenosine receptor A <sub>1</sub> agonist .....	80
4.3.6 Effects of IB-MECA, a selective A <sub>3</sub> agonist.....	82
<b>4.5 CONCLUSIONS .....</b>	<b>98</b>
<b>CHAPTER 5 - HANGING DROP DIFFERENTIATION REVEALS MULTIPLE SPONTANEOUSLY ACTIVE CELL TYPES IN Nkx2.5-GFP<sup>+</sup> CARDIAC LINEAGE CELLS: PACEMAKER CHARACTERISATION .....</b>	<b>99</b>
<b>MATERIALS AND METHODS .....</b>	<b>105</b>
ESC Propagation & Differentiation .....	106
FACS isolation .....	106
Nkx2.5-eGFP <sup>+</sup> Single Cell Calcium Imaging .....	107
Post Calcium Imaging Analysis .....	108
Immunocytochemistry of Mouse Nkx2.5-eGFP <sup>+</sup> Cells.....	109
RT-PCR of Mouse Nkx2.5-eGFP <sup>+</sup> Cells.....	109
Statistical Analysis .....	110
Drugs and Chemicals .....	111
<b>RESULTS.....</b>	<b>111</b>
Single Cell Calcium Imaging .....	111
C-kit expression .....	112
Analysis of Waveform Kinetics and Cellular Morphology .....	112
Immunocytochemistry & RT-PCR .....	113
Analysis of Intracellular Calcium Handling .....	114
I <sub>f</sub> channel blockade.....	114
The Effects of Ryanodine.....	115
The Effects of Thapsigargin .....	115
The Effects of Nifedipine, NNC 55-0396 and NiCl <sub>2</sub> .....	115
Analysis of day 13 cardiac progenitors .....	116
<b>DISCUSSION.....</b>	<b>117</b>
<b>SUMMARY .....</b>	<b>124</b>
<b>ACKNOWLEDGEMENTS .....</b>	<b>125</b>
<b>REFERENCES .....</b>	<b>125</b>
<b>CHAPTER 6 – TRASTUZUMAB AND DOXORUBICIN TOXICITY IN HUMAN ESC DERIVED EMBRYOID BODIES .....</b>	<b>136</b>
<b>6.1 INTRODUCTION .....</b>	<b>137</b>
<b>6.2 METHODS.....</b>	<b>137</b>

---

6.2.1 hESC derived embryoid bodies.....	138
6.2.2 Gene expression analysis .....	138
<b>6.3 RESULTS.....</b>	<b>139</b>
6.3.1 Differentiation .....	139
6.3.2 Function and Maturation.....	139
6.3.3 Doxorubicin Toxicity .....	143
6.3.4 Trastuzumab Toxicity .....	143
6.3.5 Mechanisms .....	148
<b>6.4 DISCUSSION.....</b>	<b>154</b>
<b>6.5 CONCLUSION.....</b>	<b>161</b>
<b>CHAPTER 7 – CONCLUDING REMARKS .....</b>	<b>161</b>
<b>REFERENCES .....</b>	<b>169</b>
<b>APPENDIX I.....</b>	<b>197</b>
<b>APPENDIX II - CHAPTER 5 SUPPLEMENTAL MATERIAL .....</b>	<b>197</b>

---

## **Summary**

Drug discovery and development requires preclinical models to eliminate flawed compounds from development pipelines. Unfortunately, current models have limitations, occasionally resulting in toxic or ineffective compounds progressing to the clinic at great cost and patient risk. Utilising stem cell technology, it is now possible to generate sophisticated models with human biology and physiological context, potentially overcoming the limitations of more established preclinical models. In this thesis I have investigated the use of embryonic stem cell derived cardiac cells for use as models in pharmacology, physiology and toxicology studies.

Mouse embryonic stem cells were differentiated to generate cardiomyocytes in multicellular aggregates containing not only myocytes, but also pacemaker cells, fibroblasts and endothelium. These aggregates were used for pharmacology studies, where the signaling resulting from  $\beta$ -adrenoceptor and adenosine receptor stimulation was explored. Using the same differentiation method, in combination with a pan-cardiac reporter for cell enrichment, the function of individual cardiac cells was measured using calcium imaging. Following extensive method development, multiple phenotypes were identified in the enriched population based on spontaneous calcium oscillations. These distinct phenotypes were characterised based on calcium oscillation kinetics, pharmacology and immunocytochemistry. Using human stem cell derived cardiomyocyte aggregates I studied the effects of doxorubicin (a known cardio-toxin) and Trastuzumab, a humanised antibody with disputed cardio-toxicity.

---

Following extensive method development, toxicity was observed for both doxorubicin and Trastuzumab. Mechanistic studies implicated multiple cell types mediating Trastuzumab toxicity via a complicated signaling pathway.

These results suggest that stem cell derived cardiomyocytes may be used as physiologically heterogeneous models for pharmacological screening of on- and off-target cardiac activity. My results suggest the complexity of multicellular aggregates limits their use in characterizing less established, or complicated receptor signaling pathways. Results from calcium imaging studies indicate that at a single cell level, there is considerable heterogeneity of stem cell derived cardiac cells. Focusing on cells with spontaneous calcium oscillations, that are presumably pacemaker cells, it may be possible to gain greater insight into the mechanisms required to maintain spontaneous cardiac activity and identify drugs that disrupt it. The results of the Trastuzumab toxicity study provide evidence of a novel mechanism of Trastuzumab cardio-toxicity. Importantly, these results support the use of stem cell derived models for toxicology screening, particularly of humanised antibodies whose toxicity may not be identified in classical models. The work presented in this thesis identified novel pacemaker phenotypes previously unreported, and a novel mechanism for Trastuzumab toxicity. Ultimately, this thesis highlights the strengths and weaknesses of stem cell derived models for use in pharmacology, physiology and toxicology assays.

---

## List of figures

Figure 1.1 – Diagrams of excitation contraction coupling and pacemaker ion currents.....	22
Figure 1.2 – Molecular effects of $\beta$ -adrenoceptor activation.....	25
Figure 3.1 – Optimisation of culture conditions for growth and maintenance mESC .....	48
Figure 3.2 – Optimisation of mESC cardiac differentiation.....	54
Figure 3.3 – Effects of low oxygen tension of cardiomyocyte differentiation.....	56
Figure 3.4 – Videomorphometry: effects of ouabain and forskolin on mESC EBs.. .....	60
Figure 3.5 – Antioxidant stabilization of spontaneous calcium oscillations.....	65
Figure 3.6 – Effects of confocal laser imaging on cell viability .....	66
Figure 3.7 – Spontaneous waveform analysis template .....	68
Figure 3.8 – Spontaneous calcium waveform analysis logic map .....	69
Figure 4.1 – Effects of $\beta$ AR activation on mESC EBs .....	77
Figure 4.2 – Effects of $\beta$ AR antagonists on mESC EBs .....	78
Figure 4.3 – Isoprenaline induced desensitisation of $\beta$ AR .....	79
Figure 4.4 – Effects of NECA on mESC EBs .....	83
Figure 4.5 – Effects of Selective adenosine receptor agonists on mES EBs .....	84
Figure 4.6 – Interaction of CPA and isoprenaline signaling.....	86
Figure 4.7 – Effects of Iso and CPA on cAMP levels .....	87
Figure 5.1 – Table: Different kinetic waveforms and key features .....	130
Figure 5.2 – Immunohistochemical characterisation of spontaneously active cells .....	131
Figure 5.3 – HCN channel expression and function in spontaneously active cells .....	132
Figure 5.4 – Effects of Ryanodine and ZD7288 on spontaneously active cells... ..	133
Figure 5.5 – Effects of Thapsigargin and 2-APB on spontaneously active cells . ..	134
Figure 5.6 – Characterisation of immature spontaneously active cells .....	135
Figure 6.1 – Cardiac differentiation and gene expression of hESC .....	141
Figure 6.2 – Spontaneous rates and functional sensitivity of hESC EBs.....	142
Figure 6.3 – Effects of Doxorubicin and Trastuzumab on spontaneous rate of contraction .....	145
Figure 6.4 – Effects of Doxorubicin on Cardiomyocyte viability.....	146
Figure 6.5 – Effects of Trastuzumab on Cardiomyocyte viability.....	147
Figure 6.6 – Effects of Doxorubicin and Trastuzumab on lipid peroxidation ....	150
Figure 6.7 – Caspase activation by Trastuzumab .....	151
Figure 6.8 – Effects of CP 724 714 on Cardiomyocyte viability .....	152
Figure 6.9 – Effects of Trastuzumab on NO release from endothelial cells.....	153

---

## **List of Tables**

Table 3.1 – mESC differentiation methods trialled.....	55
Table 5.1 – Spontaneous waveform classification and characteristics.....	129

## **List of Supplementary videos**

Supplementary movie 1 – Calcium imaging of cells seeded at high density – connection

Supplementary movie 2 – Calcium imaging of cells seeded at lower density – varying spontaneous kinetics

Supplementary movie 3 – Calcium imaging of connected cells – basal

Supplementary movie 4 – Calcium imaging of connected cells – after 100 nM CPA

Supplementary movie 5 – Calcium imaging of connected cells – after 1  $\mu$ M CPA

Supplementary movie 5 – Calcium waves at high magnification

---

## **Declaration**

I declare that the material contained in this thesis has not been presented for award of any other degree or diploma in any university or other institution. To the best of my knowledge the thesis contains no material previously published or written by another person, except where due reference is made in the text of the thesis. The work in Chapter 5 was conducted in collaboration with Dr. Louise Lagerqvist and her contribution is outlined in Chapter 5. The work in Chapter 6 was conducted in collaboration with Dr. David Elliot and his contribution is outlined in Chapter 6.

I certify that the writing of the thesis, the results and interpretations are entirely my own work.

.....  
Benjamin Arthur Llewellyn Finnin

---

## Acknowledgements

I have to start by thanking my supervisors, John and Colin, for providing me with opportunity, funding, guidance and freedom. I have been exposed to numerous techniques, involved with a variety of different projects and been challenged along the way. The lessons I have learnt from you are invaluable.

Special thanks to my family, particularly my parents, for supporting me in every possible sense throughout this project. Your assistance, encouragement, witticisms and criticisms have shaped me forever more. I wonder now if I might not have turned out a very different boy indeed if you had administrated a few fatal beatings earlier on.

Past and present students, Steph, Brad, Cam, Carl, Caroline, Jon, Katherine, Marina, Nel, and Tori, thank you for the 5 O'clock unwind on Fridays and the occasional random party.

Warren, Stewart, and Erica, thank you for the vent sessions, the 'get on with it's, and most importantly for the random hallway chats.

Adrian, thank you for your support, it's easy to overlook your contribution to the department because you never ask for praise. I cannot count the number of times I made my problems your problems, and more often than not, they were solved without complaint.

Andrew, for being patient, rarely asking how the 'thesis' was going, and for distracting me just the right amount. I cannot imagine life without your friendship.

Jason, Tom, Craig and Matt, the lads, for all the stress-relieving nights, the training sessions, steak nights, wine tastings and coffee, especially the coffee.

To Louise, my comrade, thank you for our time together, for agreeing to be part of the team. Personally and professionally, you were always available, always helping, and for that I am forever in your debt.

Special thanks to Brig for talking to me. It might seem like a small thing but our discussions are something that I treasure. You have challenged me and kept me sane, never underestimate your potential; I look forward to seeing what your endeavors produce.

---

## Communications

2012 **Poster presentation** at the Annual Australian Flow Cytometry Group meeting. Unstable calcium transients of the cardiac conduction system – Artefact or fiction?

2012 **Oral presentation** at Australian Stem Cell Centre Stream 3 retreat. Unstable calcium transients of the cardiac conduction system – Artefact or fiction?

2012 **Oral presentation** at the Annual SydFlow meeting. The use of cell sorting and stem cells to develop better biology models.

2009 **Poster presentation** at the Annual Monash Institute of Pharmaceutical Science Postgraduate Research Symposium. Acute Adrenergic and Purinergic Stimulation of Mouse Embryonic Stem Cell Derived Cardiomyocytes.

2009 **Poster presentation** at the Annual ISSCR meeting in Barcelona. Acute Adrenergic and Purinergic Stimulation of Mouse Embryonic Stem Cell Derived Cardiomyocytes.

---

## Publications

Lagerqvist, E. L., **Finnin, B. A.**, Pouton, C. W. & Haynes, J. M. Endothelin-1 and angiotensin II modulate rate and contraction amplitude in a subpopulation of mouse embryonic stem cell-derived cardiomyocyte-containing bodies. *Stem Cell Research* 6, 23–33 (2011). Refer to Appendix I.

**BA Finnin**, EL Lagerqvist, S Wu, CW Pouton and JM Haynes. Hanging drop differentiation reveals multiple spontaneously active cell types in Nkx2.5-GFP<sup>+</sup> cardiac lineage cells. Submitted to *Stem Cell Research*

Other publications by the author:

**Finnin, B.**, O'Neill, M. & Gaisford, S. Performance validation of step-isothermal calorimeters. *Journal of thermal analysis and microcalorimetry* (2006).

---

## Abbreviations

2-APB	2-Aminoethoxydiphenyl borate
AC	Adenylate cyclase
ADME	Absorption, distribution, metabolism and excretion
aMHC	Alpha myosin heavy chain
Ang II	Angiotensin II
ANP	Atrial natriuretic peptide
AP	Action potential
AR	Adrenoceptor
aSMA	Alpha smooth muscle actin
ATCC	American type culture collection
ATP	Adenosine Triphosphate
AV	Atrioventricular
AVN	Atrioventricular node
βAR	β-Adrenoceptor
BMP	Bone morphogenetic protein
BSA	Bovine serum albumin
[Ca <sup>2+</sup> ] <sub>i</sub>	Intracellular calcium concentration
Ca <sup>2+</sup>	Calcium ion
cAMP	Cyclic adenosine monophosphate
CHO	Chinese hamster ovary
CICR	Calcium induced calcium release
CM	Cardiomyocyte
CPA	N <sup>6</sup> -Cyclopentyladenosine
cTnI	Cardiac troponin I subunit
cTnT	Cardiac troponin T subunit
Cx	Connexin
DMEM	Dulbeccos modified eagle medium
DMSO	Dimethyl sulfoxide
DNA	Deoxyribonucleic acid`
Dox	Doxorubicin
DPCPX	Dipropylcyclopentylxanthine
EB	Embryoid body
EDS	Early differentiation stage
eGFP	Enhanced green fluorescent protein
EGFR	Epidermal growth factor receptor
ELISA	Enzyme-linked immuno sorbent assay
EpiSC	Eplibast derived stem cell
ERK	Extracellular signal-regulated kinase
ESC	Embyronic stem cells
ESC-CMs	Embryonic stem cell-derived cardomyocytes
ET-1	Endothelin-1
FACS	Fluorescent activated cell sorting
FBS	Foetal bovine serum

---

FDA	Food and drug administration
FGF	Fibroblast growth factor
GPCR	G-Protein coupled receptor
HCN	Hyperpolarisation-activated cyclic nucleotide-gated cation channel
HE	Hydroethidine
hEB	Human embryoid body
HEK	Human embryonic kidney
hERG	Human Ether-a-go-go K <sub>v</sub> 11.1 K <sup>+</sup> channel
hESC	Human embryonic stem cells
HIF	Hypoxia inducible factor
ICM	Inner cell mass
IP3	Inositol Triphosphate
iPSC	Induced pluripotent stem cells
Iso	Isoprenaline
K <sup>+</sup>	Potassium ion
KSR	Knockout serum replacement
LDS	Late differentiation stage
LIF	Leukemia inhibitory factor
MAPK	Mitogen-activated protein kinase
MEK	Mitogen-activated protein kinase kinase
mESC	Mouse embryonic stem cells
MISCL	Monash immunology and stem cell laboratories
MLC2v	Ventricular specific myosin light chain kinase
mRNA	Messenger ribonucleic acid
Na <sup>+</sup>	Sodium ion
NCX	Sodium calcium exchanger
NEAA	Non-essential amino acids
NECA	5'-(N-Ethylcarboxamido)adenosine
NiCl <sub>2</sub>	Nickel Chloride
NMR	Nuclear magnetic resonance
PBS	Phosphate buffered saline
PD	Pharmacodynamics
PE	R-Phycoerythrin
PK	Pharmacokinetics
PKA	Protein kinase A
PKC	Protein kinase C
PLC	Phospholipase C
qPCR	Quantitative polymerase chain reaction
RNA	Ribonucleic acid
roGFP	Reactive oxygen green fluorescent protein
ROS	Reactive oxygen species
RT	Room temperature
RT-PCR	Reverse transcription polymerase chain reaction
RyR	Ryanodine receptor
SA	Sinoatrial
SAN	Sinoatrial node

---

SAR	Structure activity relationship
SERCA	Sarco/endoplasmic reticular calcium ATPase
SPG	Sucrose-phosphate-glyoxylic acid
SR	Sarcoplasmic reticulum
TBARS	Thiobarbituric acid reactive substances
TMRM	Tetramethylrhodamine
VMAT	Vesicular monoamine transporter

## **CHAPTER 1 – GENERAL INTRODUCTION**

The research and development sections of the pharmaceutical industry are undergoing a revolution as the result of economic downturn, patent expiry and the escalating costs of getting new chemical entities to market. The cost of failure in the clinical phase has lead to a ‘fail fast, fail cheap’ focus, recognition of the importance of identifying unsuitable drug candidates as early as possible. (Ford et al. 2004). To eliminate flawed compounds from the pipeline there are well-established preclinical models for developing biologically active compounds into drugs with verified activity and safety. However, industry is constantly evolving to make use of emerging technologies to better identify drug candidates that have a low probability of proceeding past clinical testing(Korfmacher 2005). This thesis investigates stem cell derived systems as models for cardiac drug discovery, development and testing, and tests the hypothesis that stem cell derived models address some of the limitations of more traditional *in vitro* and *in vivo* systems.

## **1.1 Target Discovery – ID and Validation**

Basic biological research, particularly focused on pathophysiology, is continually identifying new target molecules that play a role in initiating or maintaining a disease state including orphan receptors, kinases, enzymes, gene products and other RNA derived molecules. Once identified as being integral to a disease state further characterisation of these biological molecules using methods such as x-ray crystallography, NMR and molecular biology further define the target(Middleton 2006; Crowther 2002; Rudin et al. 1999). This facilitates development of high throughput assays, which can then be used to screen large compound libraries for a hit, which is a compound with relatively high affinity

for a target. Increased understanding of key biochemical processes has enabled development of sophisticated screening models that identify specific biological outcomes rather than simple interactions. An example of this approach is development of omecamtiv mecarbil, an activator of cardiac myosin which increases cardiac contractility without affecting intracellular calcium concentrations, thereby negating the side effects of prolonged calcium elevation(Malik & Morgan 2011; Cleland et al. 2011).

## 1.2 Drug Discovery

### 1.2.1 Hit to Lead

Hit to lead development is the process of taking a chemical compound with high affinity for a biological target and further refining the structure until a molecule with drug-like characteristics is obtained(Alanine et al. 2003; Bleicher et al. 2003). This involves numerous streams of research by teams of medicinal chemists, physical chemists, biologists and pharmaceutical scientists. Firstly, a structure activity relationship (SAR) is determined by screening hundreds of analog compounds to identify key molecular motifs that contribute to the compounds target affinity. This is often performed in parallel with simple *in vitro* testing to determine functional efficacy where appropriate models are available. Having established the core molecular structure required for target affinity, computer modeling can be used to select a restricted number of candidates for further physiochemical testing. The use of *in silico* prediction software to screen larger numbers of analogs is already a part of the development process. However, it is unlikely to completely usurp the

experimental determination of a lead compounds physical, chemical and biological properties(Gleeson et al. 2011).

### **1.22 Lead Optimisation**

Lead optimisation seeks to identify compounds with the necessary characteristics to make a successful drug, allowing progression of a limited number of compounds into rigorous preclinical animal studies. During lead optimisation, the lead compounds are tested for parameters other than activity that will also contribute to their efficacy. To be a useful prospective drug candidate a compound must have suitable physicochemical properties such as solubility and partitioning behaviour(G. W. Caldwell et al. 2001). These properties will be influenced by molecular weight, polar surface area, crystallinity and ionisation equilibria or pKa. Drug candidates must also have suitable pharmacokinetics, determined in part by dosing strategy, route of administration and the toxicity profile of the drug class. Lead optimization is followed by *in vitro* and *in vivo* preclinical testing.

### **1.3 Preclinical Testing**

Extensive preclinical testing is required before drugs can enter human trials to minimize incidental toxicity and prevent the expensive initiation of trials on unsuitable compounds. The tools used at these stages start at the *in vitro* level where activity and toxicity is screened in high throughput cellular or biochemical assays(Li 2001; Slater 2001). Beyond simple cellular assays, compound efficacy and off target effects can be measured in more complicated *in vitro* or *ex vivo* assays such as organ baths or isolated perfused organs. The first live animal

subjects tested are generally rodents, followed by non-rodent testing, as described in more detail below. Only after rigorous *in vivo* testing of efficacy and toxicity, do drug candidates proceed to clinical studies, and yet despite this, there are still unsuitable compounds that make it through to trial, sometimes even to market(Waxman 2005).

Between 1992 and 2002, 90% of withdrawals of drug products from the market were due to toxicity, with hepatic and cardiac toxicity being the major causes for withdrawal of two out of three drugs. In drug development trials at clinical phases I-III, 43% failed due to insufficient efficacy and 33% due to toxicity(Schuster et al. 2005). As previously mentioned, clinical efficacy depends not only on affinity for a receptor but also in suitable ADME properties, where a drug candidate may not succeed owing to a poor PK/PD profile, i.e.: rapid metabolism, poor distribution, protein binding. Drug failure is sometimes due to previously unidentified issues with toxicity or ADME not predicted by current screening protocols. This has resulted in regulatory bodies and industry scrambling to add screening of recently identified adverse biological interactions to preclinical requirements. This reactionary approach was seen when hERG toxicity occurred with astemizole (amongst other drugs) and has led to inclusion of screening for hERG channel blockade in most development pipelines. To prevent adverse clinical outcomes, pharmaceutical models that are more predictive of human physiological responses to drugs are critically needed, and the earlier they can be employed the greater the impact.

### 1.3.1 In Vitro models

Initial screens of drug candidates for toxicity and activity are performed using simple, well-characterised *in vitro* models. The simplest format, based on biochemical assays can be used to determine properties including target affinity, metabolic interactions, metabolic degradation and activity. Highly characterised cell lines such as human embryonic kidney cells (HEK) or Chinese hamster ovary cells (CHO) can be genetically modified and used to test for cellular responses including target affinity, activity, proliferation and apoptosis(Eglen et al. 2008; Korn & Krausz 2007). The use of primary or immortalized cell lines is considered to carry more predictive power of the *in vivo* activity of compounds as receptors or target proteins should be at physiologically relevant levels with appropriate second messenger coupling. Simple biochemical and cellular assays allow for high throughput and high content screening, facilitating a broad characterisation of a number of candidate compounds; however, the simplicity of these models limits their utility for *in vivo* prediction.

Modeling physiological responses to drug candidates requires more than a homogenous cell population as organs contain a mixture of the primary functional or target cells, blood vessels, nerves, and accessory cells. In order to account for the effects of all of these integrated systems various *ex vivo* models are employed. Organ baths and isolated perfused organs (such as the liver or the heart) contain all relevant cell types contextually arranged, such that measurement of contraction, spontaneous action potentials or other parameters should accurately reflect the *in vivo* response to a compound of whatever animal the organ has come from(Wakefield et al. 2002; Bell et al. 2011). While not

feasible for screening of vast libraries of candidates, *ex vivo* methods can be useful for identifying compounds with off target effects in select organs. *Ex vivo* models also aid in extrapolating activity identified in *in vitro* screens to *in vivo* efficacy.

### **1.3.2 Animal models**

Rodents are usually the first live animal on which a new chemical entity is tested, and are used to determine safety, PK and occasionally efficacy. In basic toxicity testing mice or rats are injected with increasing concentrations of compound to determine the dose required to kill 50% of the cohort (LD<sub>50</sub>). Following these studies, post mortems can also provide clues as to the mechanism of toxicity. Pharmacokinetic studies, usually in rats, are used to determine parameters such as metabolism, excretion and distribution that can be used to predict how the drug will behave in humans. In some cases, where appropriate models of diseases exist such as genetically modified mice, studies may be conducted to assist in the prediction of compound efficacy. *In vivo* rodent data is combined with allometric scaling to predict human parameters for toxicity and PK. However, specific aspects of mouse and human physiology and biology vary significantly, and thus testing in non-rodent animals is required.

Non-rodent animal testing of drug compounds is usually the last checkpoint before a compound goes into human clinical trials. The goal of these studies is to ensure that compounds will not have serious deleterious effects in human subjects. Informed by predicted toxicity, and approximated dosing (concentration and frequency), studies will be conducted in non-rodent animals

to ascertain any species differences that limit prediction from the rodent models ((Fielden & Kolaja 2008; Wall & Shani 2008; Pritchard et al. 2003)). The gold standard for this are primates based on their genetic homology with humans, however the ethically motivated push to minimize primate studies has practically limited their use in standard PK studies(Prescott 2010; Herodin et al. 2005). Other non-rodent animals used include pigs, sheep and dogs, which are particularly used for orally dosed compounds, as their alimentary canals are a similar length to humans. Despite diverse models and extensive testing, there are still deficiencies of currently prescribed models, which limit their predictive power.

### **1.3.3 Model deficiencies**

Screening of humanized drugs (eg. Monoclonal antibodies) requires use of human cell lines or recombinant expression of human genes in non-human cell lines. In vitro models have been used for this; however, their success is limited by their lack of physiological context. For example, human hepatocytes, which can be purchased cryopreserved for *in vitro* assays, are highly predictive of human metabolism, however, they cannot be used to study kidney excretion or effects on other cell types, such as endothelial cells or hepatic stellate cells that may affect distribution of the compound within the liver. The absence of systems that model both human tissue and physiological relevance, limits the predictive power of *in vitro* preclinical testing.

Species differences limit the predictive power of animal models for the purposes of toxicology and PK studies. The species differences that occur between

humans and animals may be physiological, such as differences in blood flow patterns, or genetic, resulting in proteins with different activity. In the case of physiological differences these may sometimes be accounted for using allometric scaling to adjust predicted values(Hunter 2010a; Hunter 2010b; Tang & Mayersohn 2005). However, this is not always the case: the inability of non-primates to sweat is a fundamental difference in biology that may effect drug disposition in the skin and cannot be dealt with via modeling. Similarly, genetic differences that result in expression of proteins or enzymes with different activities can sometimes be accounted for with an understanding of the inter-species variation, e.g. exogenous expression of a missing or deficient metabolic enzyme. However, failing to address species-specific variability may have seriously dire outcomes(J. Caldwell 1992; Eastwood et al. 2010). One possible tool to help address the deficiencies of current models is embryonic stem cells.

Availability of healthy heart tissue for scientific research is limited by organ donation and poor supply. This has inspired stem cell researchers to develop differentiation techniques to generate cardiac tissue from stem cells. These cells could assist not only in cell replacement therapy but also in drug development assays. The prediction of adverse biological events by models based on these cells could reduce the likelihood of toxic or inefficacious drugs going to the clinic.

## 1.4 Stem Cell derived models

### 1.4.1 Embryonic Stem cells

Embryonic stem cell biology has developed over the last 30 years to the point where our understanding of hESCs may allow their use in drug development and testing. The following is a summary of some highlights from the development of embryonic stem cell biology.

In July 1981 Cambridge scientists Evans & Kaufman first described a method to culture cells from the inner cell mass of a mouse blastocyst(Evans & Kaufman 1981). 5 months later Gail Martin from UCSF described a different process to culture these cells, going on to coin the term Embryonic Stem Cell (ESC)(Martin 1981). These cells were isolated from the inner cell mass of a 3-day-old mouse blastocyst and had two unique properties: self-renewal capacity and pluripotency. Self-renewal capacity means that the cells could be grown indefinitely under the appropriate culture conditions, while remaining undifferentiated in culture. Pluripotent cells are capable of differentiating upon induction into any cell in the adult body(DeChiara et al. 2010). This work heralded a new era of biomedical research, including the birth of regenerative medicine.

The potential utility of mouse embryonic stem cells, and the ease with which they could be genetically manipulated, resulted in an exponential growth of stem cell research. Investigators explored the mechanisms of differentiating different tissues while animal studies were conducted to determine the potential clinical

applications (Tropepe et al. 2001; Kubo et al. 2004; Yuasa et al. 2005; Murry & Keller 2008). The key to further development was an understanding of the fundamental nature of the stem cell. Among many contributors, two researchers stand out for additions to our understanding of pluripotency and self-renewal. Work conducted under the guidance of Rudolph Jaenisch utilizing somatic cell nuclear transfer, the process of transferring the nucleus from one cell to another, highlighted the importance of DNA methylation and the epigenetic state in maintenance of the stem cell phenotype(Rideout 2001; Blelloch et al. 2006). The work of Austin Smith's group has led to the depiction of the stem cell in a constant balancing act between self renewal and lineage commitment, even identifying kinase inhibitors capable of trapping the cell in what he called the 'ground state'(Ying et al. 2008). As understanding of mouse embryonic stem cells continued to grow, the race was on to reach the next major milestone: derivation of a human line.

In 1998 James Thomson's group from Wisconsin was the first to report the isolation of *human* embryonic stem cells, which differed from *mouse* ESCs based on their morphology and maintenance requirements(Thomson 1998). While initially grown on mouse embryonic fibroblast feeder cells(Martin 1981), researchers had successfully cultured mESCs on gelatin in media supplemented with LIF and BMP4 alone(Ying et al. 2003). Unlike *mouse* ESCs, *human* ESCs cannot be maintained on gelatin. Furthermore, maintenance of *mouse* ESCs requires supplementation of media with LIF while *human* ESCs require supplementation with FGF2. Beyond basic culture conditions *mouse* ESCs were passaged enzymatically, by contrast *human* ESCs required manual passage with

each colony being sliced up and passaged ‘organotypically’(Thomson 1998). Despite their differences, mESC and hESC were shown to share upregulation of key pluripotency genes such as OCT4, KLF2/4 and NANOG, while secreting a different profile of morphogens (Boyer et al. 2005; Loh et al. 2006). The differences between the two cell types had researchers questioning the validity of calling such cells embryonic stem cells. Indeed one hypothesis put forward was that hESCs were a slightly later stage of stem cell from the epiblast(Tesar et al. 2007). In 2007, Ronald McKay published a study comparing mESC, hESC and mouse Epiblast Stem Cells (EpiSC) and presented strong evidence that hESC are more akin to mouse EpiSC than mESC(Tesar et al. 2007; Chenoweth et al. 2010). This work was supported by a comparative metabolic study(W. Zhou et al. 2012). While understanding of the stem cell state continued to develop, a fundamental change in the way we view a cell would arise from the work of Shinya Yamanaka, whose work on reprogramming resulted in a Nobel prize(K. Takahashi & Yamanaka 2006).

Cellular reprogramming of adult cells via nuclear transfer was established by Nobel Laureate John Gurdon 50 years ago. In 2006 Yamanaka extended this work by reprogramming adult fibroblasts to pluripotent cells by delivery of a simple vector encoding four transcription factors(K. Takahashi & Yamanaka 2006). Described as ‘induced pluripotent stem cells’ (iPSC), these cells demonstrated all the characteristics of embryonic stem cells, even able to achieve germ line transmission. Less than one year later, Yamanaka repeated the feat by reprogramming human fibroblasts to pluripotent cells using a vector delivering the same genes(K. Takahashi et al. 2007). This advance removed the

need to destroy embryos to make cell lines and enabled researchers to compare in vitro assays with adult patient phenotypes. However, incomplete understanding of iPSC biology has distracted from progression of stem cell research. Many researchers, including Yamanaka, have indicated that iPSCs generated from different labs show different capacity for germline transmission and that thorough characterization of every pluripotent stem cell line is required to ensure karyotypic and phenotypic stability and pluripotency(Liao et al. 2009; Nakagawa et al. 2010; Kou et al. 2010; S. Zhou et al. 2010). However, there is debate regarding the importance of germ line transmission, especially for the purpose of in vitro investigations(Ellis et al. 2009). Researchers have spent the last 5 years, and vast research funding, comparing iPSCs from different sources to established hESC lines, with mixed conclusions regarding their similarities(Marchetto et al. 2009; Wilson et al. 2009; Newman & Cooper 2010). While iPSC offer a source of patient-specific stem cells for use in clinical treatment, the cost, time and low efficiency currently prohibits such use, at least until a future development changes some of these factors. Expanding our understanding of the molecular mechanisms governing stem cell characteristics while also enabling the possibility of patient derived stem cell lines, iPSC has attracted significant attention from researchers worldwide.

#### **1.4.2 Cardiac Differentiation**

Any study involving the use of tissue derived from stem cells requires a certain amount of attention to the complex task of differentiation. The capacity of ESCs to generate tissues from all three germ layers has resulted in a plethora of work to identify methods that control and direct differentiation towards specific

tissues. Early studies employed rudimentary protocols combining withdrawal of sera and addition of specific cytokines and morphogens (Ying & Smith 2003; Sachinidis et al. 2003). These protocols were generally inefficient and rarely generated functionally mature cells(Dambrot et al. 2011). Differentiation via co-culture with stromal induction cell lines such as END2 for mesoderm differentiation or PA6 for midbrain neuron differentiation increased yields and led to more physiologically relevant phenotypes(Murry & Keller 2008; Morizane et al. 2010). However, the variability introduced via the extra cell lines, as well as the inability to completely define and control these methods led investigators to explore other options. The ideal differentiation method would utilize a robust, fully defined, sera-free medium employing cheap, stable and small drug like compounds to drive differentiation. This approach to control differentiation using cheap and robust consumables has yet to be achieved, however considerable advances have been made. For example, Lorenz Studer's group, who utilized small molecule inhibitors to efficiently generate a high yield of cells whose transcriptional and immunochemical profile indicated a mature mid brain dopaminergic phenotype(Kriks et al. 2011).

The differentiation of ESCs towards different tissues holds great potential for drug testing. For example, cardiac tissue would be particularly useful for toxicity and functional screening assays. One of the early cardiac differentiation methodologies still currently employed today is the formation of aggregates via 'hanging drop' termed embryoid bodies (EB). Originally used with embryonic carcinoma cell lines to generate cells with a cardiomyocyte-like phenotype(Wobus et al. 1994), this method was rapidly adapted by ESC

scientists to generate cells of the mesoderm lineage(Mummery et al. 2007). Two aspects drive EB differentiation; firstly endogenous morphogens and growth factors, and secondly a physical hypoxic core which increases levels of the Hypoxia Inducible Factor (HIF) transcription factor(Ateghang et al. 2006; Sachlos & Auguste 2008). EB formation is an inexpensive and accessible method to differentiate ESC. While not efficient, it allows investigators access to this differentiation model without requiring extensive understanding of developmental biology and the recombinant factors that would be required for directed cardiac differentiation.

The use of END2 stromal cells to supply a matrix of connective tissue, growth factors, and morphogens to drive cardiac differentiation of mESC and hESC is well established(Mummery et al. 2007). Co-culture of ESCs with stromal cells has been demonstrated to achieve high efficiency differentiation with reasonable reproducibility at low cost; many of the factors which have limited EB differentiation(Mummery et al. 2007). However, the addition of a stromal cell line to cultures affects reproducibility of differentiation, and has made lab-to-lab comparison more difficult(Klimanskaya et al. 2008). Additionally, co-culture, like EB differentiation, is limited with respect to scalability. Most differentiation work has been aimed at providing a source of cells for cell replacement therapy; however, the complexities of co-culture and loss of defined conditions are unattractive to industrial and commercial uses.

Recently published methods have aimed to remove some of the variability and inefficiency of EB differentiation, by reducing serum, using specific recombinant

growth factors and controlling aggregate formation(Elliott et al. 2011; Burridge et al. 2011). The use of low-attachment U bottom plates and centrifugation to generate ‘Spin EBs’ has both increased the reproducibility of EB formation as well as allow for greater scalability. In combination with carefully timed addition of carefully titrated recombinant factors, Spin EBs allow for efficient cardiomyocyte differentiation(Elliott et al. 2011). Another approach to improving EB differentiation involves ‘priming’ the hESC for differentiation, which presumably aligns cell cycles and prepares the cells to respond to stimuli(Taha & Valojerdi 2008; Bauwens et al. 2008). This approach has been combined with low oxygen tension for high efficiency differentiation in a variety of hESC and hiPSC cell lines(Burridge et al. 2011).

A completely different method to induce differentiation is the use of transcription factors, introduced either directly as proteins or more commonly in expression vectors. The use of transcription factors to reprogram a cell towards becoming a cardiomyocyte has been studied extensively and is already in use for preclinical studies of cell replacement therapy(Hartung et al. 2013; Ieda et al. 2010). The approach has been taken one step further, a recent study investigating *in vivo* reprogramming of non-myocytes in the heart(Qian et al. 2012). The costs involved in utilising transcription factors remain prohibitive for screening applications, and does not necessarily provide the physiologically relevant heterogeneity present in EBs. Each differentiation methodology yields different types of tissue that make standardizing analytical methods difficult. Furthermore, the characteristics of the tissue resulting from some differentiation

methods (homogeneity for example) can be regarded as a strength and a weakness depending on choice of assay and desired output.

In a step towards the use of stem cell derived tissues for toxicity and pharmacology screening, GE Health has recently started selling 'Cytiva' cryopreserved cardiomyocytes, derived from hESC cells using a differentiation method licensed from Geron. The patent application for this technology suggests the differentiation protocol involves controlled EB formation with addition of recombinant proteins and small molecules(Gold et al. 2008). They claim that their cells are a representative mix of myocytes including nodal cells, with ventricular-like myocytes the majority(Minger 2012). The commercial availability of tools such as hESC-derived cardiomyocytes will allow drug companies to incorporate human embryonic stem cell derived cardiomyocytes into their safety and activity screening without the need to establish protocols for hESC maintenance and differentiation.

## 1.5 Heart physiology

### 1.5.1 Cardiac development and Physiology

Differentiation research is in a symbiotic relationship with developmental biology. Differentiation is an *in vitro* paradigm that replicates processes that occur naturally during development. Developmental biology informs which morphogens induce differentiation, and which proteins and genes can be used to identify cells of interest. Understanding of the different developmental stages and processes can help characterisation of *in vitro* differentiation.

The first stage of development, gastrulation, is triggered by formation of the primitive streak, which denotes the midline of the developing embryo, a process driven by nodal signaling and BMP4(Bellairs 1986). From the primitive streak, all three germ layers arise. One of these is the mesoderm, identified via expression of brachyury, which leads to cardiogenic, hematopoietic, osteogenic, endothelial and adipogenic lineages. FGF signaling induces cardiac-specified cells to migrate around the embryonic midline forming the cardiac crescent, which is identified by expression of the key cardiac gene Nkx2-5 (Harvey 2002; Sun et al. 1999).

The next stage of development is formation of the first and second heart fields, each contributing to distinct regions and cell type fates(Abu-Issa & Kirby 2007). The first heart field gives rise to the majority of the left ventricle and both atria while the second heart field gives rise to the outflow tracts and right ventricle(Cai et al. 2003). Prior to initiation of cardiac automaticity, the linear heart tube is formed from the medial and lateral sides of the primary heart field. The second heart field contributes to the ends of the heart tube and the formation of outflow tracts(Jiang et al. 2000). A complicated transcriptional program governs looping of the heart tube which allows formation of the four chambered structure of the adult heart(Christoffels et al. 2000).

### **1.5.2 Heart Structure**

The mammalian heart consists of four chambers, two atria and two ventricles. Blood enters the right atrium via the vena cava, is pumped into the right

ventricle and is then in turn pumped to the lungs via the pulmonary artery(Vander et al. 2007). Oxygenated blood is then returned to the left atrium via the pulmonary vein, then pumped in to the left ventricle, the largest of the four chambers. The thick, strong muscles of the left ventricle then contract (systole) and pump the blood to the peripheral circulation via the aorta. Valves at the opening of each chamber prevent the back flow of blood during contraction thereby maximizing efficiency. The continuous, and at times strenuous, work rate of the myocardium requires extensive vascularization to ensure adequate delivery of oxygen and nutrients to the cells at all times. In addition to the basic architecture of the myocardium an extensive network of cells forming a conductive network is necessary for the generation and propagation of the action potentials controlling myocardial contraction(Noble 2004).

The different cell types that are present in the heart can be broken down into three subsets: contractile, conductive and accessory. The contractile cells primary role is rhythmical and forceful contraction. The contractile cells can be further distinguished as ventricular myocytes, which account for around 40% of the cells in the ventricles and atrial myocytes, which have their own pacemaker activity. The conductive cells provide spontaneous action potentials that drive rhythmical contraction, namely pacemaker cells from the SA and AV node, and subsequent propagation of that action potential to ensure coordinated contraction, namely cells of the HIS bundle and purkinje fibers(Vander et al. 2007).

In addition, the heart contains accessory cells including endothelium for perfusion of the heart and fibroblasts, which are integral to normal function as well as inflammation and myocardial remodeling in response to injury. The somewhat simple structure of the heart relies on a number of cell types with vastly different characteristics working in concert to maintain a continual heartbeat.

## **1.6 Heart cellular physiology**

### **1.6.1 Myocytes**

The myocyte is a highly specialized cell type with many unique cellular and molecular components that facilitate contraction, relaxation and energy generation. The contractile proteins - actin, myosin, troponin and tropomyosin - act in concert as a molecular motor by contracting in response to  $\text{Ca}^{2+}$  ions and consuming ATP to relax. Thus a carefully controlled cycle of calcium and contraction, known as excitation contraction coupling, is driven by a host of molecular channels and pumps including calcium-induced calcium release from the sarcoplasmic reticular store regulated by the ryanodine receptor, sodium/calcium exchange regulated by the NCX antiporter and replenishment of sarcoplasmic reticular calcium stores via the ATPase SERCA. All of these processes are energy dependent and cardiomyocytes have a large volume of mitochondria to meet these energy needs. The unique contractile fibers and high mitochondrial concentration in cardiomyocytes allow for the continual excitation and contraction required to maintain circulation.

### 1.6.2 Pacemakers

The cardiac conduction system is just as essential to heart function as the cardiomyocytes themselves. Coordinated spontaneous and rhythmical contraction requires that the conduction system both generates action potentials, and then distributes them using the AV node to offset atrial contraction from ventricular contraction(Anderson et al. 1981). This allows the atria to contract and fill the ventricles with blood prior to ventricular contraction. The spread of the action potentials relies on specialized cells in the bundle of His and purkinje fibers that are almost neuronal in function.

Generation of the action potentials in nodal based pacemaker cells is sensitive to the dynamic interaction of a membrane clock and intracellular calcium cycling(Maltsev & Lakatta 2007). The membrane clock relies on the hyperpolarisation-activated cyclic nucleotide (HCN), or funny channel. After repolarisation, the funny channel permits slow entry of  $\text{Na}^+$  and  $\text{K}^+$  ions resulting in a slow depolarization that triggers opening of T-type  $\text{Ca}^{2+}$  channels(Robinson & Siegelbaum 2003). Depolarization activates L-type  $\text{Ca}^{2+}$  channels, which causes ryanodine receptor mediated calcium release from sarcoplasmic stores. This spike in intracellular calcium results in activation of both NCX antiporter and SERCA, replenishing sarcoplasmic calcium and activating several  $\text{K}^+$  channels, allowing efflux and repolarisation. It is these interacting cycles that underlie production of action potentials in the heart, facilitating spontaneous rhythmical contraction(Maltsev & Lakatta 2007; Lakatta et al. 2010).

A

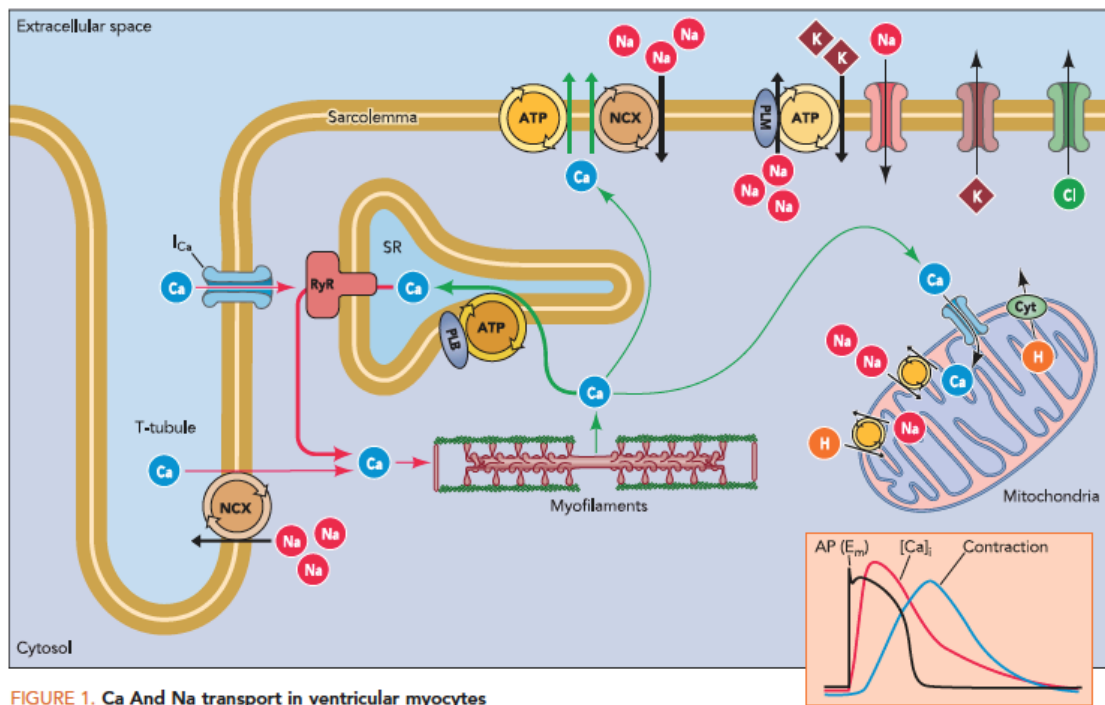


Image taken from Bers 2006.

B

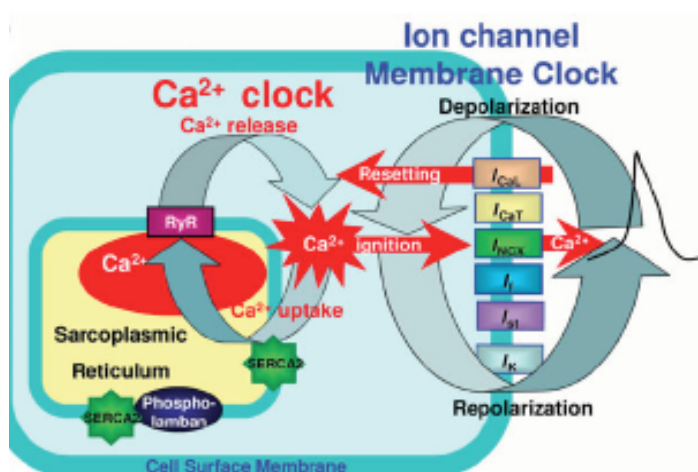


Image taken from Maltsev & Lakatta 2007

Figure 1.1

Panel A is a diagram highlighting important molecular components controlling  $[Ca^{2+}]_i$ , contraction and relaxation of cardiomyocytes. Panel B depicts the inter-dependant ion current clocks (membrane and  $Ca^{2+}$ ) that regulate the spontaneous activity of pacemaker cells.

## 1.7 Model receptor targets and drugs

### 1.7.1 Adrenergic receptors

The adrenoceptors (AR) are a class of G-Protein Coupled Receptors (GPCRs) that mediate the sympathetic signaling of adrenalin and noradrenalin. The class can be divided into  $\alpha$  and  $\beta$ -adrenoreceptors, and then further into the  $\alpha_1$  and  $\alpha_2$  which couple to the  $G_q$  and  $G_i$  proteins respectively, and the  $\beta_1$ ,  $\beta_2$ , and  $\beta_3$  which have been shown to couple with multiple G proteins. In the myocardium the  $\beta$ ARs couple to  $G_s$ , causing activation of adenylate cyclase, which converts adenosine tri phosphate (ATP) to cyclic adenosine monophosphate (cAMP) and in turn activates second messengers such as Protein Kinase A (PKA). The  $\beta_2$ AR has also been shown to couple to  $G_i$  which in turn causes a reduction in adenylate cyclase activity(Brodde 1993; McGrath et al. 2006; Hieble et al. 1995; Trautwein & Hescheler 1990).

The  $\beta$  adrenoceptors are key regulators of cardiac function, and dysregulation of their signaling has been implicated in diseases, including heart failure and cardiomyopathy(Post et al. 1999). Cardiac  $\beta$ AR pharmacology is extremely well characterized with clinically used agonists and antagonists. This makes  $\beta$ ARs an appropriate target to investigate mESC-derived EBs as models for drug development (refer to Chapter 4).

Isoprenaline is a non-selective  $\beta$ -adrenergic agonist which causes activation of the  $\beta_1$ AR resulting in increased adenylate cyclase activity, and subsequently

increased levels of cAMP and PKA phosphorylation. In turn, PKA phosphorylates several downstream targets in the myocardium, including L-Type calcium channels, phospholamban (a modulator of SERCA), the ryanodine receptor and the sodium calcium exchanger. The net effect of this signaling is increased intracellular calcium concentration and increased speed of sarcoplasmic reticular cycling permitting both increases in force and rate of contraction. The selectivity of isoprenaline for  $\beta$ ARs and the extensive data available in the literature make it an ideal control compound for exploring the uses of EBs for pharmacology studies.

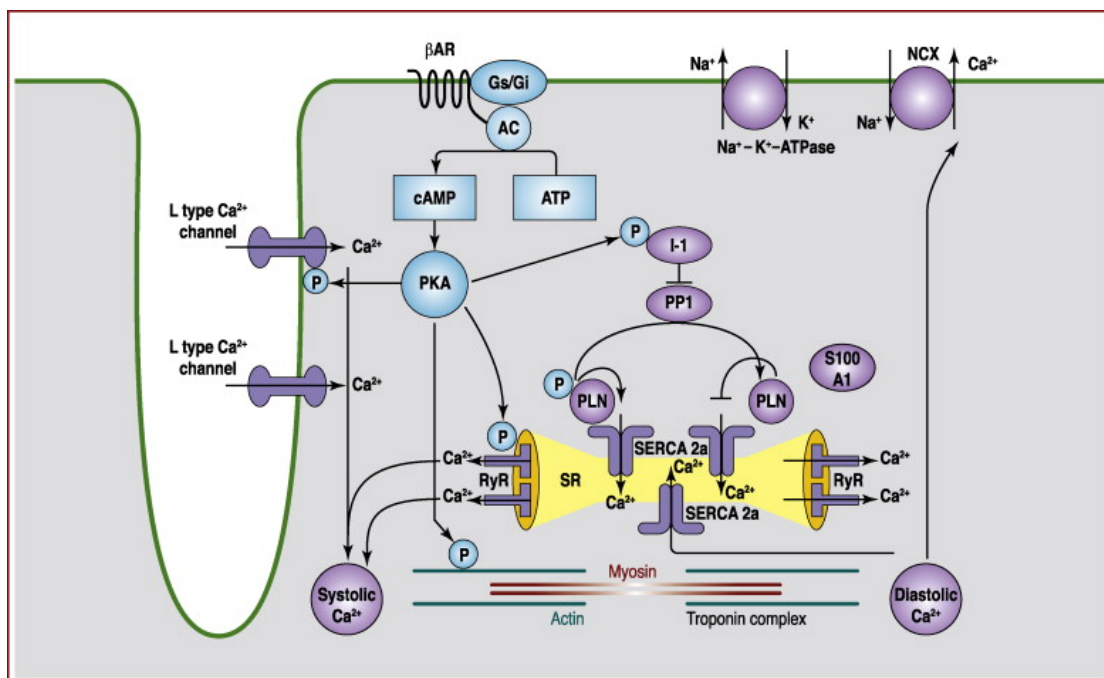


**Figure 1.2**

Diagram illustrating the effect of  $\beta$ -Adrenoceptor activation in the myocardium. Activation of the  $\beta_1$ AR stimulates adenylate cyclase through G<sub>s</sub>-Proteins. Adenylate cyclase converts ATP to cAMP, which subsequently activates PKA. PKA then phosphorylates L-Type calcium channels, phospholamban (PLN), the ryanodine receptor (RyR), and the actin-troponin complex. This results in increased intracellular calcium ( $[Ca^{2+}]_i$ ), increased force of contraction and increased speed of relaxation.

Image taken from Njeim & Hajjar 2010.

### **1.7.2 Adenosine receptors**

The adenosine receptors are a class of GPCRs that affect numerous cardiovascular functions such as coronary vessel dilation, pacemaker activity, and conduction. Adenosine is well known for its physiological inhibition of adrenergic signaling, primarily via post-synaptic inhibition of noradrenalin signaling. There are four distinct adenosine receptor subtypes, the A<sub>1</sub>, A<sub>2A</sub>, A<sub>2B</sub> and A<sub>3</sub>, which are all expressed at some level in the different parts of the myocardium(Shryock & Belardinelli 1997). A<sub>2A</sub> and A<sub>2B</sub> receptors are expressed on cardiac endothelium and while there is evidence of A<sub>2A</sub> mRNA in cultured cardiomyocytes this does not hold true for A<sub>2B</sub>, implying that A<sub>2B</sub> receptors may not be expressed in the myocardium(Olah & Stiles 1995; Shryock & Belardinelli 1997). The different levels and subtypes of adenosine receptors expressed on cardiomyocytes, endothelium and pacemaker cells suggests that purified cardiomyocytes are unlikely to be predictive of the physiological effects of adenosine receptor ligands.(Shryock & Belardinelli 1997).

Adenosine receptors represent an attractive drug class for use in the treatment of myocardial infarction; they have been shown to reduce the effects of reperfusion injury via a phenomenon termed ‘post-conditioning(Kin et al. 2005; Schipke et al. 2006). Post-conditioning was first thought to be primarily mediated through the A<sub>3</sub> subtype, but is now thought to involve multiple subtypes and signaling pathways(Urmaliya et al. 2010; Urmaliya et al. 2009).

Pharmacology of the adenosine receptor is complicated by multiple subtypes, mixed signaling, and limited selectivity of pharmacological tools. A major

difficulty when studying the adenosine receptor family in physiological tissues is the choice of commercially available ligands. Adenosine itself is highly labile(Van der Weyden & Kelley 1976). To overcome this limitation, NECA is widely used as a nonspecific ligand, although it has less affinity for the A<sub>2B</sub> receptor than the other subtypes(Olah & Stiles 1995). There are several selective A<sub>1</sub> agonists and antagonists, e.g., CPA and DPCPX, respectively. With respect to the A<sub>2A</sub> and A<sub>2B</sub>, subtypes there are not many potent selective agonists. CGS 21680 is selective for the A<sub>2A</sub> over the A<sub>2B</sub> however is also a potent agonist of the A<sub>1</sub> and A<sub>3</sub>. Selective agonists and antagonists for the A<sub>3</sub> are widely available; IB-MECA and MRS-1523 widely used examples. The variety of adenosine receptor subtypes and their downstream signaling pathways make adenosine receptors an interesting target for testing the capacity of EB models to investigate pathways that are more complex (refer Chapter 4).

### **1.7.3 Doxorubicin**

The anthracycline class of therapeutics was initially identified from a strain of Streptomyces bacteria during a screen for anticancer compounds(Weiss et al. 1986). Anthracyclines are used to treat a wide range of cancers including leukemias, lymphomas, breast and lung cancers and are considered among the most effective chemotherapeutic agents(RB 1992). However, their use is limited by their cardiac toxicity(Weiss et al. 1986). The prototypical anthracycline, Doxorubicin (Dox) has been the subject of hundreds of studies, focusing on efficacy, modified regimens and toxicity ((Zhang et al. 2009; Menna et al. 2010; Wallace 2003)). Despite this work, the exact mechanisms of anthracycline toxicity are contentious(Octavia et al. 2012). The extensive characterisation of

doxorubicin toxicity in a plethora of models makes it the ideal control compound for development and comparison in a novel toxicological assay (refer to Chapter 5).

#### **1.7.4 Monoclonal antibodies and Trastuzumab**

The development of molecular approaches to humanize monoclonal antibodies has created the opportunity for new drugs with exquisite specificity and selectivity to be developed. The first humanized antibody to be approved by the FDA in 1997, Daclizumab, paved the way for a host of new antibody-based drugs. Between 2000 and 2008, 39 humanised and 45 human monoclonal antibodies went through clinical stage testing(Brekke & Løset 2003; Nelson et al. 2010). There has been extensive review of the developability of monoclonal antibody therapies with respect to their potential market sizes, cost of development and ease of targeting orphan diseases(Hughes 2008; Reichert 2008). While providing several advantages over traditional therapies, monoclonal antibodies present a serious challenge for preclinical toxicity testing; one potentially mitigated by stem cell derived models.

Trastuzumab is a humanised antibody designed to block the HER2 (neuregulin) receptor to treat HER2-expressing breast cancer. HER2 is an orphan EGFR that stimulates cell proliferation and is often over expressed in early-stage breast cancers. Blockade of HER2 signaling by Trastuzumab inhibits cellular proliferation and angiogenesis, and may induce immune-mediated cytotoxicity(Hudis 2007). Selectivity of Trastuzumab is vital as non-selective EGFR blockade causes a number of unfavorable of side effects. There is question

surrounding the safety of Trastuzumab, specifically clinically observed cases of cardiotoxicity, often when used in combination with anthracyclines. As a monoclonal antibody with disputed cardiotoxicity, Trastuzumab is an excellent test compound to explore the use of stem cell derived toxicity models (refer to chapter 6).

## **1.8 Stem cell models in drug discovery - work to date**

The use of iPSC reprogramming technology to develop models for genetic diseases has already begun to yield promising drug candidates previously unidentified. One leader in the field, Lorenz Studer, has published considerable work combining iPSC reprogramming technology and small molecule directed neuronal differentiation to generate models for pathophysiology and drug screening

(Chambers et al. 2012; Kriks et al. 2011; Lee & Studer 2011). This has culminated in a recent publication identifying target molecules that can rescue the disease state of cells derived from patients with the genetic disease familial dysautonomia (Ramirez et al. 2012). The importance of this work extends beyond the identification of target molecules to treat dysautonomia; it provides a framework for the use of context relevant iPSC derived models for drug screening of genetic diseases.

Electrophysiology is a fundamental analytical technique commonly used to assess cardiac cell function. Advanced electrophysiological techniques, such as microelectrode arrays, have been studied for use with stem cell derived cardiac tissue as models for drug discovery screening (Möller & Witchel 2011; Desbordes

& Studer 2012; Cohen et al. 2011). However, not all cardiac functions are governed by the ionic currents measured by electrophysiology. Drugs such as omecamtiv mecarbil (which affect binding affinity of calcium with contractile fibers) would display little effect in an electrophysiology assay despite having great therapeutic promise. The combination of stem cell derived tissues and electrophysiology has great promise in drug discovery, however, it has already been extensively investigated and has limitations with the functional responses it can measure.

An alternative form of analysis that has previously been used to assess function of stem cell derived cardiomyocytes is videomorphometry. Videomorphometry employs various modes of microscopy and sophisticated software algorithms to detect changes in cell location (movement) or cell shape. With respect to ESC derived cardiac cells videomorphometry has been used to study the responses of embryoid bodies to classical cardio-active drugs(Ali et al. 2004; Lagerqvist et al. 2011; Sedan et al. 2008). The capacity of videomorphometry to identify clear functional outcomes independent of molecular mechanisms was considered an advantage for the purposes of this study. Owing to the extensive prior work surrounding electrophysiology and the benefits associated with videomorphometry, this method of analysis was selected for initial studies described in Chapter 4.

## 1.9 Aims

The utility of stem cell derived models in drug discovery is entirely dependant on assays that yield interpretable data from heterogeneous cultures, ideally yielding data that is predictive of the *in vivo* setting. While methods have been developed to reduce stem cell culture heterogeneity, physiological heterogeneity is an advantage stem cell cultures may provide over standard preclinical models. To test the utility of stem cell derived models of cardiac tissue in pharmacological, functional and toxicological studies, the aims of this project are to:

1. Test the hypothesis that mESC embryoid bodies are a suitable organotypic model for investigation of adrenoceptor and adenosine receptor pharmacology.
2. Test the hypothesis that mESC-derived cardiac populations are suitable physiological models for characterizing calcium oscillations.
3. Test the hypothesis that hESC-derived cardiomyocytes are a suitable model for investigating Trastuzumab cytotoxicity.

## CHAPTER 2 - MATERIALS AND METHODS

## 2.1 Mouse ESC lines

The Nkx2.5-eGFP mESC transgenic reporter line was obtained from Dr. Sean Wu ((S. M. Wu et al. 2006). This line was adapted from the original culture conditions in CJ7 media to the conditions described below. The E14Tg2a ESC line was obtained from Stem Cell Sciences for experiments outlined in Chapter 4 and then directly from the ATCC, catalogue number CRL-1821<sup>TM</sup>, for experiments in Chapter 5.

## 2.2 Mouse ESC propagation

Both mESC lines were propagated in Dulbecco's Minimum Essential Medium (DMEM) supplemented with 2 mM GlutaMAX<sup>TM</sup>, 1 mM Sodium Pyruvate, 0.2 mM  $\beta$ -mercaptoethanol and 10% ESC qualified Foetal Bovine Serum (FBS; Invitrogen, Australia). The pluripotency of cells was maintained using  $2 \times 10^3$  U/mL of murine leukemia inhibitory factor (LIF; Chemicon, Australia) and an additional 3  $\mu$ M CHIR 99021 and 1  $\mu$ M PD0325901 (Axon Chemicals, Germany)(Ying et al. 2008). Cultures were incubated at 37°C, 5% CO<sub>2</sub> in air in a humidified incubator. Cultures were passaged every 2-3 days when at approximately 85% confluence using Accutase<sup>TM</sup> (Invitrogen, Australia).

## 2.3 Cardiac differentiation of mouse ESCs

Cardiac differentiation of mESC lines was initiated using the hanging drop method ((Boheler et al. 2002)). Briefly, cells were suspended at a density of  $2.4 \times 10^4$  cells/mL in differentiation media consisting of DMEM supplemented with 2 mM GlutaMAX<sup>TM</sup>, 1%

Non-Essential Amino Acids (NEAA; Invitrogen, Australia), 1 mM Sodium Pyruvate, 0.2 mM,  $\beta$ -mercaptoethanol, 20% Foetal Bovine Serum (Thermo, Australia),  $10^4$  U/mL penicillin and 10 mg/mL streptomycin. The FBS was batch tested for maximum capacity to induce cardiomyocyte differentiation. 25 $\mu$ L droplets (containing approximately 600 cells) were seeded onto the lid of a culture dish, which was inverted to form hanging drops. The droplet shape forced cells into aggregates that developed into embryoid bodies (EBs). Lids were incubated over diluted phosphate buffered saline (PBS) to reduce droplet evaporation. At indicated time points the EBs were transferred via pipette to gelatin coated wells for further differentiation. For differentiation efficiency studies, EBs were seeded at a density of 1 EB / well of a 96 well plate. For contractility studies EBs were seeded at 3 EBs / well of a 24 well plate and for calcium imaging studies EBs were seeded at >1200 EBs / flask. Media was exchanged for fresh differentiation media every 2 days until FACS at day 8 (early developmental stage) or day 18 (late developmental stage). All contractility studies were done between days 18-21 of differentiation.

## 2.4 Mouse ESC-Derived embryoid body contractility studies

Videomorphometry was used to measure contraction rate and contractility of spontaneously beating bodies between days 18-21 of differentiation. On the day prior to measurement, fresh media was added to each well. Embryoid body cultures were superfused with a physiological salt solution consisting of 140 mM NaCl, 6 mM KCl, 2 mM CaCl<sub>2</sub>, 1 mM MgCl<sub>2</sub>, 20 mM HEPES, 10 mM glucose, and 1.4% (w/v) bovine serum albumin (pH 7.4). Each superfused well was maintained at 37°C using an inline heater

(Warner, USA) (measured with a thermocouple) at 1 mL total volume / well. A field of view containing an area with spontaneous beating was visualized using a Nikon Eclipse TS100 inverted microscope with Hoffman modulation contrast optics. Video captures were acquired at 80 frames per second using a Basler A602f camera controlled by the Quick Caliper program (SDR Clinical Technologies, Australia). Video was captured before agonist addition and at several time points after agonist addition, in the absence and presence of antagonists. Following 10-20 min equilibration, a 10 s capture was taken to quantify basal contractility and contraction frequency of the selected region. Subsequently antagonists: Atenolol (1 – 10 $\mu$ M), Propranolol (100 nM), ICI 118551 (100 nM), DPCPX (100 nM), ZM241385 (25 nM), or MRS 1523 (100 nM) were added for 10 min prior to a second capture. Drugs were then added: Isoprenaline (10 nM - 3  $\mu$ M), Salbutamol (10 nM – 3  $\mu$ M), Forskolin (5  $\mu$ M), Ouabain (10  $\mu$ M), NECA (10 nM – 100  $\mu$ M), CPA (10 nM – 100  $\mu$ M), or IB-MECA (10nM - 10  $\mu$ M) and then 10 s captures were taken at multiple time points for up to 20 min.

## 2.5 Data analysis

Video captures were analysed using Metamorph® Imaging System (Molecular Devices LTS, United States of America). An intensity threshold was applied to each frame of the capture to identify light or dark particles, the movement of which was tracked and quantified using the object tracking plug-in. These particles were the result of using Hoffman modulation contrast microscopy on EB cultures, small areas of high or low optical density in contracting areas. Tracking movement of these particles allowed measurement of the rate and amplitude of contraction. Absolute X Y values were plotted

to identify and eliminate particles with non-linear motion, then displacement from origin (the object position in the first frame) was plotted versus time. The amplitude of this value, expressed in pixels, was treated as relative to contractility while the number of spontaneous contractions within the capture was converted to a rate of beats per minute representing contraction frequency. The contraction amplitude and frequency was measured after addition of agonist, in the absence or presence of antagonist(s), and expressed as a percentage of the amplitude and frequency prior to chemical addition.

## **2.6 Immunolabelling of mESC-Derived embryoid bodies**

Embryoid body cultures were fixed with fresh 4% paraformaldehyde for 30 min or Acetone/Methanol (1:1) at -20°C for 10 min. 0.1% Triton-X in phosphate buffered saline (PBS) was used to permeabilise tissue at 4°C for 30 min, followed by blocking using 10% donkey serum in PBS for 30 min at room temperature, followed by 4 washes with PBS containing 1% (w/v) BSA and 0.1% Sodium Azide, 5 min each. Tissue was then incubated with primary antibodies overnight at 4°C at optimized dilutions (1:50-1:500). Cells were washed thoroughly before addition of secondary donkey antibodies labeled with combinations of Alexa 488, 594, 647, R-phycoerthrin (PE) or allophycocyanin (APC) used at 1:500 – 1:1000 (as needed), were added to wells for 2 hours at room temperature or 4°C overnight. Secondary only controls (tissue incubated without the primary antibody) were included with each experiment.

## 2.7 Fluorescence activated cell sorting

Fluorescence activated cell analysis and sorting was used both to identify cardiac progenitors using c-kit expression, and for assessment and purification of differentiated cells using the Nkx2.5-eGFP reporter line.

### 2.7.1 Cell digestion

Following 7-20 days of differentiation, embryoid bodies were incubated in accutase supplemented with collagenase (type II, 4mg/mL) for 30 min on a shaker at 37°C. Cell suspensions were filtered using a 100 $\mu$ m cell strainer to remove undigested aggregates followed by centrifugation (200g for 5 min). The digested pellets were re-suspended in FACS analysis buffer (PBS supplemented with 5% differentiation media, 5% FBS and 10 nM SYTOX® Red (Invitrogen, USA), or 10 nM SYTOX® Blue (Invitrogen, USA) or 100ng/mL Propidium Iodide). Late stage (day 18-20) cultures required DNase (10U/mL; Sigma Aldrich) to facilitate complete dissociation.

### 2.7.2 Analysis

Populations were analysed on the BD FACScanto II (Becton Dickinson, Australia). eGFP was detected using 488 nm laser excitation and a 530 $\pm$ 30 nm emission filter. SYTOX™ Red was detected using 633 nm laser excitation and a 660 $\pm$ 20 nm emission filter. Following exclusion of debris, doublets and non-viable SYTOX™ Red positive cells, the gate for eGFP positive cells was drawn on a dot plot of 488 nm excited 530 nm vs. 585 nm emission, using control (wild-type differentiated cells) as a non-fluorescent reference population. Propidium Iodide and Phycoerthrin (PE) labeled anti-cKit antibody (Beckman Coulter, Australia) were detected after excitation with the 488 nm

laser at  $585\pm40$  nm. SYTOX® Blue was detected after excitation with a 405 nm laser at  $450\pm50$  nm.

### **2.7.3 Sorting**

Cells were sorted on either a BD Influx cell sorter (Becton Dickinson, Australia) or a MoFlo Astrios cell sorter (Beckman Coulter, Australia) using a 100  $\mu\text{m}$  nozzle at 20 pounds/square inch (psi) sheath pressure. The gating strategy outlined above was again used to identify eGFP positive cells. The event rate was controlled to maintain a minimum sort efficiency of 80% and cells were collected into a 1:1 mix of PBS and filtered conditioned media. When using the Astrios soft aborts were collected and resorted, following which the final purity was analysed and found to be no less than 96% across all sorts.

### **2.8 Mouse Nkx2.5-eGFP<sup>+</sup> calcium imaging**

Following sorting (as detailed in 2.7), cells were plated at  $8-13 \times 10^3$  cells/cm<sup>2</sup> onto collagen coated 96 well plates. For studies investigating cellular connection, cells were plated at  $6.5 \times 10^4$  cells/cm<sup>2</sup>. Subsequent studies were performed 3-4 days post plating. Imaging media consisting of DMEM supplemented with 20% KnockOut™ Serum Replacement (KSR; Invitrogen, Australia), 1% NEAA, 0.1 mM  $\beta$ -mercaptoethanol, and 1x B27® where indicated, was made up fresh for each experiment. Cells were incubated with 10  $\mu\text{M}$  Fluo-4-AM (Invitrogen) in imaging media for 15 min ( $37^\circ\text{C}$ , 5% CO<sub>2</sub>). After loading the media was replaced with fresh imaging media and cells were incubated for a further 15 min ( $37^\circ\text{C}$ , 5% CO<sub>2</sub>). Cells were then transferred to the pre-warmed, heated ( $37^\circ\text{C}$ ) stage of an A1-R confocal microscope (Nikon, Japan). Cells were allowed to

equilibrate for 10 min before the baseline acquisition of 30 s. The compounds used for calcium imaging studies were ryanodine (10 $\mu$ M), forskolin (1 $\mu$ M), Thapsigargin (1 $\mu$ M), 2-APB (2 $\mu$ M), ZD7288 (10 -100 $\mu$ M), nifedipine (1 $\mu$ M), NNC 55-0396 (1  $\mu$ M) and NiCl<sub>2</sub> (10 $\mu$ M). Following addition of drugs 30 s captures were periodically acquired after 2, 5, 10 and 15 minutes. The 488 nm laser power was maintained at 10 % (approximately 16mW) and the frame rate at 30 frames per second (FPS). To confirm the waveform kinetics of some cells the frame rate was increased up to 120 FPS.

### **2.8.1 Post Calcium Imaging Analysis Mouse Nkx2.5-eGFP<sup>+</sup> Cells**

Analysis of calcium imaging captures was performed using NIS elements software (Nikon, Japan). Briefly, a threshold was used to identify cells from background, followed by binary overlay and transfer to region. This facilitated automatic selection of whole cells, following which multi-cellular aggregates were excluded from analysis (identified by morphology). Total Fluorescence intensity was measured over time and exported as text files for further analysis. An Excel analysis template was designed to not only identify peaks but also to summarise key peak features including width at half height, up slope and down slope, this is described in further detail in chapter 3.5.2. After each Excel file was imported into the analysis template, a manual inspection was required to ensure that the automated equations correctly identified each peak. Functional data were then correlated to morphological features and cellular immunolabelling profiles.

### **2.8.2 Post calcium imaging immunocytochemistry of Mouse Nkx2.5-eGFP<sup>+</sup> cells**

Following calcium imaging, plates were fixed for immunocytochemistry according to an adaption of a previously published protocol ((Schmid et al. 1991)). Cells were fixed with 0.4% paraformaldehyde for 10 min at room temperature (RT), followed by

permeabilization with 0.05% triton-X or 0.2% tween-20 at RT for 15 minutes. Cells were then blocked with 10% donkey serum for 30 minutes at RT, washed and incubated overnight with primary antibodies at optimized dilutions (table 2.1). Cells were carefully washed and then incubated with donkey secondary antibodies labeled with Alexa 488, 594, 647, R-phycoerthrin (PE) or allophycocyanin (APC) used at 1:500 overnight at 4°C.

### **2.8.3 Post calcium imaging TO-PRO®-3 cell death assay**

Calcium imaging was carried out as described in section 2.9 with the following modifications. Imaging media was supplemented with 1 µM TO-PRO®-3 and 1x B-27® where indicated. 50 µL mineral oil (Sigma Aldrich) was added to each well to prevent evaporation and alkalization of media during prolonged imaging. Following an initial 30 s capture to establish base line activity (10% laser power ~16mW), each field of view was then imaged for 60 s at 1, 10 or 70% laser power (5, 16 and 90 mW respectively). An image of each field of view was captured at 10 minute intervals for 8 hours using the 488 nm and 647 nm laser and 525 and 700 nm band pass emission filters to record Fluo-4 and TO-PRO®-3 fluorescence, respectively.

### **2.9 Hydroethidine (HE) reactive oxygen imaging**

Measurement of the generation of reactive oxygen species was adapted from a previously published protocol ((Abramov et al. 2007)). Calcium imaging was carried out as described in section 2.9 but with the addition of 50 µL mineral oil to each well to prevent evaporation and alkalization of media during prolonged imaging. Following calcium imaging, 100µL KSR media containing 10µM HE was added to each well. Fields

of view were then imaged at 10, 70 and 100% laser power for 60 s. An image of each field of view was captured at 20 minute intervals for 2 hours using the 488 nm laser with 525 and 590 nm band pass emission filters to measure intracellular Ca<sup>2+</sup> and nuclear labelling of the oxidized form of HE, ethidium, respectively.

## **2.10 Human embryoid body toxicity studies**

Human embryonic stem cell culture was established and several different differentiation protocols trialed in an attempt to generate hESC derived cardiomyocytes for the work described in Chapter 6. None of these methods was successful in our hands using numerous cell lines and minor modifications of established protocols(Burridge et al. 2011; Jang et al. 2008; Ng et al. 2011). Collaborators from Monash Immunology and Stem Cell Laboratories (MISCL) kindly supplied both differentiated cells and defined media for these studies.

### **2.10.1 Troponin ELISA**

The Human Cardiac Troponin I (cTnI) ELISA kit (Abnova, United States of America) was used to determine presence, and when suitably concentrated, quantity of cardiac troponin in supernatant following toxic insult. cTnI was measured in supernatant following incubation of hESC-derived embryoid bodies with toxins using a protocol adapted from the manufacturers instructions. Briefly, at each time point 450 µL supernatant was removed from each well to be replaced with 500 µL of fresh media containing toxin. Standards supplied in the kit were made up in hESC-EB media and used fresh. 200 µL of standards, controls, and sample supernatants were dispensed into separate wells in duplicate for analysis. 100 µL of Enzyme Conjugate Reagent was

dispensed into each well followed by thorough mixing. The plate was incubated at room temperature for 90 min followed by thorough washing with deionised water to remove all media components not bound to anti cTnI. 150µL of TMB reagent was added to each well, gently mixed, and then plate was incubated at room temperature for 30 minutes. The reaction was stopped by addition of 100µL of Stop Solution to each well followed by thorough mixing. The absorbance was read at 450 nm using an Envision (Perkin Elmer, Australia) within 15 minutes.

#### **2.10.2 TBARS assay for lipid peroxidation**

The TBARS Assay Kit (Cayman Chemicals, Australia) was used to measure the lipid peroxidation of hESC-EBs following incubation with and without toxin using a protocol adapted from the manufacturers instructions. Briefly, cells were treated with toxins for defined time, detached from plates using accutase/collagenase mix (refer 2.8.1) and sonicated to disrupt membranes. Cell lysates were transferred to tubes with 100µL of SDS solution and 4mL of the colour reagent. Tubes were placed in a beaker containing water on a hot plate and boiled vigorously for 1 hr, incubated on ice for 10 min, and centrifuged at 1,600 g at 4°C for 5 min. Samples were transferred to a 96 well plate and fluorescence read by exciting at 525 nm and emitting at 575 nm using the envision plate reader (Perkin Elmer, USA).

#### **2.10.3 TO-PRO®-3 cell death assay – Acute and chronic chemical toxicity**

Culture media was supplemented with 1 µM TO-PRO®-3 and incubated for 1 hour. Media was replaced and 50 µL mineral oil (Sigma Aldrich) was added to each well to prevent evaporation and alkalization of media during prolonged imaging. Plate was transferred to an A1-R confocal microscope, each EB identified and its location saved to

a coordinate list. Each EB was then imaged for 5 Z-planes from bottom to top of the EB at high (4096\*4096) resolution. eGFP, TO-PRO®-3 and SytoBlue were imaged as previously described. Each frame was then analysed for objects displaying co-localization of TO-PRO®-3 and eGFP, this was quantified as the number of double positive nuclei.

#### **2.10.4 CaspGLOW red assay**

Caspase assays utilized the CaspGLOW Red Active Caspase Staining Kit (BioVision, USA). Following two weeks of Trastuzumab exposure, media was replaced with 250µL fresh media containing a 1 in 500 dilution of Red-VAD-FMK. Cells were incubated for 1 hr in the dark in a CO<sub>2</sub> incubator, after which time the media was replaced with fresh media and they were transferred to a Nikon A1-R microscope. Images of SytoBlue, eGFP, and TO-PRO®-3 were acquired of each embryoid body as described previously. CaspGLOW Red was detected following excitation with a 488 laser using a 590 nm band pass emission filter.

#### **2.11 Drugs and Chemicals**

All drugs and chemicals were purchased from Sigma Aldrich (Australia) unless otherwise stated. Carbachol, ryanodine, and ouabain were dissolved in PBS. Nifedipine, thapsigargin & ZD7288 were dissolved in DMSO. Forskolin was dissolved in ethanol. 2-APB was dissolved in methanol. Isoprenaline was dissolved in 0.2 mM ascorbic acid, 1mg/mL BSA in PBS. The final concentration of DMSO, methanol or ethanol did not exceed 0.01% of the final incubation volume. Primary antibodies against MHC, SMA, HCN1, HCN4, vWF and PGP9.5 were purchased from Abcam (USA), or against cTnT from

Santa Cruz Biotechnology (USA). Secondary antibodies were from Invitrogen (Australia). ZD7288, 2-APB and ryanodine were purchased from Tocris bioscience (UK). HE, TMRM, Fluo-4 AM, TO-PRO®-3 and B-27® were purchased from Invitrogen (Australia).

## **CHAPTER 3 - METHOD DEVELOPMENT**

### **3.1 Foreword**

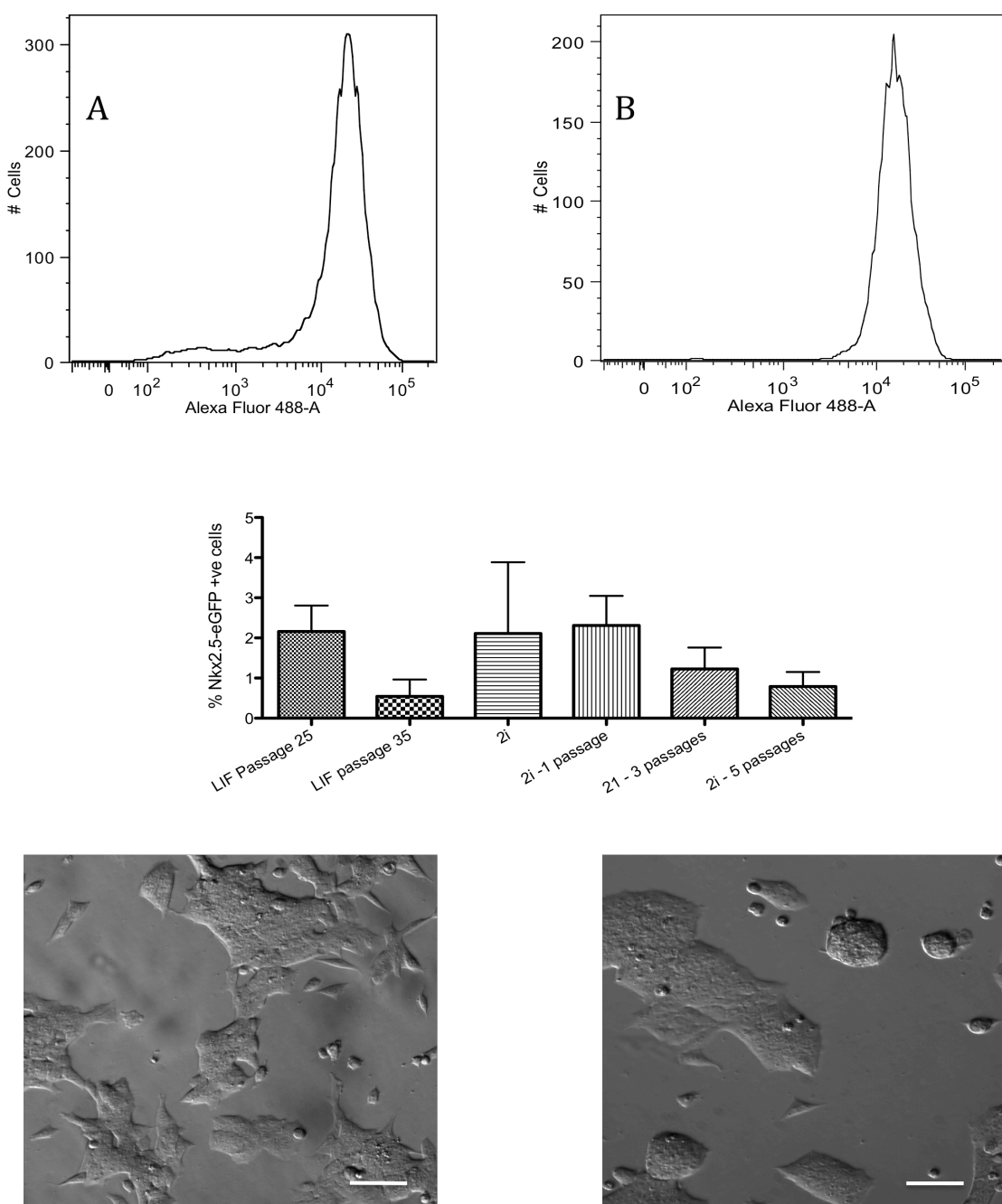
To address the questions raised in Chapter 1 considerable effort was required to optimize a number of protocols and analytical methods.

The true utility of stem cell derived models will only be realized when they are used in assays that were designed to make use of their strengths and overcome their limitations. Progress in the development of cardiac drugs could be expedited with standardized methods to analyse ESC-derived cardiomyocytes. Progress in the field of differentiation has occurred parallel to assay development, causing difficulty in translation. Specifically, EB formation is still a commonly used method of differentiation, but heterogeneity of the EB limits the number of traditional analytical techniques that can be used. This chapter includes method development and optimisation that was required for the experimental work discussed in later chapters.

### **3.2 Embryonic stem cell culture**

As discussed in Chapter 1, techniques for culturing embryonic stem cells have evolved since they were pioneered in the early 1980's by Evans, Kaufman and Martin ((Evans & Kaufman 1981; Martin 1981)). Austin Smith's work has highlighted the inherent instability of the 'pluripotent' state, and established defined culture conditions to maintain cells in a quasi stable state termed the 'ground state'(Ying et al. 2008; Silva et al. 2008). However, while methods are well described, maintaining embryonic cultures in an undifferentiated state while preventing germ layer and differentiation bias has

proved a challenge throughout this project. Using the Oct4-eGFP and Nkx2.5-eGFP reporter cell lines to measure stem cell homogeneity and cardiogenic differentiation potential respectively, a modified version of Austin Smiths ‘2i’ protocol was adapted for maintenance of mouse embryonic stem cells. Addition of the GSK3- $\beta$  inhibitor CHIR99021 and MEK inhibitor PD0325901 to our standard propagation media resulted in more homogenous expression of Oct4. Unfortunately, prolonged culture in 2i had a negative effect on cardiogenesis as determined by nKX2.5 reporter expression measured using FACS following EB differentiation. It is most likely this differentiation bias may be due to altered  $\beta$ -catenin levels caused by the GSK3- $\beta$  inhibitor, although it is possible that altered FGF-2 signaling following withdrawal of the MEK inhibitor was responsible. An interesting side note, other students in the lab noticed that culturing cells in 2i caused a rapid decrease in neurogenic potential as measured via SOX-1 expression during differentiation. To overcome this differentiation bias I investigated the effects of withdrawing 2i briefly before differentiation. These studies found that withdrawing 2i for one passage before differentiation provided the highest yields of Nkx2.5-eGFP cells. Distinct morphological differences between cells cultured in adapted ‘2i’ protocol and the standard protocol were also quite evident when visualized using white light microscopy (Figure 3.1).

**Figure 3.1**

FACS and morphology assessment of 2i treatment on pluripotency and differentiation potential. Oct4-eGFP indicated a heterogeneous population with high, medium and low Oct4 expression (A), 2i treatment abolished the presence of the medium and low levels of Oct4 expression (B). The effect of passage and 2i treatment on cardiogenic differentiation potential (C). White light images of cells grown under standard conditions (D) and those grown in the presence of 2i (E). Scale bar =  $100 \mu\text{m}$ .

### 3.3 Cardiac Differentiation

Embryoid body differentiation in hanging drop cultures is well established for the mesodermal differentiation of embryonic stem cells(Dambrot et al. 2011).

Differentiation is initiated by seeding cells in droplets suspended upside down on the lid of a dish. Factors affecting this method of differentiation include the initial number of cells and the duration of suspended culture, chemical supplementation of media during suspension or following attachment, as well as the oxygen tension throughout culture(Wiese et al. 2011; Czyz & Wobus 2001; Sachlos & Auguste 2008; Dang 2004). EB differentiation can yield cells from all three germ layers, in the EBs generated for this study mesodermal differentiation was observed based on brachyury expression (not shown). Aside from myocardium, smooth muscle is also derived from the mesodermal germ layer. Using videomorphometry to track movement based on cellular contraction, smooth muscle capable of spontaneous contraction has the potential to confound analysis of responses of EBs. The rhythmical contraction of cardiomyocytes can easily be separated from the spastic contractions of smooth muscle visually. A study was conducted to determine the optimal number of cells per droplet to achieve maximal cardiac differentiation (determined as % of EBs contracting spontaneously and rhythmically) while limiting smooth muscle differentiation (spontaneous non-rhythmical contraction). EB size was also measured throughout the time-course. EB size on day 5 was used in future studies as a quality control measure of successful differentiation.

### **3.3.1 Results and Discussion – EB differentiation**

Cell aggregation occurred during the first 48 hours of suspension, after which time aggregates could be clearly identified and measured (Figure 3.2 A). Rate of growth of the EB, measured by microscopy, expressed as total diameter, was dependant on the initial number of cells seeded into each droplet. The data was fitted to a one-phase association equation with an apparent plateau at 1000 µm (Figure 3.2 B). This plateau is most likely explained by two parallel processes. Firstly, the growth of the diameter of the sphere was likely limited by requiring geometric growth of cell proliferation as the increasing diameter incorporated increasing numbers of cells, and secondly, the gradual consumption of nutrients and buildup of byproducts within the suspended drop likely slowed cell division. Presumably, the kinetics of formation and size of the hypoxic region of the EB core was dictated by the initial seeding density, balanced by necrosis in the center. These two processes are likely the key determinates of the optimum number of cells for cardiac differentiation. The efficiency of cardiac differentiation was measured by assessing the proportion of embryoid bodies with detectable spontaneous contraction. Cardiac differentiation was detectable at 200 cells/droplet and increased up to 1000 cells/droplet. Smooth muscle differentiation could be readily detected from 800 cells/droplet. 600 cells/droplet was determined to be a suitable compromise (Figure 3.2 C).

### **3.3.2 Maximising cardiomyocyte yield**

Although the EB method consistently produced beating aggregates, I evaluated the differentiation efficiency of several other published differentiation methods(T.

Takahashi 2003; Zhu et al. 2009; X. Wu et al. 2004; Willems & Leyns 2008; Hao et al. 2008; Jang et al. 2008; Kawai et al. 2004). The goal of this optimization was primarily to generate a greater number of cells for later studies utilising the Nkx2.5-eGFP reporter line, which would have benefited from greater differentiation yields.

Many chemical and process-based approaches have been published utilising various methods to increase cardiac differentiation efficiency(Sachinidis et al. 2003; Rajala et al. 2011; Lyssiotis et al. 2010; Willems et al. 2009). Several of these were trialed with limited success. Two of the differentiation methods trialed were limited by toxicity(Zhu et al. 2009; Hao et al. 2008). Three of them produced no significant increase in differentiation efficiency(X. Wu et al. 2004; Willems & Leyns 2008; Kawai et al. 2004). One method based on monolayer culture with ascorbic acid showed promise in 96 well plates, however, when scaled up to flasks the efficiency dropped to unacceptable levels(T. Takahashi 2003). The one method that showed the biggest increase in cardiac differentiation efficiency involved the use of DAPT, a  $\gamma$ -secretase inhibitor that indirectly blocks Notch signaling. It significantly increased the % of Nkx2.5-eGFP positive cells, however it also had an effect on the level of GFP expression, resulting in a significantly higher number of cells with 'high' levels of GFP.

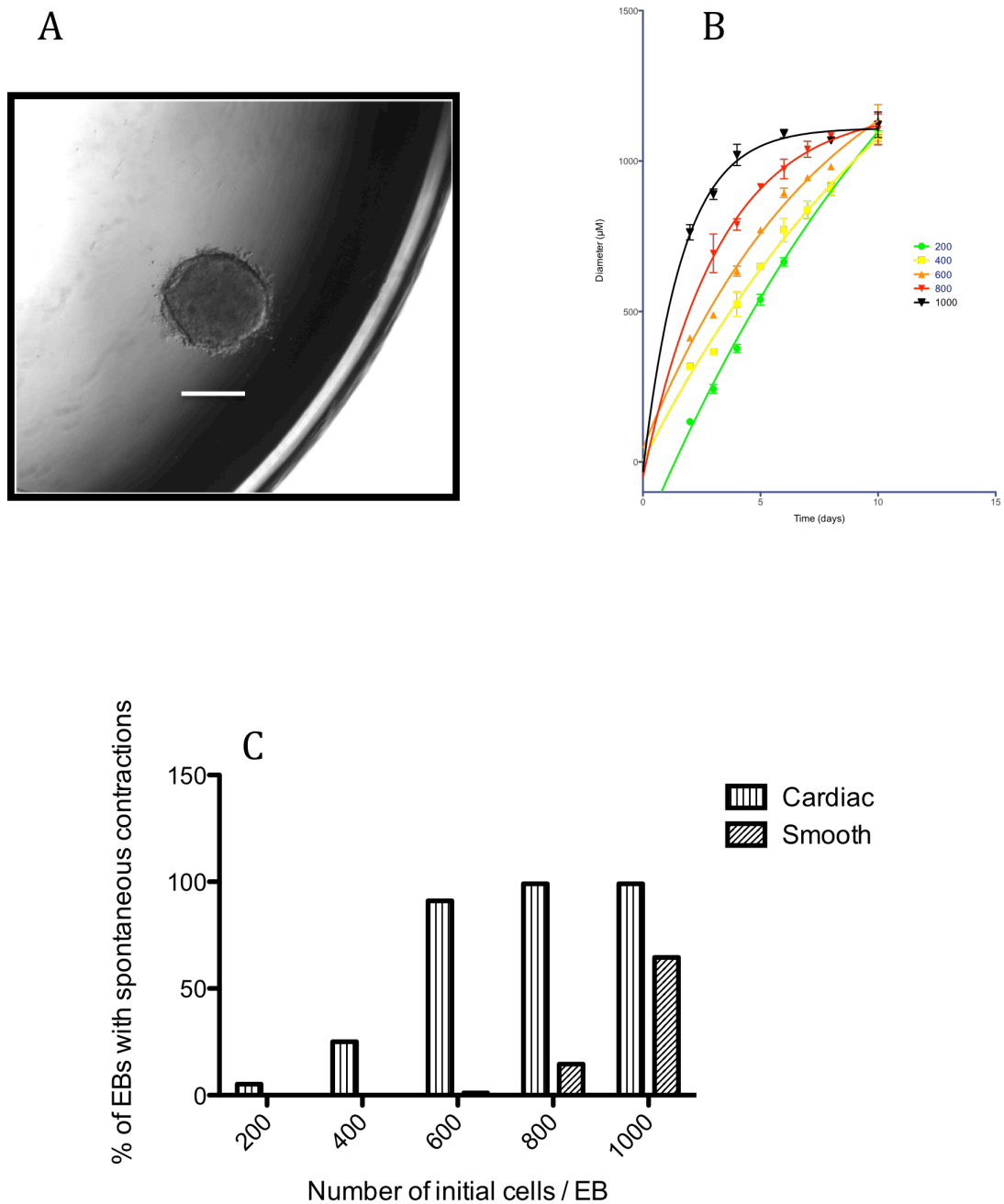
During cardiac development Nkx2.5 is expressed at low, high, and then intermediate levels depending on how mature the cells are(Yang et al. 2008; S. M. Wu et al. 2006). Assuming the changes in the GFP expression were reflective of changes in the levels of Nkx2.5, this would indicate that DAPT is having an effect on maturity; specifically it is reducing the proportion of cells leaving the transient 'high' nkx2.5 stage. The role of

Notch signaling during differentiation changes over the course of development, however it has been shown to be an inhibitor of cardiac differentiation(Rochais et al. 2009). There is also evidence that suggests Notch acts through  $\beta$ -catenin to drive commitment of cardiac progenitor cells(Kwon et al. 2009). The complexity of Notch signaling, and the resultant need for extensive characterisation before functional studies could proceed was considered outside the scope of this thesis. Instead, the standard EB differentiation method used for Chapter 4 and outlined in Chapter 2.3 was used for further studies. The different chemical approaches attempted, and their efficacies, are outlined in Table 3.1

### **3.3.3 Effect of oxygen tension on cardiogenesis**

One alternative approach to chemically driven differentiation is the use of low oxygen tension, which has been shown to have a positive effect on cardiac differentiation(van Oorschot et al. 2011; Csete 2005). To investigate if low oxygen tension would increase the CM yields required for future studies, I examined the feasibility and effect of low oxygen tension on our optimized differentiation protocol. A chamber was built to facilitate control of the atmosphere within the incubator. The effect on the differentiation of the Nkx2.5-eGFP reporter line was then accessed using FACS (Figure 3.3). Differentiation was assessed based on % of positive and the total number as positive cells as low oxygen tension has been shown to increase cellular proliferation which may have masked any observed increase in cardiomyocyte numbers. While 2 and 6 days of reduced oxygen tension showed significantly increased CM differentiation this was not consistently observed. It's likely this inconsistency was due to difficulty in

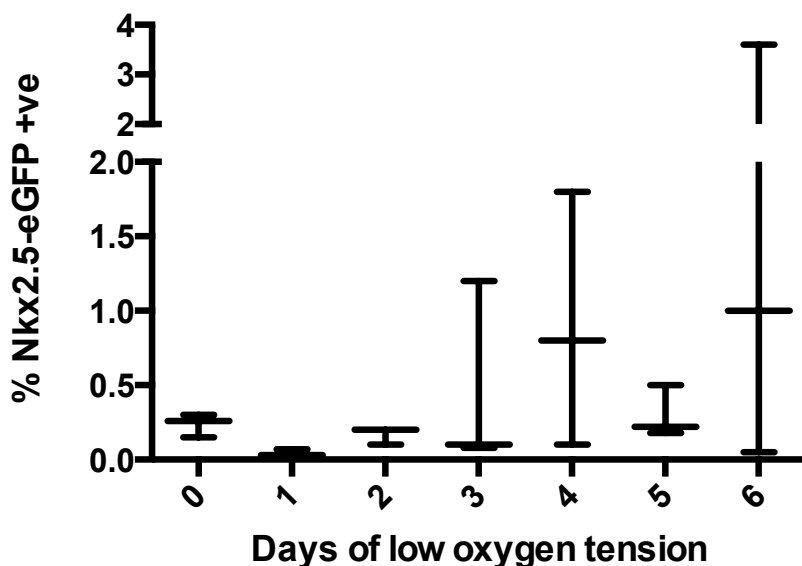
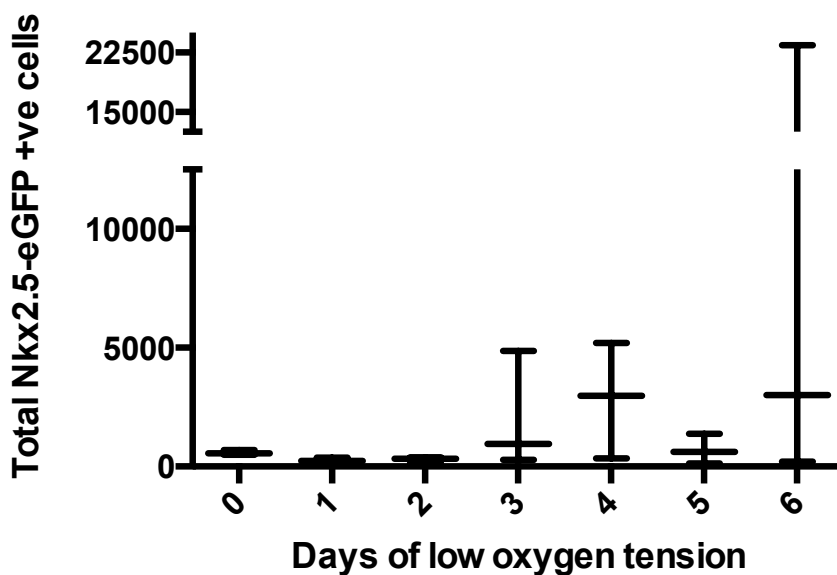
controlling oxygen tension without expensive and elaborate environmental control equipment. Future studies were performed at atmospheric oxygen levels.

**Figure 3.2**

Optimisation of hanging drop differentiation. A representative embryoid body plated after 5 days of suspension culture, scale bar = 500 µm (A). Kinetics of embryoid body growth and the effect of initial cell number on diameter (B). The effect of initial cell number on the development of different types of spontaneous contractile tissue (C)

Source	Morphogen(s)	Process	Results	Comments
(Takahashi 2003)	Ascorbic acid	Monolayer	Reasonable efficiency (0.4% Nkx2.5-eGFP by FACS)	When scaling from 96 well plates to flasks efficiency was lost
(Zhu et al. 2009)	Stauprime	Hanging Drop	Cytotoxic at concentrations specified in paper	No significant activity when diluted below toxic concentrations
(Wu et al. 2004)	Cardiogenol C	Hanging Drop	No statistical increase in efficiency	
(Willems & Leyns 2008)	Activin A and BMP 4	Hanging Drop	No statistical increase in efficiency	
(Hao et al. 2008)	Dorsomorphin	Hanging Drop	Cytotoxic at concentrations specified in paper	No significant activity when diluted below toxic concentrations
(Jang et al. 2008)	DAPT	Hanging Drop	Increased efficiency	Altered levels of Nkx2.5 expression, possible affect on maturity
(Kawai et al. 2004)	FGF2 & BMP2	Hanging Drop	No statistical increase in efficiency	

**Table 3.1**  
mESC cardiac differentiation methods and the resultant outcomes in our lab.

**A****B****Figure 3.3**

The effects of low oxygen tension during hanging drop. Following hanging drop suspension cells were placed in an airtight container under low (4%) oxygen tension for up to 6 days. Cells were FACS sorted on day 7 quantifying the proportion of Nkx2.5-eGFP cells (A) and the total number (B). Data is expressed as mean with the range.

### 3.4 Videomorphometry – Object tracking

To measure the effects of different drugs on the function of the mESdCM we developed a method utilising high contrast optics, high-speed imaging, and object tracking. Using motion tracking to determine changes in rate of contraction is a common technique(Ali et al. 2004), however there is no clear standard for measuring contractility using videomorphometry. To investigate the potential of object tracking to measure changes in contractility we compared the effects of two drugs, ouabain and forskolin. Ouabain is an inhibitor of the  $\text{Na}^+/\text{K}^+$ -ATPase, which causes an increase in the intracellular  $[\text{Na}^+]$ , which in turn drives the NCX antiporter to efflux  $\text{Na}^+$  while importing  $\text{Ca}^{2+}$ . Due to this activity ouabain has a potent ionotropic effect causing an increase in contraction with little to no effect on the rate of contraction (Mason & Braunwald 1963) (Sonnenblick et al. 1966). Forskolin acts on the same signaling pathway as isoprenaline (discussed in Chapter 1), however it bypasses the adrenoceptor and acts directly on adenylate cyclase to stimulate cAMP production; as such it should cause an increase in rate and contractility owing to multiple downstream signaling targets(Vinogradova et al. 2010; Bround et al. 2012).

#### 3.4.1 Results and discussion

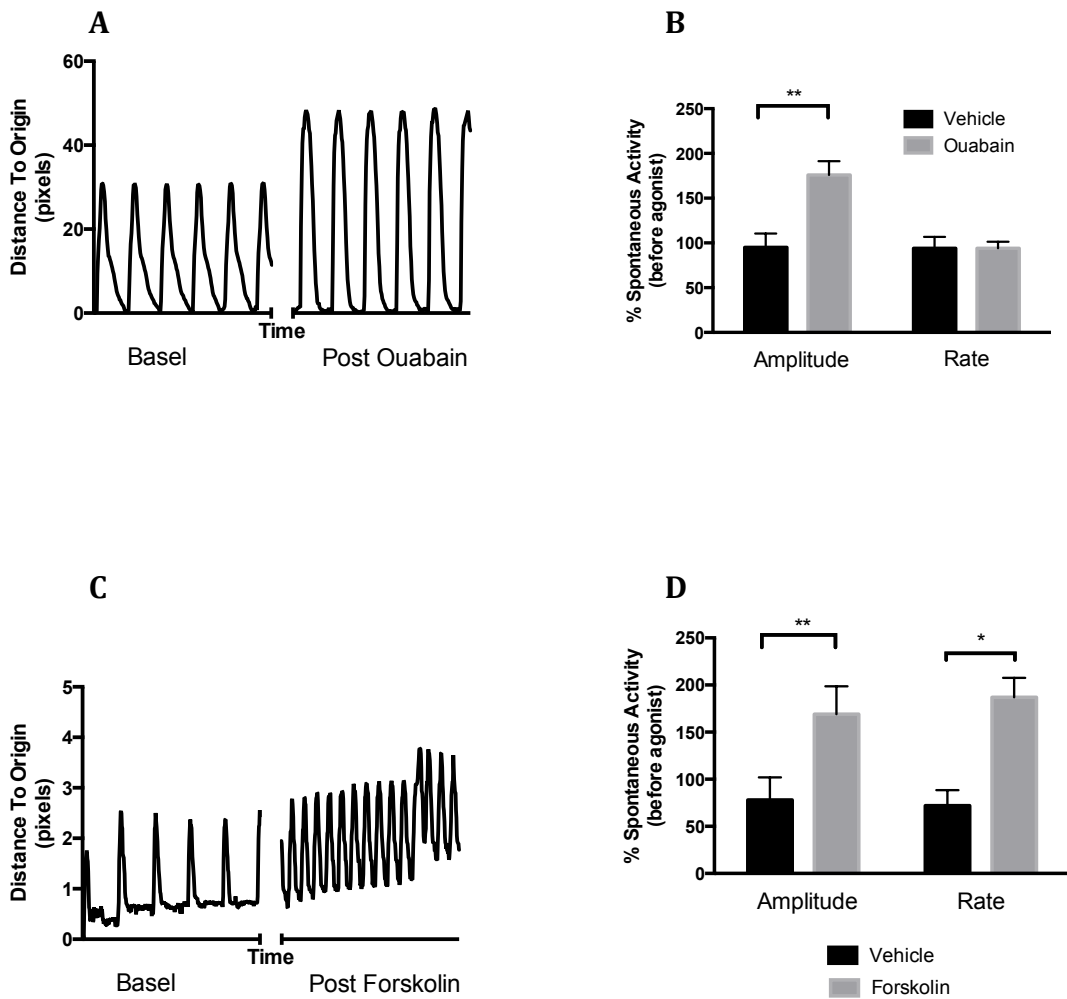
To validate the videomorphometry method I developed, two compounds were investigated that have different cardiac effects. Ouabain, the most widely used cardiac glycoside, inhibits the  $\text{Na}^+/\text{K}^+$  ATPase. This results in increased intracellular  $\text{Na}^+$ , which in turn causes activation of the  $\text{Na}^+/\text{Ca}^{2+}$  antiporter, ultimately resulting in increased

intracellular  $\text{Ca}^{2+}$ (Hansen 1984). This manifests physiologically as increased force of contraction, with little effect on rate of contraction. The other compound, forskolin, directly activates adenylate cyclase, resulting in increased cAMP and all the subsequent functional effects described in Chapter 1(Hartzell & Fischmeister 1987; Insel & Ostrom 2003). The physiological result of increased cAMP is increases in both rate and force of contraction. These two compound have allowed me to validate the capacity of my imaging method to differentiate between agents that have effects of both rate and force of contraction (also known as chronotropic and ionotropic) and agents that only affect one parameter.

The representative traces show the effects of both ouabain (Figure 3.4A) and forskolin (Figure 3.4B) on rate and contractility of EBs when imaged according to the methods outlined in chapter 2. All tracking data is presented as two parameters, contraction amplitude (measured by distance to origin) and rate of contraction (measured as contractions per min). Previously it has been shown that measurement of the contraction amplitude (or contractility) relates to contractile force using dynamic traction force microscopy(Jacot et al. 2010). As expected forskolin causes increases in rate and amplitude of contraction while ouabain only increases contraction amplitude. This validates the use of both parameters to measure effect of compounds on myocytes (contraction amplitude) and pacemakers (contraction rate) in the EB

Parameters other than peak height and rate, such as rate of contraction or relaxation, peak area and width at half height were examined for forskolin and ouabain. Robust results were only achieved with peak height and rate. The fundamental problem with

image tracking is the occurrence of non-linear motion, which can be identified in the x and y but not the z-axis using standard microscopy. This results in potential changes in the velocity (a vector), which would affect peak shape and thereby other parameters outside of height and rate. Other groups have used videomorphometry to determine parameters such as rate of relaxation(Ali et al. 2004). That this was not possible using my imaging method highlights the need for development of standardized methods that have been rigorously tested

**Figure 3.4**

The effect of Ouabain (an ionotropic drug) on mESC EBs. (A) Representative trace demonstrating change in contraction amplitude without change in rate of contraction. (B) The responses were quantified and expressed as a % of spontaneous activity prior to addition of compound (basal) (\*\* $p > 0.01$ , two way ANOVA, post-hoc Bonferroni's n=6).

The effect of forskolin (ionotropic and chronotropic drug) on mESC EBs. (C) Representative trace demonstrating change in contraction amplitude without change in rate of contraction. (D) The responses were quantified and expressed as a % of spontaneous activity prior to addition of compound (basal) (\* $p > 0.05$ , \*\* $p > 0.01$ , two way ANOVA, post-hoc Bonferroni's n=6).

## 3.5 Calcium imaging

Following the EB studies in Chapter 4 it became clear that a method was required that would allow us to look at the function and responses of specific cells, allowing elucidation of the interaction of the heterogeneous cell types present in the EB. Calcium imaging is a well-established method allowing measurement of responses of individual cells; moreover, calcium is a key regulator of both pacemaker activity and contractile activity. Pilot experiments identified a problem, rhythmical and spontaneous waveforms could be identified but they were especially unstable. The instability appeared to be dependent on imaging, as cells that were loaded and left to incubate for several hours still displayed the waveforms briefly before succumbing to the same instability as freshly loaded cells. The following experiments were done to identify the cause of this instability and a mechanism to prevent it, the work here crucial to the results presented in Chapter 5.

### 3.5.1 Stability and reactive oxygen species

The generation of free radicals by laser excitation of fluorescent dyes is a phenomenon that has been investigated for several sensors, including calcium sensing dyes (Knight et al. 2003; Schaffer et al. 1994). The effects of free radical generation during calcium imaging have largely been ignored in many recent publications, of particular relevance to this study, those involving calcium imaging of ESC derived CMs and neurons (Zahanich et al. 2011; Malmersjö et al. 2010; Kim et al. 2010). The effects of confocal calcium imaging on cellular viability were measured using the To-Pro-3© assay described in chapter 2.12. In cells loaded with Fluo4-AM, those exposed to the confocal

laser showed cell death, but those without laser exposure did not (Fig 3.6b). This was done in parallel with studies where the stability of the spontaneous waveforms described in chapter 5 was dependent on the time cells were exposed to the confocal laser rather than incubation time (results not shown). The hypothesis was that confocal calcium imaging was generating free radicals, which in turn affected cell viability and function. Prior to studies described in chapter 5, the mechanisms of instability, and a method for stabilization were required. To this end, the effects of confocal imaging on FACS sorted cardiomyocytes was investigated, focusing on cell viability, reactive oxygen generation and dye toxicity.

Measurement of reactive oxygen species in single cells is a complicated methodology. The natural generation and detoxification of reactive oxygen species within cells with high mitochondrial content, such as cardiomyocytes, confounds many assays, especially at a single cell level. Small changes in the levels of free radicals can have significant effects on cell function while not being readily detectable using currently available methods. Thus, indirect measurement must be relied upon to support trends shown with direct free radical measurement.

To investigate the effect of laser induced ROS generation on cell viability I treated ESC cultures with anti-oxidants and examined the effect of ROS generation. The loss of cell viability displayed following various laser strengths (Figure 3.6 A) was evidence of the generation of a toxic product that was related to laser exposure. Antioxidant stabilization of the spontaneous waveforms unveiled long lasting rhythmical calcium transient waveforms of varying phenotypes previously not described in the literature

(Figure 3.5). The experimental data I have described here and in chapter 5 point to an underlying artefact that may explain both the instability described by Zahanich *et al* (Zahanich et al. 2011), and also the absence of reports in the literature of the different spontaneous calcium waveforms I have observed.

Calcium flux was measured using Fluo-4-AM, where Fluo-4 is coupled to a methoxy ester (AM) to allow it to cross the cell membrane, before esterase cleavage traps it in the cell generating a molecule of formaldehyde. It is plausible that toxicity observed during confocal calcium imaging may be due to formaldehyde from the dye, rather than ROS generation. The lack of death following Fluo-4 AM loading without laser exposure (Figure 3.6 B) is strong evidence that formaldehyde toxicity is not directly causing cell death. Addition of the anti-oxidant B-27® during imaging reversed laser-induced cell death, consistent with a role for generation of toxic ROS.

Direct measurement of reactive oxygen species was attempted but results were limited by technical constraints, specifically the dyes available for use in my system. Measurement of reactive oxygen species at a cellular level requires the use of dyes such as 2',7'-dichlorodihydrofluorescein diacetate (H2DCFDA) or HE. Due to the GFP and Fluo4 already present in these cells, most widely used reactive oxygen sensors were unusable, hence the use of HE. However, the excitation wavelength used to measure calcium flux also activated (and potentially bleached HE, preventing reliable readouts of ROS. Another issue was that all available fluorescent free radical dyes act irreversibly, which precludes dynamic measurement of the redox state of the cell.

Future studies to directly measure the effect of microscope laser activation on ROS generation could make use of fluorescent proteins based on GFP that have been generated to react dynamically to the redox state of the cell, and allow dynamic measurement of insult and recovery(Dooley 2004; Dooley et al. 2012; Hanson 2003). While we have obtained one expression construct for such a protein (roGFP), extensive work was required for optimization, and its use was therefore outside the scope of the current study. Despite not having an optimal method to measure free radical generation at a single cell level, the indirect evidence I gathered indicated a strong causal link between laser exposure and loss of cell function and viability. In the absence of toxicity owing to the dye, this evidence suggests an artefact of live cell imaging that is likely to have implications for many studies already published. Of particular importance to this study, the addition of antioxidants to eliminate the effects of ROS, stabilized previously dismissed waveforms and permitted further characterisation as described in Chapter 5.

Figure 3.5

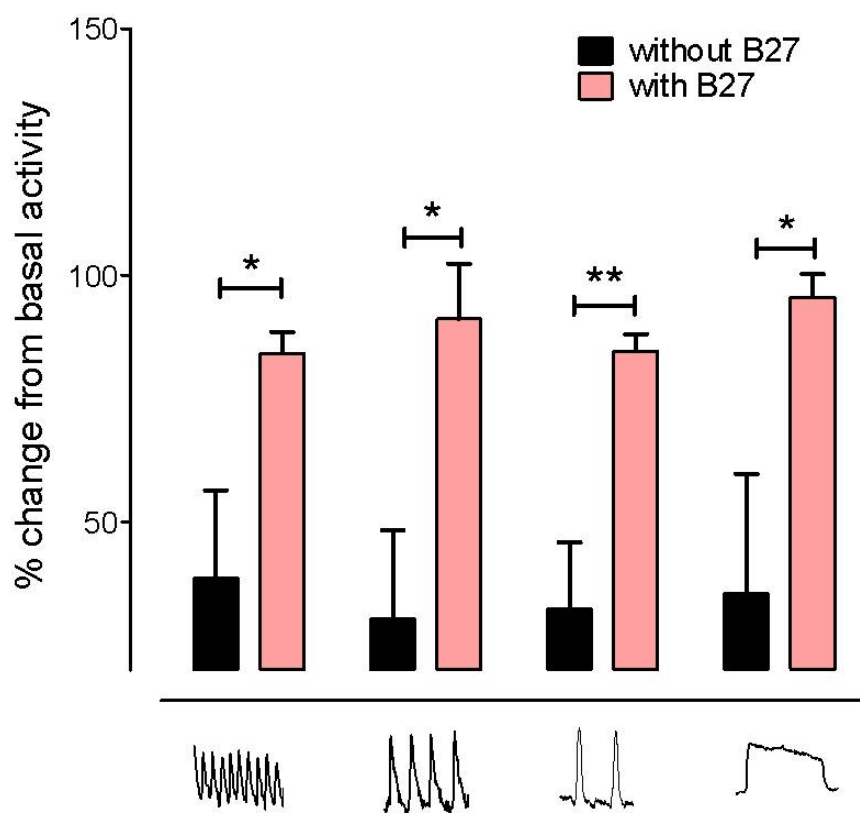
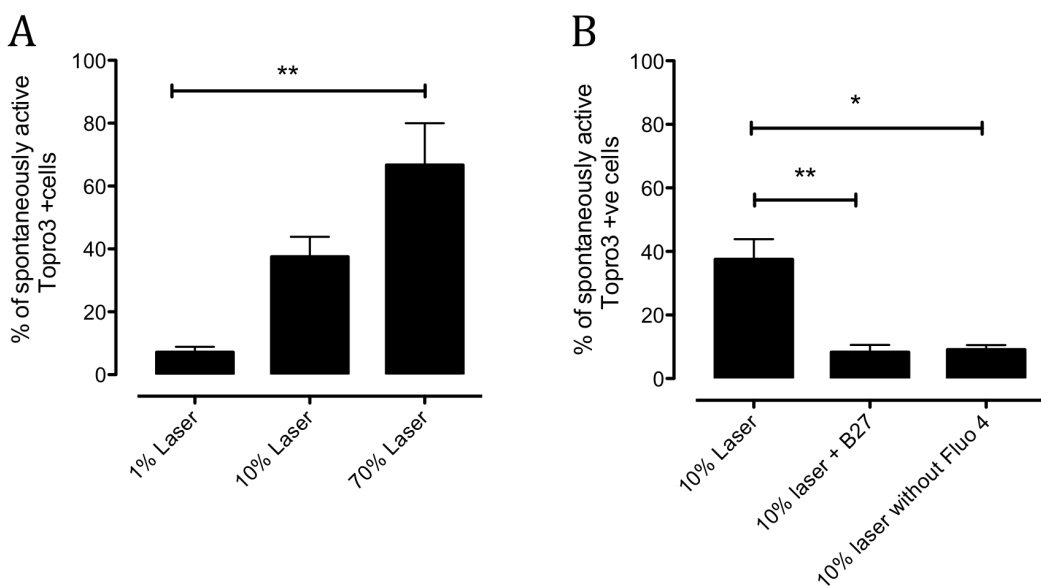


Figure 3.5

Stabilization of spontaneous calcium oscillation following addition of B-27®. Use of the anti-oxidant supplement B-27® during confocal  $\text{Ca}^{2+}$  imaging significantly maintains functional integrity of spontaneous  $[\text{Ca}^{2+}]$  activity. (\* $P>0<0.05$ , \*\* $P<0.01$ , two way ANOVA, post-hoc Bonferroni's n=3-19).

Figure 3.6



C

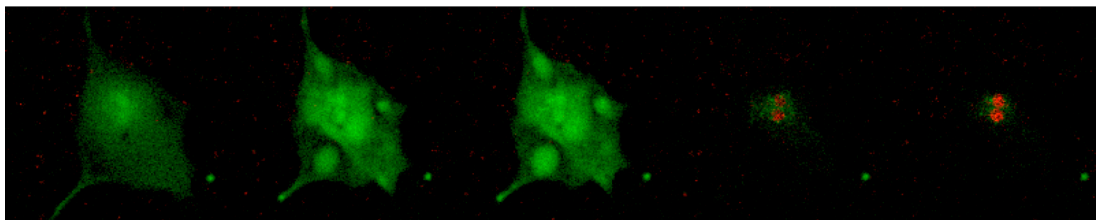


Figure 3.6

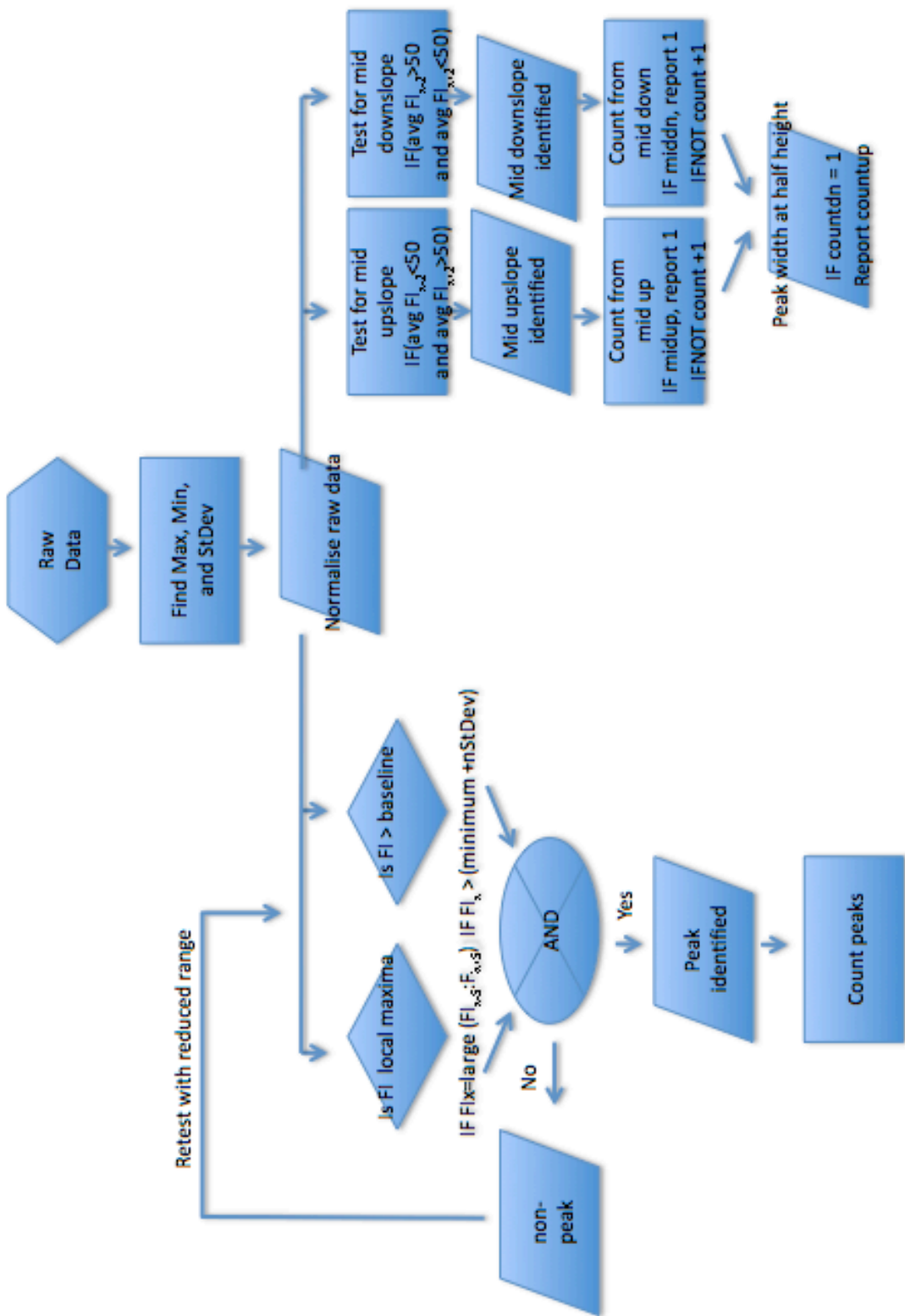
Confocal imaging and cell death. Proportion (%) of spontaneously active cells that die after 8 hours, following five minutes of continuous imaging at different laser strengths (A, \*\*P<0.01, one-way ANOVA, post-hoc Dunnett's, n=3). Proportion (%) of spontaneously active cells that die after 8 hours, following five minutes of continuous imaging with and without B27 (B, \*P<0.05, \*\*P<0.01, one-way ANOVA, post-hoc Dunnett's, n=3). Representative time lapse images of cell death following laser exposure (C).

### 3.5.2 Waveform analysis

While there are several data analysis packages available for analyzing the complex data generated from object tracking or calcium imaging we were unable to identify one that consistently extracted the key information from our raw data without first having to select the data for each individual peak. Without a semi-automated method to analyse the kinetics of total fluo-4 fluorescence intensity from each cell, the work presented in Chapter 5 would have been insurmountable. To increase the throughput and thoroughness of data analysis an excel template was constructed which identified peaks and key peak parameters (Figure 3.7). The approach used relied on normalization of fluorescence intensity data, which allows formulaic testing for maximums, minimums, mid peak (50%) values and other peak parameters. A break down of the logic is depicted as a process chart in Figure 3.8. The high variability of the waveforms identified in chapter 5 precluded the use of commercially available analysis software. The excel template I developed enabled efficient analysis of the kinetic parameters of calcium flux facilitating the thorough characterisation presented in Chapter 5.

**Figure 3.7**

This foldout is a representative example of the automated analysis template developed for analysis of calcium waveform data discussed in 3.5.2

**Figure 3.8**

Logic process chart demonstrating the approach required to identify kinetic parameters from heterogeneous calcium waveform data.

### 3.6 Conclusion

The heterogeneous cellular nature of stem cell-derived cultures provides pharmaceutical models with greater physiological context than standard *in vitro* primary or immortalized cultures. However, analysis of tissue with this heterogeneity also requires development of alternative analytical methods. To allow the work that is presented in later chapters extensive effort was required to develop and test new analytical methods for pharmacology studies of EBs, calcium imaging of spontaneously active cells from EBs, and toxicity of cardiac cells in EBs. These methodologies permitted analysis of the effects of adenosine receptor and adrenoceptor activation in Chapter 4, characterisation of spontaneously active pacemaker cells in chapter 5 and Trastuzumab toxicity in Chapter 6. As stem cell differentiation methods continue to evolve, it will be necessary for the field to continue to emphasize development and standardization of analytical methods for comparison of results. Standardization of differentiation and analytical methods should encourage adoption of stem cell derived models by the pharmaceutical industry.

**CHAPTER 4 - STEM CELL DERIVED CARDIOMYOCYTES AS MODELS OF  
ORGANOTYPIC PHARMACOLOGY: ADRENOCEPTOR AND ADENOSINE RECEPTOR  
SIGNALING**

## 4.1 Introduction

One use of stem cell derived cells and tissues is in pharmacological assays. They can be used either as specific cell populations or as a heterogeneous tissue containing a range of physiologically relevant cells, without the species differences usually associated with the use of organ bath pharmacology. To facilitate their use in pharmacological assays, the methods I developed and described in chapters 2 and 3, permit the quantification of mouse embryonic stem cell derived cardiomyocyte responses to pharmacological agents. To investigate the capacity of embryoid bodies to model pharmacological signaling pathways of varying levels of complexity, I investigated the activity of two key cardiac receptor classes discussed in chapter 1: adrenoceptors and adenosine receptors.

Adrenoceptors mediate the cardiac response to sympathetic nervous stimulation, and are both a common drug target (e.g.  $\beta$ -blockers) and implicated in many disease states including cardiac hypertrophy. Adenosine receptors have been identified as a possible therapeutic target to treat myocardial infarction. While in the mouse adrenoceptor signaling is mediated via the  $\beta_1$ AR, multiple adenosine receptor subtypes are prevalent in different parts of the myocardium and signal via different second messengers. Thus, as model targets, the adrenoceptor represents a relatively simple pathway while the adenosine receptor is more complex. The varied selectivity of available agonists and the varied complexity of receptor signaling provide a good opportunity to address the question of how useful EB models are for the investigation of pharmacology.

## 4.2 Methods

Unless detailed below, the procedures used in this chapter, including hanging drop differentiation, FACS sorting and object tracking are described in Chapters 2 and 3.

### 4.2.1 cAMP AlphaScreen assays

AlphaScreen ® cAMP Assay Kits (Perkin Elmer, Australia) were used to detect relative amounts of cAMP in Nkx2.5-eGFP FACS sorted cells following incubation with either isoprenaline or CPA. The method was adapted from the manufacturer's instructions. Briefly, 1000 cells (experimentally determined as the minimum required) were seeded into collagen-coated wells of a 96 well plate (~6000 cells/cm<sup>2</sup>) and incubated at 37°C 5% CO<sub>2</sub> to recover in conditioned media. After three days media was replaced with low serum (2%) media for 12h overnight. The following morning media was replaced with the manufacturers recommended stimulation buffer containing anti-cAMP acceptor beads and isoprenaline (0.5-5 µM) or forskolin (5 µM) and CPA (0.15-1.5 µM) for 15 minutes at 37°C. The phosphodiesterase inhibitor IBMX was recommended by the manufacturer but is an adenosine receptor antagonist so rolipram (1 µM) was used instead. Biotinylated-cAMP, streptavidin donor beads and lysis buffer were added and the incubation continued for 4 hours. Fluorescence was then measured on an Envision plate reader using the AlphaScreen filter set. The detection chemistry is outlined in Figure 4.7 A.

### 4.2.2 Statistical Analysis

The maximum response following addition of agonist was measured for contraction amplitude and frequency, expressed as change from basal activity (%). All treatments

were compared to their respective vehicle controls, none of which displayed a significant effect on the basal spontaneous rate of beating. Differences between means were tested using Student's t-test and one-way ANOVA (post-hoc Bonferroni's or Dunnett's where appropriate).  $p < 0.05$  was considered statistically significant.

## 4.3 Results

### 4.3.1 Effects of Isoprenaline, a $\beta$ -adrenoceptor agonist

Isoprenaline is a non-specific  $\beta$ -adrenoceptor agonist, which activates  $\beta_1$ ,  $\beta_2$ , and  $\beta_3$  adrenoceptors. All EBs responded to isoprenaline (10 nM-10  $\mu$ M) with an increase in frequency of beating and amplitude of contraction, which allowed calculation of EC<sub>50</sub> values of 0.4  $\mu$ M and 0.7  $\mu$ M respectively. (Figures 4.1 A-B,  $p < 0.001$ , two-way ANOVA, post-hoc Dunnett's,  $n = 8$ ). Isoprenaline elicited a maximal response at 3  $\mu$ M, comparable to forskolin for rate and contractility. This maximal response would indicate the  $\beta$ ARs were well coupled to adenylate cyclase. Preincubation with the inhibitory cAMP analogue Rp-8-Br-cAMPS reduced the isoprenaline-mediated response (Figure 4.6 D, D, \* $p < 0.05$ , one way ANOVA post-hoc tukey test,  $n=4-8$ ). The effects of isoprenaline on cAMP production were investigated in Nkx2.5-eGFP FACS sorted cells using AlphaScreen interference assay to further confirm  $\beta$ AR mediated stimulation of adenylate cyclase. Isoprenaline treatment alone caused a decrease in fluorescence intensity, indicating an increase in cAMP accumulation ( $EC_{50} = 125$  nM  $\pm$  99, Figure 4.7 B). These results demonstrate that stimulation of  $\beta$ AR receptors in the EB cause increase in contraction rate and frequency with equivalent potency. These effects are

mediated via stimulation of adenylyl cyclase and subsequent phosphorylation of PKA as supported by the cAMP assay and the Rp-8-Br-cAMPS results.

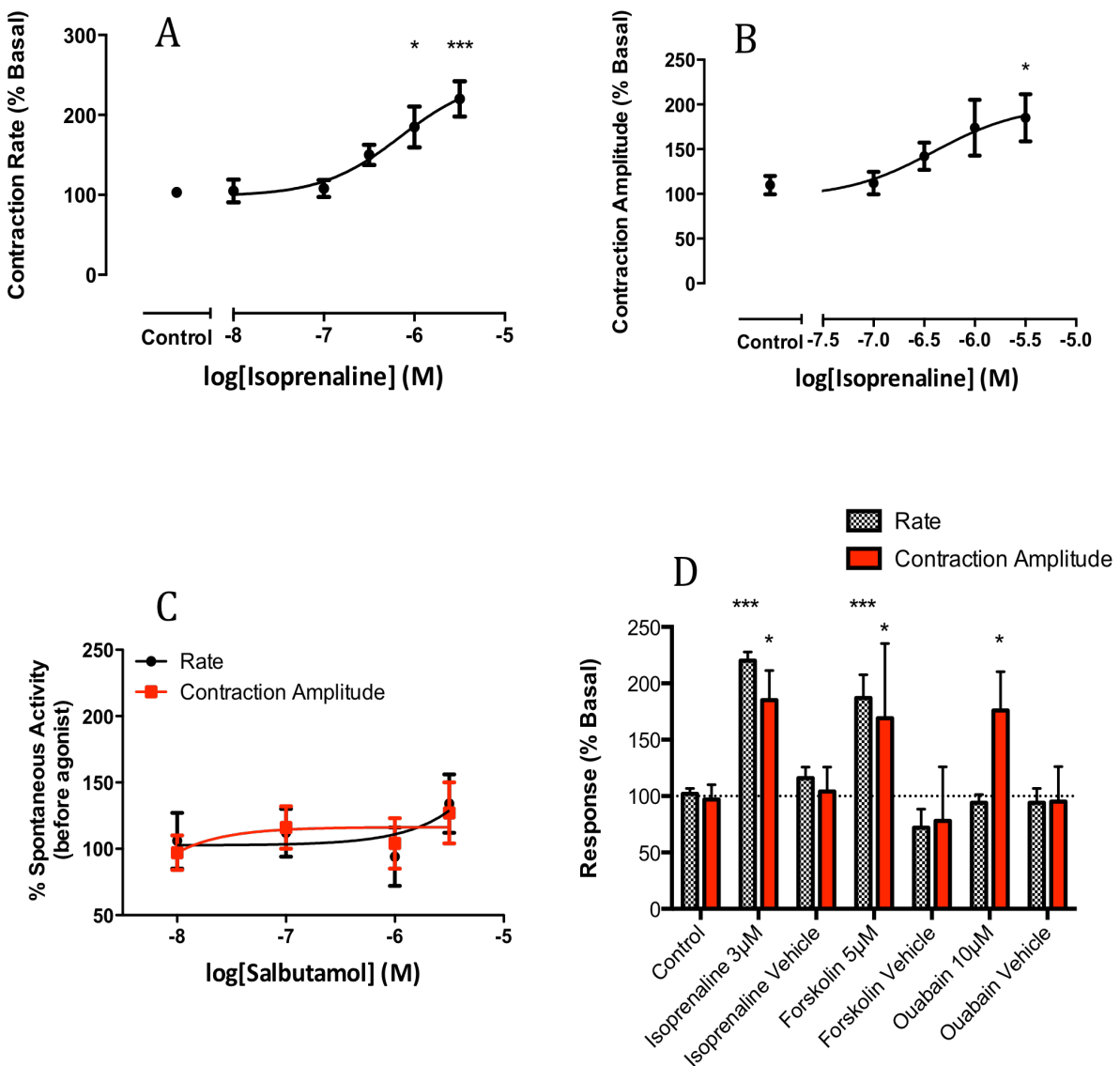
#### **4.3.2 $\beta$ -adrenoceptor subtype identification**

Salbutamol, a  $\beta_2$ -adrenoceptor selective agonist, did not affect either rate or contractility when compared with vehicle control (Figure 4.1 C, one-way ANOVA, post-hoc Bonferroni, n = 4). The selective  $\beta_1$  antagonist atenolol (1  $\mu$ M) suppressed the isoprenaline-mediated (1 and 3  $\mu$ M) increases in contraction frequency, but had no effect on the forskolin induced response (Figure 4.2 A., \*\*p < 0.01, \*\*\*p < 0.001, two way ANOVA post-hoc Dunnett's, n = 4-8). Atenolol alone caused a decrease in contraction frequency (Figure 6.2 B, \*P<0.05, two way ANOVA post-hoc Bonferroni's, n=10). The non-selective  $\beta$  blocker propanolol also caused a decrease in contraction frequency alone, but neither normetanephrine (a re-uptake inhibitor) nor the selective  $\beta_2$  antagonist ICI 118551 had any effect on contraction frequency. Propranolol (100 nM) suppressed the isoprenaline (3  $\mu$ M) mediated increase in contraction frequency, Normetanephrine and ICI 118551 (100nM) had no significant effect on isoprenaline mediated responses (Figure 6.2 C, \*p < 0.05, two way ANOVA post-hoc Dunnett's, n = 4-10). Blockade of isoprenaline-mediated responses with selective antagonists indicate that these responses are mediated by the  $\beta_1$  receptor (Figure 4.2 C). The absence of an effect in the presence of normetanephrine demonstrates insignificant extra-neuronal uptake of isoprenaline in the EB. The selective antagonist atenolol and the non-selective propanolol depressed rate in the absence of any external agonists indicating endogenous receptor activation was occurring in the EB. These findings suggest that

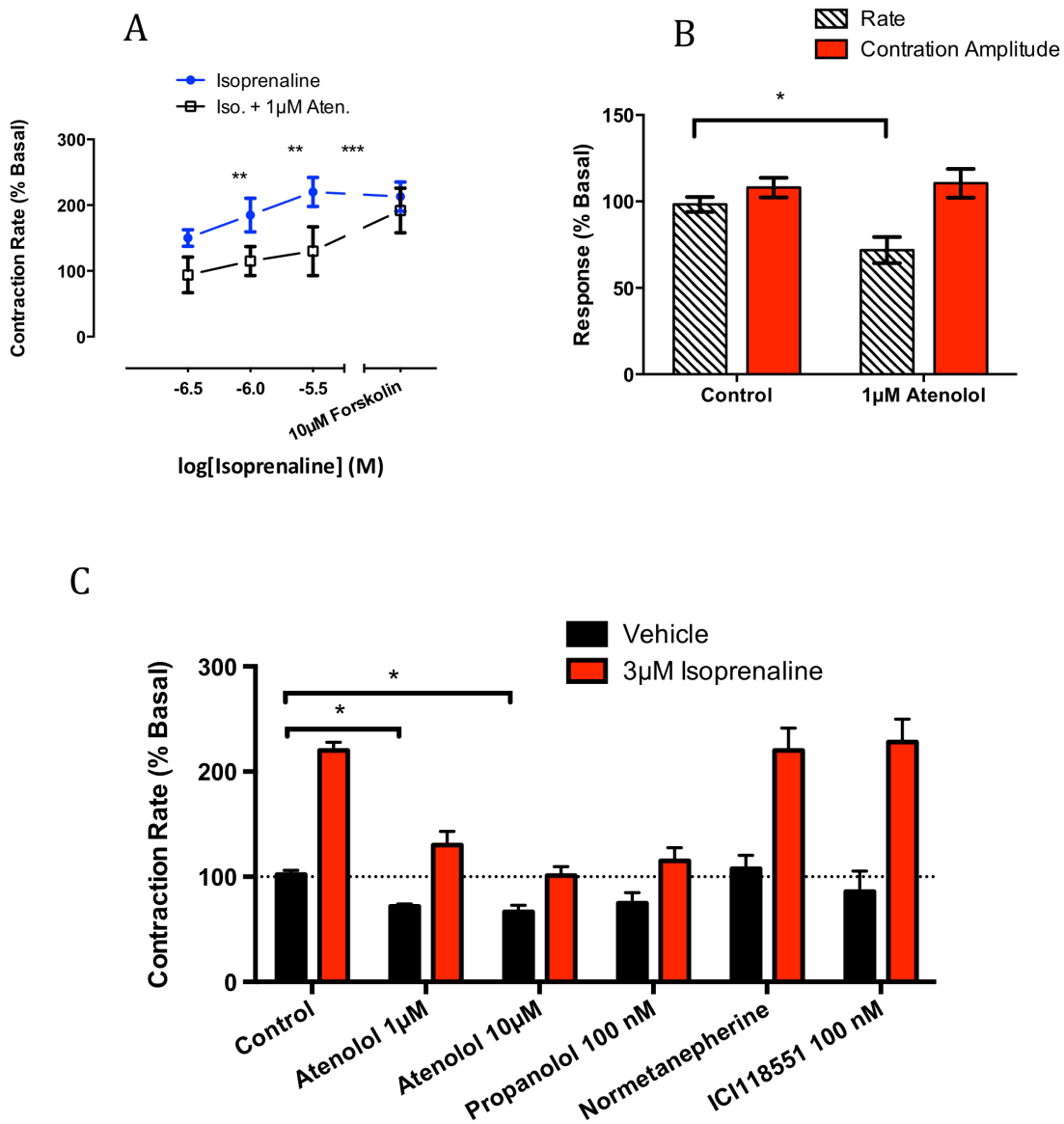
isoprenaline exerts effects via signaling through the  $\beta_1$ AR, regulating contraction frequency and rate in the EB.

#### **4.3.3 Acute $\beta$ -adrenoceptor desensitisation.**

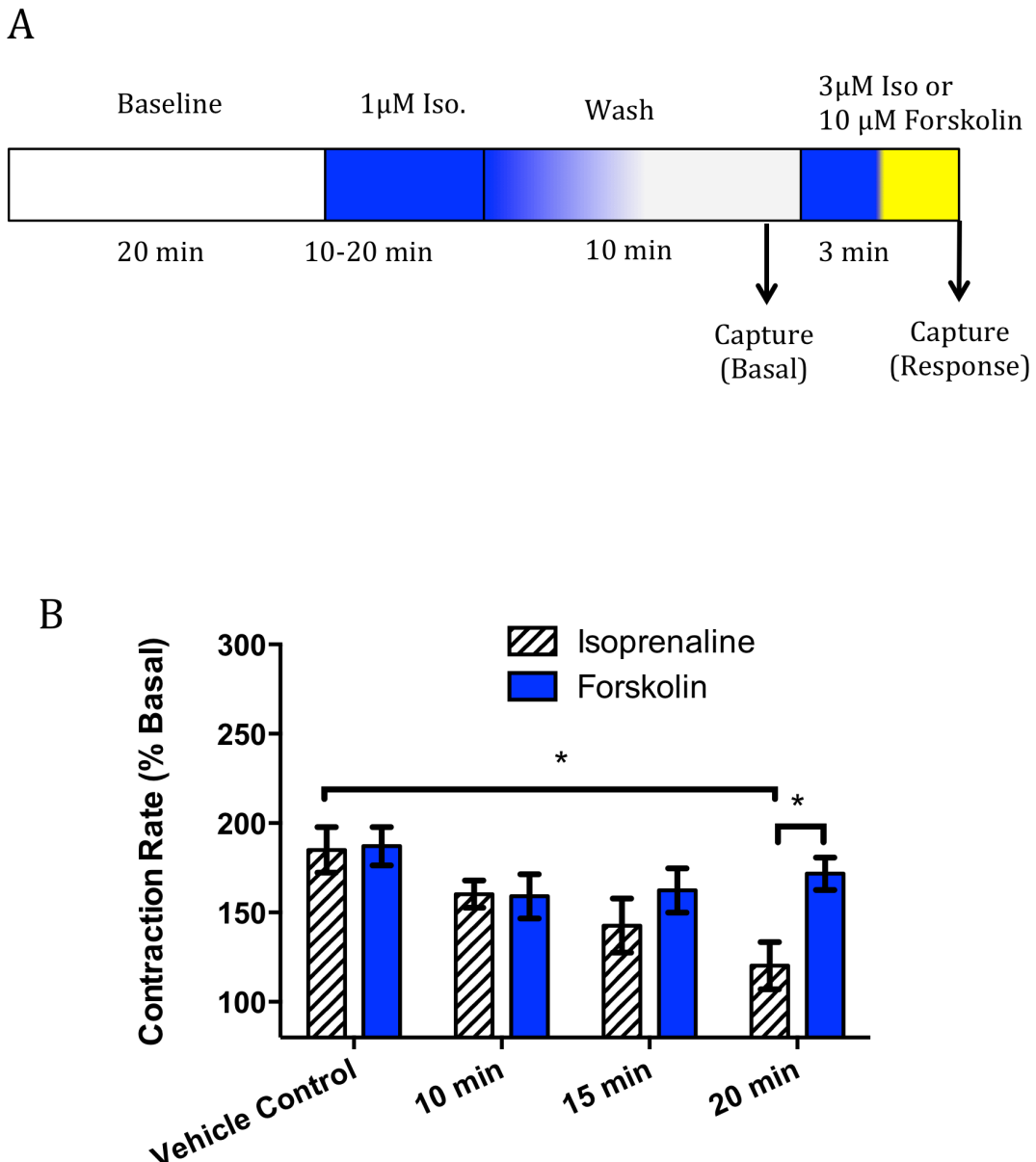
Isoprenaline (1  $\mu$ M) pretreatment for 20 minutes significantly reduced subsequent responses to isoprenaline (3  $\mu$ M), but did not affect the forskolin mediated responses. (Figure 4.3 B, two way ANOVA, post-hoc Dunnett's test, n = 4). The loss of sensitivity to subsequent isoprenaline exposure indicated receptor desensitisation; based on the timing this is likely mediated via receptor internalization.

**Figure 4.1**

EB response to Isoprenaline and Salbutamol. Mean responses ( $\pm$ SD) to the addition of Isoprenaline which increases contraction frequency and amplitude; lines represent three-parameter dose response curves fitted to the data (A & B respectively, \*\*\*P<0.001, \*P<0.05, two way ANOVA, post-hoc Dunnett's test, n=8). Mean responses ( $\pm$ SD) to the addition of Salbutamol which had no effect on either rate or contractility of EB (C, one way ANOVA, post-hoc Dunnett's test, n=4). Maximal responses to Isoprenaline, Forskolin, Ouabain and respective vehicles (D, mean  $\pm$ SD, \*\*\*P<0.001, \*P<0.05, two way ANOVA, post-hoc Dunnett's test, n=4-8)

**Figure 4.2**

EB response to Isoprenaline with and without antagonists. Mean responses to the addition of Isoprenaline with and without Atenolol (A, \*\*P<0.01, \*\*\*P<0.001, two way ANOVA post-hoc Dunnett's, n=4-8). Mean responses to Atenolol (B, \*P<0.05, two way ANOVA post-hoc Bonferroni's, n=10). Mean changes in contraction rate following addition of isoprenaline in the presence and absence of antagonists (C, \*P<0.05, two way ANOVA post-hoc Dunnett's, n=4-10)

**Figure 4.3**

Effect of isoprenaline pretreatment on desensitisation to isoprenaline or forskolin. Panel A shows a diagram depicting experimental process and timing. Mean responses to the addition of Isoprenaline or (following pretreatment and wash) which increases contraction frequency depending on pretreatment, and forskolin which does not; (B, two way ANOVA, post -hoc Dunnett's test, n=4).

#### **4.3.4 Effects of NECA, a non-selective adenosine receptor agonist.**

N-ethylcarboxamidoadenosine (NECA) is a non-selective adenosine receptor agonist that activates A<sub>1</sub>, A<sub>2A</sub> and A<sub>3</sub> adenosine receptors with relatively equal affinity. Furthermore, NECA also activates A<sub>2B</sub> receptors but with much lower affinity. NECA (10 μM) induced a decrease in frequency and amplitude of contraction in EBs (Figure 4.4 A, \*p < 0.05, \*\*\*p < 0.001, one-way ANOVA, post-hoc Dunnett's, n = 4-6). At higher concentrations (100 μM), the inhibitory effects of NECA were not apparent. This was presumably due to opposing responses mediated via different receptor subtypes that have different sensitivity to NECA. In the presence of the selective A<sub>1</sub> antagonist DPCPX (100 nM), NECA (1 μM) caused an increase in rate, followed by a NECA concentration-dependent decrease in rate (Figure 4.3B). This indicates that the A<sub>1</sub> subtype is present in the EB and mediates a negative chronotropic response. In the presence of the selective A<sub>2A</sub> antagonist, ZM 241385 (25 nM) NECA had no effect until 100 μM, at which point it inhibited all spontaneous beating. This suggests the A<sub>2A</sub> receptor mediated a positive chronotropic response. Adenosine receptor activation displayed mixed effects in the presence of selective antagonists, indicative that receptor subtypes mediated opposing responses in EBs.

#### **4.3.5 Effects of CPA, a selective adenosine receptor A<sub>1</sub> agonist**

CPA (10 nM-100 μM) induced a decrease in frequency and amplitude of contraction in EBs with EC<sub>50</sub> values of 34 nM and 3.2 μM respectively. (Figure 4.4 A, p < 0.001, two-way ANOVA, post-hoc Dunnett's, n = 4-6). Note the large difference between the EC<sub>50</sub> values determined using the different parameters.

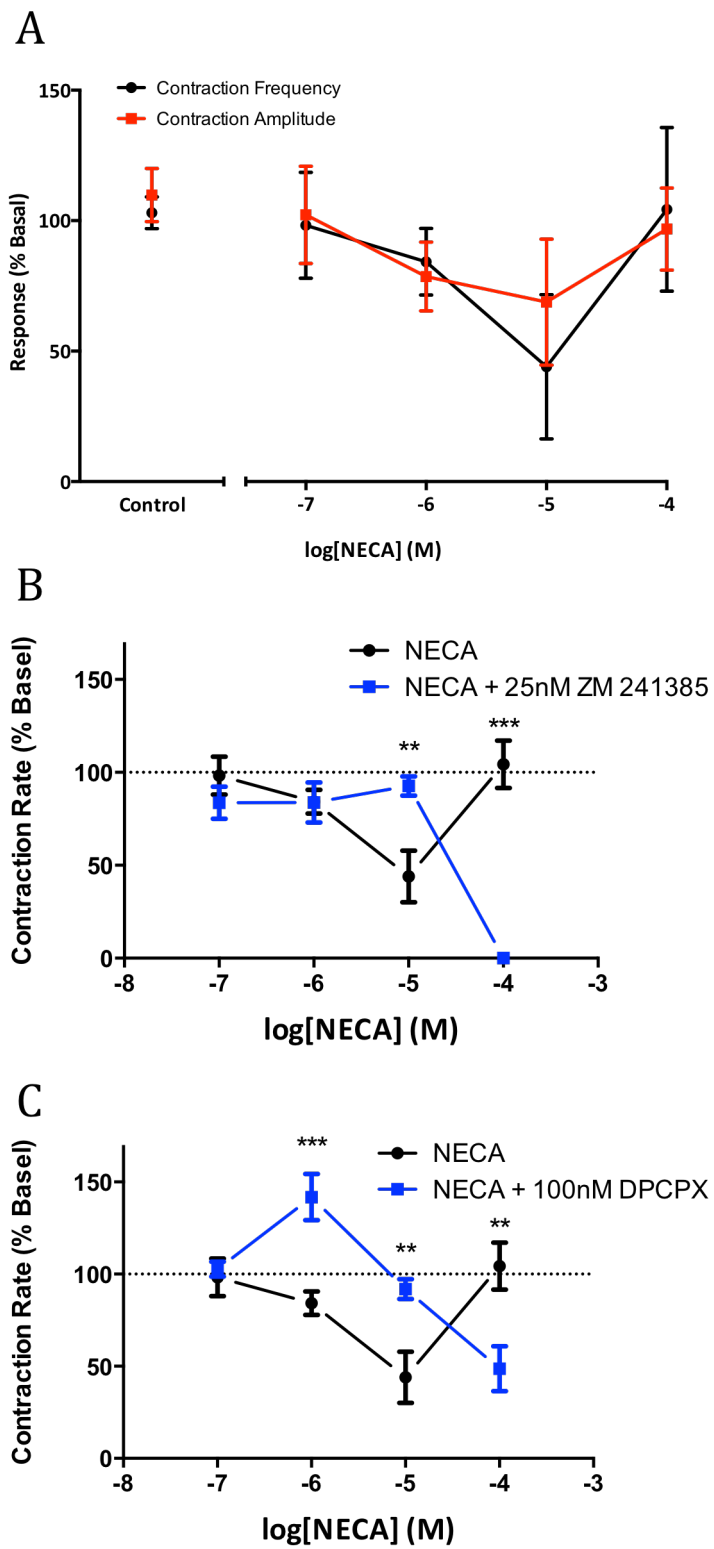
The effects of CPA on cAMP production were investigated in Nkx2.5-eGFP FACS sorted cells using AlphaScreen interference assay. CPA had minimal effect on cAMP levels in cells without pretreatment with forskolin (data not shown). Presumably, AC activity was too low (and as a result levels of cAMP) without exogenous stimulation to show a reduction of cAMP using AlphaScreen assay. There are two reasons why this may not affect results in the EB. Firstly, the pacemaker cells that drive rate (which was the more sensitive parameter to CPA) are likely to be a small fraction of the sorted cells, thus this plate-based assay would be weighted towards the myocyte populations. Secondly, the apparent  $\beta$ AR receptor activity reported in 4.3.2 could be explained by endogenous catecholamines, which may not be present in this sorted population thus requiring exogenous stimulation. CPA treatment simultaneously with forskolin stimulation caused an increase in fluorescence intensity, indicating a decrease in cAMP ( $EC_{50} = 111 \text{ nM} \pm 49$ ).

Preincubation with Sp-8-Br-cAMPS non-significantly reduced the CPA mediated response. Based on the experimental power of this study, calculations indicate a need for 30 repetitions to confirm a statistical significance of the effect of Sp-8-Br-cAMPS on CPA response. The A<sub>1</sub> adenosine receptor agonist CPA mediated a decrease in contraction frequency and at higher concentrations a decrease in contraction amplitude, in EBs. Results from cAMP assays of FACS enriched populations indicate the A<sub>1</sub> adenosine receptor to be inhibiting adenylate cyclase, reducing cAMP levels; but only when AC activity was exogenously stimulated. While the PKA activator Sp-8-Br-cAMPS

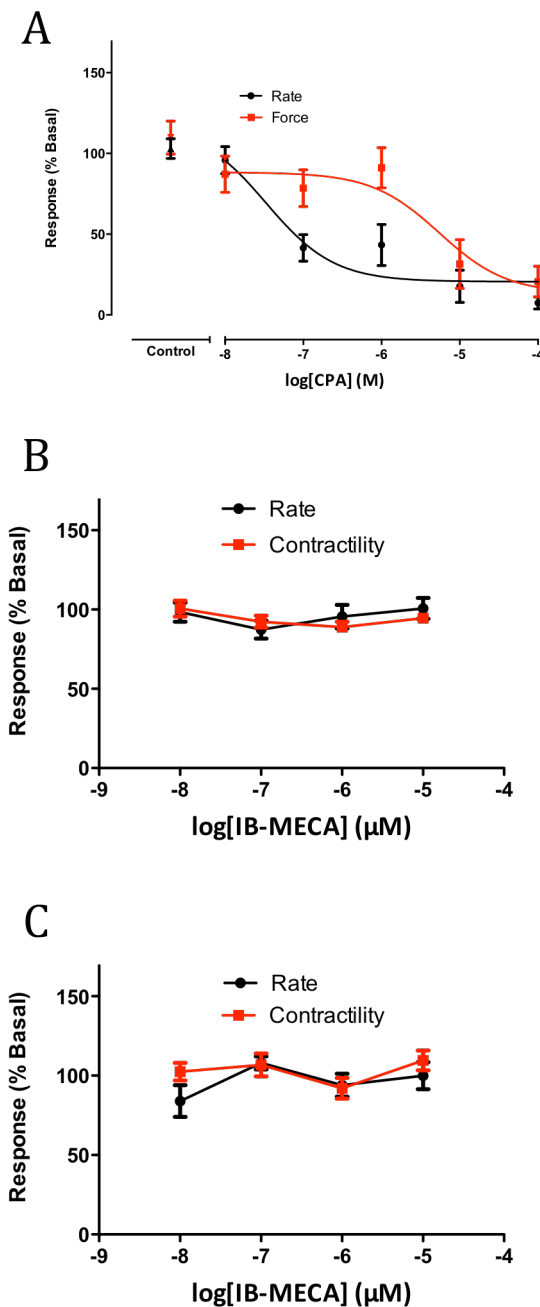
did not significantly reduce the effects of CPA, the results from this experiment do not disprove the hypothesis that CPA is acting via the A<sub>1</sub> adenosine receptor, inhibiting AC, resulting in decreased levels of cAMP and subsequent PKA phosphorylation.

#### **4.3.6 Effects of IB-MECA, a selective A<sub>3</sub> agonist**

IB-MECA, the selective A<sub>3</sub> agonist did not affect either rate or contractility (Figure 4.4 B; one-way ANOVA, post-hoc Dunnett's, n = 4). The selective A<sub>3</sub> antagonist MRS-1523 (100 nM) did not affect either rate or contractility in the presence or absence of IB-MECA 10 μM (Figure 4.4 C; one-way ANOVA, post-hoc Dunnett's, n = 4). These findings show that the A<sub>3</sub> receptor did not demonstrate direct modulation of any functional responses in the EB.

**Figure 4.4**

NECA response in the presence and absence of DPCPX (100 nM) and ZM241385 (25 nM). Mean responses to the addition of NECA which decreases contraction amplitude and frequency (A, two way ANOVA, post-hoc Dunnett's test, n=8). Mean responses to the addition of NECA in the presence of the A<sub>2A</sub> antagonist ZM 241385 (B, \*\*P<0.01, \*\*\*\*P<0.0001, two way ANOVA, post-hoc Dunnett's test, n=4). Mean responses to the addition of NECA in the presence of the A<sub>1</sub> antagonist DPCPX (C, \*\*P<0.01, \*\*\*P<0.001, two way ANOVA, post-hoc Dunnett's test, n=4).

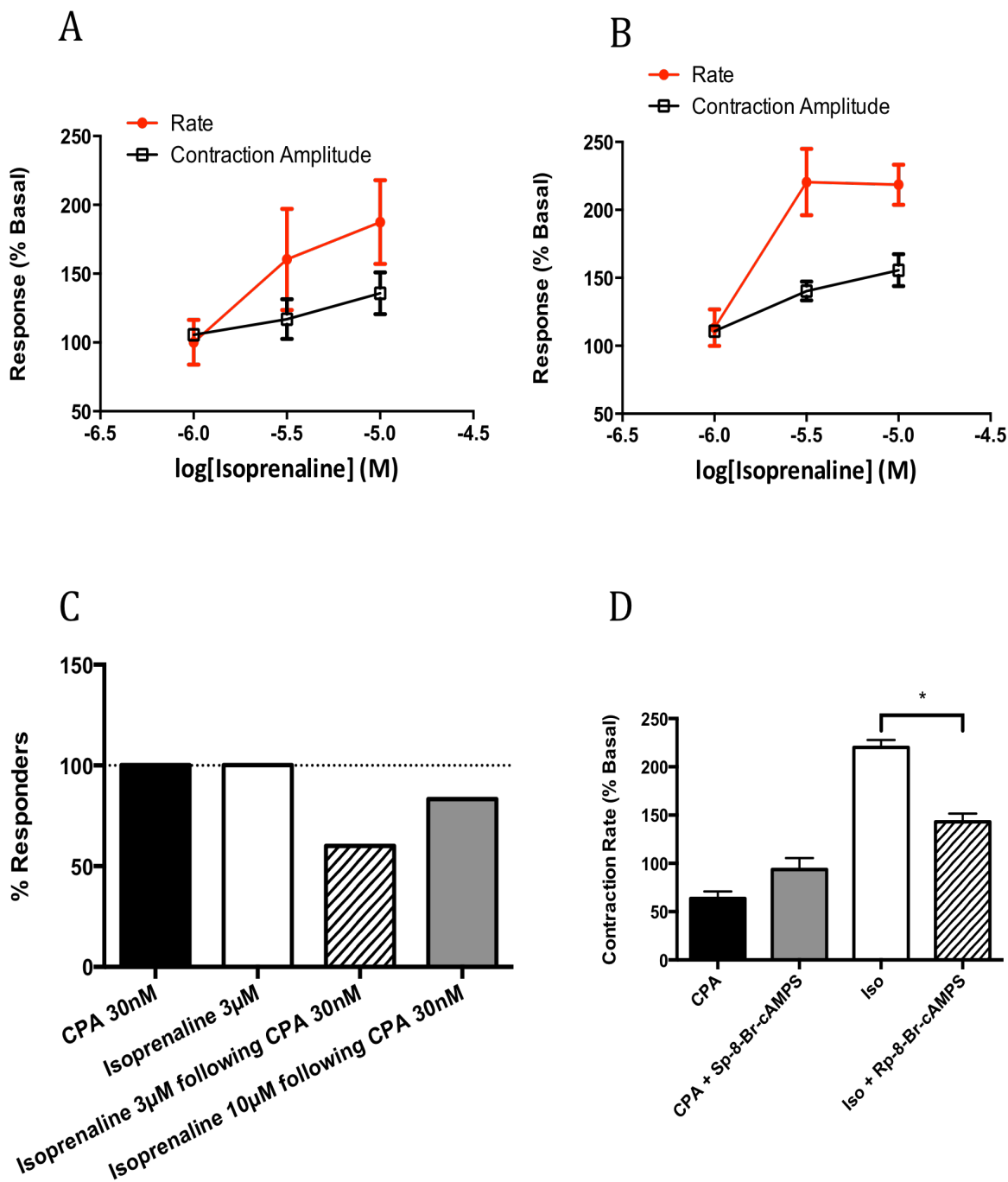
**Figure 4.5**

EB response to the selective A<sub>1</sub> adenosine receptor agonist CPA. Mean responses (±SEM) to the addition of CPA which decreases contraction frequency and amplitude; lines represent three-parameter dose response curves fitted to the data (A, n = 8).

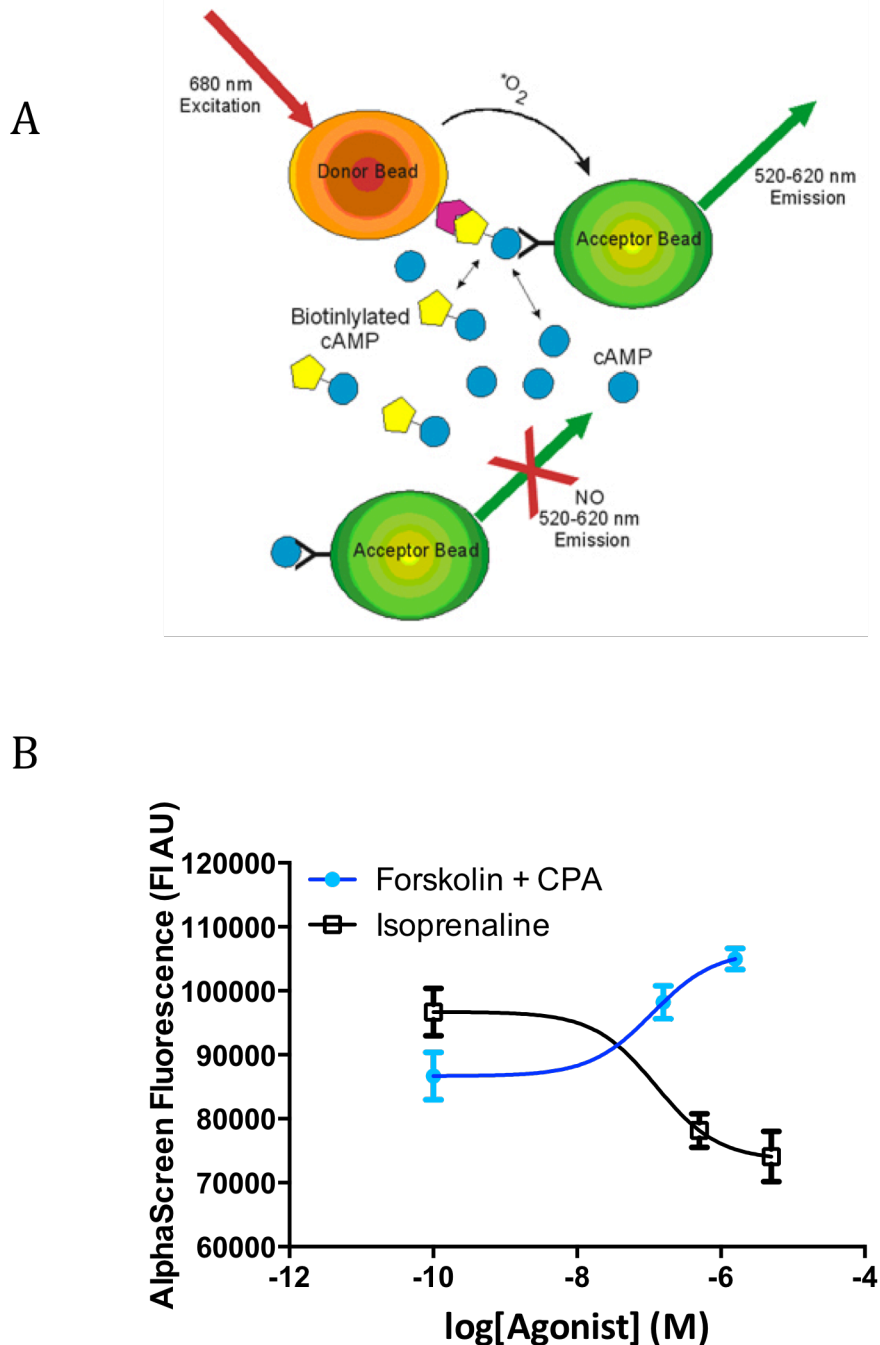
Mean responses to the selective A<sub>3</sub> adenosine receptor agonist IB-MECA in the absence (B) and presence (C) of the selective A<sub>3</sub> antagonist MRS-1523 (no significant responses, two way ANOVA post-hoc Bonferroni's, n = 4).

#### 4.3.7 Effects of combined addition of isoprenaline and CPA

Adenosine attenuates the affects of adrenergic stimulation in ventricular myocytes(Neumann et al. 1995). To investigate the capacity of EBs to model the effect of A<sub>1</sub> adenosine receptor activation on βAR signaling I treated EBs with CPA and isoprenaline simultaneously. Treatment with CPA or isoprenaline alone resulted in consistent responses by 100% of EBs. In contrast, simultaneous addition of CPA and isoprenaline resulted in some EBs that showed no response. Addition of CPA (30 nM) suppressed the isoprenaline-mediated (3 μM) increase in contraction frequency in 62% of embryoid bodies (Figure 4.6 A – C, n = 4-8). Increasing the isoprenaline concentration (10 μM) increased the proportion of EBs that responded to 85% (n = 7). Given EBs responded uniformly to each agonist individually, receptor density is unlikely to be responsible for the lack of response to multiple agonists. A more likely explanation may be variable second messenger coupling between the adenosine receptor and adrenoreceptor. The coupling of adenosine receptors and adrenoceptors has been observed to be different between ventricular and atrial cardiac tissue. It is also known that EBs tend to differentiate toward either predominant ventricular or atrial phenotype. The result of this may influence signaling in the presence of both ligands resulting in EBs that showed no response to isoprenaline and CPA treatment(Werry et al. 2003; Hernandez et al. 2012; Musser et al. 1993). Further characterisation of the dominant phenotypes generated in individual EBs and the resultant receptor expression/coupling may yield insight into the complex pharmacology of adenosine.

**Figure 4.6**

Effects of CPA on subsequent isoprenaline responses. Mean responses  $\pm$  SEM to the addition of Isoprenaline following CPA (30 nM) (A, n=6) and with non-responders removed (B, n=4). Proportion of non-responders to CPA, and Isoprenaline before and after CPA (C, n=4-8). Effect of incubation with Sp- or Rp-8-Br-cAMPS (PKA activator or inhibitor respectively) on the CPA (30nM) and Isoprenaline (3  $\mu\text{M}$ ) respectively (D, \*P<0.05, one way ANOVA post-hoc tukey test, n=4-8)

**Figure 4.7**

cAMP AlphaScreen on sorted Nkx2.5-eGFP+ve cells. AlphaScreen detection chemistry; cAMP in sample and biotinylated cAMP compete for binding to acceptor beads, the biotinylated cAMP can then bind the streptavidin bound donor beads and emit fluorescence which is inversely proportional to the concentration of cAMP (A). Mean fluorescence  $\pm$  SEM in response to Isoprenaline and CPA (in the presence of 5 $\mu$ M Forskolin), lines represent three-parameter dose response curve fitted to the data (B, n = 4).

## 4.4 Discussion

Utilising the cardiac differentiation protocol optimized in Chapter 3, spontaneously beating embryoid bodies were generated and their responses to signaling through the  $\beta$ AR and adenosine receptor pathways was investigated. Videomorphometry was used to measure frequency and amplitude of contraction. As discussed in chapter 3, contraction amplitude is a surrogate measure of contractility as determined from the responses of the ionotropic drug ouabain. Frequency of contraction and drug-induced changes to spontaneous rate are likely mediated via pacemaker and other cells of the conduction system within the EB. In contrast, contraction amplitude or contractility is likely to be principally determined by the myocytes and contractile cells within the EB, this suggests that the most appropriate *in vivo* parameter for comparison of EB contraction amplitude would be force of contractility. Measuring both contraction frequency and contraction amplitude, we have the potential to observe changes mediated via a range of cell types controlling the contractile function within the EB.

$\beta$ -Adrenoceptor activation by isoprenaline induced changes of frequency and amplitude of contraction in EBs. Fitted to a standard pharmacological three-parameter dose response curve, the EC<sub>50</sub> values for frequency and amplitude calculated were 0.4  $\mu$ M and 0.7  $\mu$ M respectively. These values are an order of magnitude higher than previously reported for mESC derived cardiac cells ((Neumann et al. 1995; Ali et al. 2004; Werry et al. 2003; Xi et al. 2010; Hernandez et al. 2012; Musser et al. 1993)), or primary tissue ((Hawthorn et al. 1985; Rub et al. 1981)). In contrast, the EC<sub>50</sub> values determined using the cAMP assay were much closer to previously published values indicating this

difference may be due to the analytical system rather than the cells(Ali et al. 2004).

Extraneous to analytical issues there is a possibility that the EBs used in this study were less sensitive than previously reported studies. Without molecular characterisation of  $\beta$ AR function, which was outside the scope of this study, and access to tissue used in other studies, there is no obvious explanation for the discrepancy between the literature and experimentally determined values presented here.

Blockade of  $\beta_1$ AR by the selective antagonist atenolol inhibited the isoprenaline-induced increase in rate which supports previous work indicating a  $\beta_1$ AR-mediated effect of isoprenaline on mES EBs(Ali et al. 2004). *In vivo* knockout of the  $\beta_1$  subtype is sufficient to attenuate stress induced elevations of heart rate in mice, providing evidence the  $\beta_1$ AR subtype is essential for noradrenalin and adrenaline mediated functional cardiac effects *in vivo*. (Rohrer et al. 1998). The most surprising result from my studies of EBs was that treatment with  $\beta$ AR antagonists decreased spontaneous contraction rate in the absence of exogenous catecholamines. This effect may be due to antagonism of endogenous catecholamines present in the culture. Physiologically, most catecholamine synthesis occurs in sympathetic nerves and the adrenal gland. However, there is evidence that many of the enzymes responsible for the production of adrenaline are present in the developing heart as well as stem cell cultures differentiating towards a cardiac fate(Ali et al. 2004; Xia et al. 2012; SPASOJEVIC et al. 2011; Ebert et al. 2004). To investigate if the effect of atenolol on spontaneous contractility may be due to endogenous catecholamine production in EBs, I used chemical staining employing sucrose-phosphate-glyoxylic acid (SPG) to directly quantify catecholamines. However,

catecholamines could not be detected in EBs (results not shown). SPG staining is utilized to identify nerve terminals where catecholamines are highly concentrated in vesicles but may not be sensitive enough to detect extra-neuronal catecholamine synthesis(Guidry 1999; Himura et al. 1993). Testing the hypothesis that EB cultures have extra-neuronal endogenous catecholamine synthesis may require HPLC with electrochemical or mass spectrometer detection to quantify very low neurotransmitter levels. Alternatively, endogenous catecholamines may be identified by treatment with a uptake inhibitor, which should show agonist-like behaviour in the presence of endogenous catecholamines, assuming that the extracellular concentrations are being controlled via uptake and not metabolism or dilution.

Alternatively,  $\beta$ AR antagonist induced decreases in the rate of spontaneous contraction may be due to inverse agonism, which is dependent on some level of constitutive receptor activity in the absence of ligand. To investigate inverse agonism of  $\beta$ -blockers physiologically, the vesicular monoamine transporter (VMAT) inhibitor reserpine has been used(Varma et al. 1999). VMAT actively transports catecholamines from the cytoplasm of nerves into vesicles where they are protected from degradation by monoamine oxidases and catechol o methyl transferases. Thus, reserpine treatment results in catecholamine metabolism and neuronal depletion. If this pathway exists in the EB, depletion of catecholamines should result in a decrease in contractile rate much like atenolol. Unfortunately, the use of Reserpine to test this hypothesis may not be straightforward due to the scarcity of knowledge regarding mechanisms of catecholamine handling and metabolism in the EB. Further investigation to determine

which mechanism is responsible, and whether  $\beta$ -blockers modulate spontaneous contractility in human derived tissues is suggested for future studies. Regardless of the mechanism of  $\beta$ -blocker modulation of contraction frequency, these studies suggest that EBs are an appropriate model to study pharmacology, toxicology or physiology of  $\beta$ AR signaling.

Selective  $\beta_2$  activation using salbutamol had no effect on the spontaneous activity of embryoid bodies, even at relatively high agonist concentrations. This concurs with work in both mESC derived cardiac cells and mice which shows that activation of the  $\beta_2$ AR does not cause a significant increase in frequency or force of contraction (Devic et al. 2001) (Ali et al. 2004). The selective antagonist ICI 118551 did not attenuate the isoprenaline-mediated effects in the EB. In combination with the salbutamol data, this provides strong evidence for no direct functional effect of the  $\beta_2$ AR.

While seemingly not functionally relevant to contractile rate and amplitude in the mouse EB the  $\beta_2$ AR is known to modulate rate and contractility in human cardiac tissue and is implicated in several disease states, including heart failure(Brodde et al. 2001). Specifically, the human  $\beta_2$ AR mediates an increase in cAMP in the myocardium that does not occur in mouse tissues (Kaumann et al. 1996) (Kaumann et al. 1999) (Sabri et al. 2000). To date many studies have investigated the effects of isoprenaline on human pluripotent cell derived cardiac cultures, assessing function using videomorphometry, electrophysiology and microscopy. However, none of these studies has looked at the receptor subtypes responsible or used selective agonists to control for this(Földes et al.

2011; Braam et al. 2010) (Pillekamp et al. 2012; Khan et al. 2012). At a molecular level the  $\beta_2$ AR can couple to  $G_s$  and  $G_i$  second messenger proteins(Xiao 2001). It is possible that differences between mouse and human  $\beta_2$ AR responses are due to receptor second messenger coupling rather than receptor expression (Sabri et al. 2000). The capacity to generate human and mouse cardiac tissue in EBs for *in vitro* studies, coupled with comparison of these results to *in vivo* mouse studies may provide unprecedented insight in the mechanisms underlying  $\beta$ AR signaling, particularly in pathophysiological states. ES cell derived models provide a novel tool to dissect out subtle nuances in tissue with physiologically relevant signaling pathways.

The desensitisation of  $\beta$ -adrenoceptors plays an important role in regulation of receptor signaling and has been implicated in multiple cardiac disease states (Lefkowitz et al. 2000; Post et al. 1999; Harding et al. 1994). Desensitisation generally refers to the loss of sensitivity of a tissue to adrenergic stimulation, generally mediated by altered second messenger coupling, receptor internalization, or decreased receptor expression occurring on short (seconds), intermediate (minutes) and long (hours) time intervals respectively. Receptor internalization following chronic exposure to excessive isoprenaline has been shown to be cardioprotective presumably by preventing excess intracellular calcium concentrations for prolonged periods of time (Tan et al. 1992). However, recent molecular pharmacology findings indicate that internalized receptors can have the potential for further downstream signaling following trafficking to endosomes, which can then lead to ERK signaling resulting in both acute (functional) and chronic (transcriptional) effects (Murphy et al. 2008). The timing of desensitisation

observed in this study would indicate acute internalization occurs in EBs in preference to other delayed phenomena. Given the increasing interest in receptor recycling and the signalosome identified using heterologous expression systems, it would be interesting to see if that extends to the EB. If so, human EBs may be a useful tool to further characterize the importance of the signalosome and signal bias in physiological relevant *in vitro* tissues. Overall, these findings suggest that EBs are a good model of well characterised pharmacological signaling.

To explore the capacity of EBs to model responses to more complex pharmacological signaling we investigated the effects of the non-selective adenosine receptor agonist NECA on EB function. EB contraction frequency and amplitude responses to NECA displayed an unusual concentration dependence on NECA indicating complicated signaling likely mediated via the different adenosine receptor subtypes. Considering the selective A<sub>1</sub> agonist CPA decreased spontaneous rate while no response was measured following IB-MECA (an A<sub>3</sub> agonist) addition, the assumption was that NECA was acting via the A<sub>2A</sub> or A<sub>2B</sub> subtypes mediating an opposing increase in rate. Antagonism of the A<sub>1</sub> effects of NECA using DPCPX had the expected effect, resulting in an increase in rate at low concentrations followed by a decrease in rate, presumably as the CPA out competed the antagonist. Antagonism of the A<sub>2A</sub> effects of NECA using ZM 241385 resulted in a loss of contraction at the highest concentration of NECA (100 µM) indicating that the A<sub>2A</sub> was opposing the A<sub>1</sub> mediated response. However, that does not explain the effect of A<sub>2A</sub> antagonism on 10 µM NECA, which without antagonism caused a decrease in rate. There are several possible explanations for this, principle among them that the A<sub>2B</sub> subtype is present in EBs and causing mixed functional effects.

Unfortunately, this could not be tested during this study, as there was limited commercial availability of a selective A<sub>2B</sub> agonist or antagonist. The other likely possibility is that considerable receptor coupling interaction between the subtypes occurred resulting in more complex signaling that could not be deconvoluted with the available ligands. While not easy to interpret, these results concur with what is known about *in vivo* responses to A<sub>1</sub> stimulation and likely G-protein coupling of A<sub>2A</sub> receptors(Shryock & Belardinelli 1997; McIntire 2001; Liang & Haltiwanger 1995). Without selective agonists and antagonists EBs are not a good tool for characterizing complicated unknown pharmacology. However, it is foreseeable that by measuring rate and contractility changes of the EB in response to unknown compounds, prediction of intended and unintended cardiac activities could be measured in an indiscriminant model with both physiological relevance and human tissue. To rephrase, drug candidates that have clinically limiting cardiac effects may be identified in human EBs earlier than current preclinical models.

The selective A<sub>1</sub> adenosine receptor agonist CPA displayed a difference in potency with respect to its effects on rate versus contractility. A<sub>1</sub> activation was two orders of magnitude more effective at reducing rate than contractility. This is in contrast to the results for isoprenaline where the EC<sub>50</sub> values were comparable. Adenosine has been reported to have four major cardiac activities outside of its vasoactivity: depression of nodal (pacemaker) activity, reduction of atrial contractility, negative dromotropy (the slowing of conduction speeds), and finally a depression in the response to catecholamines (sometimes referred to as anti-adrenergic activity)(Belardinelli et al. 1989). Of these cardiac effects, three are related to pacemaker function and mediated

through the A<sub>1</sub> adenosine receptor. Given that frequency of contraction is governed by spontaneous pacemaker activity, it is not surprising that the frequency of contraction of EBs is more sensitive to CPA than the contractility. This suggests that changes in rate of the EB are governed by a restricted population of pacemaker-like cells within the EB. The question remains as to whether the difference in potency is due to differences in receptor density in the different cells types, receptor coupling, or other signaling mechanisms. Further investigation of the pharmacology of pacemaker populations within the EB is required to address this question. Initial studies in this direction are discussed further in Chapter 5.

The role of the A<sub>3</sub> adenosine receptor in mediating protection from ischemia reperfusion injury promises a novel therapy for the treatment of myocardial infarction(Kin et al. 2005). The A<sub>3</sub> receptor appears to have little cardiac function outside minimization of reperfusion injury(Borea et al. 2009). To confirm the A<sub>3</sub> subtype has negligible effects on EB function the responses to the selective agonist IB-MECA were measured in the presence and absence of the selective inhibitor MRS. Neither agonist nor antagonist had any effect at the concentrations tested, confirming literature reports from primary tissue and supporting the use of the EB as a model of pharmacology to investigate cardiac pharmacology(Borea et al. 2009; Shryock & Belardinelli 1997).

In an EB model where receptor expression and density are intrinsically governed, selective agonists are essential to investigating the pharmacological function of different receptor subtypes. The biggest hurdle to elucidating the function of different

adenosine receptor subtypes was the lack of commercially available, selective, and potent A<sub>2A</sub> and A<sub>2B</sub> agonists. For this study the only commercially available compound that displayed suitable selectivity between the A<sub>2</sub> subtypes was CGS 21680. However, this compound has significant A<sub>1</sub> agonism, which rendered the compound useless based on previously observed A<sub>1</sub> mediated effects (see 4.3.5). Development of highly selective agonists will be essential to fully dissect the mixed pharmacology of the adenosine receptor subtypes in tissues with mixed subtype expression and function. Given the importance of adenosine receptor signaling in the pathophysiology of myocardial infarction, understanding the unique function of each receptor subtype may be integral to developing a clinically useful treatment. In that context, EBs may be a useful model to evaluate compounds with mixed subtype affinity in a physiologically relevant setting.

Outside of prevention of reperfusion injury, one main role of adenosine is attenuation of the effects of adrenergic stimulation. In ventricular myocytes this largely occurs due to overlap of the stimulatory βAR and inhibitory A<sub>1</sub> adenosine receptor signaling leading to the same phosphorylation targets (Neumann et al. 1995). Given the homogenous responses signaling through either βAR or adenosine receptors alone, the mixed response to simultaneous stimulation of both pathways in EBs indicated a complicated interaction of the two pathways. Given the complexity of the embryoid body preparation, elucidation of the mechanism driving these mixed responses is difficult. It has previously been shown that while embryoid bodies differentiate to all cells of the working myocardium, the ventricular phenotype tends to dominate, although the atrial

phenotype is also present, which may effect receptor density and coupling(Kolossov et al. 2005). Crosstalk between GPCRs such as the adrenoceptor and adenosine receptor is known to occur, and effect cellular response and function(Werry et al. 2003; Franco 2000; Rousell et al. 1996). The anti-adrenergic effects mediated via adenosine receptors are dependent on adenosine receptor and adrenoceptor second messenger coupling ((Koglin et al. 1994)). It is possible that these receptors couple differently in the different cell types of the myocardium, although to date there has been no published evidence to support this hypothesis. Better understanding the role the adenosine receptor plays in modulation of adrenergic signaling and cardiac function may facilitate the design of better drugs to treat ischemic reperfusion injury.

Because of their heterogeneous nature, use of EBs in high-throughput plate based assays is limited without careful cell purification. Measurement of the second messenger signaling of cardiomyocytes from the EB without enrichment was not suited to plate based screening because of the low efficiency of EB differentiation (< 5%). To overcome this issue I investigated second messenger responses of a pan-cardiac population FACS sorted from EBs. The EC<sub>50</sub> values calculated from these experiments matched values for cardiomyocytes from previous *in vitro* and *in vivo* studies(Germack & Dickenson 2004; Gosling et al. 2012). Generally, the majority (>70%) of cells in the pan-cardiac population are cardiomyocyte and so the correlation between experimental results and literature values is to be expected(Kolossov et al. 2005; Hidaka et al. 2003; Boheler et al. 2002). There were discrepancies between the EC<sub>50</sub> values determined using enriched population in the cAMP assay compared to those determined using the EB (4.3.1 & 4.3.5). This likely reflects the inability to separate responses of the pan-

cardiac sorted population, which is predominantly myocytes but also contains pacemaker cells and other cell types; while in the EB the different measures (rate and contractility) are mediated more specifically by distinct cell types(Maltsev et al. 1993). The inability to distinguish responses mediated via different cell types in the cAMP assay using sorted cells compromises the advantage of the heterogeneous nature of the EB. To make better use of the mixed population of cells present in the EB, methods enabling single cell analysis are required, such as those described in chapter 5.

## 4.5 Conclusions

This study provides insight to the potential uses of EBs for the purposes of drug discovery or development screening. The effects of various adrenoceptor and adenosine receptor agonists and antagonists on EB cardiomyocyte function were measured. In depth investigation of  $\beta$ -adrenoceptor pharmacology was possible thanks to selective compounds and a well-characterised pharmacological signaling pathway. Characterisation of adenosine receptor pharmacology in EBs was more challenging due to a lack of selective tools and confounding signaling pathways. These findings suggest that the use of EBs for characterizing pharmacological pathways and signaling mechanisms is limited by their inherent complexity. However, with respect to basic screening of intended or incidental cardiac effects, the EB represents a physiologically relevant model that might prevent drugs with previously unidentified toxic cardiac activity from entering the clinic.

**CHAPTER 5 - HANGING DROP DIFFERENTIATION REVEALS MULTIPLE  
SPONTANEOUSLY ACTIVE CELL TYPES IN  $\text{Nkx}2.5\text{-GFP}^+$  CARDIAC LINEAGE CELLS:  
PACEMAKER CHARACTERISATION**

## 5.1 Foreword

Chapter 5 is formatted and presented as the intact manuscript submitted to the journal Stem Cell Research. The figures are at the back of the manuscript; the supplementary figures are included as Appendix II. The references cited in the manuscript follow the text and are not included in the references section, unless cited elsewhere in this dissertation.

This work was conducted in collaboration with Louise Lagerqvist, with an equal share of experimental work directed towards the pharmacological and immunological characterisation of the mature cells. I was responsible for all work involving immature cells, the analysis template outlined in Chapter 3, and all supplementary data regarding the significance of ROS on waveform stability. Louise was solely responsible for the PCR data included in Figure 3.

## **Development of cardiac spontaneity**

### **Hanging drop differentiation reveals multiple spontaneously active cell types in Nkx2.5-GFP<sup>+</sup> cardiac lineage cells**

BA Finnin<sup>1</sup>, EL Lagerqvist<sup>1</sup>, S Wu, CW Pouton and JM Haynes\*.

Drug Discovery Biology, Monash Institute of Pharmaceutical Sciences, Monash University (Parkville Campus), Melbourne, Australia.

381 Royal Parade, Parkville. Victoria 3052, Australia.

<sup>1</sup>These authors contributed equally to this work



BA Finnin: Conception and design, collection and assembly of data, data analysis and interpretation, manuscript writing

EL Lagerqvist: Conception and design, collection and assembly of data, data analysis and interpretation, manuscript writing

S Wu: Provision of study material

CW Pouton: Conception and design, financial support, administrative support

JM Haynes: Conception and design, data interpretation, manuscript writing, financial support, administrative support

Keywords (6): pacemaker, cardiac, calcium imaging, embryonic stem cell,  $I_f$  channels, conduction system

## Abstract

Isolated cells of the human and or mouse cardiac conduction system show spontaneous pacemaker activity. The frequency and physical characteristics of this activity are defined by the anatomical location of the pacemaker cells, i.e. sinoatrial, node, atrioventricular node, Bundle of His or Purkinje fibers, and are most often described by changes in either electrical activity or in intracellular calcium ( $[Ca^{2+}]_i$ ) cycling.

Aberrant activity in these cells is central to a number of cardiac conditions but their isolation from heart tissue is difficult and time consuming. In this study we employ a simple hanging drop differentiation protocol to generate Nkx2.5-eGFP<sup>+</sup> cardiac lineage cells. FACS sorting of the Nkx2.5-eGFP<sup>+</sup> population followed by single cell high speed Ca<sup>2+</sup>imaging reveals five common  $[Ca^{2+}]_i$  waveforms with frequencies ranging from  $139 \pm 6$  to  $14 \pm 1$  oscillations per minute. Frequencies directly correlated with cell size ( $\mu m^2$ ,  $r^2 = 0.93$ ). Faster cells appeared less sensitive to the If channel blocker ZD7288 (10  $\mu M$ ), but more sensitive to the blockade of intracellular store-mediated Ca<sup>2+</sup> release by ryanodine (10  $\mu M$ ). All cells were sensitive to blockade by the SERCA inhibitor thapsigargin (1  $\mu M$ ) and the L-type voltage operated Ca<sup>2+</sup> channel inhibitor, nifedipine (1  $\mu M$ ). The slowest oscillating Ca<sup>2+</sup> waveform was immunoreactive to anti-PGP9.5, a marker of Purkinje cells. This study shows that hanging drop differentiation generates distinctly identifiable populations of spontaneously active Nkx2.5-eGFP<sup>+</sup> positive cells. These cells should prove an invaluable aid to investigations of the mechanisms and pathophysiology of cardiac pacemaker cells.

## Introduction

The adult mammalian heart is driven by the spontaneous and repetitive depolarizations of pacemaker cells located in the sinoatrial node (SAN). The action potentials arising in these cells are propagated to the atrioventricular node (AVN) and then spread to the ventricles via the ventricular conduction system which consists of the Bundle of His, the bundle branches and the Purkinje fibre network [1]. Although the cells of the AVN and ventricular conduction system are primarily conduits for the propagation of electrical impulses arising in the SAN, they are capable of automaticity themselves. Generally, the rates of spontaneous pacemaker activity in these cells decreases the further away they are from the SAN [2, 3]. Much of what we know of cardiac conduction system physiology, especially the secondary conduction system, has been derived from animal models and 3D computer representations (reviewed in [4]).

Due to both the delicate structure of the murine heart and its rapid rate of beating, there are considerable difficulties in obtaining working murine cardiac conduction system cells. In particular, Purkinje cells are not apparent by histology and appear to merge seamlessly with the surrounding myocardium [5]. The little that is known regarding the function of this diverse conduction system *in vivo* has prompted several groups to use mouse embryonic stem cell-derived cardiomyocytes (ESC-CMs) as *in vitro* models of pacemaker cell activity [6-8], primarily focusing on SAN-like cells. The simplest protocol for generating cardiac lineage cells from mESCs involves the cultivation of three-dimensional aggregates in hanging drop culture. These aggregates, when plated, give

rise to spontaneously beating cardiomyocytes within mixed cell aggregates [9]. The resultant cells show the transcriptional, electrophysiological and morphological properties of early myocardial development [10, 11]. We have previously used this method to show a high degree of variability with respect to basal rates of beating and sensitivity to bioactive peptides such as angiotensin II (Ang II) and endothelin-1 (ET-1) [12]. This previous study led us to conclude that ESC-derived beating aggregates contain pacemaker cells with heterogeneous intrinsic rates of activity and functional properties. In this study we again use the hanging drop differentiation method to generate cardiomyocytes, but in contrast to our previous study we use FACS to isolate the Nkx2.5-eGFP<sup>+</sup> cells, and investigate the functional properties of the spontaneously active cells using high speed confocal fluorescence calcium ( $\text{Ca}^{2+}$ ) imaging. We now report the presence of distinct populations of spontaneously active cells that arise at an early stage of differentiation and develop different functional characteristics during the course of differentiation. These distinct waveforms can be distinguished based on cell morphology, frequency and kinetics of the spontaneous intracellular  $\text{Ca}^{2+}$  ( $[\text{Ca}^{2+}]_i$ ) oscillations, and differential sensitivity to  $I_f$  channel, ryanodine receptor blockade and second messenger signalling activation.

## Materials and Methods

### **ESC Propagation & Differentiation**

The mouse ESC Nkx2.5-eGFP line was propagated in a culture medium consisting of GlutaMAX™ Dulbecco's Minimum Essential Medium (DMEM) supplemented with 0.1 mM MEM Non-Essential Amino Acids Solution, 10% fetal calf serum (FCS), 0.1 mM 2-mercaptoethanol,  $10^3$  U mL<sup>-1</sup> murine recombinant leukemia inhibitory factor (Chemicon, Australia) (pH 7.4). Cultures were incubated at 37°C, with 5% CO<sub>2</sub> in a humidified environment. Cardiomyocyte differentiation was induced by the hanging drop method [10]. Briefly, embryoid bodies (EBs) were formed from 600 ESCs in hanging drops of differentiation medium (propagation medium supplemented with 20% FCS, 10,000 U/mL penicillin and 10,000 µg/mL streptomycin) for 5 days. EBs were subsequently plated on gelatin-coated wells for a further 3 - 13 days.

### **FACS isolation**

Following 8-20 days of differentiation, cell aggregates were incubated in a 1:1 accutase: collagenase (type II, 2 mg/mL) mix for 45 minutes on a shaker at 37 °C. Cell suspensions were filtered to remove remaining aggregates and the single cell suspension was re-suspended in 10% PBS/FBS with 10 nM of the dead cell stain, SYTOX® Red (Invitrogen). Cells were sorted on days 8-10 (early) or 18-20 (late) of differentiation following excitation with 488 nm and 633 nm lasers. Emission of eGFP and SYTOX® Red was detected with 525 nm and 660 nm band filters, respectively. Following exclusion of doublets and SYTOX® Red positive cells, the sort gate for eGFP positive cells was established based on the forward scattered-light and eGFP

fluorescence of control cells (i.e. cardiomyocytes differentiated using the non-reporter ESC line E14Tg2a).

Nkx2.5-eGFP<sup>+</sup> cells were collected in 1:1 mix of differentiation media (as described above) and 10% PBS/FBS, plated onto collagen coated 96-well plates and maintained in differentiation media for 3 days.

### **Nkx2.5-eGFP<sup>+</sup> Single Cell Calcium Imaging**

On the day of use cells were loaded with Fluo-4 AM (10 µM; Invitrogen) for 15 minutes in KnockOut<sup>TM</sup> Serum Replacement media (KSR; Invitrogen, Australia) containing GlutaMAX<sup>TM</sup> Dulbecco's Minimum Essential Medium (DMEM), 1% NEAA, 20% KSR, 0.1 mM β-mercaptoethanol, and supplemented with 1x B-27® where indicated. B-27® is a readily available supplement from Invitrogen which contains several antioxidants such as catalase and superoxide dismutase. We observed that without this supplement, [Ca<sup>2+</sup>]<sub>i</sub> waveforms demonstrated marked sensitivity to the confocal imaging process which we attributed to the generation of reactive oxygen species. Only through addition of the B-27® antioxidant cocktail could the functional integrity of the spontaneously active Nkx2.5-eGFP<sup>+</sup> cells be maintained (Supplemental Figure S1).

After loading with Fluo-4 AM, media was replaced with fresh DMEM/KSR/B-27® media. The cells were placed in a 37 °C, 5% CO<sub>2</sub> humidified incubator to equilibrate for 20 minutes. Cell culture plates were then placed on (37°C) heated stage of a

Nikon A1-R confocal microscope for a further 10 minutes. Following the 10 minute equilibration, an initial 30 s capture was taken to establish baseline activity prior to the addition of: the ryanodine receptor antagonist, ryanodine (10  $\mu$ M), the HCN channel blocker, ZD7288 (10  $\mu$ M/ 100  $\mu$ M), the L-type  $\text{Ca}^{2+}$  channel blocker, nifedipine (1  $\mu$ M), the  $\text{IP}_3$  receptor antagonist, 2-APB (2  $\mu$ M), the sarco/endoplasmic reticular  $\text{Ca}^{2+}$ /ATPase (SERCA) inhibitor thapsigargin (1  $\mu$ M), the T-type  $\text{Ca}^{2+}$  channel blockers NNC 55-0396 (1  $\mu$ M) and nickel chloride ( $\text{NiCl}_2$ , 10  $\mu$ M) or the cyclic adenosine monophosphate (cAMP) activator, forskolin (1  $\mu$ M). 30 s captures were subsequently taken at 5, 10, 15 and 20 minutes after ligand addition at frame rates between 30 and 120 frames per second. For these studies, the 488 nm laser was at 10% power (~ 16mW).

### **Post Calcium Imaging Analysis**

Briefly, regions were drawn around spontaneously active cells using an automated selection tool. Multi-cellular aggregates were excluded from analysis. Total fluorescence intensity was measured over time and exported into Excel to enable analysis of rate and kinetic ( $\text{Ca}^{2+}$  waveform) profile. This data was subsequently correlated with the cellular immunocytochemical profiles and morphometry analyses.

Changes in  $[\text{Ca}^{2+}]_i$  oscillation frequency and peak width at half height (being the time between the points on the up- and down- slope that were closest to 50% of the maximum peak intensity) were analysed prior to and after the addition of inhibitors or agonists. Results are expressed as percentage change from basal values i.e. prior to

agonist/inhibitor addition. None of the vehicles had any effect on basal  $[Ca^{2+}]_i$  and were therefore pooled together for each waveform category. Representative traces of responses by each waveform group can be found in supplementary materials (Supplementary Figure S5).

### **Immunocytochemistry of Mouse Nkx2.5-eGFP<sup>+</sup> Cells**

Following calcium imaging, plates were fixed for immunocytochemistry according to an adapted previously published protocol [13]. Briefly, cells were fixed with 0.25% paraformaldehyde for 1 hour at 4 °C, followed by permeabilization with 0.2% tween-20 at room temperature (RT) for 15 minutes. Cells were then blocked with 10% donkey serum (Millipore) for 30 minutes at RT and incubated overnight, at 4°C, with primary antibodies for polyclonal rabbit smooth muscle actin ( $\alpha$ SMA, 1:200), mouse monoclonal alpha myosin heavy chain ( $\alpha$ MHC, 1:200), rabbit polyclonal PGP9.5 (1:50), mouse monoclonal HCN1 (1:50), rabbit polyclonal ANP (1:250) or mouse monoclonal HCN4 (1:50). Cells were then incubated with donkey anti-mouse Alexa Fluor 594 (1:600) and donkey anti-rabbit Alexa Fluor 647 (1:400) for 2 hours at RT.

### **RT-PCR of Mouse Nkx2.5-eGFP<sup>+</sup> Cells**

Nkx2.5-eGFP<sup>+</sup> cells were isolated on day 18 post differentiation using FACS (as described above). Total RNA was extracted using the RNeasy Micro kit (Qiagen, Australia) and treated with DNase I to remove the contaminating genomic DNA. Reverse transcription of mRNA into cDNA was carried out by Transcriptor Reverse Transcriptase (Roche Applied Science, Australia) using a combination of Oligo (dT)

and random primers. Reverse transcription of 10ng of RNA per sample was performed for 10 minutes at 25 °C followed by 60 minutes at 55 °C, and the reaction was inactivated by heating to 85 °C for 5 minutes. For PCR amplification, cDNAs were amplified using Phusion Flash PCR Master Mix (Finnzymes, Australia), 1 µL of cDNA and 0.5 µM of each primer pair. The tubes were placed in the thermal cycler (Veriti®, Applied Biosystems), and the PCR was run with a hot start for 10s at 98°C (initial melt); then for 40 cycles of 5s at 98°C, 7s at 55°C, and 10s at 72°C; and, at last, for 1 min at 72°C (final extension). Ten microliters of each PCR product was size fractionated by agarose gel electrophoresis. The gene-specific primer sequences used were: HCN1 Fwd: 5'-ctctttgctaaccgcga-3', HCN1 Rev: 5'-catthaaattgtccaccgaa-3', HCN2 Fwd: 5'-gtggagctctactcgt-3', HCN2 Rev: 5'-gttcacaatccctcacgca-3', HCN3 Fwd: 5'-cgtagctggtaccgtaat-3', HCN3 Rev: 5'-acttggtgtggacaaggagg-3', HCN4 Fwd: 5'-tgctgcattggtatgga-3', HCN4 Rev: 5'-ttcggcagttaaagtgtatg-3'.

### Statistical Analysis

Mean ± SEM values were calculated for rate, width at half height and cell area. Respective *n* values are shown in the figure legends. Differences between means were tested using one- or two-way ANOVA. Parameters associated with cellular morphologies (size, deviation from circularity and roughness) and spontaneous [Ca<sup>2+</sup>]<sub>i</sub> waveform activity (width at half height and downward slope) were tested against frequency using linear or non-linear regression analysis. Values of P<0.05 were considered statistically significant.

## Drugs and Chemicals

Ryanodine and NiCl<sub>2</sub> were reconstituted in PBS buffer. Nifedipine, thapsigargin, and ZD7288 were dissolved in DMSO. 2-APB was dissolved in methanol. The final concentration of DMSO or methanol did not exceed 0.01% of the final volume. Ryanodine was purchased from Calbiochem-Novabiochem (Australia) and thapsigargin was purchased from LC laboratories (USA). ZD7288 and 2-APB were purchased from Tocris Bioscience (UK). Primary antibodies against  $\alpha$ MHC,  $\alpha$ SMA, HCN1, HCN4 and PGP9.5 were purchased from Abcam (USA), Secondary antibodies were from Molecular Probes, Invitrogen (Australia). All drugs and chemicals were purchased from Sigma-Aldrich (Australia) unless otherwise stated.

## Results

### Single Cell Calcium Imaging

Under the differentiation conditions of this study the Nkx2.5-eGFP<sup>+</sup> cell line showed detectable eGFP expression from day 7 (supplemental figures S1 A-B). Spontaneous beating arose and remained within eGFP positive areas 1-3 days after the appearance of eGFP. Following sorting the cells attached to collagen coated tissue culture plates and, 72 hrs later, were loaded with Fluo-4 AM (10  $\mu$ M, supplemental figures S1 C-D). Spontaneous oscillations of  $[Ca^{2+}]_i$  were observed in approximately 5-10% of eGFP<sup>+</sup> cells. In control experiments eGFP<sup>+</sup> cells that were not loaded with Fluo-4 AM did not exhibit detectable fluorescence oscillations (data not shown). Initially, multiple kinetically distinct waveforms were evident in the spontaneously active population;

however the majority of waveforms ceased within 10 minutes of the start of imaging. The addition of the antioxidant supplement B-27® during Fluo-4 AM loading and confocal imaging stabilised all previously unstable spontaneous waveforms (Supplemental figure S3).

### **C-kit expression**

Co-expression of Nkx2.5-eGFP and c-kit was determined between days 6 and 19. The proportion of Nkx2.5-eGFP<sup>+</sup> cells expressing high levels of c-kit was relatively constant between days 6-11 until a decrease at day 13, at day 19 there was further drop in the proportion of double positive cells (Supplemental Figure S3).

### **Analysis of Waveform Kinetics and Cellular Morphology**

Once stabilised, the majority of spontaneous [Ca<sup>2+</sup>]<sub>i</sub> waveforms could be classified into groups based on their intrinsic [Ca<sup>2+</sup>]<sub>i</sub> oscillation frequency and waveform kinetics (Table 1). Significant kinetic differences were observed between the waveform groups in terms of the interval of time between baseline and peak fluorescence intensity (upslope), width of the waveform at half its peak height and the interval of time between peak fluorescence intensity and the subsequent baseline (downslope; Supplemental Figure S4).

Quantitative morphometry analysis was conducted on late stage cells using NIS elements software (Nikon, Japan) where parameters such as cell length, width,

circularity and roughness were analysed. Cell size was found to significantly correlate with the spontaneous  $[Ca^{2+}]_i$  frequency demonstrated by the different categories of pacemaker-like cells (Figure 1 A,  $P=0.01$ , Linear Regression Analysis,  $n=5-15$  per waveform category). The morphology of spontaneously active cells on the day of  $Ca^{2+}$  imaging experimentation demonstrated trends within each waveform group which correlated to previously reported morphologies observed within the conduction system. For example, the slower waveforms (Figure 1 B) developed almost neuronal like processes extending in opposite polar directions from the cell body, possibly indicative of a ventricular conduction system phenotype and the fastest oscillating cells exhibiting a small typical “pacemaker-like” morphology [14] (Figure 1 C). Cells exhibiting waveforms of intermediate frequencies were varied in their appearance and morphometric analysis could not accurately classify these cells into distinct groups. This is, however, not altogether surprising given that previous observations throughout the *in vivo* conduction system have reported multiple morphologically distinct populations [15-17].

### **Immunocytochemistry & RT-PCR**

To correlate the different waveform categories with the region of the cardiac conduction system they may represent, the incidence of sarcomeric contractile protein expression was investigated [18, 19] (Figures 2 A-B). Furthermore, PGP9.5, a marker of cardiac Purkinje cells [20, 21] could be observed in both intact ESC-derived beating body cultures as well as single cells exhibiting the slowest  $[Ca^{2+}]_i$  waveform (Figures 2 C-D). Supplementary Table 1 summarizes the immunolabelling profile of each distinct

waveform group ( $n= 7-10$  for each waveform category). Cytoplasmic organization of  $\alpha$ MHC was detected in mature cardiomyocytes (Figure 2 E) but not immature cells (Figure 2 F), which also expressed ANP, not detectable in mature cells.

RT-PCR analysis of HCN channel expression by spontaneously active Nkx2.5-eGFP<sup>+</sup> cells demonstrates that all four HCN channel subtypes are expressed (Figure 3 A). The cells of the fastest oscillating cell group express HCN4, however, we could not observe conclusive HCN4 or HCN1 labelling in other spontaneously active cell types (Figures 3 B-D). Addition of forskolin (1  $\mu$ M) increased spontaneous  $[Ca^{2+}]_i$  oscillation frequency in some waveform groups, while prolonging the waveform duration in others indicating HCN 2/4 and HCN 3 expression respectively (Figures 3 E-F).

## **Analysis of Intracellular Calcium Handling**

### **I<sub>f</sub> channel blockade**

Addition of the I<sub>f</sub> blocker, ZD7288 (10  $\mu$ M), decreased the frequency of  $[Ca^{2+}]_i$  oscillations in all waveform groups ( $P<0.05$ , one-way ANOVA, post-hoc Dunnett's,  $n=3-26$  per waveform group). At increased concentrations, ZD7288 (100  $\mu$ M) abolished activity in most waveform groups (Figure 4 A,  $P<0.001$ , one-way ANOVA, post-hoc Dunnett's,  $n=4-17$  per waveform group). Interestingly, waveform groups with decreasing intrinsic  $[Ca^{2+}]_i$  cycle rates demonstrated increasing sensitivity to ZD7288 (Figure 4 B,  $P=0.004$ , Linear Regression Analysis,  $n=3-27$  per waveform group). In addition to significantly decreasing the frequency of  $[Ca^{2+}]_i$  oscillations, ZD7288 also

significantly prolonged the duration of the  $[Ca^{2+}]_i$  cycle (Figure 4 C,  $P<0.01$ , one-way ANOVA, post-hoc Dunnett's,  $n=3-27$  per waveform group).

### **The Effects of Ryanodine**

The ryanodine receptor antagonist, ryanodine ( $10 \mu M$ ), in contrast to ZD7288 progressively decreased  $[Ca^{2+}]_i$  oscillation frequency with increasing intrinsic cycle rates (Figures 4 D-E,  $P=0.01$ , Linear Regression Analysis,  $n= 6-29$  per waveform group). In addition, ryanodine significantly prolonged the duration of the  $[Ca^{2+}]_i$  oscillation peak in the two slowest waveform categories (Figure 4 F,  $P<0.05$ , one-way ANOVA, post-hoc Dunnett's,  $n=6-29$  per waveform group).

### **The Effects of Thapsigargin**

The SERCA inhibitor thapsigargin significantly reduced spontaneous  $[Ca^{2+}]_i$  oscillation frequency in all waveforms as well as prolonging the  $[Ca^{2+}]_i$  oscillation peak in others (Figures 5 A-B,  $P<0.05$ , one-way ANOVA, post-hoc Dunnett's,  $n=4-17$  per waveform category). The IP<sub>3</sub> receptor antagonist 2-APB ( $2 \mu M$ ) did not affect either the frequency or width at half height of  $[Ca^{2+}]_i$  oscillations in any of the different waveform categories (Figures 5 C-D,  $n=4-17$  per waveform group).

### **The Effects of Nifedipine, NNC 55-0396 and NiCl<sub>2</sub>**

The L-type Ca<sup>2+</sup> channel blocker, nifedipine ( $1 \mu M$ ), rapidly abolished activity in all spontaneously active Nkx2.5-eGFP<sup>+</sup> cells (Supplementary Figure S5 A). The T-type Ca<sup>2+</sup>

channel blocker, NNC 55-0396 (1  $\mu$ M), significantly reduced the  $[Ca^{2+}]_i$  cycling frequency in all spontaneously active cells, as well as shortened their duration in all waveform categories except for the fastest oscillating cells (Supplementary Figure S5 B-C,  $P<0.001$ , one-way ANOVA, post-hoc Dunnett's,  $n=3-17$  per waveform group). Nickel chloride ( $NiCl_2$ , 10  $\mu$ M) significantly decreased the  $[Ca^{2+}]_i$  oscillation frequency of the slowest waveform group (Supplementary Figure S5 D,  $P<0.05$ , one-way ANOVA, post-hoc Dunnett's,  $n=3-9$  per waveform group). Furthermore, it progressively prolonged the width at half height of each  $[Ca^{2+}]_i$  oscillation the slower the intrinsic pacemaker-like cell activity ( $P<0.001$ ,  $P<0.05$ , one-way ANOVA, post-hoc Dunnett's,  $n=3-7$  per waveform group).

### **Analysis of day 13 cardiac progenitors**

Spontaneous calcium oscillations of cardiac progenitors at day 13 displayed a greater heterogeneity than observed in the mature cells. Activity could be categorized into 5 groups based on rate and width at half height for 91% of spontaneously active cells (Figure 6A), representative traces included. In contrast to mature cells the IP<sub>3</sub> receptor antagonist 2-APB (2  $\mu$ M) inhibited the frequency of spontaneous  $[Ca^{2+}]_i$  oscillations in 3 of the waveforms (Figure 6B,  $P<0.05$ , one-way ANOVA, post-hoc Dunnett's,  $n=4$ ) and prolonged the peak width at half height in 3 waveforms (Figure 6B,  $P<0.05$ , one-way ANOVA, post-hoc Dunnett's,  $n=3-4$ ). Ryanodine (10  $\mu$ M) inhibited the frequency of spontaneous  $[Ca^{2+}]_i$  oscillations in 4 of the waveforms, while the effects on peak width at half height were varied between waveforms. Only waveform 2 displayed a mature

phenotype, unresponsive to 2-ABP while ryanodine significantly reduced peak width at half height (Figure 6C,  $P<0.05$ , one-way ANOVA, post-hoc Dunnett's,  $n=4$ ).

## Discussion

In this study, an Nkx2.5-eGFP mESC reporter cell line was used to isolate cells of the cardiac lineage for live single cell high acquisition rate calcium imaging. Within a pacemaker cell, spontaneous cyclic variations in  $[Ca^{2+}]_i$  governs the discharge rate of the depolarizing impulse [22, 23]. Mature ventricular myocytes are not spontaneously active themselves and rely on the pacemaker depolarization stimulus to contract. We now report on the presence of five common, distinct spontaneous  $Ca^{2+}$  waveforms in Nkx2.5-eGFP<sup>+</sup> cells. These waveforms were classified on the basis of waveform kinetics, specifically rate and width, sensitivity to  $I_f$  channel blockade and SR calcium handling.

The reporter line used in this study expresses eGFP under the control of a cardiac-specific enhancer element of Nkx2.5 [24]. These cells have previously been shown to differentiate into most of the different cardiac phenotypes [24-26], however, Nkx2.5 is not expressed in the SAN region at any stage during development [27-30]. Thus, our Nkx2.5-eGFP<sup>+</sup> FACS isolated cells will include all cardiac lineage cells, with the exception of the sinoatrial pacemaker population. The potential of ESCs to differentiate into the other cells, which constitute the cardiac conduction system, while previously reported [10, 31], has not been extensively investigated.

The spontaneously active cells identified by confocal  $\text{Ca}^{2+}$  imaging constituted approximately 5-10% of the entire mature Nkx2.5eGFP $^+$  population. In contrast to previous studies showing a predominance of a single rhythmic spontaneous  $[\text{Ca}^{2+}]_i$  waveform [32-35], we now report multiple distinct  $[\text{Ca}^{2+}]_i$  waveforms in our spontaneously active population. With respect to cellular morphology, the only consistently identifiable parameter correlating with  $\text{Ca}^{2+}$  oscillation frequency was cell size; small cells showed a faster spontaneous rhythm than larger cells. That we saw no  $[\text{Ca}^{2+}]_i$  oscillation frequencies comparable to rates reported in murine isolated SAN cells ( $\sim 294 [\text{Ca}^{2+}]_i$  oscillations per minute, [36]) supports our contention that the Nkx2.50 eGFP $^+$  population is devoid of SAN-like cells. Given the wide range of spontaneous  $[\text{Ca}^{2+}]_i$  oscillations observed in single cells isolated from one nodal structure (90-250 oscillations/minute [37]), as well as previous observations that intact mouse atrioventricular cells respond with a resting frequency of 120 oscillations per minute [38], the fastest  $[\text{Ca}^{2+}]_i$  oscillation frequencies observed in this study are largely consistent with the presence of atrioventricular cell types.

While pacemaker cells are known to possess rudimentary cytoskeletal structures [39, 40] conduction system regions *in vivo* have, nevertheless, previously been isolated by sarcomeric contractile protein expression [18, 19]. To establish whether our spontaneous populations contained cardiac  $\alpha\text{MHC}$  and  $\alpha\text{SMA}$  we undertook post-experimental immunocytochemistry. In this study, the four Nkx2.5-eGFP $^+$  cell types demonstrating the fastest  $[\text{Ca}^{2+}]_i$  oscillation frequencies were  $\alpha\text{MHC}^+/\alpha\text{SMA}^0$ . Since both AVN and atrial cells exhibit spontaneous  $[\text{Ca}^{2+}]_i$  activity [41] and express  $\alpha\text{MHC}$  [42], we believe that our data may indicate the presence of an atrial/AVNO like

phenotype. Since the AVN is composed of several functionally and morphologically distinct cell types [15-17], it is not surprising that multiple waveform categories may correlate to populations in this one diverse structure.

In contrast with the faster oscillating cell types, the slowest oscillating cells were positive for both  $\alpha$ SMA and the Purkinje cell marker PGP9.5<sup>+</sup> [20, 21]. Currently there is no data showing the resting rate of Purkinje cells in mouse heart, however, the prolonged plateau-shaped  $[Ca^{2+}]_i$  profile demonstrated by the slowest oscillating Nkx2.5-eGFP<sup>+</sup> cell population is consistent with previous observations in Purkinje cells isolated from rabbit and sheep hearts [43, 44]. Furthermore, their immunoreactivity to PGP9.5 provides strong support that these cells are Purkinje-like cells.

Pacemaker cell function is dependent on the interaction of the membrane clock and the  $[Ca^{2+}]_i$  clock. The two components of these clocks attributed with the generation of pacemaker automaticity are the  $I_f$  current- generated through HCN channels on the pacemaker cell membrane- and RyR-mediated  $Ca^{2+}$  release from the SR. Other vital contributors to the  $[Ca^{2+}]_i$  cycle include the T- and L-type voltage gated  $Ca^{2+}$  channels on the pacemaker cell membrane, as well as the SERCA pumps on the SR which regulate  $Ca^{2+}$  re-uptake into the SR at the end of the  $[Ca^{2+}]_i$  cycle. Through addition of various inhibitors against different aspects of the  $[Ca^{2+}]_i$  cycle, this study examined the contribution of various ion channels and receptors vital for automaticity in mature pacemaker cell function in spontaneously active ESC-derived Nkx2.5-eGFP<sup>+</sup> cells. We investigated the changes to two properties of waveform kinetics: (1) the firing rate of these pacemaker-like cells (changes in the spontaneous  $[Ca^{2+}]_i$  frequency) and (2) the

duration of each  $[Ca^{2+}]_i$  oscillation (changes in the width at half height of each  $[Ca^{2+}]_i$  oscillation peak).

Nkx2.5-eGFP<sup>+</sup> pacemaker-like cells demonstrated varying degrees of sensitivity to the  $I_f$  blocker, ZD7288, and the ryanodine receptor antagonist, ryanodine, depending on the intrinsic frequency of the  $[Ca^{2+}]_i$  waveforms. The different HCN channel subunit isoforms, the molecular correlates of the  $I_f$  current, do not display any bias in affinity to ZD7288 [45]. These results may, therefore, indicate that the faster  $[Ca^{2+}]_i$  cycles are less dependent upon HCN channel activation. The generation of pacemaker activity in these rapidly oscillating cells appears to rely predominantly on SR-mediated  $Ca^{2+}$  release via ryanodine receptors. This is consistent with previous observations that ryanodine has a more pronounced effect on pacemaker cells with faster intrinsic rhythm [46]. By contrast, the pacemaker mechanism in the slower waveform categories is reliant on the  $I_f$  current, as demonstrated by the cessation of activity following ZD7288 addition. Ryanodine decreased the  $[Ca^{2+}]_i$  oscillation rate but, more significantly, it prolonged the duration of each  $[Ca^{2+}]_i$  oscillation peak. This is perhaps suggestive of a more modulatory role of the SR in these slower oscillating pacemaker-like cells. These observations imply distinctions in the predominance of either SR-mediated  $[Ca^{2+}]_i$  release or the  $I_f$  current in the generation of automaticity depending on the intrinsic frequency of  $[Ca^{2+}]_i$  cycling of the different pacemaker-like cell populations, and may account for the previously discussed differences in the literature.

Automaticity in the early stages of cardiac development relies almost entirely on  $IP_3$ -dependent  $[Ca^{2+}]_i$  release from the sarcoplasmic reticulum (SR) [47, 48], with no essential contribution of ryanodine receptors to excitation contraction coupling [49,

50]. Since spontaneous activity in all Nkx2.5-eGFP<sup>+</sup> cells was unaffected by the presence of the IP<sub>3</sub> receptor antagonist, 2-APB, but inhibited by ryanodine, we infer that, with respect to their SR [Ca<sup>2+</sup>]<sub>i</sub> handling, these auto-rhythmic cells appear to be mature.

The L-type Ca<sup>2+</sup> channel blocker, nifedipine, and the T-type Ca<sup>2+</sup> channel blocker, NNC 55-0396, both markedly diminished spontaneous activity in all cell types. This is in accordance with reported observations in the murine heart [51, 52] and mESC-derived pacemaker cells [53], and suggests the paramount importance of L- and T- type Ca<sup>2+</sup> channels for pacemaker activity. The T-type Ca<sup>2+</sup> channels are encoded by two subunits, Ca<sub>v</sub>3.1 and Ca<sub>v</sub>3.2. During the early developmental stages of cardiac development, T-type channels are expressed on all cardiac cell types and are predominantly composed of the Ca<sub>v</sub>3.2 subtype. Upon maturation, T-type channel expression is largely localised to the conduction system and Ca<sub>v</sub>3.1 expression progressively increases and eventually predominates over Ca<sub>v</sub>3.2 [54]. These two subtypes can be differentiated by their disparate sensitivity to nickel, where Ca<sub>v</sub>3.2 is sensitive to low μM concentrations of nickel and Ca<sub>v</sub>3.1 is not [55, 56]. In response to 10 μM nickel chloride (NiCl<sub>2</sub>), only the slowest Purkinje-like cell type of the spontaneously active populations demonstrated a decrease in [Ca<sup>2+</sup>]<sub>i</sub> oscillation frequency, however, the two slowest intrinsically active cell types had prolonged oscillation peak widths. This suggests that the Ca<sub>v</sub>3.2 isoform plays a role in the pacemaker function of slower spontaneously active cell types. Although the effect of mM concentrations of NiCl<sub>2</sub> was not investigated, the Ca<sub>v</sub>3.1 isoform, which demonstrates faster kinetics than Ca<sub>v</sub>3.2 [57], may play a role in regulating the faster spontaneously active Nkx2.5-eGFP<sup>+</sup> pacemaker-like cell types.

HCN channels are widely considered determinants of pacemaker cell identity. All four HCN isoforms are expressed in the murine cardiac conduction system [58] as well as in our Nkx2.5-eGFP<sup>+</sup> cells. Previous observations in cells of the SAN/AVN, indicate that expression of HCN4 predominates [59]. In this study, HCN4 immunolabelling was clearly observed on the fastest oscillating pacemaker-like cells, but not on any other cell types. This seems consistent with the ZD7288 response profile, where the fastest oscillating, HCN4<sup>+</sup> pacemaker-cell types appear more sensitive to HCN channel blockade. HCN1 immunolabelling was not conclusively observed on spontaneously active cells. A more sensitive technique, such as *in situ* hybridization, may therefore be required to observe HCN channel expression by the other pacemaker-like cells within these cultures. In a further attempt to elucidate the HCN subtype expression by different populations, we investigated the effect of cAMP activation on the  $[Ca^{2+}]_i$  kinetics of the different pacemaker-like populations as the four HCN channel isoforms have recently been reported to be differentially sensitive to cAMP activation. Thus, cAMP increases the activation kinetics of HCN2 and HCN4 [60, 61]. The HCN3 channel, which is most common in the ventricular conduction system region [62], is slightly inhibited by cAMP [63]. The HCN1 is relatively insensitive to changes in cAMP [60]. In this study the slowest Purkinje-like waveforms were slightly inhibited by the addition of the cAMP activator, forskolin, and exhibited prolonged waveform duration. Furthermore, an atrial/AVN-like waveform demonstrated increased  $[Ca^{2+}]_i$  oscillation frequency in response to forskolin, indicative of either HCN2 or HCN4 expression. These results are suggestive of the expression of different HCN channel subtypes by distinct spontaneously active Nkx2.5-eGFP<sup>+</sup> populations and we postulate that this may correlate to the frequency with which pacemaker-like cells initiate  $[Ca^{2+}]_i$  cycles. The

expression of HCN channels by these distinct spontaneously active groups is under continued investigation.

Given the heterogeneous nature of stem cell cultures there was a possibility that the different waveforms represented different stages of differentiation rather than a different cell type, to disprove this we sought to analyse early progenitor cells. c-Kit expression was used to determine the point at which the differentiating mesoderm became committed cardiac progenitors [24] in our culture, day 13 determined the best day for early cardiac cells. These early cells gave rise to a more heterogeneous range of waveforms, likely due to their transient nature, however 5 groups could still be classified based on their rate of oscillation and peak width at half height. To further confirm the immaturity of these cells IP<sub>3</sub> - dependent [Ca<sup>2+</sup>]<sub>i</sub> release from the sarcoplasmic reticulum was blocked using 2-APB, causing reduction of spontaneous activity in some of the waveforms measured, confirming functional immaturity. Blocking the ryanodine receptor had a range of effects (both inhibitory and stimulatory) perhaps indicating these cells were transitioning towards a mature phenotype. Given the presence of these different waveforms at such an early stage of differentiation suggests that the waveforms observed in the mature cells represent different functional phenotypes instead of different stages of differentiation.

In whole tissue, a single pacemaker cell type, typically that demonstrating the fastest kinetics, governs pacing. This is replicated with the Nkx2.5<sup>+</sup> population when seeded at a high enough density (Supplementary Video 1). However, it is only at the single cell level where one can observe the distinct intrinsic rhythms of different pacemaker cell populations (Supplementary Video 2). It may not be surprising; therefore, that the variety of [Ca<sup>2+</sup>]<sub>i</sub> transients observed in this study has not previously been reported

given that studies of the conduction system to date have focused on whole tissue preparations. It is also possible that some of these  $[Ca^{2+}]_i$  waveforms may not have been observed in reporter lines isolated using an  $\alpha$ MHC promoter [35, 64-66].

## Summary

This study has established a simple method by which the functional integrity of all rhythmical Nkx2.5-eGFP<sup>+</sup> ESC-derived spontaneously active cells can be maintained, unveiling a range of novel and previously unreported  $[Ca^{2+}]_i$  waveforms. Differences in intrinsic  $[Ca^{2+}]_i$  oscillation frequency,  $[Ca^{2+}]_i$  waveform kinetics and cytoskeletal protein expression were used to crudely correlate the populations of spontaneously active Nkx2.5-eGFP<sup>+</sup> pacemaker-like cells with different regions of the *in vivo* cardiac conduction system. Furthermore, these distinct ESC-derived pacemaker-like cellular phenotypes demonstrate distinct functional and pharmacological properties. Much of the research in the ESC-CM field has revolved around generation of homogeneous cultures of the working myocardium for use in cell replacement therapies. With cardiac toxicity issues accounting for 30% of drug withdrawals from market [67], the ability to differentiate all of the cardiac phenotypes, including the entire conduction system, is highly advantageous. Furthermore, with cellular Ca<sup>2+</sup> dysregulation implicated in ventricular conduction system arrhythmias [68], investigating the mechanisms of  $[Ca^{2+}]_i$  handling within these cells is also highly clinically relevant. This work has developed a model system whereby cells akin to those of the entire cardiac conduction system can be identified, characterised and potentially change the way drug candidates are screened for cardiac activity and toxicity.

## Acknowledgements

This work was supported by the Australian Stem Cell Centre. The authors thank the Monash University Core Flow Cytometry Facility Flowcore for their FACS work.

## References

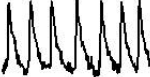
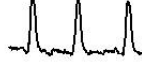
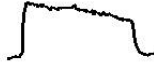
1. Silverman, M.E., D. Grove, and C.B. Upshaw, Jr, *Why Does the Heart Beat?: The Discovery of the Electrical System of the Heart*. Circulation, 2006. **113**(23): p. 2775-2781.
2. Dobrzynski, H., et al., *Site of Origin and Molecular Substrate of Atrioventricular Junctional Rhythm in the Rabbit Heart*. Circulation Research, 2003. **93**(11): p. 1102-1110.
3. Mangoni, M.E. and J. Nargeot, *Genesis and Regulation of the Heart Automaticity*. Physiol. Rev., 2008. **88**(3): p. 919-982.
4. Tusscher, K.H.W.J.T. and A.V. Panfilov, *Modelling of the ventricular conduction system*. Progress in Biophysics and Molecular Biology, 2008. **96**(1-3): p. 152-170.
5. Lev, M. and J.C. Thaemert, *Conduction System of Mouse Heart*. Acta Anatomica, 1973. **85**(3): p. 342-352.
6. Barbuti, A., et al., *Molecular composition and functional properties of f-channels in murine embryonic stem cell-derived pacemaker cells*. Journal of Molecular and Cellular Cardiology, 2009. **46**(3): p. 343-351.
7. Ou, D.-B., et al., *Using embryonic stem cells to form a biological pacemaker via tissue engineering technology*. BioEssays, 2009. **31**(2): p. 246-252.
8. Kleger, A., et al., *Modulation of Calcium-Activated Potassium Channels Induces Cardiogenesis of Pluripotent Stem Cells and Enrichment of Pacemaker-Like Cells*. Circulation, 2010. **122**(18): p. 1823-1836.
9. Wobus, A.M., et al., *Embryonic Stem Cells as a Model to Study Cardiac, Skeletal Muscle, and Vascular Smooth Muscle Cell Differentiation*. Methods in Molecular Biology, 2002. **185**: p. 127-156.
10. Boheler, K.R., et al., *Differentiation of Pluripotent Embryonic Stem Cells Into Cardiomyocytes*. Circ Res, 2002. **91**(3): p. 189-201.
11. Fijnvandraat, A.C., et al., *Cardiomyocytes purified from differentiated embryonic stem cells exhibit characteristics of early chamber myocardium*. Journal of Molecular and Cellular Cardiology, 2003. **35**(12): p. 1461-1472.
12. Lagerqvist, E.L., et al., *Endothelin-1 and angiotensin II modulate rate and contraction amplitude in a subpopulation of mouse embryonic stem cell-derived cardiomyocyte-containing bodies*. Stem Cell Research, 2011. **6**(1): p. 23-33.
13. Schmid, I., C.H. Uittenbogaart, and J.V. Giorgi, *A gentle fixation and permeabilization method for combined cell surface and intracellular staining with improved precision in DNA quantification*. Cytometry, 1991. **12**(3): p. 279-285.
14. Gassanov, N., et al., *Endothelin induces differentiation of ANP-EGFP expressing embryonic stem cells towards a pacemaker phenotype*. FASEB J., 2004: p. 04-1619fje.
15. Hancox, J.C., Yuill, K.H., Mitcheson, J.S., Convery, M.K., *Progress and Gaps in Understanding the Electrophysiological Properties of Morphologically Normal Cells*

- From the Cardiac Atrioventricular Node.* International Journal of Bifurcation and Chaos, 2003. **13**(12): p. 3675-3691.
16. Efimov, I.R., et al., *Structure-function relationship in the AV junction.* The Anatomical Record Part A: Discoveries in Molecular, Cellular, and Evolutionary Biology, 2004. **280A**(2): p. 952-965.
  17. Meijler, F.L. and M.J. Janse, *Morphology and electrophysiology of the mammalian atrioventricular node.* Physiological reviews, 1988. **68**(2): p. 608-647.
  18. Franco, D. and J.M. Icardo, *Molecular characterization of the ventricular conduction system in the developing mouse heart: topographical correlation in normal and congenitally malformed hearts.* Cardiovascular Research, 2001. **49**(2): p. 417-429.
  19. Ya, J., et al., *Expression of the smooth-muscle proteins  $\alpha$ -smooth-muscle actin and calponin, and of the intermediate filament protein desmin are parameters of cardiomyocyte maturation in the prenatal rat heart.* The Anatomical Record, 1997. **249**(4): p. 495-505.
  20. El Sharaby, A.A., et al., *Immunohistochemical Demonstration of Leu-7 (HNK-1), Neurone-Specific Enolase (NSE) and Protein-Gene Peptide (PGP) 9.5 in the Developing Camel (*Camelus dromedarius*) Heart.* Anatomia, Histologia, Embryologia, 2001. **30**(6): p. 321-325.
  21. Airey, J.A., et al., *Human Mesenchymal Stem Cells Form Purkinje Fibers in Fetal Sheep Heart.* Circulation, 2004. **109**(11): p. 1401-1407.
  22. Lakatta, E.G., et al., *Cyclic Variation of Intracellular Calcium.* Circulation Research, 2003. **92**(3): p. e45-e50.
  23. Maltsev, V.A., et al., *Diastolic Calcium Release Controls the Beating Rate of Rabbit Sinoatrial Node Cells: Numerical Modeling of the Coupling Process.* Biophysical Journal, 2004. **86**(4): p. 2596-2605.
  24. Wu, S.M., et al., *Developmental Origin of a Bipotential Myocardial and Smooth Muscle Cell Precursor in the Mammalian Heart.* Cell, 2006. **127**(6): p. 1137-1150.
  25. Hidaka, K., et al., *Chamber-specific differentiation of Nkx2.5-positive cardiac precursor cells from murine embryonic stem cells.* FASEB J., 2003: p. 02-0104fje.
  26. Christoforou, N., et al., *Mouse ES cell-derived cardiac precursor cells are multipotent and facilitate identification of novel cardiac genes.* J Clin Invest, 2008. **118**(3): p. 894-903.
  27. Bakker, M.L., V.M. Christoffels, and A.F.M. Moorman, *The Cardiac Pacemaker and Conduction System Develops From Embryonic Myocardium that Retains Its Primitive Phenotype.* Journal of Cardiovascular Pharmacology, 2010. **56**(1): p. 6-15.
  28. Christoffels, V.M., et al., *Formation of the Venous Pole of the Heart From an Nkx2-5-Negative Precursor Population Requires Tbx18.* Circ Res, 2006. **98**(12): p. 1555-1563.
  29. Espinoza-Lewis, R.A., et al., *Shox2 is essential for the differentiation of cardiac pacemaker cells by repressing Nkx2-5.* Developmental Biology, 2009. **327**(2): p. 376-385.
  30. Gittenberger-De Groot, A.C., et al., *Nkx2.5-negative myocardium of the posterior heart field and its correlation with podoplanin expression in cells from the developing cardiac pacemaking and conduction system.* The Anatomical Record: Advances in Integrative Anatomy and Evolutionary Biology, 2007. **290**(1): p. 115-122.
  31. Hescheler, J., et al., *Embryonic stem cells: a model to study structural and functional properties in cardiomyogenesis.* Cardiovascular Research, 1997. **36**(2): p. 149-162.
  32. Zahanich, I., et al., *Rhythmic beating of stem cell-derived cardiac cells requires dynamic coupling of electrophysiology and Ca cycling.* Journal of Molecular and Cellular Cardiology, 2011. **50**(1): p. 66-76.

33. Fu, J.-D., et al., *Crucial role of the sarcoplasmic reticulum in the developmental regulation of Ca<sup>2+</sup> transients and contraction in cardiomyocytes derived from embryonic stem cells*. FASEB J, 2006. **20**(1): p. 181-183.
34. Shinozawa, T., et al., *Gene Expression Profiling of Functional Murine Embryonic Stem Cell-Derived Cardiomyocytes and Comparison with Adult Heart: Profiling of Murine ESC-Derived Cardiomyocytes*. Journal of Biomolecular Screening, 2009. **14**(3): p. 239-245.
35. Kapur, N. and K. Banach, *Inositol-1,4,5-trisphosphate-mediated spontaneous activity in mouse embryonic stem cell-derived cardiomyocytes*. J Physiol, 2007. **581**(3): p. 1113-1127.
36. Cho, H.-S., M. Takano, and A. Noma, *The Electrophysiological Properties of Spontaneously Beating Pacemaker Cells Isolated from Mouse Sinoatrial Node*. The Journal of Physiology, 2003. **550**(1): p. 169-180.
37. Lyashkov, A.E., et al., *Calcium Cycling Protein Density and Functional Importance to Automaticity of Isolated Sinoatrial Nodal Cells Are Independent of Cell Size*. Circulation Research, 2007. **100**(12): p. 1723-1731.
38. Nikmaram, M.R., et al., *Characterization of the effects of Ryanodine, TTX, E-4031 and 4-AP on the sinoatrial and atrioventricular nodes*. Progress in Biophysics and Molecular Biology, 2008. **96**(1-3): p. 452-464.
39. Oliphant, L.W. and R.D. Loewen, *Filament systems in Purkinje cells of the sheep heart: Possible alterations of myofibrillogenesis*. Journal of Molecular and Cellular Cardiology, 1976. **8**(9): p. 679-684.
40. Virág, S. and C.E. Challice, *The development of the conduction system in the mouse embryo heart : II. Histogenesis of the atrioventricular node and bundle*. Developmental Biology, 1977. **56**(2): p. 397-411.
41. Kirk, M.M., et al., *Role of the Transverse-Axial Tubule System in Generating Calcium Sparks and Calcium Transients in Rat Atrial Myocytes*. The Journal of Physiology, 2003. **547**(2): p. 441-451.
42. Lyons, G.E., et al., *Developmental regulation of myosin gene expression in mouse cardiac muscle*. The Journal of Cell Biology, 1990. **111**(6): p. 2427-2436.
43. Cordeiro, J.M., J.H.B. Bridge, and K.W. Spitzer, *Early and delayed afterdepolarizations in rabbit heart Purkinje cells viewed by confocal microscopy*. Cell Calcium, 2001. **29**(5): p. 289-297.
44. Verkerk, A.O., et al., *Two types of action potential configuration in single cardiac Purkinje cells of sheep*. American Journal of Physiology - Heart and Circulatory Physiology, 1999. **277**(4): p. H1299-H1310.
45. Stieber, J., et al., *Functional Expression of the Human HCN3 Channel*. Journal of Biological Chemistry, 2005. **280**(41): p. 34635-34643.
46. Lancaster, M.K., et al., *Intracellular Ca<sup>2+</sup> and pacemaking within the rabbit sinoatrial node: heterogeneity of role and control*. The Journal of Physiology, 2004. **556**(2): p. 481-494.
47. Mery, A., et al., *Initiation of Embryonic Cardiac Pacemaker Activity by Inositol 1,4,5-Trisphosphate-dependent Calcium Signaling*. Mol. Biol. Cell, 2005. **16**(5): p. 2414-2423.
48. Rosemblit, N., et al., *Intracellular Calcium Release Channel Expression during Embryogenesis*. Developmental Biology, 1999. **206**(2): p. 163-177.
49. Takeshima, H., et al., *Embryonic lethality and abnormal cardiac myocytes in mice lacking ryanodine receptor type 2*. EMBO J, 1998. **17**(12): p. 3309-3316.
50. Chiesi, M., A. Wrzosek, and S. Grueninger, *The role of the sarcoplasmic reticulum in various types of cardiomyocytes*. Molecular and Cellular Biochemistry, 1994. **130**(2): p. 159-171.

51. Hüser, J., L.A. Blatter, and S.L. Lipsius, *Intracellular Ca<sup>2+</sup> release contributes to automaticity in cat atrial pacemaker cells*. The Journal of Physiology, 2000. **524**(2): p. 415-422.
52. Marger, L., et al., *Functional roles of Cav1.3, Cav3.1 and HCN channels in automaticity of mouse atrioventricular cells: Insights into the atrioventricular pacemaker mechanism*. Landes Bioscience, 2011. **5**(3): p. 251-261.
53. Yanagi, K., et al., *Hyperpolarization-Activated Cyclic Nucleotide-Gated Channels and T-Type Calcium Channels Confer Automaticity of Embryonic Stem Cell-Derived Cardiomyocytes*. Stem Cells, 2007. **25**(11): p. 2712-2719.
54. Niwa, N., et al., *Cav3.2 subunit underlies the functional T-type Ca<sup>2+</sup> channel in murine hearts during the embryonic period*. American Journal of Physiology - Heart and Circulatory Physiology, 2004. **286**(6): p. H2257-H2263.
55. Ferron, L., et al., *Functional and Molecular Characterization of a T-type Ca<sup>2+</sup> Channel During Fetal and Postnatal Rat Heart Development*. Journal of Molecular and Cellular Cardiology, 2002. **34**(5): p. 533-546.
56. Lee, J.-H., et al., *Nickel Block of Three Cloned T-Type Calcium Channels: Low Concentrations Selectively Block α1H*. Biophysical Journal, 1999. **77**(6): p. 3034-3042.
57. Kozlov, A.S., et al., *Distinct kinetics of cloned T-type Ca<sup>2+</sup> channels lead to differential Ca<sup>2+</sup> entry and frequency-dependence during mock action potentials*. European Journal of Neuroscience, 1999. **11**(12): p. 4149-4158.
58. Marionneau, C., et al., *Specific pattern of ionic channel gene expression associated with pacemaker activity in the mouse heart*. The Journal of Physiology, 2005. **562**(1): p. 223-234.
59. Liu, J., et al., *Role of pacemaking current in cardiac nodes: Insights from a comparative study of sinoatrial node and atrioventricular node*. Progress in Biophysics and Molecular Biology, 2007. **96**(1-3): p. 294-304.
60. Ludwig, A., et al., *Two pacemaker channels from human heart with profoundly different activation kinetics*. EMBO J, 1999. **18**(9): p. 2323-2329.
61. Azene, E.M., et al., *Non-equilibrium behavior of HCN channels: Insights into the role of HCN channels in native and engineered pacemakers*. Cardiovasc Res, 2005. **67**(2): p. 263-273.
62. Fenske, S., et al., *HCN3 Contributes to the Ventricular Action Potential Waveform in the Murine Heart*. Circulation Research, 2011.
63. Mistrík, P., et al., *The Murine HCN3 Gene Encodes a Hyperpolarization-activated Cation Channel with Slow Kinetics and Unique Response to Cyclic Nucleotides*. Journal of Biological Chemistry, 2005. **280**(29): p. 27056-27061.
64. Chu, L., et al., *Signal Transduction and Ca<sup>2+</sup> Signaling in Contractile Regulation Induced by Crosstalk Between Endothelin-1 and Norepinephrine in Dog Ventricular Myocardium*. Circ Res, 2003. **92**(9): p. 1024-1032.
65. Kolossov, E., et al., *Identification and characterization of embryonic stem cell-derived pacemaker and atrial cardiomyocytes*. FASEB J., 2005: p. 03-1451fje.
66. Hannes, T., et al., *Biological pacemakers: characterization in an in vitro coculture model*. Journal of Electrocardiology, 2008. **41**(6): p. 562-566.
67. Killeen, M.J., *Drug-induced arrhythmias and sudden cardiac death: implications for the pharmaceutical industry*. Drug Discovery Today, 2009. **14**(11-12): p. 589-597.
68. Herron, T.J., et al., *Purkinje cell calcium dysregulation is the cellular mechanism that underlies catecholaminergic polymorphic ventricular tachycardia*. Heart rhythm : the official journal of the Heart Rhythm Society, 2010. **7**(8): p. 1122-1128.

**Tables:**

Waveform	Incidence (% of total spontaneously active population, $n=504$ )	Average [Ca <sup>2+</sup> ] <sub>i</sub> oscillations per minute ( $\pm$ SEM, $n=47-173$ per group)	Average time-to- peak	Average Width at half-height	Average time from Peak to Baseline	Defining Features
	15.0%	139 ± 6	Rapid	Narrow	Rapid	Extremely rapid [Ca <sup>2+</sup> ] <sub>i</sub> cycling
	16.8%	67 ± 2	Intermediate	Intermediate	Rapid	Small amplitude, relatively rapid [Ca <sup>2+</sup> ] <sub>i</sub> cycling
	23.1%	52 ± 2	Rapid	Narrow	Rapid	Rapid upslope with a tailed down slope
	32.9%	35 ± 1	Slow	Intermediate	Intermediate	Upslope and downslope have roughly equal gradients
	12.2%	14 ± 1	Slow	Very broad	Slow	Prolonged plateau phase

**Table 1:** Kinetic properties of [Ca<sup>2+</sup>]<sub>i</sub> waveforms exhibited by the majority of the Fluo-4 AM loaded spontaneously active Nkx2.5-eGFP<sup>+</sup> population.

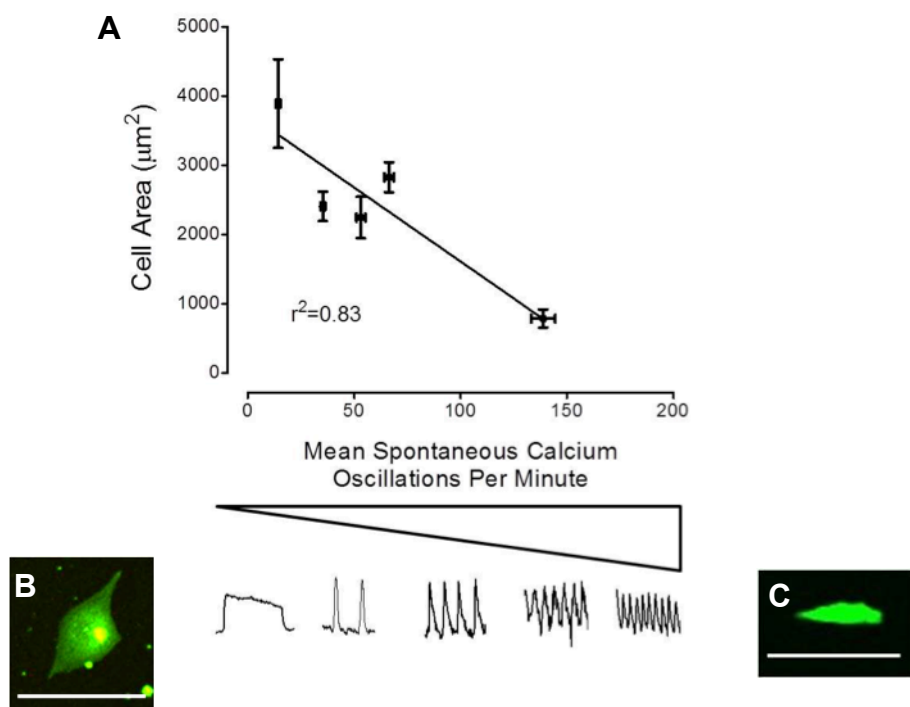


**Figure 1:** Analyses of Morphology and Cell Surface Area. (A) Cell area significantly decreases with increasing  $[\text{Ca}^{2+}]_i$  oscillation frequency ( $P=0.01$ , Linear Regression Analysis,  $n=5-15$  per waveform category). (B) The cells in the slowest oscillating population were typically observed to have processes extending from their cell bodies. The intermediate populations of cells could not be differentiated from one another based on size or morphology. (C) The fastest oscillating cells consistently exhibited typical “pacemaker-like” morphologies and were significantly smaller than those cells belonging to the slowest oscillating population. Scale bar= 100  $\mu\text{m}$ .

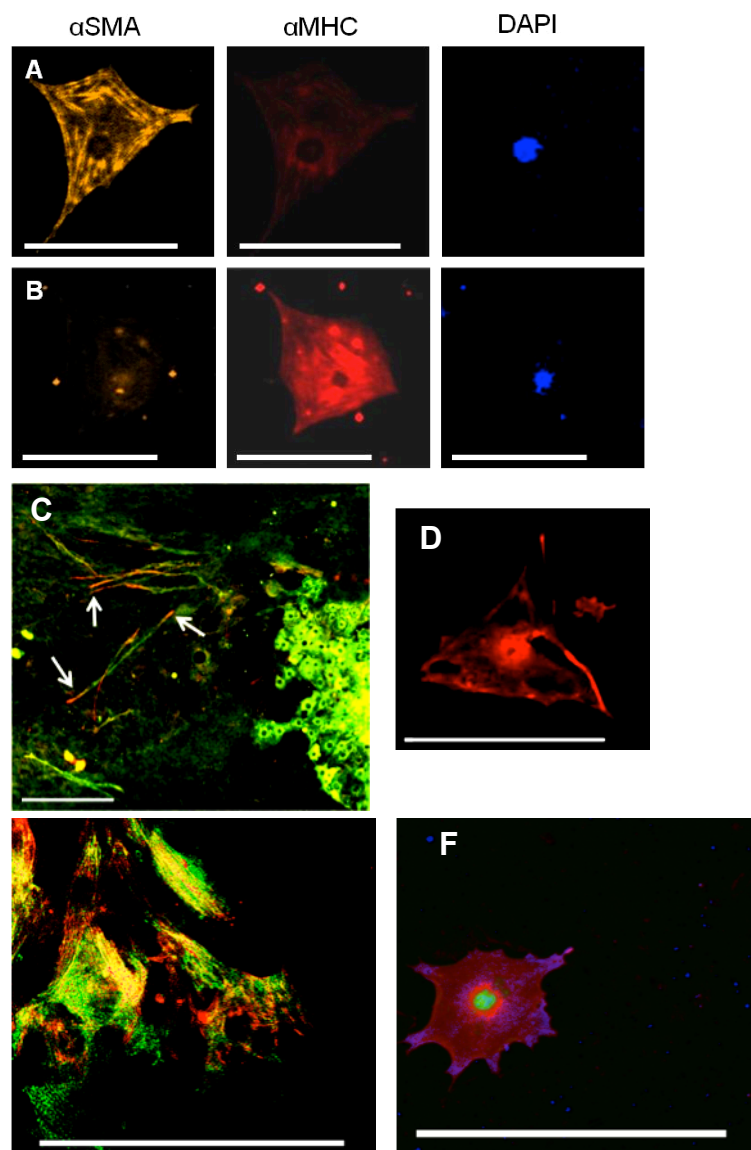


**Figure 2:** Immunocytochemical profiles of single, spontaneously active Nkx2.5-eGFP+ ESC-derived cells. The majority of autorhythmic cells had very distinct cytoskeletal expression profiles, being positive for either (A)  $\alpha$ SMA only or (B)  $\alpha$ MHC only. (C) PGP9.5+ expression was observed in the Nkx2.5 ESC derived beating body cultures (red labelling indicated by white arrows), a marker for Purkinje cells, at the ends of faintly expressing  $\alpha$ MHC+ cells (green), (D) as well as in single spontaneously active cells exhibiting the slowest  $[Ca^{2+}]_i$  oscillations. Mature cells at day 19 of differentiation display organisation of cytoskeletal proteins (E),  $\alpha$ MHC (Green) and cTT (Red) while immature cells display general cytoplasmic labelling of  $\alpha$ MHC (Green), as well as ANP (Red). Scale bar=100  $\mu$ m.

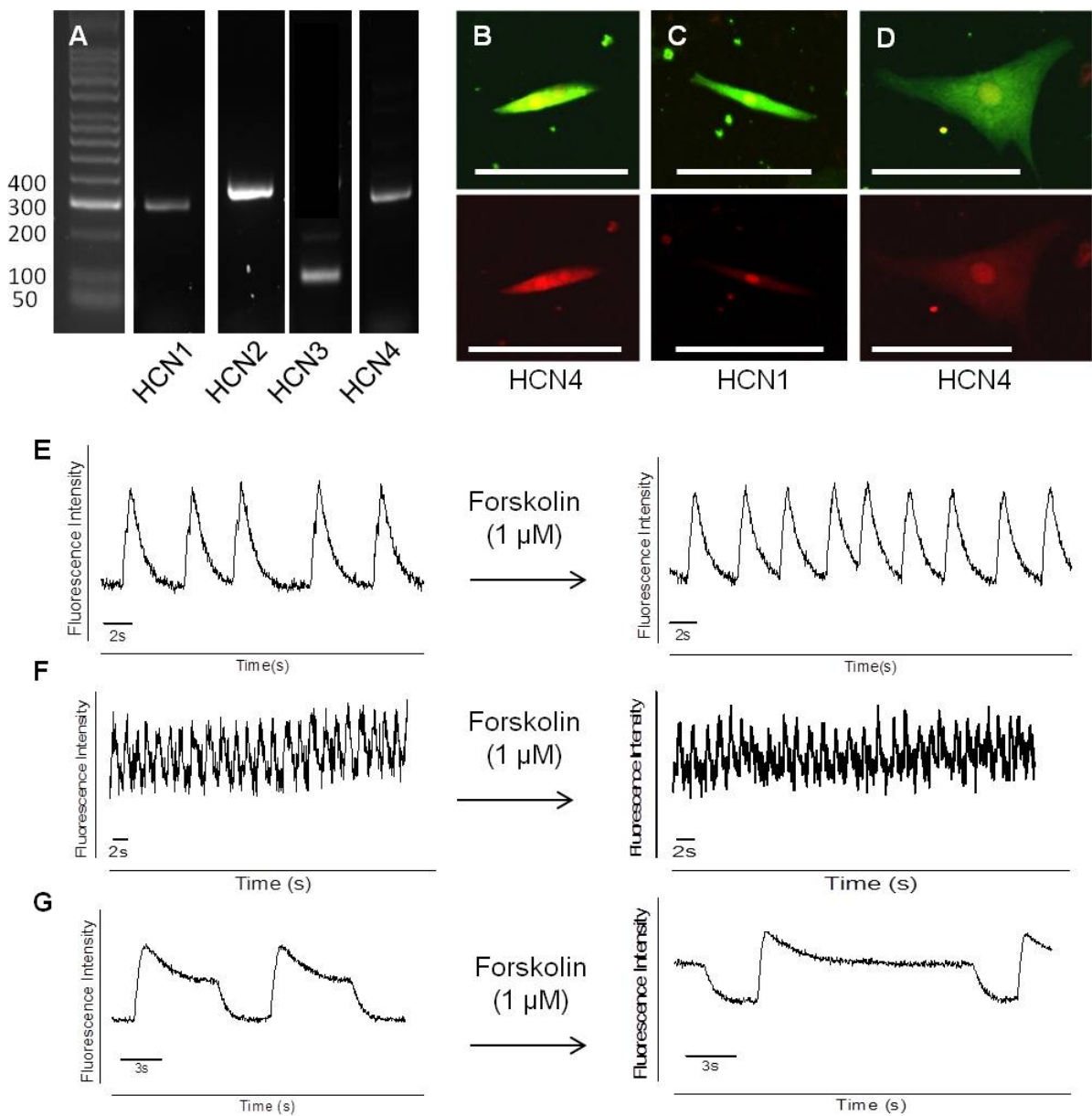


**Figure 3: HCN Channel Expression by Spontaneously Active Nkx2.5-eGFP<sup>+</sup> Cells.**

(A) Sorted Nkx2.5-eGFP<sup>+</sup> cells express all four HCN isoforms. (B) The fastest oscillating pacemaker-like cells express HCN4 (red) but not (C) HCN1 (red). (D) Other spontaneously active cells were not observed to express HCN4 (green=eGFP). (E&F) Investigation of cAMP activation in spontaneously active cells reveals that the faster oscillating pacemaker-like cells respond to forskolin (1 $\mu$ M) with an increase in spontaneous oscillation frequency, indicative of HCN4 or HCN2 expression. (G) The  $[Ca^{2+}]_i$  waveform within the slowest oscillating cells responded to forskolin (1 $\mu$ M) with a prolonged duration, suggesting HCN3 channel expression.

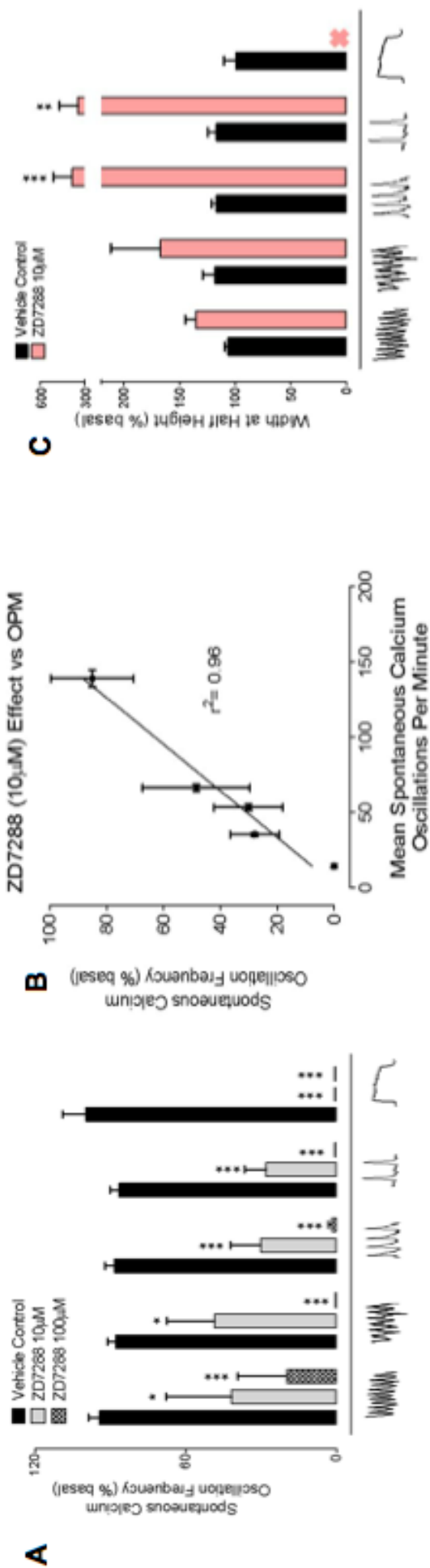


**Figure 4A-C:** (A) ZD7288 (10  $\mu$ M and 100  $\mu$ M) inhibited  $[Ca^{2+}]_i$  oscillation frequency in all waveform groups.(B) . (B) The lower the frequency of  $[Ca^{2+}]_i$  oscillations per minute (OPM) demonstrated by a spontaneously active pacemaker-like cell, the greater the inhibitory effect of ZD7288 (10  $\mu$ M, P=0.004, Linear Regression Analysis, n=3-27 per waveform group). (C) ZD7288 (10  $\mu$ M) also increasingly prolonged the duration of each  $[Ca^{2+}]_i$  oscillation (\*\*P<0.001, \*P<0.05, one-way ANOVA, post-hoc Dunnett's, n= 3-27 per waveform group).

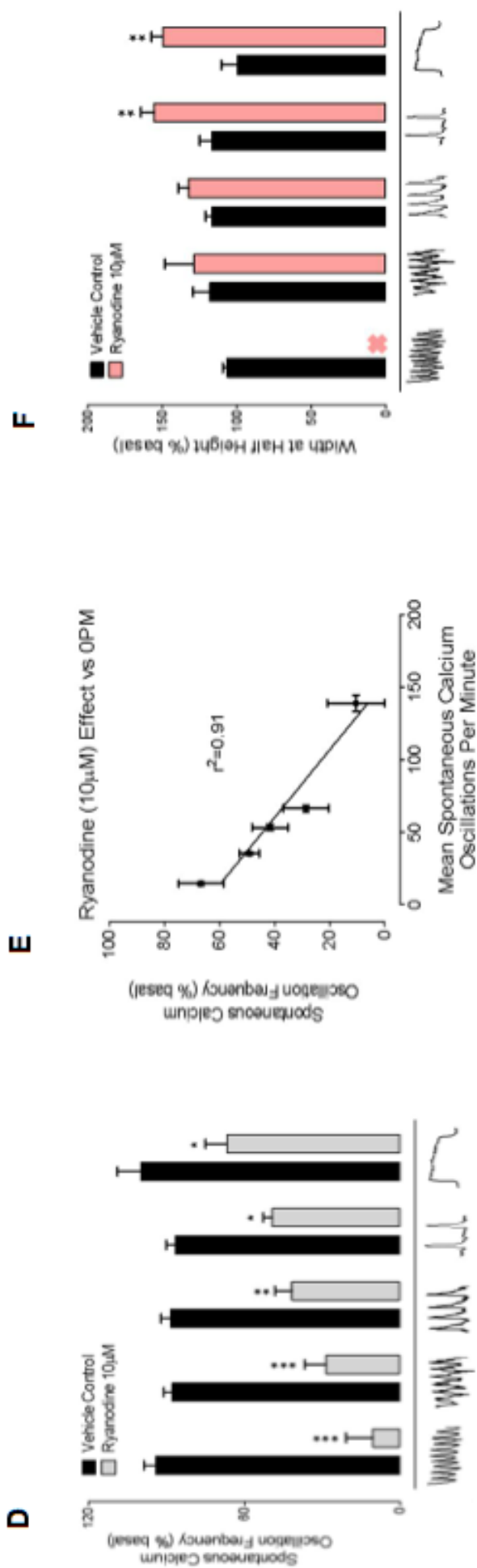


**Figure 4D-F**(D) Ryanodine (10  $\mu$ M) inhibited the frequency of spontaneous  $[Ca^{2+}]_i$  oscillations in all waveform groups (\*\* $P$ <0.001, \*\* $P$ <0.01, \* $P$ <0.05, one-way ANOVA, post-hoc Dunnett's, n=6-29 per waveform group). (E) In contrast to that observed with ZD7288, the inhibitory effect of ryanodine decreased in cells demonstrating increasing  $[Ca^{2+}]_i$  oscillations per minute (OPM,  $P$ =0.01, Linear Regression Analysis, n=6-29 per waveform group). (F) Ryanodine (10 $\mu$ M) also significantly prolonged the width at half height of the two slowest oscillating waveform categories (\*\* $P$ <0.01, one-way ANOVA, post-hoc Dunnett's, n= 6-29 per waveform group). A red cross indicates the cessation of spontaneous activity.

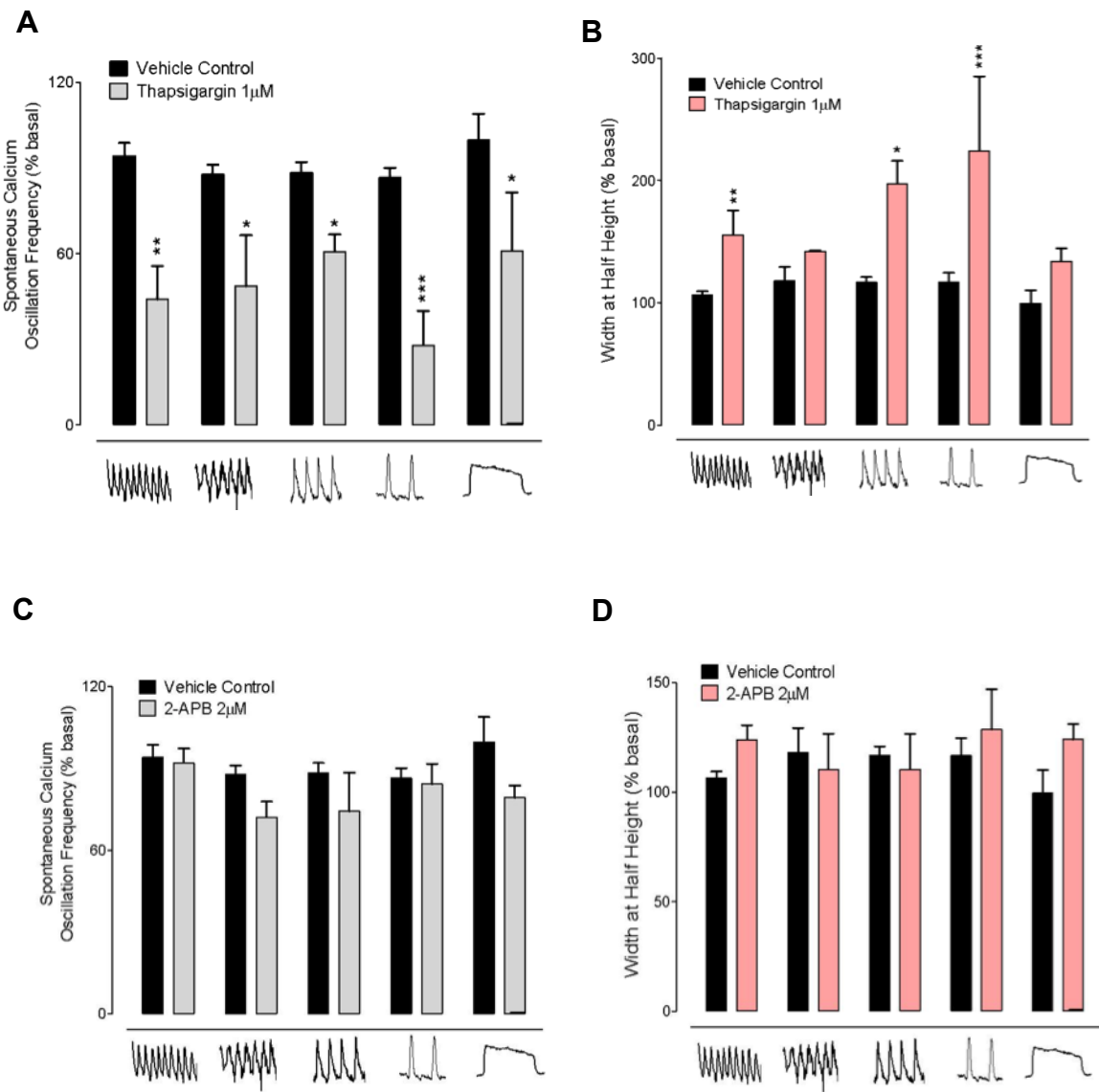


**Figure 5:** (A) Thapsigargin (1  $\mu$ M) attenuated spontaneous  $[Ca^{2+}]_i$  oscillation frequency, as well as (B) prolonged the duration of the  $[Ca^{2+}]_i$  cycle in all waveform groups (\*\* $P<0.001$ , \*\* $P<0.01$ , \* $P<0.05$ , one-way ANOVA, post-hoc Dunnett's, n=4-17 per waveform group). (C) The IP<sub>3</sub> receptor antagonist 2-APB (2  $\mu$ M) had no effect on either the  $[Ca^{2+}]_i$  oscillation frequency or (D) the duration of each  $[Ca^{2+}]_i$  oscillation (n=4-17 per waveform group).

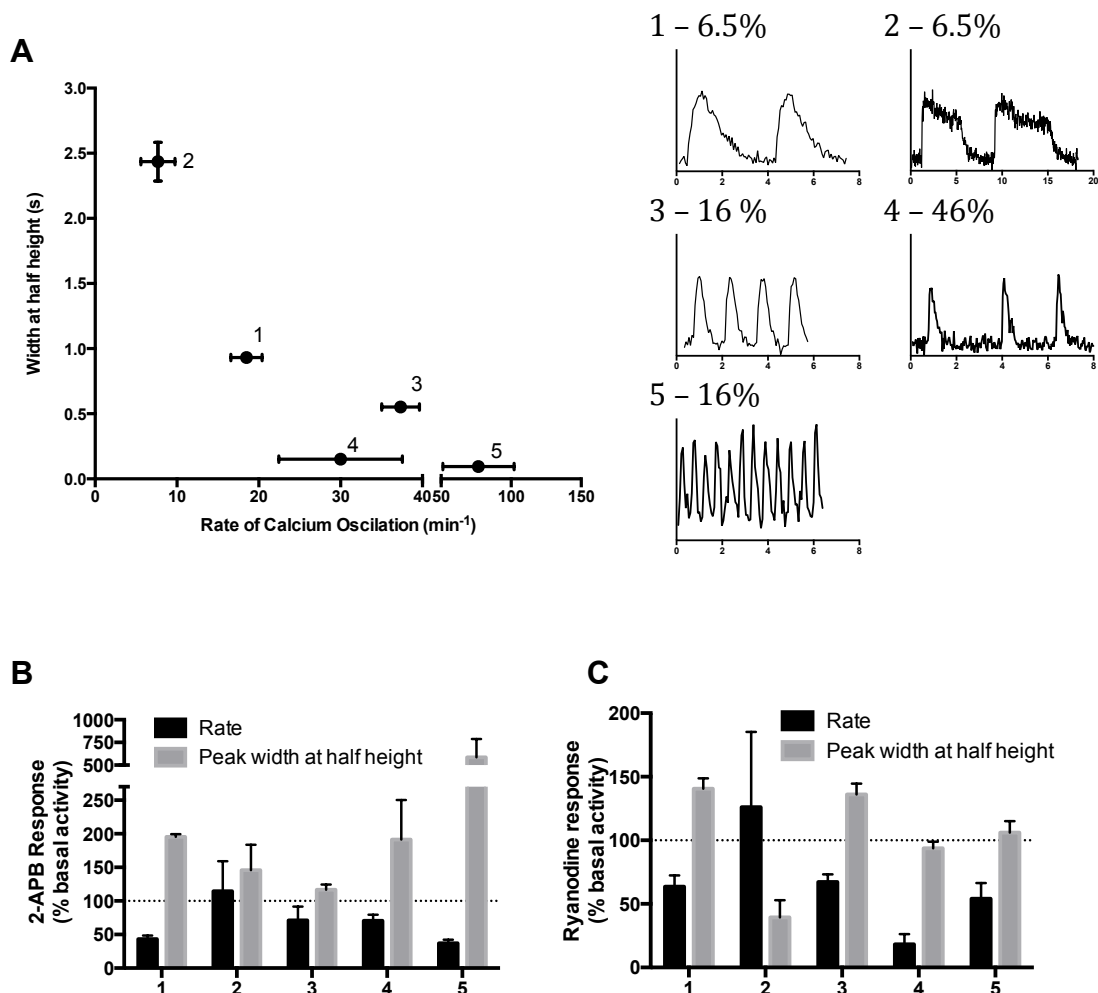


**Figure 6:** (A) Spontaneous calcium oscillations of cardiac progenitors at day 13. Activity could be categorized based on rate and width at half height, representative traces included. (B) The IP3 receptor antagonist 2-APB (2  $\mu\text{M}$ ) inhibited the frequency of spontaneous  $[\text{Ca}^{2+}]_i$  oscillations in 3 of the waveforms ( $P<0.05$ , one-way ANOVA, post-hoc Dunnett's,  $n=4$ ) and prolonged the peak width at half height in 3 ( $P<0.05$ , one-way ANOVA, post-hoc Dunnett's,  $n=3-4$ ). Ryanodine (10  $\mu\text{M}$ ) inhibited the frequency of spontaneous  $[\text{Ca}^{2+}]_i$  oscillations in 4 of the waveforms, the effects on peak width at half height were varied between waveforms.

## **CHAPTER 6 – TRASTUZUMAB AND DOXORUBICIN TOXICITY IN HUMAN ESC**

### **DERIVED EMBRYOID BODIES**

## 6.1 Introduction

Toxicity testing is frequently highlighted as major application of stem cell derived tissues in the drug discovery pipeline. To date many studies have looked at the toxicity of known cardio toxins such as doxorubicin. These agents are known to be toxic in a range of cell based assays due to the non-specific mechanism of toxicity rather than requiring specific signaling cascades {Sartipy:2011ek, Mandenius:2011ds, Cohen:2011ik}. One application, as yet unreported, for human stem cell derived tissues is to examine the toxicity of humanised monoclonal antibodies, whose toxicity cannot be measured in animal models and whose mechanisms of toxicity are likely to rely on signaling cascades only present in specialized cell types. To address this, the current project investigated the effect of the humanised antibody Trastuzumab (trade name Herceptin) on human stem cell derived cardiomyocytes was measured and the mechanism of its toxicity was investigated. The findings from this work provide insight that may help explain differences in the *in vitro* safety profile of Trastuzumab and it's clinically observed toxicity. Furthermore, the utility of human stem cell derived tissue for toxicity screening is reinforced.

## 6.2 Methods

Unless detailed below, the procedures used in this chapter are described in Chapters 2 and 3. Trastuzumab was obtained from Professor David Kaye of the Baker IDI.

### **6.2.1 hESC derived embryoid bodies**

The differentiation of hESC to cardiomyocytes using a variety of methods has been reported(Jang et al. 2008; Ng et al. 2011; Fujiwara et al. 2011; Hartung et al. 2013; Kattman et al. 2011; Burridge et al. 2011; Elliott et al. 2011). Several of these methods were trialed in our lab using the H9 cell line established by James Thompson supplied by WiCell and the HES3 line from MISCL. Despite extensive testing, I was unable to get either cell line to differentiate to spontaneously contracting tissue. Cell survival was an issue during early stages of differentiation, however once this was resolved, I was still unable to generate cardiomyocytes. To ensure the quality of the hESC cultures IHC was performed to confirm the expression of pluripotency markers NANOG and SSEA4, expression was detected in all cultures tested. In the interest of progressing the work cells were obtained from David Elliot (MISCL) differentiated according to his published protocol between days 12 and 14(Elliott et al. 2011). Cells were then maintained until day 90 with a weekly media change, after which monothioglycerol (MTG) and Ascorbic Acid (AA) were withdrawn for 2 weeks prior to toxicity assays.

### **6.2.2 Gene expression analysis**

RNA was prepared using the High Pure RNA Isolation kit according to manufacturer's instructions (Roche). Gene expression was examined on the Illumina HumanWG-6 v3.0 BeadChip at the Australian Genome Research Facility. Labeling, hybridization and scanning performed in accordance with manufacturer's instructions. Expression profiles were established from three independent samples for day 14 eGFP+ve populations sorted from spin EBs. Samples from adult hearts were also analyzed by

microarray. Data was analyzed using Beadstudio Gene Expression Module version 3.4 (Illumina) using average normalization across all samples.

## 6.3 Results

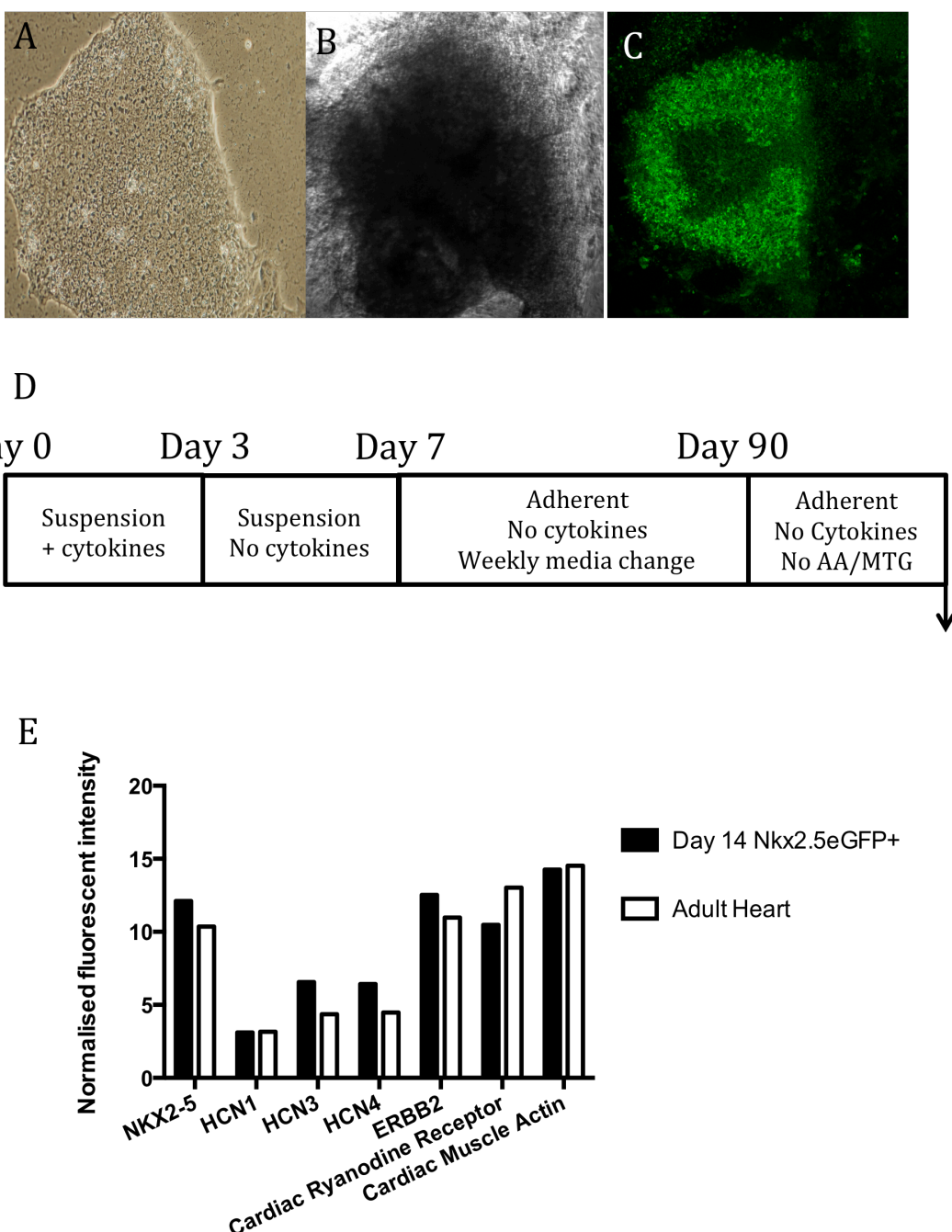
### 6.3.1 Differentiation

The Nkx2.5-eGFP hESC cell line was differentiated towards the cardiac lineage yielding spontaneously beating embryoid bodies from day 7. These cultures contained a high proportion of Nkx2.5-eGFP positive cells (15-40% as determined by FACS), which expressed key cardiac genes as determined by RNA sequencing (Figure 6.1 C).

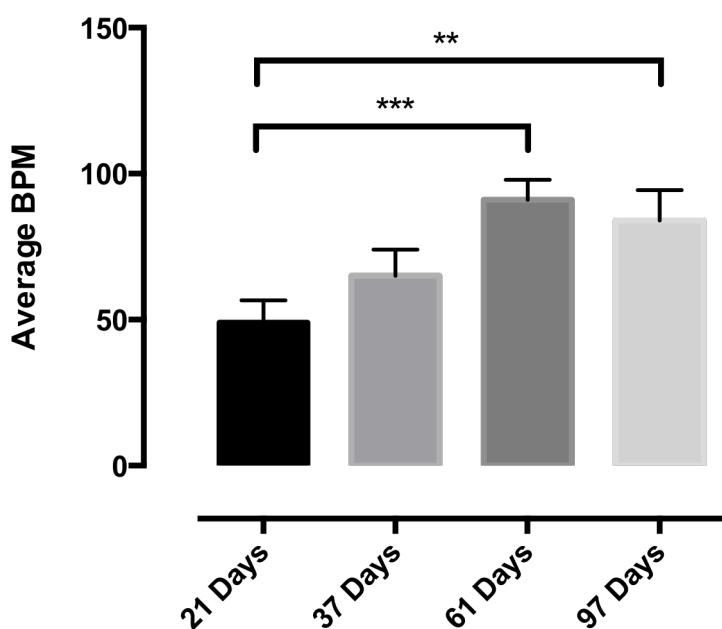
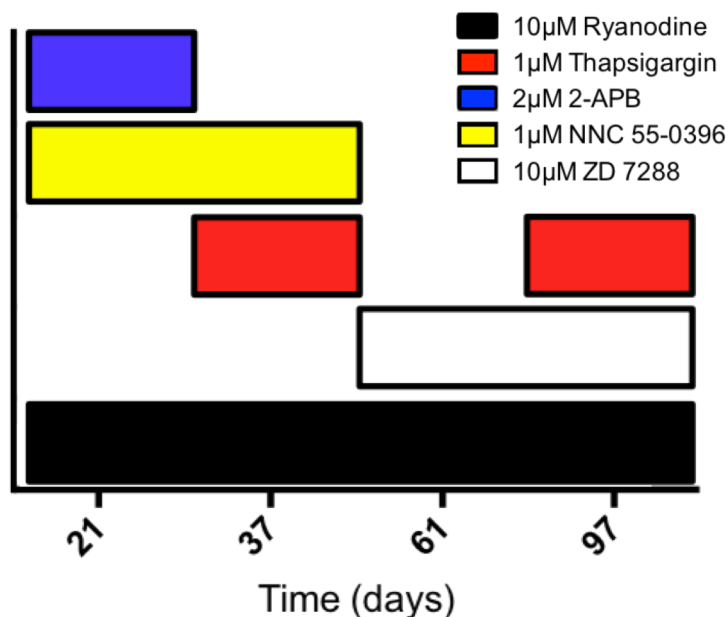
### 6.3.2 Function and Maturation

The molecular mechanisms controlling spontaneous contraction were examined to determine functional maturity (Table 6.1). The spontaneous rate of contraction increased from day 21 to day 61 after which time it did not significantly change. Ryanodine (an inhibitor of calcium sensitive calcium release from the SR) significantly reduced the spontaneous rate of contraction at all time points tested. Thapsigargin (an inhibitor of SERCA) had no significant effect on cultures at day 21 or 61 but significantly reduced contraction amplitude at day 97. 2-APB (an inhibitor of IP<sub>3</sub> induced calcium release) reduced contraction frequency at day 21, but had no significant effect on cultures from day 37. NNC 55-0396 (T Type Ca<sup>2+</sup> channel blocker) abolished beating in cultures up to day 37, after which it had no significant effect. ZD7288 (HCN channel blocker) decreased the spontaneous rate of contraction from day 61 onwards. Reliance on SR calcium, both release and uptake, and HCN channels in EB cultures at day 97

suggests these cells have acquired a mature phenotype by that time point. This is further supported by the lack of response to blockade of IP<sub>3</sub> induced calcium release and T-Type calcium channel blockade at day 97.

**Figure 6.1**

Differentiation of human embryonic stem cells to cardiomyocytes. Undifferentiated hESCs and a day 14 embryoid body (A & B respectively). Cells expressed eGFP under the control of the Nkx2.5-eGFP promoter from day 7 (C). Pictographic representation of differentiation and assay timing (D). Illumina BeadChip Gene expression analysis of Nkx2.5-eGFP + cells demonstrates comparable expression of cardiac genes (Nkx2.5, cardiac actin, HCN, RyR) and HER2 to Adult heart tissue.

**A****B****Figure 6.2**

The spontaneous rate of beating of Nkx2.5-GFP+ hESC-EBs increases during time in culture up until around day 61 post differentiation (\*\*P<0.01, \*\*\*P<0.001, one way ANOVA, post-hoc Dunnett's test, n=12-19 per differentiation time point). Effects of modulators of spontaneous contraction displayed diagrammatically, bars represent time points where spontaneous rate was affected by the indicated compound. EBs were dependant on different molecular mechanisms to maintain spontaneous contraction during differentiation, developing a mature-like phenotype from day 97.

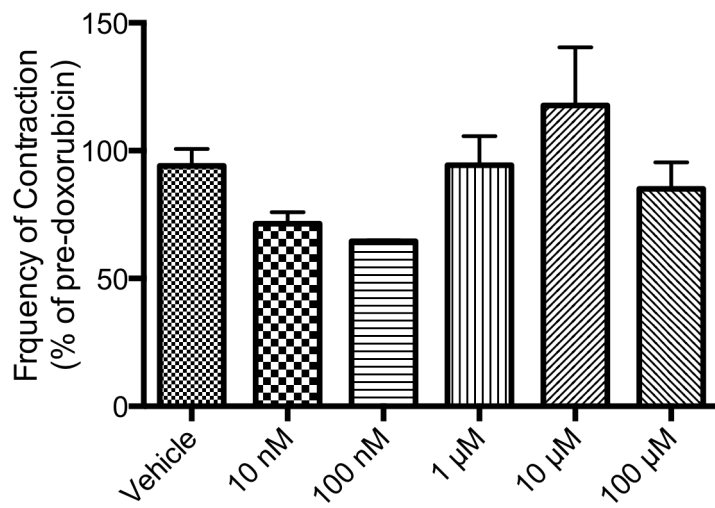
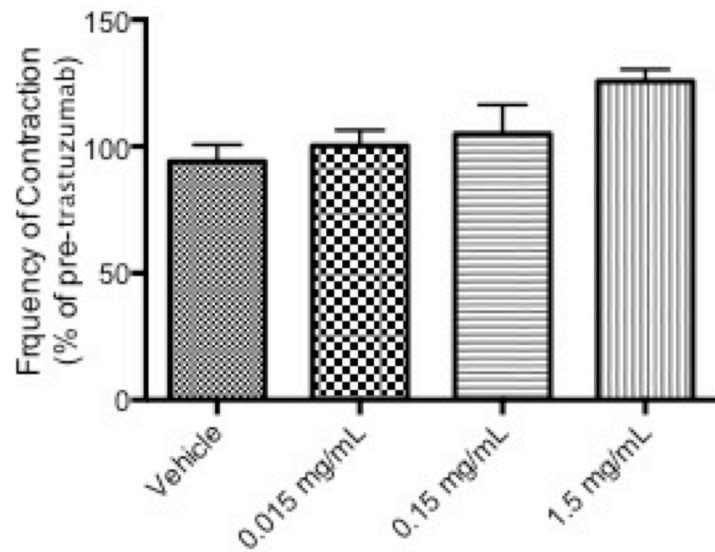
### 6.3.3 Doxorubicin Toxicity

To confirm that EBs are an appropriate model to study cardiotoxicity we examined the effect of doxorubicin treatment. 24 hours of doxorubicin exposure resulted in extensive cell death, including a large number of Nkx2.5-eGFP+ cardiomyocytes as measured using the To-Pro®-3 assay (Figure 6.3). Doxorubicin's effect on rate of contraction during this time was not significant when compared with vehicle. However, treatment with 100 nM showed significantly slower rate than treatment with 10 uM which may be due to disruption of calcium homeostasis as the cell moves from attempting to detoxify at lower (100 mM) calcium levels but suffers from increased membrane permeability at higher (10uM) concentrations followed by a decrease from 10 $\mu$ M to 100 $\mu$ M (Figure 6.2, P<0.05, one way ANOVA bonferroni post-hoc). Biphasic effects of doxorubicin on SR calcium channels have been observed previously, add to the that the importance of mitochondrial calcium stores which doxorubicin interrupts and the complicated functional response to doxorubicin could well be due to altered calcium homeostasis(Wallace 2003; Ondrias et al. 1990). TBARS assay was used to investigate the effect of Dox on lipid peroxidation, which is a measure of free-radical induced toxicity. Dox significantly increased lipid peroxidation, confirming this as a mechanism of Dox toxicity (Figure 6.5 C)(Zhang et al. 2009).

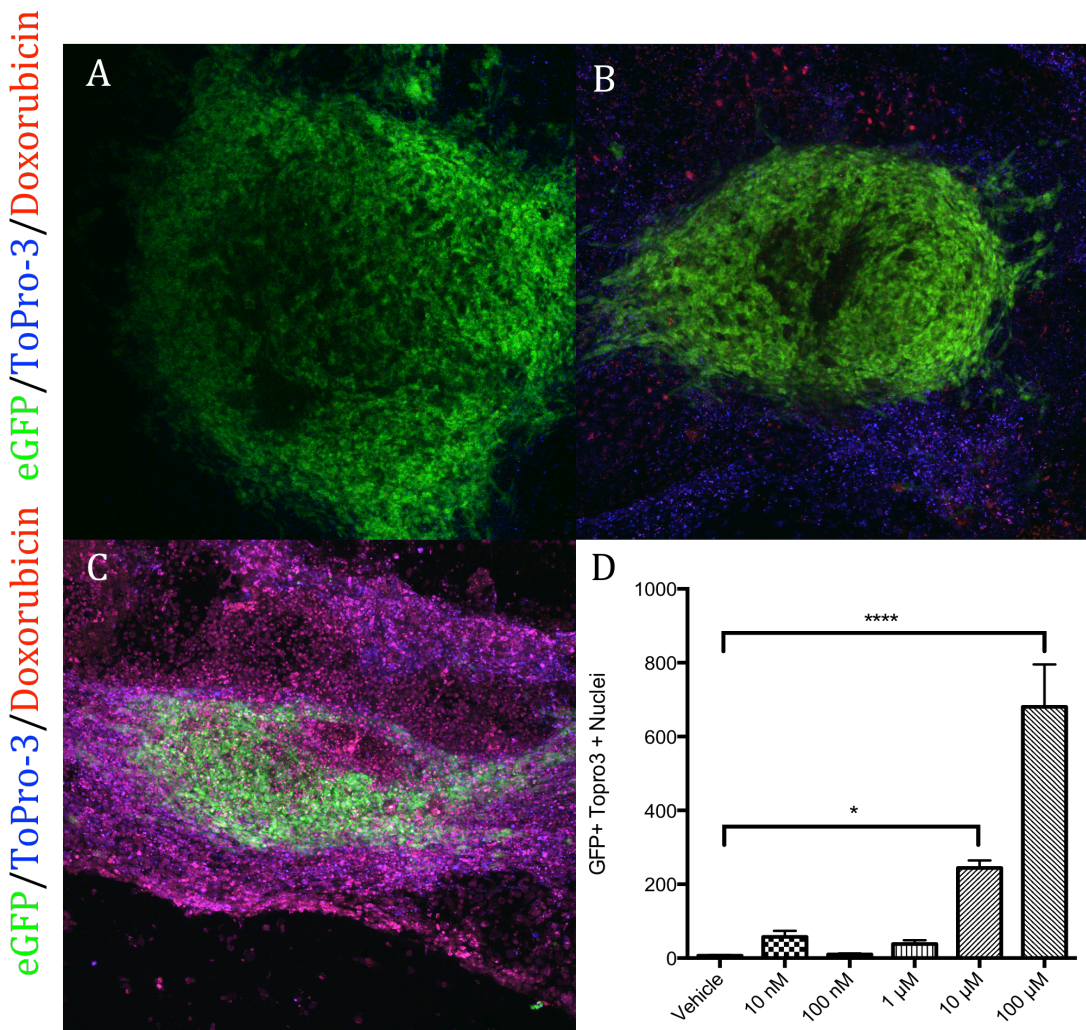
### 6.3.4 Trastuzumab Toxicity

Troponin, being a major component of cardiomyocytes, is released when cardiomyocytes die. Treating cultures with 1.5mg/mL Trastuzumab for 48 hours resulted in no detectable levels of Troponin measured using ELISA. Consistent with this, cell death using To-Pro3® assay showed no significant death. Adding to this

videomorphometry analysis of contraction showed no significant changes during 48 hours of exposure. In contrast to acute exposure, 14 days of Trastuzumab exposure resulted in cardiomyocyte death (To-Pro<sup>©</sup>-3 assay, Figure 6.4 A) troponin release (Figure 6.4 B) and caspase activation (measured using CaspGLOW, Figure 6.6). Caspase activation was detected not only in cardiomyocytes but also in circular structures in close proximity. To determine if these were endothelial cells immunolabelling was attempted using an anti-von Willebrand factor antibody. However, the caspase positive cells were displaced during washing, possibly because they had lost the necessary structure for fixation. Trastuzumab did not cause a significant increase in lipid peroxidation as measured by the TBARS assay at the concentration used in this study (Figure 6.5 D)

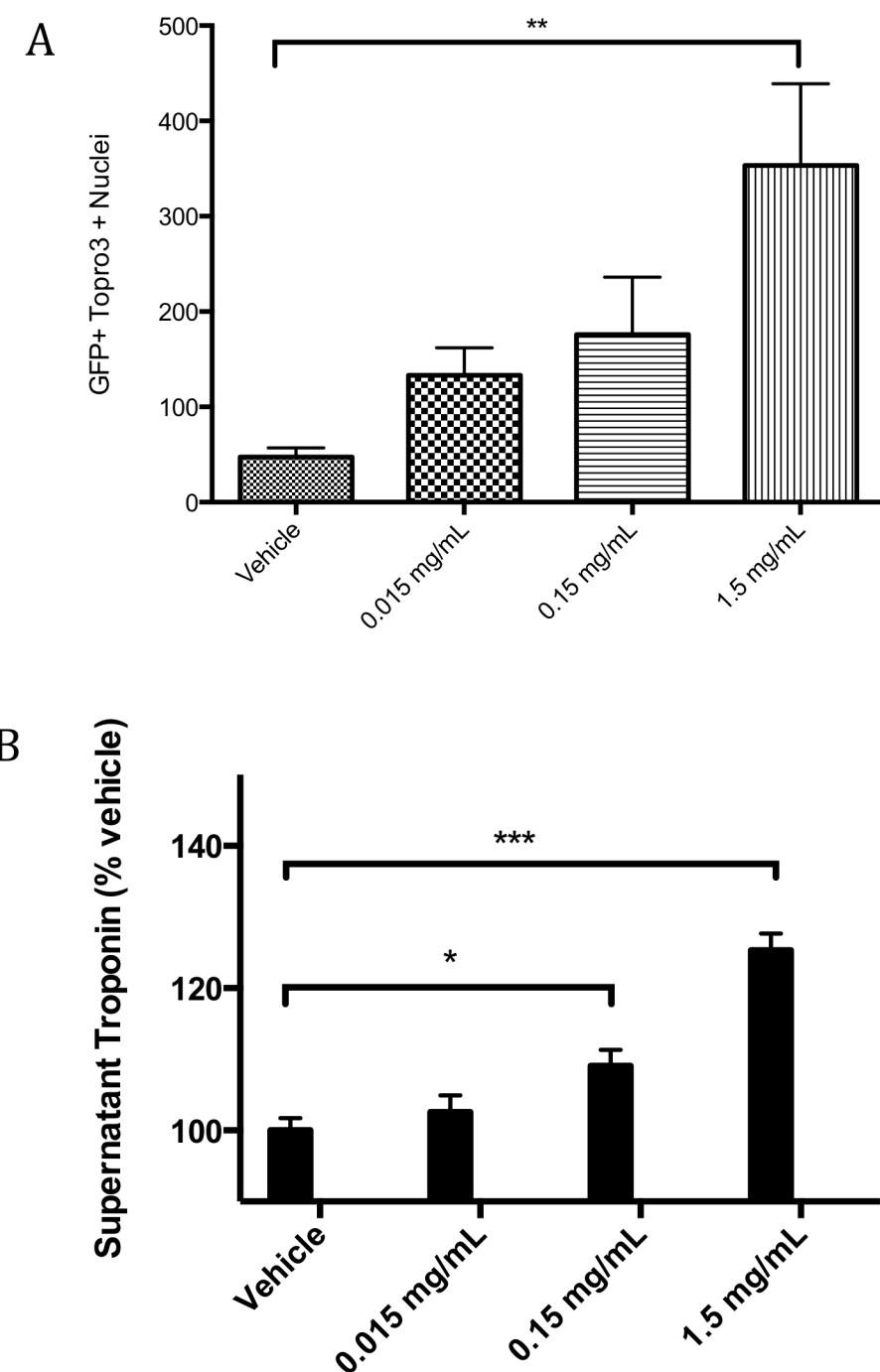
**A****B****Figure 6.3**

Effects of toxic insult on frequency of contraction. Spontaneous frequency of contraction was measured before and after addition of Doxorubicin (A) for 24 hrs, and Trastuzumab (B) for 10 days (mean  $\pm$  SEM).



**Figure 6.4**

Doxorubicin induced cell death determined using To-Pro®-3 cell death assay. Nkx2.5-eGFP (green), Doxorubicin (red) and To-Pro®-3 (blue) in human embryoid bodies treated with vehicle (A), 1  $\mu$ M Doxorubicin (B), and 100  $\mu$ M Doxorubicin (C). The number of number of nuclei that were both eGFP + and To-Pro®-3 + were quantified (D, mean  $\pm$ SEM, \*\*\*P<0.0001, \*P<0.05, one way ANOVA, post-hoc Dunnett's test, n=8-14)

**Figure 6.5**

Trastuzumab induced cell death of embryonic stem cell derived cardiomyocytes. Cell death measured using To-Pro®-3 assay after two weeks of Trastuzumab exposure (A, \*\* $P<0.01$ , one way ANOVA, post-hoc Dunnett's test, n=9-12). ELISA detection of Cardiac Troponin in supernatant of cultures treated with Trastuzumab for 2 weeks (B, \* $P<0.05$ , \*\*\* $P<0.001$ , one way ANOVA, post-hoc Dunnett's test, n=3)

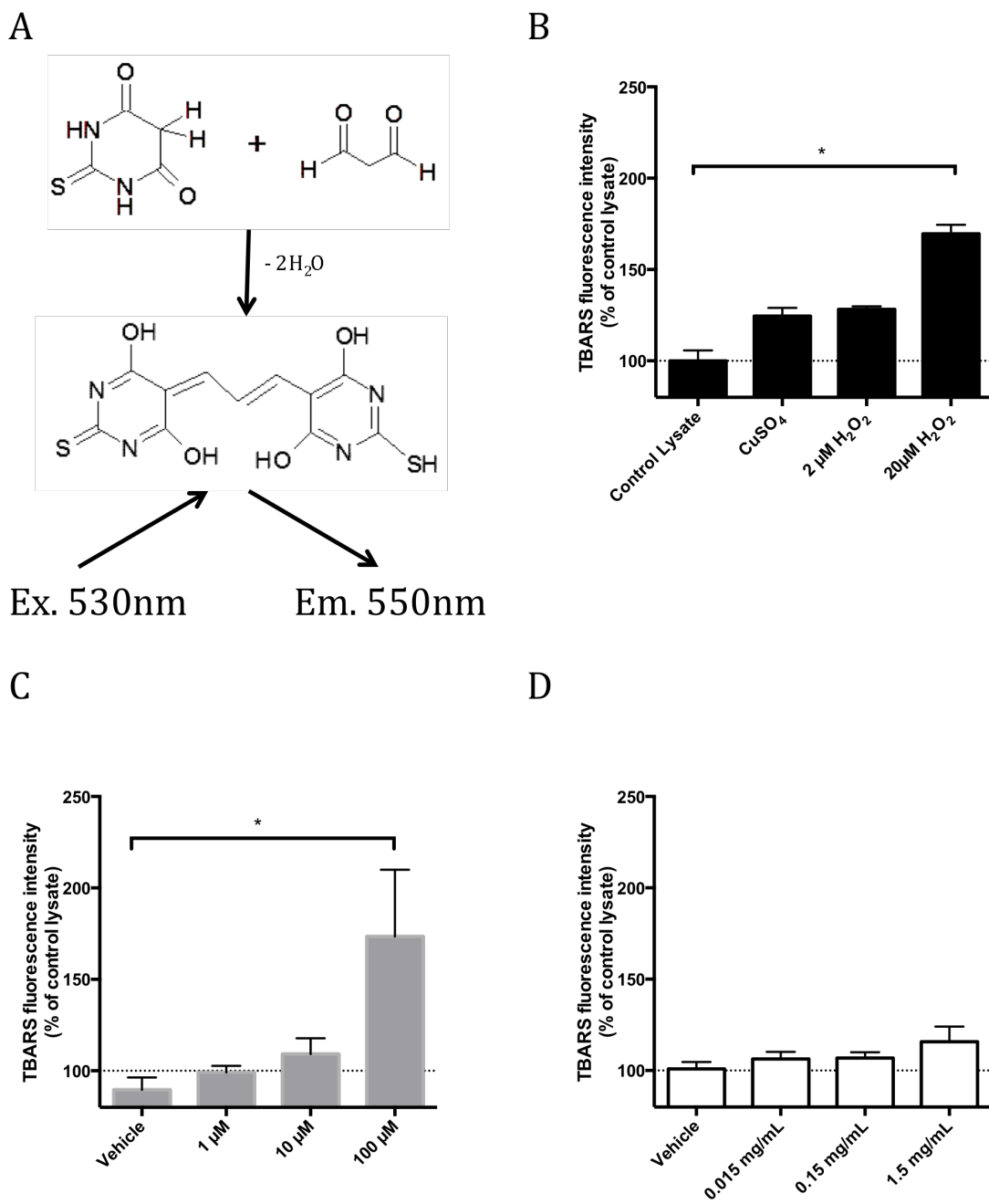
### 6.3.5 Mechanisms

To test the hypothesis that Trastuzumab induces toxicity by disrupting cell signaling downstream of the HER2 receptor, I used a kinase inhibitor that targets the HER2 receptor. CP 724714 is a kinase inhibitor shown to have selective activity on erbB2 as opposed to other EGFR receptors(Jani et al. 2007). Sustained exposure to CP 724714 resulted in cardiomyocyte death and caspase activation in the same manner as Trastuzumab.

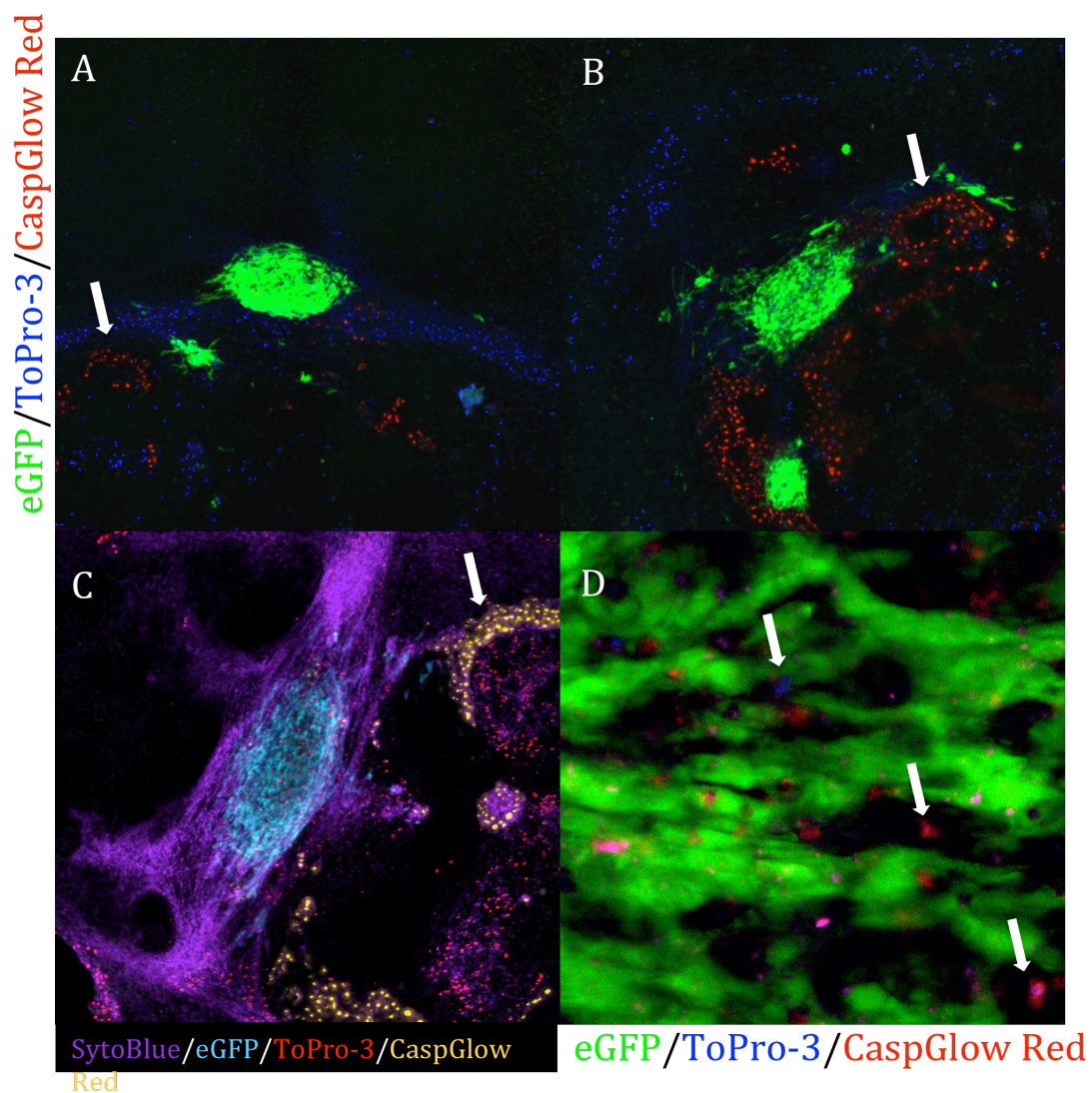
Trastuzumab-induced caspase activation in endothelial-like structures within the EBs (Figure 6.6), indicated a potential mechanism of toxicity. While not previously observed with Trastuzumab, anthracyclines including Dox have been shown to stimulate nitric oxide release from endothelium, which contributes to Dox toxicity(Foglie et al. 2004). Nitric oxide generation following Trastuzumab and CP 724714 treatment of HMVEC cells was measured using the nitric oxide sensing DAF. CP 724714 inhibition of HER2 signaling increased DAF fluorescence indicating increased nitric oxide synthesis. Trastuzumab similarly (but non-significantly) increased DAF fluorescence (Fig 6.9C), suggesting that receptor-mediated toxicity may be mediated through local NO production, possibly from endothelium.

To support the hypothesis that toxicity is mediated by non-cardiomyocytes in the heterogeneous EBs, I sorted Nkx2.5-eGFP cells from mature EB cultures and exposed them to Trastuzumab or CP 724714. Following two weeks of exposure to the same concentrations used in the previous studies neither troponin release nor To-Pro©-3

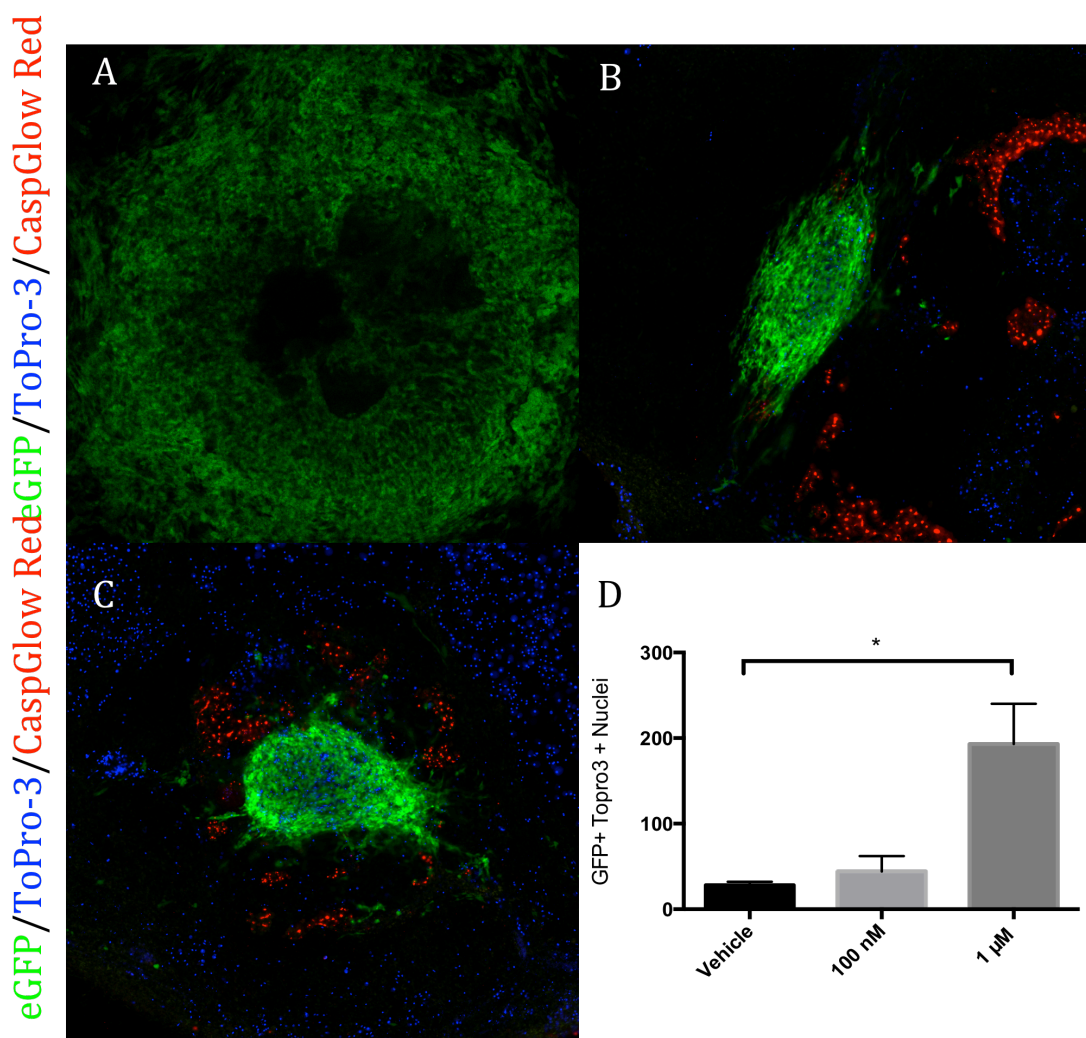
positive nuclei were detected. This suggests that Trastuzumab toxicity depends on effects on endothelial-like cells, or possibly other accessory cells in the EB.

**Figure 6.6**

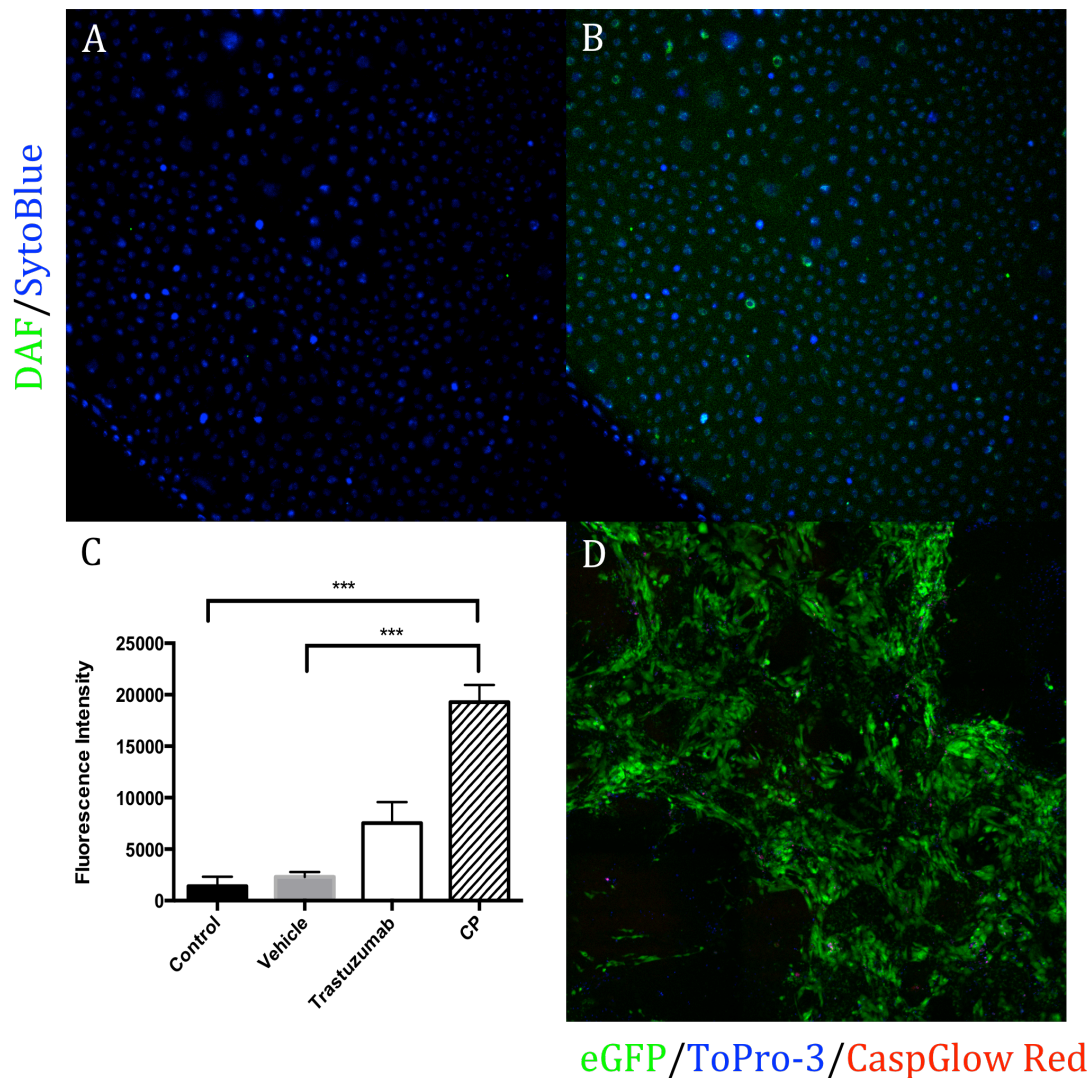
Lipid peroxidation following toxic insult measured using TBARS assay. The reaction between TBA and the lipid oxidative product MDA yields a fluorescent product (A). TBARS production following exposure of hEB to pro-oxidants CuSO<sub>4</sub> and H<sub>2</sub>O<sub>2</sub> (B, \*P<0.05, one way ANOVA, post-hoc Dunnett's test, n=3). TBARS production following exposure of hEB to Dox for 24h (C, \*P<0.05, one way ANOVA, post-hoc Dunnett's test, n=3). TBARS production following exposure of hEB to Trastuzumab for 2 weeks (D).

**Figure 6.7**

Mechanism of Trastuzumab induced cell death determined using To-Pro®-3 and CaspGLOW Red assay. Nkx2.5-eGFP (green), CaspGLOW Red (red) and To-Pro®-3 (blue) in human embryoid bodies treated with Trastuzumab (A&B, white arrows highlight CaspGLOW + 'vessel-like' structures). SytoBlue (violet), Nkx2.5-eGFP (cyan), CaspGLOW Red (yellow) and To-Pro®-3 (red) in human embryoid bodies treated with Trastuzumab (C). High magnification image of eGFP (green), CaspGLOW Red (red) and To-Pro®-3 (blue) (D, white arrows highlight cells that are single positive for either stain, or double positive for both).

**Figure 6.8**

Toxicity of the ErbB2 (HER2) kinase inhibitor CP 724 714 determined using To-Pro®-3 and CaspGLOW Red assay. Nkx2.5-eGFP (green), CaspGLOW Red (red) and To-Pro®-3 (blue) in human embryoid bodies treated with vehicle, 100 nM and 1  $\mu$ M CP 724 714 (A, B, and C respectively). The number of nuclei that were both eGFP + and To-Pro®-3 + were quantified (D, mean  $\pm$  SEM, \*P<0.05, one way ANOVA, post-hoc Dunnett's test, n=3)

**Figure 6.9**

Nitric oxide release induced by Trastuzumab or CP 724714 in HMVEC cells at 5 mins (A) and 30 mins (B) measured by DAF fluorescence. Cells were selected using SytoBlue counter stain, and then the sum of DAF fluorescence intensity was measured (C, mean  $\pm$  SEM, \*\*\*P<0.001, \*P<0.05, two way ANOVA, post-hoc Dunnett's test, n=3). FACS sorted Nkx2.5-eGFP cells displayed significantly reduced toxicity to CP 724714 (D, Nkx2.5-eGFP (green), CaspGLOW Red (red) and To-Pro®-3 (blue)).

## 6.4 Discussion

To date, no published studies have used human stem cell derived tissues to test for the toxicity of a humanized antibody. To address this, the current study investigated the use of human embryonic stem cell derived cardiomyocytes to examine the cellular and molecular basis for toxicity of the humanized antibody Trastuzumab. Trastuzumab is known to have a developmental cardiotoxicity that was not the intended focus of this study. For this reason, it was necessary to confirm the functional maturity of the EB cultures prior to toxicity studies.

Previous work demonstrating embryonic stem cell derived cardiomyocytes as toxicology models have included functional characterisation to various extents. Groups presenting differentiation methods have included functional results often concluding that the cells displayed an abnormal, non-physiological, immature phenotype until cultured beyond standard culture protocols (up to three months)(Sedan et al. 2010; Liu et al. 2009; Kim et al. 2010). The question that remains unanswered is what importance this immaturity has on toxicity assays, and until this is dealt with it is necessary to demonstrate that cells used in these assays display functional integrity. To this end the functional data described in 6.4.2 indicates that by day 97 the cells used in this study have acquired a mature calcium handling phenotype, relying on sarcoplasmic calcium store cycling and HCN channels to maintain spontaneous activity while being insensitive to IP<sub>3</sub> calcium release inhibition or T-Type calcium channel blockade. Comparison of primary human myocardium to the late stage differentiated cells using

metabolomic, proteomic and transcriptomic approaches, however important, were considered outside the scope of this study, the main aim of which was to assess the utility of stem cell derived cultures for use in models of toxicity.

There are many methods used to assess phenotype and functional maturity of cardiomyocytes including immunochemistry, mRNA profiling, electrophysiology and calcium imaging, however there isn't a prescribed method employed by all researchers internationally making comparisons between findings difficult. Embryonic stem cell derived models may present an opportunity for advanced biological models, but until standardized approaches to phenotyping are developed it will be unlikely to see widespread adoption. Standardization and rigorous testing is a major requirement prior to acceptance of new models by regulatory bodies and industry, and is a critical step before establishing novel toxicology models.

The cardiotoxicity of the anthracyclines, such as Doxorubicin (Dox), is well established and while there is some contention regarding the exact mechanism of clinical toxicity, there are well-defined toxic actions of this class of drugs(Doroshow 1991; Zhang et al. 2009). Widely considered to be integral to the toxicity of Dox is free radical-induced oxidative stress, which can be identified in many compartments within the cell but most critically in the mitochondria where Dox has been shown to act directly and indirectly to cause damage to mitochondrial DNA, ultimately resulting in apoptosis (Wallace 2003). The acute toxicity of doxorubicin observed in this study confirms what has been reported by other groups with respect to the timing of insult (Farokhpour et al. 2009) (Andersson et al. 2010). However the cells used in this study appear to be more

sensitive than previous observations, possibly due to the extended aging protocol used here, or the removal of protective components of the media such as ascorbic acid (AA) and monothioglycerol (MTG).

Acute toxicity studies often ignore the effects of protective media components during assays. This may not be a big problem when preparing an *in vitro* LD<sub>50</sub> on an acute time scale as most of these *in vitro* screens will be comparing candidate compounds against known toxins and are largely comparative. However, on a chronic time scale the protective effects of antioxidants and other components have the potential to overcome and conceal toxicities. ESC maintenance and differentiation media often contain multiple protective components – for example the ascorbic acid and monothioglycerol in the differentiation media used for this chapter. Ascorbic acid and monothioglycerol are free radical scavengers. Furthermore, MTG is capable of reducing proteins via a thiol group enabling regeneration of cellular glutathione (GSH) from the oxidized form of glutathione disulphide (GSSG). These functions clearly have protective effects and are likely to affect any biological readout with respect to toxicity. The absence of ascorbic acid and monothioglycerol enhanced doxorubicin toxicity and unveiled previously undetected Trastuzumab toxicity.

In contrast to Doxorubicin there is much contention regarding the occurrence and potential mechanisms of toxicity of trastuzumab. At the clinical level, studies investigating the association of trastuzumab and cardiac toxicity have reported mixed findings, some establishing a positive correlation while others have reported a non-significant correlation(Bird & Swain 2008) (Seidman 2002) (Suter et al. 2004). These

studies are difficult to compare due to the different measures employed to determine outcomes such as; the number of patients with progression free survival, incidence of congestive heart failure, or proportion of patients that achieved complete cardiac recovery following withdrawal of chemotherapy. This is further complicated by the lack of an appropriate *in vitro* model. One study, (Yoshiyama et al. 2003), conducted in chick embryos, showed an acute dose dependent response resulting in a reduced rate of contraction and the development of an arrhythmia. This study failed to address the clinically observed chronic toxicity profile of Trastuzumab, and is highly dependent on assumed structural homology between the chicken and human target protein. The specificity of monoclonal antibodies is one their key strengths, however, this limits the use of standard preclinical models for testing of toxicity and tolerance.

Knockout mice provide one mechanism to explore the possible toxicity of monoclonal antibody therapies, however, developmental toxicity, compensatory gene expression, species differences, and lack of possible immune mediated responses limit their utility in predicting human toxicity of antibody therapies. Toxicity testing of monoclonal antibodies typically relies on extensive characterisation of the effect of target knock down in animal models and human derived cell lines, assuming that any phenotype identified in knock-down models is representative of immunotherapy toxicity. The systemic knockdown of ErbB2 (HER2) in a mutant mouse resulted in fatal cardiac malformations before embryonic day E11(Negro 2004). To examine the effects of HER2 knockout on adult myocardium conditional knockout mice were produced by crossing mice with floxed ErB2 alleles with mice expressing Cre recombinase driven by either the promoter for muscle creatine kinase (MCK) or myosin light chain 2v (MLC2v). Both

conditional knockouts display a similar cardiac phenotype, developing dilated cardiomyopathy commensurate with the cardiac expression of genes driving Cre expression(Negro 2004). Dilated cardiomyopathy was characterised by increased ventricular dilation and decreased cardiac contractility, however in contrast to most forms of dilated cardiomyopathy the conditional knockouts myocardium was still responsive to  $\beta$ -adrenergic stimulation. A major limitation of using conditional knockouts to model immunotherapy toxicities is the selective knockdown of target signaling, if the toxicity is mediated via an alternate cell type or interaction it will be overlooked.

Developmental toxicity of trastuzumab is mediated via disruption of a critical signaling pathway involving a heterodimer of erbB2 and erbB4(Force, Krause & Van Etten 2007a). Dilated cardiomyopathy is also thought to occur via this mechanism; reducing contractility of the mature myocardium. The molecular mechanism that is thought to explain reduced contractility does not involve any sort of oxidative stress, and as a result one would not expect to see lipid peroxidation following trastuzumab exposure, concurring with the results presented above. However, Loss of contractility and onset of clinical dilated cardiomyopathy does not explain cases of clinical toxicity where withdrawal of Trastuzumab does not resolve the dilated cardiomyopathy(Ewer et al. 2005). Furthermore, frequency and severity of toxic responses to dual trastuzumab/anthracycline treatments would suggest an unexpected symbiotic relationship between the relatively innocuous signal based toxicity of trastuzumab and the highly reactive Dox(Tarantini et al. 2012). The more established and accepted

pathway of trastuzumab related cardiotoxicity does not adequately explain the clinically observed toxicity of trastuzumab.

Having established trastuzumab toxicity in our model, it seemed pertinent to determine what mechanism was causing cell death. The first step to address a mechanism of toxicity is to confirm if cell death is occurring via apoptosis or necrosis. Using a fluorescent caspase ligand, we have shown that the cardiomyocytes in Trastuzumab treated cultures are undergoing caspase activation suggesting apoptosis-mediated toxicity. Surprisingly, caspase activation and death in response to Trastuzumab toxicity was also observed in discrete vessel-like structures. Immunochemical labelling of the dying/dead cells was attempted with limited success; however, we have previously seen structures like this stain with Von Willebrands factor, a marker of endothelial cells. The possibility of other cell types being sensitive to Trastuzumab toxicity has not been discussed widely in the literature. Assuming the tight gap junctions of the myocardial endothelium are intact, unlike those of the target tumor, the amount of trastuzumab penetrating to the myocardium is presumably quite low. With this in mind, an endothelial component to trastuzumab cardiotoxicity is quite a reasonable hypothesis.

Assuming the toxicity of Trastuzumab is facilitated primarily through the erbB2 receptor then presumably kinase inhibitors that affect this receptor should display a similar toxicity *in vitro*. The latest generation of kinase inhibitors has far superior selectivity and efficacy than the last generation, making them viable options for substitution of humanised antibodies and useful tools for biological studies. Those characteristics also make them useful tools for exploring the mechanism of trastuzumab

toxicity. CP 724714 is a highly selective kinase inhibitor of erbB2 showing little affinity for other EGFR isoforms. The similarity of toxicity profile of CP 724714 to trastuzumab in this model supports the hypothesis that the observed toxicity is driven by a signaling mechanism rather than a chemical one such as free radical generation. The toxicity of CP 724714 could indicate a toxicity that will carry through all drugs that target the HER2 receptor. There is also the possibility, like with Vioxx, where the unique selectivity of each compound will impact the potential safety profile. This finding may have implications for proposed treatment regiments, but also support shESC EBs to be used for further studies to understand this toxicity.

Here I have presented strong evidence of an HER2 dependent toxicity that extends beyond previously published work. I have put forward persuasive evidence that within the heterogeneous system of the EB an intercellular crosstalk mediates chronic Trastuzumab induced cell death. The presence of activated caspases in vessel-like structures indicates that an endothelial component might be contributing to trastuzumab-induced toxicity. It is known that NO is a key mediator of anthracycline toxicity(Foglie et al. 2004). It is also known that the endothelium plays an important role in regulation of cardiac NO(Belhassen 1996). This led to the hypothesis that trastuzumab toxicity was, at least in part, driven by endothelial cell death and NO release.

In order to test this hypothesis HMVECs were treated with Trastuzumab and CP 724714 and then NO oxide was measured using DAF. The significant increase in DAF fluorescence suggests that treatment of HMVECs with CP 724714 increases NO release.

In a separate experiment the human Nkx2.5-eGFP +ve cardiac cells were sorted from mature cultures, excluding any endothelial like cells, replated and then tested for trastuzumab sensitivity. Sorted cultures of Nkx2.5-eGFP cells were highly insensitive to Trastuzumab or CP 724714 induced toxicity, further supporting the hypothesis that toxicity is being facilitated by an alternate cell type present in heterogeneous cultures.

The methods established for this investigation are novel with respect to their selective analysis of the subset of cardiac cells within the heterogeneous environment of the EB. In a high content setting, the reporter line and selective dyes combined with confocal microscopy provide a method for both quantification of cell death and avenues for exploring the potential mechanisms. In a screening environment, the ELISA detected troponin release assay would provide higher throughput and sensitivity while providing greater selectivity than simple LDH assays. An extension of this approach would be to engineer a cell line using luciferase as well as GFP as a reporter as the enzymatic detection of luciferase bioluminescence would likely provide greater sensitivity than both the methods employed for this study. Another tool that may extend the utility of these models is the inclusion of fluorescent proteins sensitive to calcium ions or the redox state of the cells. These would facilitate investigations to further clarify the mechanism of toxicity of trastuzumab, or for that matter, any other contentious cardio toxin.

## 6.5 Conclusion

The findings from this study add important information to the contentious issue of Trastuzumab toxicity. The combination of physiologically relevant heterogeneity, sophisticated analytical techniques and human derived tissues has unveiled a previously unidentified mechanism for Trastuzumab toxicity. Using these methods, further investigation may yield mechanistic insight, possibly allowing for identification of adjuvant therapies to prevent or reverse toxicity. Extending this approach to patient derived iPSCs may permit identification of clinical markers predictive of toxicity, which could be used to better direct chemotherapy strategies. Beyond the clinical implications of these findings, which have the potential to save both money and lives, the broader implication of these results could see this sort of study as a regulatory requirement for preclinical toxicity screening of humanised antibodies.

## CHAPTER 7 – CONCLUDING REMARKS

The inadequacy of models currently used in drug discovery and development for prediction of pharmacology, off-target effects and toxicology have lead to the occasional preclinical and clinical failure of drug candidates. Stem cell derived tissues are a possible solution to these shortcomings, as they allow generation of models with native human biology, and cellular heterogeneity within a physiological context. This has the potential for greater accuracy in prediction of clinical outcomes. Tissues generated from embryonic stem cells (ESCs) more closely reflect human tissue than those currently used in *in vitro* models, due to both their heterogeneity and complex 3D architecture. However, this limits their usefulness in standard pharmacological, toxicological and biochemical analysis techniques. This study set out to investigate the pharmacology, function and toxicity of stem cell-derived cardiomyocytes in a variety of purpose-developed assays to test the hypothesis that stem cell derived models can be used in place of more traditional *in vitro* models; thereby delivering models with greater human and physiological relevance. Extensive method development and optimisation was undertaken which showed that complexity arising from hESC culture heterogeneity and 3D architecture may be resolved to allow for measurement of specific and non-specific cellular function in both 3D and monolayer paradigms. This work suggests that stem cell derived tissues may make important contribution to various stages of drug development and drug discovery with scope to incorporate them into the regulatory requirements. Furthermore, the work presented here highlights the potential of stem cell-derived models to answer questions not addressable by current *in vitro* or *in vivo* methods.

A key finding from this study is that ESC-derived embryoid bodies may be used as pharmacological models, particularly for drug screening of well-characterised systems. The most up-to-date methods of cardiomyocyte differentiation rely on embryoid body formation, which is prone to heterogeneous outcomes with variable efficiency. Generation of multiple cell types has complicated translation to pharmacological models. In order to meet the requirements of a useful model, methods were developed that were capable of overcoming these limitations by separately measuring effects on pacemakers cells (rate of contraction) and cardiomyocytes (contraction amplitude). Furthermore, advanced imaging methods utilising reporters, selective dyes and confocal microscopy allowed selective analysis of intact EBs. Embryoid bodies provided a sophisticated tool for analyses of adrenoceptor pharmacology, which is well characterised with highly selective inhibitors and agonists. In contrast, EBs were less useful for dissection of adenosine receptor biology which is less well characterized, the complicated signaling of the different adenosine receptor subtypes and the lack of selective agonists limited complete elucidation of the pathways involved in adenosine receptor signaling in EBs. These findings highlight both the strength of EB screening assays that involve well-characterized pharmacology and biology but emphasize the limitations of heterogeneous systems for dissecting complex phenomena.

ESC-derived EBs may find particular use as models in drug validation in the context of complex biological systems. While our understanding of the greater architecture and function of the cardiac conduction system is well understood, the molecular mechanisms of that facilitate the spontaneous electrical activity in the different parts of the conduction system is still unclear. These studies have been limited by use of

organotypic methods, such as canine purkinje preparations, or isolated cells from well-defined regions, such as the SA node or the AV node. While these models allow us to investigate important parts of the conduction system, they contain a very limited number of cell types when compared with the variety of cells types identified in the entire intact conduction system. The studies presented here showed that ESC-derived EBs are highly complex and comprise many of the cell types found in the intact heart. Cellular subsets may be extracted by FACS and characterised for complex behaviour such as spontaneous calcium waveforms. These studies demonstrate that ESC-derived EBs may provide insight into the cellular interactions and molecular mechanisms of complex phenomena such as generation and propagation of action potentials in the heart. These findings may facilitate identification of novel drug targets and have broader implications for modeling conduction disease states. Furthermore, the characterisation and generation of nodal and conductive cells may prove important for the cell replacement therapies and tissue engineering(Xue et al. 2005).

In addition to their role in pharmacological validation, the heterogeneous nature of ESC-derived systems is well suited to investigating intercellular and complex interactions. ESC-derived EBs may be particularly powerful for addressing biological questions that are difficult to address with simplified *in vitro* models or inaccessible and inflexible *in vivo* models. Due to the ease of digestion/separation, the ease of genetic manipulation, and ready availability of healthy and genetic diseased tissue, the EB provides an ideal tool to identify previously uncharacterized cardiac waveforms. Extensive evidence presented in Chapter 5 suggested that these waveforms arose from functionally mature cells that may come from different levels of the cardiac conduction system. Additional

data from our lab that was not presented in this dissertation indicates that hESC-derived cardiomyocytes also give rise to diverse waveforms, indicating that this phenomenon is not restricted to murine-derived cardiac tissue. To formally test the hypothesis that these previously unrecognized waveforms derived from mature cells represent different parts of the cardiac conduction system, it is not essential to determine if these waveforms are present in the intact heart. This question may be addressed using reporter mice that express GFP in different parts of the cardiac conduction system(MIQUEROL et al. 2004; Gros et al. 2010). Analyses of waveforms from cells isolated from digested tissue using the reporter would provide information about the diversity of waveforms generated by cells from different levels of the conduction system of the mature heart.

While cardiac toxicity has long been linked to Trastuzumab usage, the underlying molecular and cellular mechanisms have been difficult to determine(Azim et al. 2009; Yoshiyama et al. 2003; Force, Krause & Van Etten 2007b; Fedele et al. 2012). Consistent with previous research, enriched or purified cardiomyocytes were less sensitive to antibody toxicity(Riccio et al. 2009; Barth et al. 2012). However, the complex multicellular microenvironment of stem cell-derived EBs permitted identification of a role for endothelial-like cells in trastuzumab toxicity and implicated NO as a component of the response. These findings suggest novel targets for pharmacotherapy, e.g. by blocking NO during trastuzumab administration. Additionally, these findings suggest that screening for biomarkers of trastuzumab toxicity might focus on cardiac stromal tissue rather than cardiomyocytes, which have been the focus to date(Force & Kerkelä 2008; Force, Krause & Van Etten 2007a). One possible approach is to generate iPSCs

from patients with known trastuzumab responses, followed by cardiac differentiation and trastuzumab toxicity screening, which may help to identify genetic links and/or sub groups. Combined with genetic sequencing it may be possible to identify patients with a high propensity towards trastuzumab toxicity. Identification of genetic markers that will direct usage of trastuzumab will both limit premature therapy withdrawal and cardio toxic events saving money and lives.

Humanised and recombinant antibodies have provided a leap forward in the search for highly specific drugs, and yet are a significant challenge for assuring clinical safety. The findings presented here support clinical observations of trastuzumab toxicity, but more critically, raise the specter that current preclinical screening in simplified *in vitro* systems (usually single cell type) may not detect selective toxicity of an engineered antibody. SC-derived EBs may fill this gap by providing an intermediate platform for context-rich analyses of human biology. Advanced immunotherapies and biologicals are consistently growing market share when compared with traditional compound based drugs(Dickson & Gagnon 2004). With the increasing introduction of new drugs based on biological molecules, so too comes an increasing risk that dangerous therapies will enter the clinic due to the previously explained deficiencies in current preclinical models. Biologists must address the shortcomings of standard preclinical models to provide regulatory bodies and pharmaceutical companies tools to prevent clinical failures and toxic outcomes.

The complex human context of SC-derived EBs may provide an ideal system for addressing other specific pharmacological questions. For example, common  $\beta_2$ AR

polymorphisms that influence receptor expression, recycling and function have been linked to many cardiac-related disease states. However, the pharmacology of  $\beta$ ARs in human cardiomyocytes differs significantly from rodents, which has limited translation of preclinical findings. Specifically, biased signaling and differences observed between receptor polymorphisms are not easily investigated in rodents, making the translation of these phenomena to clinical studies limited. Models based on hESC-derived cardiac cells may provide appropriate systems to investigate underlying molecular pharmacology such as polymorphisms and biased signaling in human cardiomyocytes, with physiological context not present in standard heterologous expression systems such as HEK cells(Eglen et al. 2008). Starting with a single parental hESC line one could use homologous recombination to knock in the polymorphic alleles, generating isogenic cell lines that differ only at the polymorphic gene expressed under the native promoter. Combining this approach with the videomorphometry method developed for this project it would possible to address the question of whether polymorphic differences observed in *in vitro* models are likely to manifest in physiological systems. This would give pharmacologists and drug discoverers an *in vitro* tool to study pharmacogenomics, signal bias or allosteric modulation in a physiologically relevant human model, perhaps leading to novel treatments or next generation versions of current drugs.

As SC-derived models become more commonly used for drug screening and validation it will be essential that current federal regulatory policies and requirements evolve to better utilize new technologies for establishing safety profiles of novel therapeutics. Currently regulation of preclinical data relies on predominantly on pharmacological and

toxicology findings in rodent and non-rodent models, or *in vitro* assays for humanized antibodies. Recent data presented by GE using their high content imaging systems and Cytiva© SC-derived cardiomyocytes indicates a high prediction of clinical cardiac reactions. Adoption of stem cell derived models, such as those already on offer from GE (under license from Geron), are likely to become standard practice for the screening of preclinical candidates. However, if regulatory bodies were to proactively legislate for adoption of SC-derived models as part of the registration process for new drugs, this would expedite the acceptance of such models. In the meantime, stem cell biologists must standardize culture, differentiation and analytical methods to assist stem cell derived models to become part of regulatory compliance before registration of new drug applications.

The limitations of current models for cardiac drug discovery and development have resulted in expensive, harmful and occasionally fatal clinical failures. These problems have arisen from a lack of appropriate context in over simplified *in vitro* models or lack of homology in complex animal models. Stem cell derived cardiomyocyte models present a solution to both of these deficits. Development of new methods that harness the physiology present in stem cell cultures while minimizing (or at least controlling for) the heterogeneity will facilitate better screening of preclinical candidates. By providing physiologically relevant functional and toxicological data, in a human context, stem cell derived *in vitro* models may reduce the number preclinical drug candidates that fail, potentially saving money and lives.

## References

- Abramov, A.Y., Scorziello, A. & Duchen, M.R., 2007. Three distinct mechanisms generate oxygen free radicals in neurons and contribute to cell death during anoxia and reoxygenation. *Journal of Neuroscience*, 27(5), pp.1129–1138.
- Abu-Issa, R. & Kirby, M.L., 2007. Heart Field: From Mesoderm to Heart Tube. *Annual Review of Cell and Developmental Biology*, 23(1), pp.45–68.
- Alanine, A. et al., 2003. Lead generation--enhancing the success of drug discovery by investing in the hit to lead process. *Combinatorial chemistry & high throughput screening*, 6(1), pp.51–66.
- Ali, N.N. et al., 2004. Beta-adrenoceptor subtype dependence of chronotropy in mouse embryonic stem cell-derived cardiomyocytes. *Basic Research in Cardiology*, 99(6), pp.382–391.
- Anderson, R.H. et al., 1981. Anatomico-electrophysiological correlations in the conduction system--a review. *British heart journal*, 45(1), pp.67–82.
- Andersson, H. et al., 2010. Assaying cardiac biomarkers for toxicity testing using biosensing and cardiomyocytes derived from human embryonic stem cells. *Journal of Biotechnology*, 150(1), pp.175–181.
- Ateghang, B. et al., 2006. Regulation of cardiotrophin-1 expression in mouse embryonic stem cells by HIF-1 $\alpha$  and intracellular reactive oxygen species. *Journal of cell science*, 119(6), pp.1043–1052.
- Azim, H., Azim, H.A. & Escudier, B., 2009. Trastuzumab versus lapatinib: the cardiac side of the story. *Cancer treatment reviews*, 35(7), pp.633–638.
- Barth, A.S. et al., 2012. Functional impairment of human resident cardiac stem cells by the cardiotoxic antineoplastic agent trastuzumab. *Stem cells translational medicine*, 1(4), pp.289–297.
- Bauwens, C.L. et al., 2008. Control of Human Embryonic Stem Cell Colony and Aggregate Size Heterogeneity Influences Differentiation Trajectories. *Stem Cells*, 26(9), pp.2300–2310.
- Belardinelli, L., Linden, J. & Berne, R.M., 1989. The cardiac effects of adenosine. *Progress in cardiovascular diseases*, 32(1), pp.73–97.
- Belhassen, L., 1996. Endothelial Nitric Oxide Synthase Targeting to Caveolae. SPECIFIC INTERACTIONS WITH CAVEOLIN ISOFORMS IN CARDIAC MYOCYTES AND ENDOTHELIAL CELLS. *Journal of Biological Chemistry*, 271(37), pp.22810–22814.

- Bell, R.M., Mocanu, M.M. & Yellon, D.M., 2011. Retrograde heart perfusion: The Langendorff technique of isolated heart perfusion. *Journal of molecular and cellular cardiology*, 50(6), pp.940–950.
- Bellairs, R., 1986. The primitive streak. *Anatomy and Embryology*, 174(1), pp.1–14.
- Bers, D.M., 2006. Altered Cardiac Myocyte Ca Regulation In Heart Failure. *Physiology*, 21(6), pp.380–387.
- Bird, B.R.J.H. & Swain, S.M., 2008. Cardiac Toxicity in Breast Cancer Survivors: Review of Potential Cardiac Problems. *Clinical Cancer Research*, 14(1), pp.14–24.
- Bleicher, K.H. et al., 2003. Hit and lead generation: beyond high-throughput screening. *Nature Reviews Drug Discovery*, 2(5), pp.369–378.
- Blelloch, R. et al., 2006. Reprogramming Efficiency Following Somatic Cell Nuclear Transfer Is Influenced by the Differentiation and Methylation State of the Donor Nucleus. *Stem Cells*, 24(9), pp.2007–2013.
- Boheler, K.R. et al., 2002. Differentiation of pluripotent embryonic stem cells into cardiomyocytes. *Circulation Research*, 91(3), pp.189–201.
- Borea, P.A. et al., 2009. A3 adenosine receptor: pharmacology and role in disease. *Handbook of experimental pharmacology*, (193), pp.297–327.
- Boyer, L.A. et al., 2005. Core Transcriptional Regulatory Circuitry in Human Embryonic Stem Cells. *Cell*, 122(6), pp.947–956.
- Braam, S.R. et al., 2010. Inhibition of ROCK improves survival of human embryonic stem cell-derived cardiomyocytes after dissociation. *Annals of the New York Academy of Sciences*, 1188(1), pp.52–57.
- Brekke, O.H. & Løset, G.Å., 2003. New technologies in therapeutic antibody development. *Current Opinion in Pharmacology*, 3(5), pp.544–550.
- Brodde, O.E., 1993. Beta-adrenoceptors in cardiac disease. *Pharmacology & Therapeutics*, 60(3), pp.405–430.
- Brodde, O.E. et al., 2001. Presence, distribution and physiological function of adrenergic and muscarinic receptor subtypes in the human heart. *Basic Research in Cardiology*, 96(6), pp.528–538.
- Brund, M.J. et al., 2012. Cardiac ryanodine receptors control heart rate and rhythmicity in adult mice. *Cardiovascular Research*, 96(3), pp.372–380.
- Burridge, P.W. et al., 2011. A Universal System for Highly Efficient Cardiac Differentiation of Human Induced Pluripotent Stem Cells That Eliminates Interline Variability M. Pera, ed. *PloS one*, 6(4), p.e18293.

- Cai, C.-L. et al., 2003. *Isl1 identifies a cardiac progenitor population that proliferates prior to differentiation and contributes a majority of cells to the heart.* *Developmental Cell*, 5(6), pp.877–889.
- Caldwell, G.W. et al., 2001. The new pre-preclinical paradigm: compound optimization in early and late phase drug discovery. *Current Topics in Medicinal Chemistry*, 1(5), pp.353–366.
- Caldwell, J., 1992. Problems and opportunities in toxicity testing arising from species differences in xenobiotic metabolism. *Toxicology Letters*, 64-65, pp.651–659.
- Chambers, S.M. et al., 2012. Combined small-molecule inhibition accelerates developmental timing and converts human pluripotent stem cells into nociceptors. *Nature Publishing Group*, 30(7), pp.715–720.
- Chenoweth, J.G., McKay, R.D.G. & Tesar, P.J., 2010. Epiblast stem cells contribute new insight into pluripotency and gastrulation. *Development, growth & differentiation*, 52(3), pp.293–301.
- Christoffels, V.M. et al., 2000. Chamber formation and morphogenesis in the developing mammalian heart. *Developmental Biology*, 223(2), pp.266–278.
- Cleland, J.G.F. et al., 2011. The effects of the cardiac myosin activator, omecamtiv mecarbil, on cardiac function in systolic heart failure: a double-blind, placebo-controlled, crossover, dose-ranging phase 2 trial. *Lancet*, 378(9792), pp.676–683.
- Cohen, J.D. et al., 2011. Use of human stem cell derived cardiomyocytes to examine sunitinib mediated cardiotoxicity and electrophysiological alterations. *Toxicology and Applied Pharmacology*, pp.1–10.
- Crowther, D., 2002. Applications of microarrays in the pharmaceutical industry. *Current Opinion in Pharmacology*, 2(5), pp.551–554.
- Csete, M., 2005. Oxygen in the cultivation of stem cells. *Annals of the New York Academy of Sciences*, 1049, pp.1–8.
- Czyz, J. & Wobus, A., 2001. Embryonic stem cell differentiation: the role of extracellular factors. *Differentiation*, 68(4-5), pp.167–174.
- Dambrot, C. et al., 2011. Cardiomyocyte differentiation of pluripotent stem cells and their use as cardiac disease models. *Biochemical Journal*, 434, pp.25–35.
- Dang, S.M., 2004. Controlled, Scalable Embryonic Stem Cell Differentiation Culture. *Stem Cells*, 22(3), pp.275–282.
- DeChiara, T.M. et al., 2010. Producing fully ES cell-derived mice from eight-cell stage embryo injections. *Methods in enzymology*, 476, pp.285–294.
- Desbordes, S.C. & Studer, L., 2012. Adapting human pluripotent stem cells to high-

- throughput and high-content screening. *Nature Protocols*, 8(1), pp.111–130.
- Devic, E. et al., 2001.  $\beta$ -Adrenergic receptor subtype-specific signaling in cardiac myocytes from  $\beta 1$  and  $\beta 2$  adrenoceptor knockout mice. *Molecular Pharmacology*, 60(3), pp.577–583.
- Dickson, M. & Gagnon, J.P., 2004. Key factors in the rising cost of new drug discovery and development. *Nature Reviews Drug Discovery*, 3(5), pp.417–429.
- Dooley, C.T., 2004. Imaging Dynamic Redox Changes in Mammalian Cells with Green Fluorescent Protein Indicators. *Journal of Biological Chemistry*, 279(21), pp.22284–22293.
- Dooley, C.T. et al., 2012. Toxicity of 6-hydroxydopamine: live cell imaging of cytoplasmic redox flux. *Cell Biology and Toxicology*, 28(2), pp.89–101.
- Doroshow, J.H., 1991. Doxorubicin-induced cardiac toxicity. *New England Journal of Medicine*, 324(12), p.843.
- Eastwood, D. et al., 2010. Monoclonal antibody TGN1412 trial failure explained by species differences in CD28 expression on CD4+ effector memory T-cells. *British journal of pharmacology*, 161(3), pp.512–526.
- Ebert, S.N. et al., 2004. Targeted insertion of the Cre-recombinase gene at the phenylethanolamine n-methyltransferase locus: A new model for studying the developmental distribution of adrenergic cells. *Developmental Dynamics*, 231(4), pp.849–858.
- Eglen, R.M., Gilchrist, A. & Reisine, T., 2008. The use of immortalized cell lines in GPCR screening: the good, bad and ugly. *Combinatorial chemistry & high throughput screening*, 11(7), pp.560–565.
- Elliott, D.A. et al., 2011. NKK2-5eGFP/w hESCs for isolation of human cardiac progenitors and cardiomyocytes. *Nature Methods*, 8(12), pp.1037–1040.
- Ellis, J. et al., 2009. Alternative Induced Pluripotent Stem Cell Characterization Criteria for In Vitro Applications. *Cell Stem Cell*, 4(3), pp.198–199.
- Evans, M.J. & Kaufman, M.H., 1981. Establishment in culture of pluripotential cells from mouse embryos. *Nature*, 292(5819), pp.154–156.
- Ewer, M.S. et al., 2005. Reversibility of trastuzumab-related cardiotoxicity: new insights based on clinical course and response to medical treatment. *Journal of Clinical Oncology*, 23(31), pp.7820–7826.
- Farokhpour, M. et al., 2009. Embryonic stem cell-derived cardiomyocytes as a model system to study cardioprotective effects of dexamethasone in doxorubicin cardiotoxicity. *Toxicology in Vitro*, 23(7), pp.1422–1428.

- Fedele, C. et al., 2012. Mechanisms of cardiotoxicity associated with ErbB2 inhibitors. *Breast Cancer Research and Treatment*, 134(2), pp.595–602.
- Fielden, M.R. & Kolaja, K.L., 2008. The role of early in vivotoxicity testing in drug discovery toxicology. *Expert Opinion on Drug Safety*, 7(2), pp.107–110.
- Foglie, S., NIERI, P. & Breschi, M.C., 2004. The role of nitric oxide in anthracycline toxicity and prospects for pharmacologic prevention of cardiac damage. *FASEB journal : official publication of the Federation of American Societies for Experimental Biology*, 18(6), pp.664–675.
- Force, T. & Kerkelä, R., 2008. Cardiotoxicity of the new cancer therapeutics – mechanisms of, and approaches to, the problem. *Drug Discovery Today*, 13(17-18), pp.778–784.
- Force, T., Krause, D.S. & Van Etten, R.A., 2007a. Molecular mechanisms of cardiotoxicity of tyrosine kinase inhibition. *Nature Reviews Cancer*, 7(5), pp.332–344.
- Force, T., Krause, D.S. & Van Etten, R.A., 2007b. Molecular mechanisms of cardiotoxicity of tyrosine kinase inhibition. *Nature Reviews Cancer*, 7(5), pp.332–344.
- Ford, M.G., Pitt, W.R. & Whitley, D.C., 2004. Selecting compounds for focused screening using linear discriminant analysis and artificial neural networks. *Journal of Molecular Graphics and Modelling*, 22(6), pp.467–472.
- Földes, G. et al., 2011. Modulation of human embryonic stem cell-derived cardiomyocyte growth: a testbed for studying human cardiac hypertrophy? *Journal of molecular and cellular cardiology*, 50(2), pp.367–376.
- Franco, R., 2000. Evidence for Adenosine/Dopamine Receptor Interactions Indications for Heteromerization. *Neuropsychopharmacology*, 23(4), pp.S50–S59.
- Fujiwara, M. et al., 2011. Induction and enhancement of cardiac cell differentiation from mouse and human induced pluripotent stem cells with cyclosporin-A. *PloS one*, 6(2), p.e16734.
- Germack, R. & Dickenson, J.M., 2004. Characterization of ERK1/2 signalling pathways induced by adenosine receptor subtypes in newborn rat cardiomyocytes. *British journal of pharmacology*, 141(2), pp.329–339.
- Gleeson, M.P., Hersey, A. & Hannongbua, S., 2011. In-silico ADME models: a general assessment of their utility in drug discovery applications. *Current Topics in Medicinal Chemistry*, 11(4), pp.358–381.
- Gold, J.D. et al., 2008. Direct differentiation method for making cardiomyocytes from human embryonic stem cells. Patent # US 7,452,718 B2
- Gosling, J.I. et al., 2012. Synthesis and Biological Evaluation of Adenosines with

- Heterobicyclic and Polycyclic N6-Substituents as Adenosine A1 Receptor Agonists. *ChemMedChem*, 7(7), pp.1191–1201.
- Gros, D. et al., 2010. Connexin 30 is expressed in the mouse sino-atrial node and modulates heart rate. *Cardiovascular Research*, 85(1), pp.45–55.
- Guidry, G., 1999. A method for counterstaining tissues in conjunction with the glyoxylic acid condensation reaction for detection of biogenic amines. *The journal of histochemistry and cytochemistry : official journal of the Histochemistry Society*, 47(2), pp.261–264.
- Hansen, O., 1984. Interaction of cardiac glycosides with ( $\text{Na}^+ + \text{K}^+$ )-activated ATPase. A biochemical link to digitalis-induced inotropy. *Pharmacological reviews*, 36(3), pp.143–163.
- Hanson, G.T., 2003. Investigating Mitochondrial Redox Potential with Redox-sensitive Green Fluorescent Protein Indicators. *Journal of Biological Chemistry*, 279(13), pp.13044–13053.
- Hao, J. et al., 2008. Dorsomorphin, a Selective Small Molecule Inhibitor of BMP Signaling, Promotes Cardiomyogenesis in Embryonic Stem Cells P. Callaerts, ed. *PLoS one*, 3(8), p.e2904.
- Harding, S.E. et al., 1994. Mechanisms of beta adrenoceptor desensitisation in the failing human heart. *Cardiovascular Research*, 28(10), pp.1451–1460.
- Hartung, S. et al., 2013. Directing Cardiomyogenic Differentiation of Human Pluripotent Stem Cells by Plasmid-Based Transient Overexpression of Cardiac Transcription Factors. *Stem cells and development*, 22(7), pp.1–14.
- Hartzell, H.C. & Fischmeister, R., 1987. Effect of forskolin and acetylcholine on calcium current in single isolated cardiac myocytes. *Molecular Pharmacology*, 32(5), pp.639–645.
- Harvey, R.P., 2002. Organogenesis: Patterning the vertebrate heart. *Nature Reviews Immunology*, 3(7), pp.544–556.
- Hawthorn, M.H. et al., 1985. The use of forskolin to investigate the site of cardiac  $\beta$ -adrenoceptor supersensitivity. *Journal of autonomic pharmacology*, 5(3), pp.231–240.
- Hernandez, J. et al., 2012. Evidence for a cooperation between adenosine A2 receptors and  $\beta$ 1-adrenoceptors on cardiac automaticity in the isolated right ventricle of the rat. *British journal of pharmacology*, 111(4), pp.1316–1320.
- Herodin, F. et al., 2005. Nonhuman primates are relevant models for research in hematology, immunology and virology. *European cytokine network*, 16(2), pp.104–116.

- Hidaka, K. et al., 2003. Chamber-specific differentiation of Nkx2.5-positive cardiac precursor cells from murine embryonic stem cells. *FASEB journal : official publication of the Federation of American Societies for Experimental Biology*, 17(6), pp.740–742.
- Hieble, J.P., Bondinell, W. & Ruffolo, R.R., 1995. .alpha.- and .beta.-Adrenoceptors: From the Gene to the Clinic. Part 1. Molecular Biology and Adrenoceptor Subclassification. *Journal of Medicinal Chemistry*, 38(18), pp.3415–3444.
- Himura, Y. et al., 1993. Cardiac noradrenergic nerve terminal abnormalities in dogs with experimental congestive heart failure. *Circulation*, 88(3), pp.1299–1309.
- Hudis, C.A., 2007. Trastuzumab—mechanism of action and use in clinical practice. *New England Journal of Medicine*, 357(1), pp.39–51.
- Hughes, B., 2008. 2007 FDA drug approvals: a year of flux. *Nature Reviews Drug Discovery*, 7(2), pp.107–109.
- Hunter, R.P., 2010a. Interspecies allometric scaling. *Handbook of experimental pharmacology*, (199), pp.139–157.
- Hunter, R.P., 2010b. Interspecies allometric scaling. *Comparative and Veterinary Pharmacology*, 199, pp.139–157.
- Ieda, M. et al., 2010. Direct Reprogramming of Fibroblasts into Functional Cardiomyocytes by Defined Factors. *Cell*, 142(3), pp.375–386.
- Insel, P.A. & Ostrom, R.S., 2003. Forskolin as a tool for examining adenylyl cyclase expression, regulation, and G protein signaling. *Cellular and molecular neurobiology*, 23(3), pp.305–314.
- Jacot, J.G. et al., 2010. Cardiac myocyte force development during differentiation and maturation. *Annals of the New York Academy of Sciences*, 1188(1), pp.121–127.
- Jang, J. et al., 2008. Notch inhibition promotes human embryonic stem cell-derived cardiac mesoderm differentiation. *Stem Cells*, 26(11), pp.2782–2790.
- Jani, J.P. et al., 2007. Discovery and Pharmacologic Characterization of CP-724,714, a Selective ErbB2 Tyrosine Kinase Inhibitor. *Cancer Research*, 67(20), pp.9887–9893.
- Jiang, X. et al., 2000. Fate of the mammalian cardiac neural crest. *Development*, 127(8), pp.1607–1616.
- Kattman, S.J. et al., 2011. Stage-Specific Optimization of Activin/Nodal and BMP Signaling Promotes Cardiac Differentiation of Mouse and Human Pluripotent Stem Cell Lines. *Stem Cell*, 8(2), pp.228–240.
- Kaumann, A. et al., 1999. Activation of beta2-adrenergic receptors hastens relaxation and mediates phosphorylation of phospholamban, troponin I, and C-protein in

- ventricular myocardium from patients with terminal heart failure. *Circulation*, 99(1), pp.65–72.
- Kaumann, A.J. et al., 1996. Beta 2-adrenoceptor activation by zinterol causes protein phosphorylation, contractile effects and relaxant effects through a cAMP pathway in human atrium. *Molecular and cellular biochemistry*, 163-164, pp.113–123.
- Kawai, T. et al., 2004. Efficient cardiomyogenic differentiation of embryonic stem cell by fibroblast growth factor 2 and bone morphogenetic protein 2. *Circulation journal : official journal of the Japanese Circulation Society*, 68(7), pp.691–702.
- Khan, J.M., Lyon, A.R. & Harding, S.E., 2012. The Case for Induced Pluripotent Stem Cell-derived Cardiomyocytes in Pharmacological Screening. *British journal of pharmacology*.
- Kim, C. et al., 2010. Non-Cardiomyocytes Influence the Electrophysiological Maturation of Human Embryonic Stem Cell-Derived Cardiomyocytes During Differentiation. *Stem cells and development*, 19(6), pp.783–795.
- Kin, H. et al., 2005. Postconditioning reduces infarct size via adenosine receptor activation by endogenous adenosine. *Cardiovascular Research*, 67(1), pp.124–133.
- Klimanskaya, I., Rosenthal, N. & Lanza, R., 2008. Derive and conquer: sourcing and differentiating stem cells for therapeutic applications. *Nature Reviews Drug Discovery*, 7(2), pp.131–142.
- Knight, M.M. et al., 2003. Live cell imaging using confocal microscopy induces intracellular calcium transients and cell death. *American Journal of Physiology - Cell Physiology*, 284(4), pp.C1083–9.
- Koglin, J. et al., 1994. Antiadrenergic effect of carbachol but not of adenosine on contractility in the intact human ventricle in vivo. *Journal of the American College of Cardiology*, 23(3), pp.678–683.
- Kolossov, E. et al., 2005. Identification and characterization of embryonic stem cell-derived pacemaker and atrial cardiomyocytes. *FASEB journal : official publication of the Federation of American Societies for Experimental Biology*, 19(6), pp.577–579.
- Korfmacher, W.A., 2005. Principles and applications of LC-MS in new drug discovery. *Drug Discovery Today*, 10(20), pp.1357–1367.
- Korn, K. & Krausz, E., 2007. Cell-based high-content screening of small-molecule libraries. *Current Opinion in Chemical Biology*, 11(5), pp.503–510.
- Kou, Z. et al., 2010. Mice cloned from induced pluripotent stem cells (iPSCs). *Biology of reproduction*, 83(2), pp.238–243.
- Kriks, S. et al., 2011. Dopamine neurons derived from human ES cells efficiently engraft

- in animal models of Parkinson's disease. *Nature*, 480(7378), pp.547–551.
- Kubo, A. et al., 2004. Development of definitive endoderm from embryonic stem cells in culture. *Development*, 131(7), pp.1651–1662.
- Kwon, C. et al., 2009. A regulatory pathway involving Notch1/beta-catenin/Isl1 determines cardiac progenitor cell fate. *Nature cell biology*, 11(8), pp.951–957.
- Lagerqvist, E.L. et al., 2011. Endothelin-1 and angiotensin II modulate rate and contraction amplitude in a subpopulation of mouse embryonic stem cell-derived cardiomyocyte-containing bodies. *Stem Cell Research*, 6(1), pp.23–33.
- Lakatta, E.G., Maltsev, V.A. & Vinogradova, T.M., 2010. A Coupled SYSTEM of Intracellular Ca<sup>2+</sup> Clocks and Surface Membrane Voltage Clocks Controls the Timekeeping Mechanism of the Heart's Pacemaker. *Circulation Research*, 106(4), pp.659–673.
- Lee, G. & Studer, L., 2011. Modelling familial dysautonomia in human induced pluripotent stem cells. *Philosophical Transactions of the Royal Society B: Biological Sciences*, 366(1575), pp.2286–2296.
- Lefkowitz, R.J., Rockman, H.A. & Koch, W.J., 2000. Catecholamines, cardiac beta-adrenergic receptors, and heart failure. *Circulation*, 101(14), pp.1634–1637.
- Li, A.P., 2001. Screening for human ADME/Tox drug properties in drug discovery. *Drug Discovery Today*, 6(7), pp.357–366.
- Liang, B.T. & Haltiwanger, B., 1995. Adenosine A2a and A2b receptors in cultured fetal chick heart cells. High- and low-affinity coupling to stimulation of myocyte contractility and cAMP accumulation. *Circulation Research*, 76(2), pp.242–251.
- Liao, J. et al., 2009. Generation of induced pluripotent stem cell lines from adult rat cells. *Cell Stem Cell*, 4(1), pp.11–15.
- Liu, J. et al., 2009. Facilitated maturation of Ca<sup>2+</sup> handling properties of human embryonic stem cell-derived cardiomyocytes by calsequestrin expression. *AJP: Cell Physiology*, 297(1), pp.C152–C159.
- Loh, Y.-H. et al., 2006. The Oct4 and Nanog transcription network regulates pluripotency in mouse embryonic stem cells. *Nature Genetics*, 38(4), pp.431–440.
- Lyssiotis, C.A. et al., 2010. Chemical Control of Stem Cell Fate and Developmental Potential. *Angewandte Chemie International Edition*, 50(1), pp.200–242.
- Malik, F.I. & Morgan, B.P., 2011. Cardiac myosin activation part 1: from concept to clinic. *Journal of molecular and cellular cardiology*, 51(4), pp.454–461.
- Malmersjö, S. et al., 2010. Ca<sup>2+</sup> and cAMP Signaling in Human Embryonic Stem Cell-Derived Dopamine Neurons. *Stem cells and development*, 19(9), pp.1355–1364.

- Maltsev, V.A. & Lakatta, E.G., 2007. Dynamic interactions of an intracellular Ca<sup>2+</sup> clock and membrane ion channel clock underlie robust initiation and regulation of cardiac pacemaker function. *Cardiovascular Research*, 77(2), pp.274–284.
- Maltsev, V.A., Rohwedel, J. & Hescheler, J., 1993. ScienceDirect.com - Mechanisms of Development - Embryonic stem cells differentiate in vitro into cardiomyocytes representing sinusnodal, atrial and ventricular cell types. *Mechanisms of ....*
- Marchetto, M.C.N. et al., 2009. Transcriptional Signature and Memory Retention of Human-Induced Pluripotent Stem Cells. *PloS one*, 4(9), p.e7076.
- Martin, G.R., 1981. Isolation of a pluripotent cell line from early mouse embryos cultured in medium conditioned by teratocarcinoma stem cells. *Proceedings of the National Academy of Sciences*, 78(12), pp.7634–7638.
- Mason, D.T. & Braunwald, E., 1963. Studies of digitalis IX. Effects of ouabain on the nonfailing human heart. *Journal of Clinical Investigation*, 42(7), pp.1105–1111.
- McGrath, J.C., Brown, C.M. & Wilson, V.G., 2006. Alpha-adrenoceptors: A critical review. *Medicinal research reviews*, 9(4), pp.407–533.
- McIntire, W.E., 2001. The G Protein beta Subunit Is a Determinant in the Coupling of Gs to the beta 1-Adrenergic and A2a Adenosine Receptors. *Journal of Biological Chemistry*, 276(19), pp.15801–15809.
- Menna, P., Salvatorelli, E. & Minotti, G., 2010. Anthracycline degradation in cardiomyocytes: a journey to oxidative survival. *Chemical research in toxicology*, 23(1), pp.6–10.
- Middleton, D.A., 2006. NMR Methods for Characterising Ligand-Receptor and Drug-Membrane Interactions in Pharmaceutical Research. *Annual Reports on NMR Spectroscopy*, 60, pp.39–75.
- Minger, S.L., 2012. Developing technologies to unlock the therapeutic and research potential of human stem cells. *New biotechnology*.
- MIQUEROL, L. et al., 2004. Architectural and functional asymmetry of the His-Purkinje system of the murine heart. *Cardiovascular Research*, 63(1), pp.77–86.
- Morizane, A. et al., 2010. A simple method for large-scale generation of dopamine neurons from human embryonic stem cells. *Journal of neuroscience research*, 88(16), pp.3467–3478.
- Möller, C. & Witchel, H., 2011. Automated Electrophysiology Makes the Pace for Cardiac Ion Channel Safety Screening. *Frontiers in Pharmacology*, 2, pp.1–7.
- Mummery, C. et al., 2007. Cardiomyocytes from human and mouse embryonic stem cells. *Methods in molecular medicine*, 140, pp.249–272.

- Murphy, E., Wong, R. & Steenbergen, C., 2008. Signalosomes: delivering cardioprotective signals from GPCRs to mitochondria. *American journal of physiology. Heart and circulatory physiology*, 295(3), pp.H920–H922.
- Murry, C.E. & Keller, G., 2008. Differentiation of Embryonic Stem Cells to Clinically Relevant Populations: Lessons from Embryonic Development. *Cell*, 132(4), pp.661–680.
- Musser, B. et al., 1993. Species comparison of adenosine and β-adrenoceptors in mammalian atrial and ventricular myocardium. *European Journal of Pharmacology: Molecular Pharmacology*, 246(2), pp.105–111.
- Nakagawa, M. et al., 2010. Promotion of direct reprogramming by transformation-deficient Myc. *Proceedings of the National Academy of Sciences of the United States of America*, 107(32), pp.14152–14157.
- Negro, A., 2004. Essential Roles of Her2/erbB2 in Cardiac Development and Function. *Recent Progress in Hormone Research*, 59(1), pp.1–12.
- Nelson, A.L., Dhimolea, E. & Reichert, J.M., 2010. Development trends for human monoclonal antibody therapeutics. *Nature Reviews Drug Discovery*, 9(10), pp.767–774.
- Neumann, J. et al., 1995. Interaction of beta-adrenoceptor and adenosine receptor agonists on phosphorylation. Identification of target proteins in mammalian ventricles. *Journal of molecular and cellular cardiology*, 27(8), pp.1655–1667.
- Newman, A.M. & Cooper, J.B., 2010. Lab-Specific Gene Expression Signatures in Pluripotent Stem Cells. *Cell Stem Cell*, 7(2), pp.258–262.
- Ng, K.-M. et al., 2011. Cobalt chloride pretreatment promotes cardiac differentiation of human embryonic stem cells under atmospheric oxygen level. *Cellular reprogramming*, 13(6), pp.527–537.
- Njeim, M.T. & Hajjar, R.J., 2010. Gene therapy for heart failure. *Archives of cardiovascular diseases*, 103(8-9), pp.477–485.
- Noble, D., 2004. Modeling the heart. *Physiology*, 19(4), pp.191–197.
- Octavia, Y. et al., 2012. Doxorubicin-induced cardiomyopathy: From molecular mechanisms to therapeutic strategies. *Journal of molecular and cellular cardiology*, 52(6), pp.1213–1225.
- Olah, M.E. & Stiles, G.L., 1995. Adenosine receptor subtypes: characterization and therapeutic regulation. *Annual review of pharmacology and toxicology*, 35, pp.581–606.
- Ondrias, K. et al., 1990. Biphasic effects of doxorubicin on the calcium release channel

- from sarcoplasmic reticulum of cardiac muscle. *Circulation Research*, 67(5), pp.1167–1174.
- Pillekamp, F. et al., 2012. Contractile Properties of Early Human Embryonic Stem Cell-Derived Cardiomyocytes: Beta-Adrenergic Stimulation Induces Positive Chronotropy and Lusitropy but Not Inotropy. *Stem cells and development*, 21(12), pp.2111–2121.
- Post, S.R., Hammond, H.K. & Insel, P.A., 1999. Beta-adrenergic receptors and receptor signaling in heart failure. *Annual review of pharmacology and toxicology*, 39, pp.343–360.
- Prescott, M.J., 2010. Ethics of primate use. *Adv. Sci. Res.*, 5, pp.11–22.
- Pritchard, J.F. et al., 2003. Making better drugs: Decision gates in non-clinical drug development. *Nature Reviews Drug Discovery*, 2(7), pp.542–553.
- Qian, L. et al., 2012. In vivo reprogramming of murine cardiac fibroblasts into induced cardiomyocytes. *Nature*, 485(7400), pp.593–598.
- Rajala, K., Pekkanen-Mattila, M. & Aalto-Setälä, K., 2011. Cardiac Differentiation of Pluripotent Stem Cells. *Stem Cells International*, 2011, pp.1–12.
- Ramirez, C.N. et al., 2012. Large-scale screening using familial dysautonomia induced pluripotent stem cells identifies compounds that rescue IKBKAP expression. *Nature Publishing Group*, 30(12), pp.1244–1248.
- RB, W., 1992. The anthracyclines: will we ever find a better doxorubicin? *Seminars in oncology*, 19(6), pp.670–686.
- Reichert, J.M., 2008. Monoclonal Antibodies as Innovative Therapeutics. *Current Pharmaceutical Biotechnology*, 9(6), pp.423–430.
- Riccio, G. et al., 2009. Cardiotoxic effects, or lack thereof, of anti-ErbB2 immunoagents. *The FASEB Journal*, 23(9), pp.3171–3178.
- Rideout, W.M., III, 2001. Nuclear Cloning and Epigenetic Reprogramming of the Genome. *Science (New York, N.Y.)*, 293(5532), pp.1093–1098.
- Robinson, R.B. & Siegelbaum, S.A., 2003. Hyperpolarization-activated cation currents: from molecules to physiological function. *Annual review of physiology*, 65, pp.453–480.
- Rochais, F., Mesbah, K. & Kelly, R.G., 2009. Signaling pathways controlling second heart field development. *Circulation Research*, 104(8), pp.933–942.
- Rohrer, D.K. et al., 1998. Alterations in dynamic heart rate control in the  $\beta$ 1-adrenergic receptor knockout mouse. *American journal of physiology. Heart and circulatory physiology*, 274(4), pp.H1184–H1193.

- Rousell, J. et al., 1996. Beta-Adrenoceptor-mediated down-regulation of M<sub>2</sub> muscarinic receptors: role of cyclic adenosine 5'-monophosphate-dependent protein kinase and protein kinase C. *Molecular Pharmacology*, 49(4), pp.629–635.
- Rub, H.P., Thommen, H. & Porzig, H., 1981. Quantitative changes in β-adrenergic responses of isolated atria from hyper- and hypothyroid rats. *Cellular and Molecular Life Sciences*, 37(4), pp.399–401.
- Rudin, M. et al., 1999. In vivo magnetic resonance methods in pharmaceutical research: current status and perspectives. *NMR in Biomedicine*, 12(2), pp.69–97.
- Sabri, A. et al., 2000. Coupling function of endogenous α<sub>1</sub>-and β-adrenergic receptors in mouse cardiomyocytes. *Circulation Research*, 86(10), pp.1047–1053.
- Sachinidis, A. et al., 2003. Cardiac specific differentiation of mouse embryonic stem cells. *Cardiovascular Research*, 58(2), pp.278–291.
- Sachlos, E. & Auguste, D.T., 2008. Embryoid body morphology influences diffusive transport of inductive biochemicals: A strategy for stem cell differentiation. *Biomaterials*, 29(34), pp.4471–4480.
- Schaffer, P. et al., 1994. Di-4-ANEPPS causes photodynamic damage to isolated cardiomyocytes. *Pflügers Archiv - European Journal of Physiology*, 426(6), pp.548–551.
- Schipke, J.D. et al., 2006. Postconditioning: a brief review. *Herz-Kardiovaskuläre Erkrankungen*, 31(6), p.600.
- Schmid, I., Uittenbogaart, C.H. & Giorgi, J.V., 1991. A gentle fixation and permeabilization method for combined cell surface and intracellular staining with improved precision in DNA quantification. *Cytometry Part A*, 12(3), pp.279–285.
- Schuster, D., Laggner, C. & Langer, T., 2005. Why drugs fail--a study on side effects in new chemical entities. *Current pharmaceutical design*, 11(27), pp.3545–3559.
- Sedan, O. et al., 2008. 1,4,5-Inositol trisphosphate-operated intracellular Ca(2+) stores and angiotensin-II/endothelin-1 signaling pathway are functional in human embryonic stem cell-derived cardiomyocytes. *Stem Cells*, 26(12), pp.3130–3138.
- Sedan, O. et al., 2010. Human embryonic stem cell-derived cardiomyocytes can mobilize 1,4,5-inositol trisphosphate-operated [Ca<sup>2+</sup>]<sub>i</sub> stores: the functionality of angiotensin-II/endothelin-1 signaling pathways. *Annals of the New York Academy of Sciences*, 1188, pp.68–77.
- Seidman, A., 2002. Cardiac Dysfunction in the Trastuzumab Clinical Trials Experience. *Journal of Clinical Oncology*, 20(5), pp.1215–1221.
- Shryock, J.C. & Belardinelli, L., 1997. Adenosine and adenosine receptors in the

- cardiovascular system: biochemistry, physiology, and pharmacology. *The American journal of cardiology*, 79(12A), pp.2–10.
- Silva, J. et al., 2008. Promotion of Reprogramming to Ground State Pluripotency by Signal Inhibition M. A. Goodell, ed. *PLoS Biology*, 6(10), p.e253.
- Slater, K., 2001. Cytotoxicity tests for high-throughput drug discovery. *Current opinion in biotechnology*, 12(1), pp.70–74.
- Sonnenblick, E.H. et al., 1966. Studies on digitalis: XV. Effects of cardiac glycosides on myocardial force-velocity relations in the nonfailing human heart. *Circulation*, 34(3), pp.532–539.
- SPASOJEVIC, N., GAVRILOVIC, L. & DRONJAK, S., 2011. Regulation of catecholamine-synthesising enzymes and beta-adrenoceptors gene expression in ventricles of stressed rats. *Physiological research / Academia Scientiarum Bohemoslovaca*, 60 Suppl 1, pp.S171–6.
- Sun, X. et al., 1999. Targeted disruption of Fgf8 causes failure of cell migration in the gastrulating mouse embryo. *Genes & Development*, 13(14), pp.1834–1846.
- Suter, T.M., Cook-Bruns, N. & Barton, C., 2004. Cardiotoxicity associated with trastuzumab (Herceptin) therapy in the treatment of metastatic breast cancer. *The Breast*, 13(3), pp.173–183.
- Taha, M.F. & Valojerdi, M.R., 2008. Effect of bone morphogenetic protein-4 on cardiac differentiation from mouse embryonic stem cells in serum-free and low-serum media. *International Journal of Cardiology*, 127(1), pp.78–87.
- Takahashi, K. & Yamanaka, S., 2006. Induction of Pluripotent Stem Cells from Mouse Embryonic and Adult Fibroblast Cultures by Defined Factors. *Cell*, 126(4), pp.663–676.
- Takahashi, K. et al., 2007. Induction of Pluripotent Stem Cells from Adult Human Fibroblasts by Defined Factors. *Cell*, 131(5), pp.861–872.
- Takahashi, T., 2003. Ascorbic Acid Enhances Differentiation of Embryonic Stem Cells Into Cardiac Myocytes. *Circulation*, 107(14), pp.1912–1916.
- Tan, L.B., Benjamin, I.J. & Clark, W.A., 1992. Adrenergic receptor desensitisation may serve a cardioprotective role. *Cardiovascular Research*, 26(6), pp.608–614.
- Tang, H. & Mayersohn, M., 2005. A novel model for prediction of human drug clearance by allometric scaling. *Drug metabolism and disposition: the biological fate of chemicals*, 33(9), pp.1297–1303.
- Tarantini, L. et al., 2012. Trastuzumab Adjuvant Chemotherapy and Cardiotoxicity in Real-World Women With Breast Cancer. *Journal of Cardiac Failure*, 18(2), pp.113–

119.

- Tesar, P.J. et al., 2007. New cell lines from mouse epiblast share defining features with human embryonic stem cells. *Nature*, 448(7150), pp.196–199.
- Thomson, J.A., 1998. Embryonic Stem Cell Lines Derived from Human Blastocysts. *Science (New York, N.Y.)*, 282(5391), pp.1145–1147.
- Trautwein, W. & Hescheler, J., 1990. Regulation of cardiac L-type calcium current by phosphorylation and G proteins. *Annual review of physiology*, 52, pp.257–274.
- Tropepe, V. et al., 2001. Direct neural fate specification from embryonic stem cells: a primitive mammalian neural stem cell stage acquired through a default mechanism. *Neuron*, 30(1), pp.65–78.
- Urmaliya, V.B. et al., 2009. Cardioprotection induced by adenosine A1 receptor agonists in a cardiac cell ischemia model involves cooperative activation of adenosine A2A and A2B receptors by endogenous adenosine. *Journal of cardiovascular pharmacology*, 53(5), pp.424–433.
- Urmaliya, V.B. et al., 2010. Cooperative cardioprotection through adenosine A1 and A2A receptor agonism in ischemia-reperfused isolated mouse heart. *Journal of cardiovascular pharmacology*, 56(4), pp.379–388.
- Van der Weyden, M.B. & Kelley, W.N., 1976. Human adenosine deaminase. Distribution and properties. *The Journal of biological chemistry*, 251(18), pp.5448–5456.
- van Oorschot, A.A.M. et al., 2011. Low oxygen tension positively influences cardiomyocyte progenitor cell function. *Journal of Cellular and Molecular Medicine*, 15(12), pp.2723–2734.
- Vander, A., Sherman, J. & Luciano, D., 2007. *Vander's human physiology: the mechanisms of body function (8th ed)*,
- Varma, D.R. et al., 1999. Inverse agonist activities of β-adrenoceptor antagonists in rat myocardium. *British journal of pharmacology*, 127(4), pp.895–902.
- Vinogradova, T.M. et al., 2010. Sarcoplasmic Reticulum Ca<sup>2+</sup> Pumping Kinetics Regulates Timing of Local Ca<sup>2+</sup> Releases and Spontaneous Beating Rate of Rabbit Sinoatrial Node Pacemaker Cells. *Circulation Research*, 107(6), pp.767–775.
- Wakefield, I.D. et al., 2002. The application of in vitro methods to safety pharmacology. *Fundamental & clinical pharmacology*, 16(3), pp.209–218.
- Wall, R.J. & Shani, M., 2008. Are animal models as good as we think? *Theriogenology*, 69(1), pp.2–9.
- Wallace, K.B., 2003. Doxorubicin-induced cardiac mitochondrionopathy. *Pharmacology & toxicology*, 93(3), pp.105–115.

- Waxman, H.A., 2005. The Lessons of Vioxx — Drug Safety and Sales. *New England Journal of Medicine*, 352(25), pp.2576–2578.
- Weiss, R. et al., 1986. Anthracycline analogs The past, present, and future. *Cancer Chemotherapy and Pharmacology*, 18(3), pp.185–197.
- Werry, T.D., Wilkinson, G.F. & Willars, G.B., 2003. Mechanisms of cross-talk between G-protein-coupled receptors resulting in enhanced release of intracellular Ca<sup>2+</sup>. *Biochemical Journal*, 374(Pt 2), pp.281–296.
- Wiese, C. et al., 2011. Differentiation induction of mouse embryonic stem cells into sinus node-like cells by suramin. *International Journal of Cardiology*, 147(1), pp.95–111.
- Willem, E. & Leyns, L., 2008. Patterning of mouse embryonic stem cell-derived pan-mesoderm by Activin A/Nodal and Bmp4 signaling requires Fibroblast Growth Factor activity. *Differentiation*, 76(7), pp.745–759.
- Willem, E., Bushway, P.J. & Mercola, M., 2009. Natural and Synthetic Regulators of Embryonic Stem Cell Cardiogenesis. *Pediatric Cardiology*, 30(5), pp.635–642.
- Wilson, K.D. et al., 2009. MicroRNA Profiling of Human-Induced Pluripotent Stem Cells. *Stem cells and development*, 18(5), pp.749–757.
- Wobus, A.M. et al., 1994. Cardiomyocyte-like cells differentiated in vitro from embryonic carcinoma cells P19 are characterized by functional expression of adrenoceptors and Ca<sup>2+</sup> channels. *In Vitro Cellular & Developmental Biology - Animal*, 30(7), pp.425–434.
- Wu, S.M. et al., 2006. Developmental Origin of a Bipotential Myocardial and Smooth Muscle Cell Precursor in the Mammalian Heart. *Cell*, 127(6), pp.1137–1150.
- Wu, X. et al., 2004. Small Molecules that Induce Cardiomyogenesis in Embryonic Stem Cells. *Journal of the American Chemical Society*, 126(6), pp.1590–1591.
- Xi, J. et al., 2010. Comparison of contractile behavior of native murine ventricular tissue and cardiomyocytes derived from embryonic or induced pluripotent stem cells. *The FASEB Journal*, 24(8), pp.2739–2751.
- Xia, J. et al., 2012. Targeting of the Enhanced Green Fluorescent Protein Reporter to Adrenergic Cells in Mice. *Molecular biotechnology*.
- Xiao, R.P., 2001. Beta-adrenergic signaling in the heart: dual coupling of the beta2-adrenergic receptor to G(s) and G(i) proteins. *Science's STKE*, 2001(104), p.re15.
- Xue, T. et al., 2005. Functional integration of electrically active cardiac derivatives from genetically engineered human embryonic stem cells with quiescent recipient ventricular cardiomyocytes: insights into the development of cell-based pacemakers. *Circulation*, 111(1), pp.11–20.

- Yang, L. et al., 2008. Human cardiovascular progenitor cells develop from a KDR+ embryonic-stem-cell-derived population. *Nature*, 453(7194), pp.524–528.
- Ying, Q.-L. & Smith, A.G., 2003. Defined conditions for neural commitment and differentiation. *Methods in enzymology*, 365, pp.327–341.
- Ying, Q.-L. et al., 2003. BMP induction of Id proteins suppresses differentiation and sustains embryonic stem cell self-renewal in collaboration with STAT3. *Cell*, 115(3), pp.281–292.
- Ying, Q.-L. et al., 2008. The ground state of embryonic stem cell self-renewal. *Nature*, 453(7194), pp.519–523.
- Yoshiyama, Y., Sugiyama, T. & Kanke, M., 2003. Cardiotoxicity of trastuzumab (herceptin) in chick embryos. *Biological & pharmaceutical bulletin*, 26(6), pp.893–895.
- Yuasa, S. et al., 2005. Transient inhibition of BMP signaling by Noggin induces cardiomyocyte differentiation of mouse embryonic stem cells. *Nature Biotechnology*, 23(5), pp.607–611.
- Zahanich, I. et al., 2011. Rhythmic beating of stem cell-derived cardiac cells requires dynamic coupling of electrophysiology and Ca cycling. *Journal of molecular and cellular cardiology*, 50(1), pp.66–76.
- Zhang, Y.-W. et al., 2009. Cardiomyocyte death in doxorubicin-induced cardiotoxicity. *Archivum immunologiae et therapiae experimentalis*, 57(6), pp.435–445.
- Zhou, S. et al., 2010. Successful generation of cloned mice using nuclear transfer from induced pluripotent stem cells. *Cell Research*, 20(7), pp.850–853.
- Zhou, W. et al., 2012. HIF1 $\alpha$  induced switch from bivalent to exclusively glycolytic metabolism during ESC-to-EpiSC/hESC transition. *The EMBO Journal*, 31(9), pp.2103–2116.
- Zhu, S. et al., 2009. A Small Molecule Primes Embryonic Stem Cells for Differentiation. *Stem Cell*, 4(5), pp.416–426.

available at [www.sciencedirect.com](http://www.sciencedirect.com)[www.elsevier.com/locate/scr](http://www.elsevier.com/locate/scr)

## REGULAR ARTICLE

# Endothelin-1 and angiotensin II modulate rate and contraction amplitude in a subpopulation of mouse embryonic stem cell-derived cardiomyocyte-containing bodies

E.L. Lagerqvist, B.A. Finnin, C.W. Pouton, J.M. Haynes\*

*Medicinal Chemistry and Drug Action, Monash Institute of Pharmaceutical Sciences, Monash University (Parkville Campus), Melbourne, Australia*

Received 8 March 2010; received in revised form 8 September 2010; accepted 10 September 2010

**Abstract** Embryonic stem cell-derived cardiomyocytes (ESC-CMs) have applications in understanding cardiac disease pathophysiology, pharmacology, and toxicology. Comprehensive characterization of their basic physiological and pharmacological properties is critical in determining the suitability of ESC-CMs as models of cardiac activity. In this study we use video microscopy and quantitative PCR to investigate the responses of mouse ESC-CMs to adrenoreceptor, muscarinic, angiotensin II (Ang II), and endothelin-1 (ET-1) receptor activation. Isoprenaline (10 nM–10 μM) increased beating rate and contraction amplitude in all beating bodies (BBs), whereas carbachol (up to 1 μM) and the  $I_{\text{Ca}}$  channel blocker ZD-7288 (10 μM) decreased contraction frequency. ET-1 (0.01–100 nM) reduced contraction amplitude in all BBs and increased contraction frequency in 50% of BBs; these effects were blocked by the ET<sub>A</sub> receptor antagonist BQ123 (250 nM). Ang II (0.01 nM–1 μM) increased both contraction amplitude (all BBs) and frequency (in 50% of BBs); effects blocked, respectively, by losartan (100 nM) and PD123,319 (200 nM). These results indicate the presence of functional ET<sub>A</sub> and both AT<sub>1</sub> and AT<sub>2</sub> receptors in murine ESC-CMs, but their expression and/or activity appears to be evident only in a limited set of BBs.

© 2010 Elsevier B.V. All rights reserved.

## Introduction

Embryonic stem cells (ESCs) are undifferentiated cells that can differentiate into all adult cell types. Following the initial isolation of mouse ESCs (mESCs) in 1981 (Evans and Kaufman, 1981), methods for the *in vitro* differentiation of mESC-derived cardiomyocytes (mESC-CMs) have been well

established. The most common protocol involves the cultivation of three-dimensional aggregates called embryoid bodies (EBs) which, when plated, give rise to spontaneously beating cardiomyocytes within a mixed cell aggregate (Wobus et al., 2002).

Expression profiling of the transcription factors involved with heart development *in vivo*, as well as electrophysiological and morphological studies, has shown that ESC-CMs exhibit properties indicative of early myocardial development (Boheler et al., 2002; Fijnvandraat et al., 2003). Nevertheless, some studies have reported the successful engraftment of these developing ESC-CMs to injured myocardium (Laflamme et al., 2007; Klug et al., 1996; Hodgson et al., 2004). In addition, these ESC-CMs can potentially serve as readily available and functional *in vitro*

\* Corresponding author. 381 Royal Parade, Parkville, Victoria 3052, Australia.

cardiac models for basic research and in drug discovery and development programs (Pouton and Haynes, 2007). Consideration for the use of ESC-CMs in replacement therapies and as models of cardiac activity must be linked to a comprehensive characterization of their basic physiological and pharmacological properties, an area not well established.

Most studies investigating cardiomyocyte differentiation from ESCs have used isoprenaline and carbachol as the "standard" agonists to confirm that the physiological or electrophysiological properties of the derived cardiomyocytes resemble native tissue (Banach et al., 2003; He et al., 2003; Fu et al., 2006). However, little is known about ESC-CM responsiveness to other endogenous neurotransmitters, peptides, and cardioactive drugs. Some work on the effect of angiotensin II (Ang II) and endothelin-1 (ET-1) has been carried out on single, isolated mESC-CMs (Kapur and Banach, 2007), as well as in paced human ESC (hESC)-CMs (Sedan et al., 2008). However, the specific receptor(s) mediating these responses, and the effects of these bioactive peptides on both the contraction frequency and the amplitude of spontaneously contracting mESC-CMs, is unknown. In this study, we investigate the responsiveness of mESC-CMs to two physiologically relevant peptides, Ang II and ET-1, and compare their effects with those of standard agonists such as isoprenaline and carbachol. We report that the acute effects of these peptides on ESC-CM contractility are mediated through ET<sub>A</sub>, AT<sub>1</sub>, and AT<sub>2</sub> receptors, and also that, in contrast to the effects of other agonists, the chronotropic effects of these peptides are only evident in a limited subset of beating ESC-CM-containing bodies.

## Results

### Quantitative PCR

Nkx2.5-EGFP-positive cells were sorted by FACS at Days 8 and 18 of differentiation for qPCR analysis of cardiac-specific gene expression. Whereas there were no significant differences in the expression levels of the AT<sub>1a</sub>, ET<sub>A</sub>, and the ET<sub>B</sub> receptor between cardiomyocytes differentiated over seven (EDS) and 18 (LDS) days, the AT<sub>2</sub> receptor was only expressed in LDS cardiomyocytes (Fig. 1).

### Effects of isoprenaline (ISO) and carbachol

All LDS beating bodies (BBs) responded to ISO (10 nM–10 μM) with an increase in both contraction amplitude and frequency (Figs. 2A and B,  $P<0.001$ , one-way ANOVA, post hoc Dunnett's,  $n=8$ ), and to carbachol (100 nM–1 μM) with a decrease in both contraction amplitude and frequency (Fig. 2C).

### Effects of ZD-7288, ryanodine, and thapsigargin

The L<sub>r</sub> blocker ZD-7288 over a period of 20 min decreased contraction frequency in every LDS BB (Fig. 2D). Ryanodine (10 μM) and thapsigargin (0.5 μM) significantly decreased both contraction amplitude and frequency in every BB (Fig. 3;  $P<0.01$ , Student's *t* test,  $n=4$ –5).

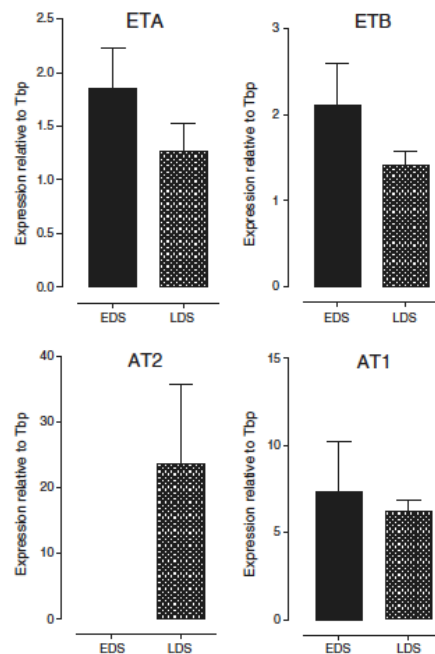


**Figure 1** qPCR of Nkx2.5-EGFP-positive cells reveals no differential expression of AT<sub>1</sub>, ET<sub>A</sub>, or ET<sub>B</sub> receptors between EDS (seven day) and LDS (18 day) cardiomyocytes. The AT<sub>2</sub> receptor, however, is only expressed in LDS cardiomyocytes. Tbp indicates the TATA binding protein housekeeping gene control.

### Effects of ET-1

All EDS BBs responded to ET-1 (10 nM) with an increase in contraction amplitude, whereas this response was reversed in LDS BBs (0.01–100 nM) ( $P<0.05$ , one-way ANOVA, post hoc Dunnett's,  $n=2$ –8, Figs. 4A and B). Only 50% of the BBs responded to ET-1 with an increase in contraction frequency in both EDS and LDS BBs (Fig. 4C, EDS data not shown), with LDS responding bodies showing a concentration-dependent increase in the number of responders ( $EC_{50}$  2.14±0.41 nM; Fig. 4D). As the maximum effect of ET-1 on contraction amplitude, frequency, and number of responding BBs was observed following the addition of 10 nM ET-1, this concentration was used for subsequent antagonist studies.

The decrease in contraction amplitude mediated by 10 nM ET-1 was abolished by the ET<sub>A</sub> receptor antagonist BQ123 (250 nM) and incubation with pertussis toxin (PTX; 1 μg mL<sup>-1</sup>;  $P<0.05$ , one-way ANOVA, post hoc Dunnett's,  $n=4$ –5). The ET<sub>B</sub> receptor antagonist BQ3020 (10 nM), the IP<sub>3</sub> receptor inhibitor 2-aminoethoxydiphenyl borate (2-APB; 2 μM), and the protein kinase C (PKC) inhibitor GF109203x (1 μM) had no effect on the ET-1-mediated decrease in contraction amplitude (Fig. 5A).

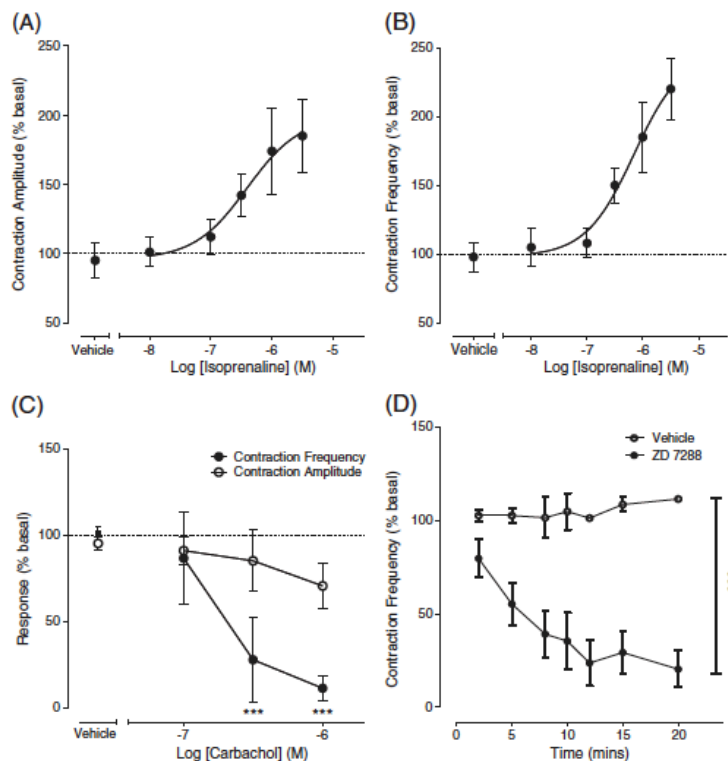


**Figure 2** Mean responses to the addition of ISO (10 nM–3 μM) which increased both (A) contraction amplitude and (B) contraction frequency ( $P<0.001$ , one-way ANOVA, post hoc Dunnett's test,  $n=8$ ). (C) Carbachol (100 nM–1 μM) decreased both contraction frequency and amplitude ( $P<0.001$ , one-way ANOVA, post hoc Dunnett's test,  $n=8$ ). (D)  $I_{\beta}$ -blocker ZD7288 significantly decreased spontaneous beating rate (10 μM,  $P<0.001$ , Student's  $t$  test,  $n=7$ ).

The ET-1-mediated increase in contraction frequency was blocked by BQ123 (250 nM) and GF109203x (1 μM;  $P<0.05$ , one-way ANOVA, post hoc Dunnett's;  $n=5$ ). Incubation of the mESC-CMs with BQ3020 (10 nM), 2-APB (2 μM), or PTX (1 μg mL<sup>-1</sup>) had no effect on the contraction frequency response to ET-1 (Fig. 5B). Addition of the PKC activator phorbol 12,13-diacetate (PDA) increased contraction frequency in every BB (by 77±13% at 10 μM, respectively,  $P<0.05$ , one-way ANOVA, post hoc Dunnett's,  $n=5$ –6; Fig. 5C).

#### Effects of Ang II

Ang II (10 pM–1 μM) increased contraction amplitude in LDS BBs, maximally at 100 nM ( $P<0.05$ , one-way ANOVA, post hoc Dunnett's,  $n=2$ –8, Fig. 6A), but had no effect in EDS BBs (data not shown). Similar to ET-1, both EDS and LDS BBs demonstrated a concentration-dependent increase in the contraction frequency responders to Ang II, up to 50% of BBs ( $EC_{50}$  0.49±0.26 nM; Figs. 6B and C).

This increase in contraction amplitude was reduced by the selective AT<sub>1</sub> antagonist losartan (200 nM) and by 2-APB (2 μM;  $P<0.05$ , one-way ANOVA, post hoc Dunnett's,  $n=4$ –6), but the AT<sub>2</sub> receptor antagonist PD123,319 (200 nM), PTX (1 μg mL<sup>-1</sup>), and GF109203x (1 μM) did not have any effect (Fig. 7A).

The Ang II (100 nM)-mediated increase in contraction frequency was reduced by PD123,319 (200 nM), GF109203x (1 μM), and 2-APB (2 μM;  $P<0.01$ , one-way ANOVA, post hoc Dunnett's,  $n=3$ –6). Incubation with losartan (200 nM) or PTX (1 μg mL<sup>-1</sup>) had no effect on the frequency response to Ang II (Fig. 7B).

#### Discussion

In this study, we have successfully differentiated mESCs into cardiomyocyte-containing BBs and measured their responsiveness to several agonists vital for the physiological functioning of cardiomyocytes *in vivo*. One of the parameters measured was changes in contraction amplitude; the second parameter of interest was contraction frequency. The cessation of contractile

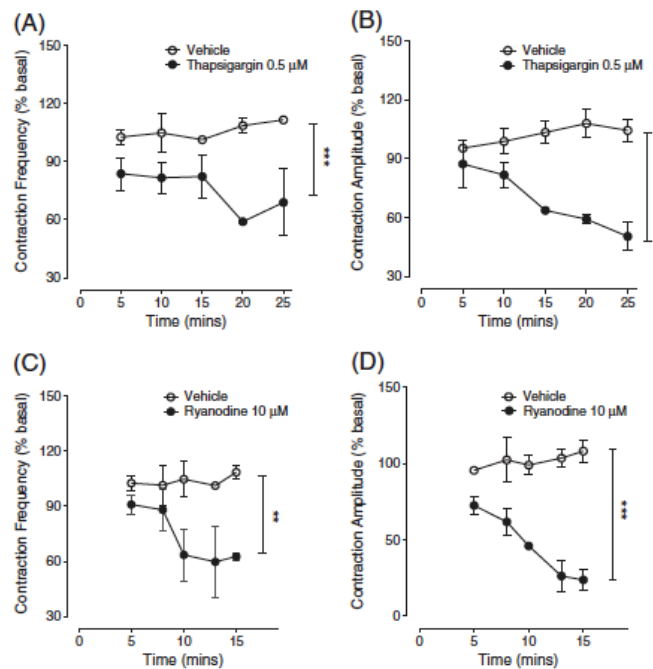


**Figure 3** Investigation of sarcoplasmic reticular function. 0.5 μM thapsigargin and 10 μM ryanodine significantly decrease both (A and C) contraction frequency and (B and D) contraction amplitude, respectively.

activity in these ESC-BBs in the presence of ZD7288 indicates a significant contribution of  $I_r$  to spontaneous contraction frequency, a finding consistent with the presence of pacemaker cells driving either, or both, atrial or ventricular cardiomyocyte contractions in these cardiac bodies (Boheler et al., 2005; Maltsev et al., 1993). Therefore, changes in contraction frequency can be interpreted as effects mediated via changes in pacemaker cell activity (Kang et al., 2007). We have shown positive and negative effects on both contraction amplitude and frequency in response to isoproterenol and carbachol, respectively, findings consistent with observations of  $\beta$ -adrenoceptor and muscarinic effects in the native mouse heart and previous studies in mESC-CMs (Lee et al., 2008; Ali et al., 2004; Kitazawa et al., 2009).

ET-1 serves as an autocrine/paracrine factor produced and released by both cardiomyocytes (Suzuki et al., 1993) and endothelial cells (Brutsaert, 2003). This potent peptide mediates its effects through two G-protein-coupled receptors:  $ET_A$  and  $ET_B$ . Both ET receptor subtypes have been localized to the atrial and ventricular myocardium, the atrioventricular conducting system, and endocardial cells (Molenaar et al., 1993; Pönöcke et al., 1998; Pieske et al., 1999; Del Ry et al., 2001; Fareh et al., 1996). Activation of  $ET_A$  and  $ET_B$  receptors may initiate signaling through several pathways. Their effects are commonly mediated through  $G_{q/11}$  activation; however, they have been reported to be coupled through  $G_s$  or  $G_i$  in particular cell types and species (Ono et al., 1998; Aramori and Nakanishi, 1992). In general, larger

mammals tend to respond to ET-1 with increased contractility (Endoh, 2006); however, during development the mouse heart response to ET-1 changes from positive to negative effects on cell shortening (Sekine et al., 1999; Izumi et al., 2000; Nagasaka et al., 2003; Namekata et al., 2008; Sakurai et al., 2002). The reversal of the ET-1-mediated increase in contraction amplitude in our EDS BBs to a decrease in contraction amplitude in LDS BBs provides strong support for the functional maturation of mESC-CMs 18 days after the initiation of differentiation.

LDS BBs were found to respond to ET-1 stimulation with a decrease in cell shortening. Furthermore, our findings that BQ123, but not BQ3020, blocked the negative shortening response to ET-1 are consistent with those of Izumi and co-workers (Izumi et al., 2000) and indicate an  $ET_A$  receptor-mediated effect. Curiously, ET-1, in the presence of the  $ET_A$  receptor antagonist BQ123, produced an increase in cell shortening. Furthermore, ET-1 concentrations above 10 nM show a reduced negative response. These findings may indicate that ET-1 acts at both  $ET_A$  and  $ET_B$  receptors to elicit negative and positive changes in cell shortening, with the  $ET_A$  receptor effect predominating at low concentrations. Physiological antagonism between the  $ET_A$  and the  $ET_B$  receptors has been observed in several studies (for a review, see Brunner et al. (Brunner et al., 2006). Thus, we conclude that  $ET_A$  mediates a decrease in cell shortening via activation of  $G_{i/o}$  proteins, but we cannot rule out an  $ET_B$ -mediated positive effect in these cells.

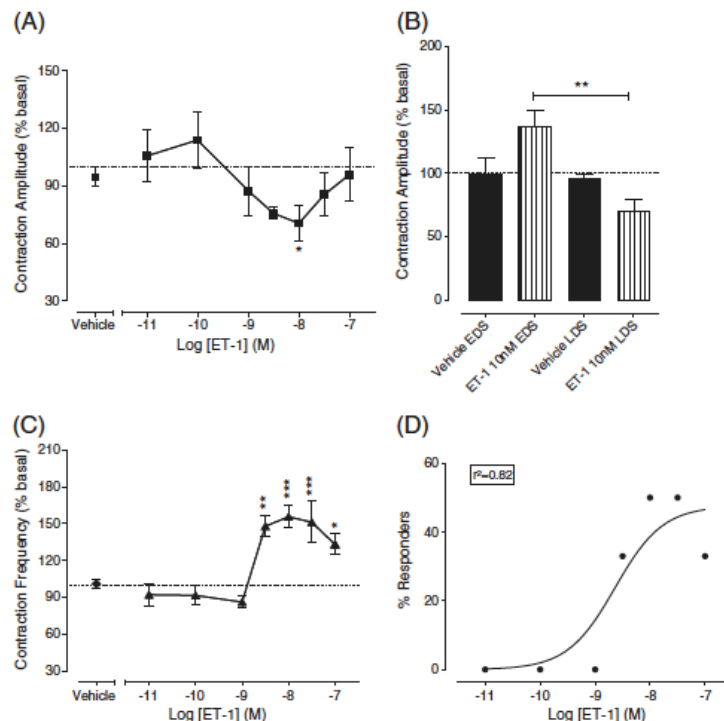


**Figure 4** Mean responses to the addition of ET-1. (A) LDS BBs respond to ET-1 stimulation with a decrease in contraction amplitude, maximal at 10 nM ( $P<0.05$  Student's  $t$  test,  $n=4-8$ ). (B) However, EDS BBs respond to 10 nM ET-1 with an increase in contraction amplitude. (C) ET-1 increased contraction frequency in LDS BBs, again maximal at 10 nM ET-1 ( $P<0.05$ , Student's  $t$  test,  $n=2-8$ ). (C) However, only a maximum of 50% of the cultures responded to ET-1 (up to 100 nM) with an increase in contraction frequency.

In contrast to previous studies that attributed the ET-1-mediated cell shortening response to PKC activation (Izumi et al., 2000; Namekata et al., 2008), we found that PTX blocked the ET-1-mediated decrease, implicating  $G_{i/o}$  protein coupling, rather than  $G_{q/11}$ .  $G_{i/o}$  coupling of ET receptors is common in other species (Ono et al., 1998; Liu et al., 2003; Kim, 1991). However, even though studies have demonstrated ET receptor coupling to both  $G_{q/11}$  and  $G_{i/o}$  in adult mouse heart (Jiang et al., 1996; Hilal-Dandan et al., 1992; Hilal-Dandan et al., 2000), it has not been associated with negative cell shortening effects of ET-1 in the mouse.

The renin angiotensin system plays a central role in the regulation of cardiac function. Ang II is the system's main effector and is known to mediate a wide range of physiological and pathophysiological effects following acute and chronic stimulation (Mehta and Grindling, 2007). In the heart, Ang II mediates both inotropic and chronotropic effects via two G-protein-coupled receptor types, AT<sub>1</sub> and AT<sub>2</sub>. These two receptors have similar affinities for Ang II, and are currently distinguished by affinities for antagonists such as losartan (AT<sub>1</sub>) and PD123,319 (AT<sub>2</sub>). The AT<sub>1</sub> receptor is thought to be the prime mediator of Ang II effects and has been linked to several signaling cascades, most commonly  $G_{q/11}$  coupling

with subsequent PLC and PKC activation (De Gasparo et al., 2000). The Ang II-mediated effect on the contractility of the mouse heart varies depending on the tissue being examined (Sakurai et al., 2002; Nishimaru et al., 2003). In this study, Ang II induced a slight increase in contraction amplitude, a finding consistent with effects seen in mouse atria (Nishimaru et al., 2003). This effect was blocked by losartan and 2-APB, but not by PTX, PD123,319, or GF109203x, and is consistent with a previous study of Ang II effects in human ESC-CMs acting via  $G_{q/11}$  proteins with subsequent PLC and IP<sub>3</sub> production (Sedan et al., 2008).

One of the most interesting aspects of this study is that the PKC-mediated positive chronotropic response to both ET-1 and to Ang II was only observed in a maximum of 50% of BBs. To determine whether this was due to the lack of developed second messenger signaling pathways in the nonresponding population, the effect of the PKC activator PDA was investigated. However, all BBs were found to respond to direct PKC activation, indicating that the second messenger pathway is intact in every culture even though half of the BBs are unresponsive to peptide addition. Previous studies using human ESC-CMs have also reported the presence of nonresponding cultures, which has been attributed to the lack of a functional sarcoplasmic

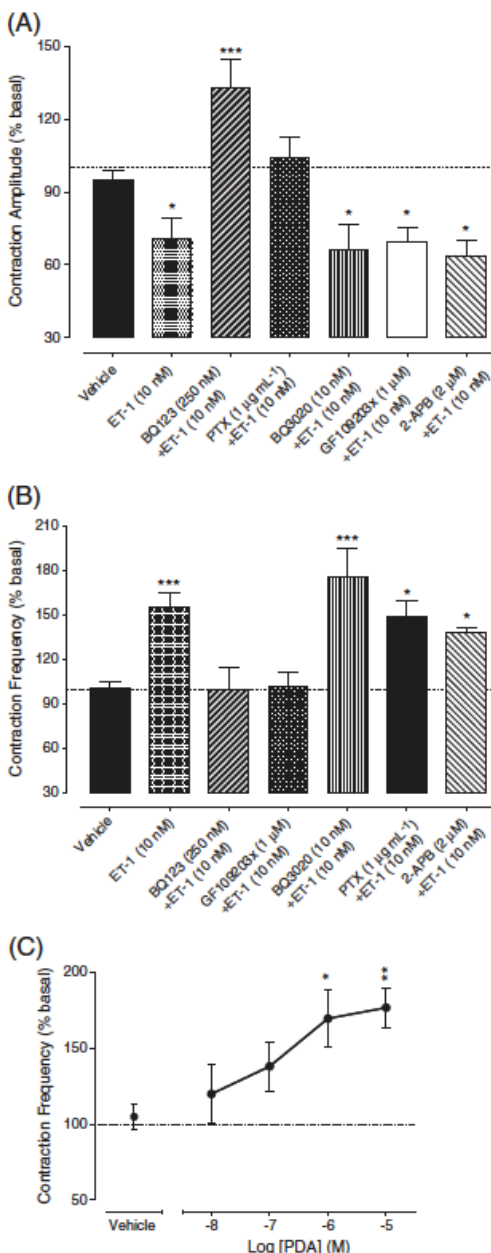


**Figure 5** Mean responses to the addition of ET-1 in the presence of antagonists. (A) Both BQ123 (250 nM) and PTX (1  $\mu$ g mL $^{-1}$ ) inhibited the ET-1 (10 nM) decrease in contraction amplitude ( $P<0.05$ , one-way ANOVA, post hoc Dunnett's,  $n=4-5$ ). (B) BQ123 (250 nM) and GF109203x (1  $\mu$ M) blocked the ET-1-mediated increase in contraction frequency ( $P<0.05$ , one-way ANOVA, post hoc Dunnett's,  $n=5$ ). (C) The PKC activator PDA significantly increased contraction frequency ( $P<0.05$ , one-way ANOVA, post hoc Dunnett's,  $n=5-6$ ).

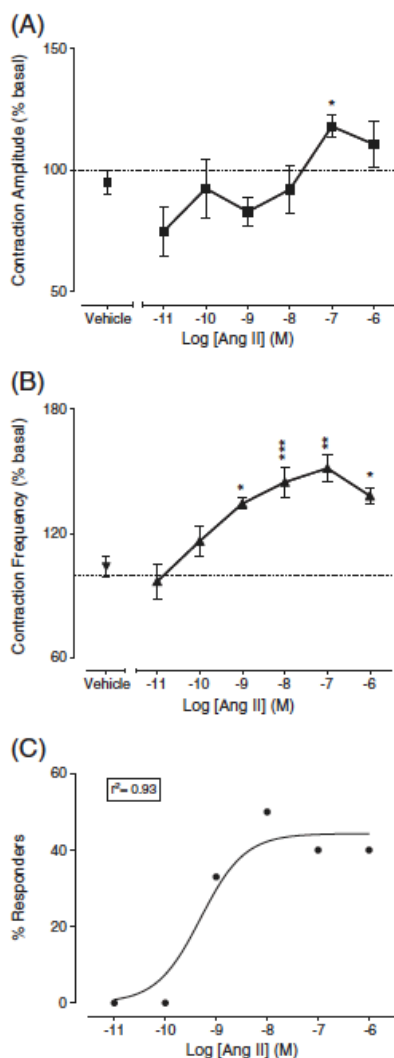


**Figure 6** Mean responses to the addition of Ang II. (A) Ang II increases contraction amplitude at 100 nM ( $P<0.05$ , Student's  $t$  test,  $n=4-8$ ) (B) with a concentration-dependent increase in contraction frequency, maximal at 100 nM ( $P<0.05$ , Student's  $t$  test,  $n=2-8$ ). (C) A maximum of 50% of the cultures responded to Ang II (up to 1  $\mu$ M) with an increase in contraction frequency.

reticulum in cardiomyocytes at varying stages of differentiation (Sedan et al., 2008). However, in our study, this observation appears to be specific to peptide effects since (1) all BBs responded to thapsigargin and ryanodine, indicating the presence of a functional sarcoplasmic reticulum, (2) all BBs responded to isoproterenol and carbachol addition, and (3) beating in all bodies was reduced by the  $I_f$  channel blocker. Furthermore, no correlation was found between a nonresponding BB and other observable properties, such as the initial

## Subpopulation of mouse embryonic stem cell-derived cardiomyocyte-containing bodies

29

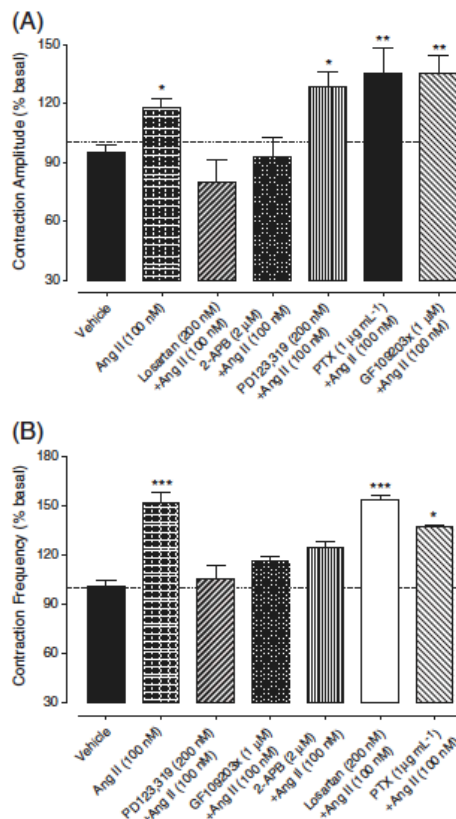


**Figure 7** Mean responses to the addition of Ang II in the presence of antagonists. (A) Losartan (200 nM) and 2-APB (2 μM) abolished the Ang II (100 nM) increase in contraction amplitude ( $P < 0.05$ , one-way ANOVA, post hoc Dunnett's,  $n = 4–6$ ). (B) PD123,319 (200 nM), GF109203x (1 μM), and 2-APB (2 μM) inhibited the Ang II (100 nM) increase in contraction frequency ( $P < 0.05$ , one-way ANOVA, post hoc Dunnett's,  $n = 3–6$ ).

beating frequency or individual batches of differentiated cells. A recent study in mESC-CMs identified two separate pacemaker populations based on hyperpolarization-activated cyclic nucleotide gated channel expression, activation kinetics, and cAMP sensitivity (Barbuti et al., 2009). We think it possible that an analogous situation exists in our cultures where approximately one-half of our beating body contains pacemakers insensitive to peptide effects. This is consistent with the idea of "functional inhomogeneity" resulting from a significant variation in receptor densities within the sinus node (Ophof, 2007). As investigating the function of individual pacemaker cells within an EB is near impossible, studies at the single cell level are ongoing to determine differences in receptor expression and signaling pathway activation within the pacemaker population.

Of the population that does respond to the peptides with changes in chronotropy ET-1, acting via ET<sub>A</sub> receptors, elicited a

PKC-dependent, pertussis toxin- and 2-APB-insensitive positive chronotropic response. This finding is broadly consistent with a previous study in mESC-CMs (Kapur and Banach, 2007). However, in contrast to our findings, Kapur and Banach (Kapur and Banach, 2007) showed that the positive chronotropic effects were mediated by phospholipase C (PLC) with subsequent IP<sub>3</sub> receptor activation. In this study the IP<sub>3</sub> receptor antagonist 2-APB was without effect, indicating either that we have not used enough 2-APB or that the majority of ET<sub>A</sub> signaling in these cells is mediated via PKC effects. The former hypothesis is unlikely since the same concentration of 2-APB reduced the effects of Ang II, leaving us to conclude that, in these cardiomyocytes, the ET-1 effect is largely attributable to the action of PKC.

In this study the AT<sub>2</sub> receptor antagonist PD312,319 blocked the GF109203x-, 2-APB-sensitive Ang II-mediated increase in contraction frequency. Previous studies have demonstrated an AT<sub>2</sub> receptor (PKC-dependent)-mediated effect on contractility (Allen et al., 1988; Kohout and Rogers, 1995); however, the AT<sub>2</sub> receptor is normally highly expressed in the fetus and dramatically reduced in the adult; where it is predominantly located on the vascular endothelium (Grady et al., 1991; Wang et al., 1998).

In these ESC-CMs, onset of AT<sub>2</sub> receptor expression does not occur until at least Day 8 postdifferentiation and is definitively present in LDS CMs. Together with its demonstrated effect on contractile activity, this could imply a less developed Ang II system compared to ET-1, an observation consistent with what is known about Ang II signaling in rodents (Kang et al., 2007). Current studies are investigating the developmental progression of Ang II signaling in these ESC-CMs in more detail.

## Conclusion

Use of ESC-CMs for cell-based therapy and *in vitro* applications during drug discovery necessitates comprehensive characterization of their functional activity. In this study, we have used video microscopy to (i) compare the modulation of cardiac contractile activity by various agonists vital for the physiological function of cardiomyocyte *in vivo*, (ii) investigate which second messenger systems the peptide agonists activate to produce their responses, and (iii) used these data to establish just how like normal adult heart tissue these ESC-CMs are.

We have demonstrated that these mESC-CM cultures respond to stimulation through functional adrenoceptor, muscarinic, Ang II, and ET-1 receptors, and possess intact G<sub>q/11</sub> and G<sub>i/o</sub> signaling cascades in a manner comparable to previous studies in the native mouse myocardium. However, even though we demonstrate the progressive maturation of these CMs by the reversal of their cell shortening response to ET-1 between EDS and LDS BBs, and that all BBs have functional sarcoplasmic reticulum, the pacemaker population within the BBs can be divided on the incidence of their response to Ang II and ET-1. Further investigations are required to better characterize the pacemaker populations in these differentiated cultures.

## Materials and methods

### ESC propagation

The mouse ESC lines E14Tg2a (ATCC, catalogue number CRL-1821) and Nkx2.5-EGFP line (a kind gift from Dr. Sean Wu)

were propagated in a culture medium consisting of GlutaMAX Dulbecco's minimum essential medium (DMEM, pH 7.4) supplemented with 0.1 mM MEM nonessential amino acids solution, 10% fetal calf serum (FCS), 0.1 mM 2-mercaptoethanol, 10<sup>3</sup> U mL<sup>-1</sup> murine recombinant leukemia inhibitory factor (Chemicon, Australia). Cultures were incubated at 37 °C, 5% CO<sub>2</sub> in a humidified environment.

### ESC-CM differentiation

Cardiomyocyte differentiation was induced by the hanging drop method (Boheler et al., 2002). Briefly, embryoid bodies were formed in hanging drops of differentiation medium (propagation medium supplemented with 20% FCS, 10,000 U mL<sup>-1</sup> penicillin and 10,000 µg mL<sup>-1</sup> streptomycin) for 5 days. EBs were subsequently plated on gelatin-coated wells for the remainder of the differentiation period. Contractility studies were used to investigate cardiomyocyte responsiveness at both early and late developmental stages, i.e., Days 7 (EDS) and 18 (LDS) post differentiation. Fu et al. have shown that by this LDS, mESC-CMs demonstrate a functional sarcoplasmic reticulum (SR) with ryanodine receptor-mediated SR calcium release, and pharmacological maturity in response to β-adrenergic stimulation (Fu et al., 2006).

### Quantitative real-time PCR

Nkx2.5-EGFP-positive cells were collected on Days 8 and 18 postdifferentiation by fluorescence-activated cell sorting. Total RNA was extracted using the RNeasy Micro kit (Qiagen, Australia), treated with DNase I to remove the contaminating genomic DNA, before reverse transcription into cDNA by Transcripter Reverse Transcriptase (Roche Applied Science, Australia) and random primers according to the manufacturer's specifications. Quantitative real-time PCR analysis was carried out in triplicate for each sample and each gene using the Rotor Gene 3000 (Corbett Robotics, Australia). For PCR amplification, cDNAs were amplified using Roche SYBR Green PCR Master Mix (Roche Applied Science, Australia) and 1 µm of each primer pair. Amplification was carried out starting with 10 min template denaturation/hot start step at 95 °C, followed by 35 cycles (95 °C for 15 s, 59 °C for 20 s, and 72 °C for 20 s). Relative gene expression values were obtained by normalizing C<sub>T</sub> (threshold cycle) values of the target genes in comparison with C<sub>T</sub> values of the housekeeping gene (TATA binding protein) using the ΔΔC<sub>T</sub> method. Gene-specific primer sequences are provided in Table 1.

### Experimental methodology

On the day of use, the E14Tg2a EB outgrowths were washed twice and superfused with a physiological salt solution (PSS) buffer consisting of (in mM) NaCl 140, KCl 6, CaCl<sub>2</sub> 2, MgCl<sub>2</sub> 1, HEPES 20, and glucose 10 (pH 7.4, 37 °C), supplemented with 1.4% (w/v) BSA. A single beating region within an EB outgrowth was selected and viewed through a Basler (Model A602f) camera coupled to a Nikon Eclipse TS100 inverted microscope with Hoffman modulation contrast optics. The Quick Caliper program (SDR Clinical Technologies, Australia) enabled image acquisition at a rate of 50

**Table 1** Quantitative PCR primer sequences

Gene	Primer sequence	Product size (bp)
TATA binding protein	CTGCTGTTGGTATTGTTGG AACTGGCTTGTTGGGAAAG	100
AT <sub>1a</sub> receptor	CCAACTCAACCCAGAAAAGC CCACCACAAAGATGATGCTG	147
AT <sub>2</sub> receptor	GGAGCTCGGAACCTGAAAGC CTGCAGCAACTCCAAATTCTT	131
ET <sub>A</sub> receptor	ATCGGGATCCCCTGATTAC TTGAGCATGCAGGTCTATG	140
ET <sub>B</sub> receptor	GCTCTGAAGTTCAAAGCCAAC AGATTGGCGAGTGTTCTTG	94

a beating cardiac region pre- and postagonist addition, in the absence and presence of antagonists.

Following a 10 min equilibration period, a 10 s capture was taken of the selected beating region to quantify basal activity. Subsequently, Ang II (0.01–1 µM), ET-1 (0.01–100 nM), isoprenaline (10 nM–10 µM), carbachol (100 nM–1 µM), ryanodine (10 µM), thapsigargin (0.5 µM), the I<sub>F</sub> blocker ZD-7288 (10 µM), or the protein kinase C activator phorbol 12,13-diacetate (10 nM–10 µM) was added to the well and 10 s image captures were taken at various time points up to 20 min postagonist or vehicle addition.

For antagonist and inhibitor studies, BBs were superfused with the AT<sub>1</sub> and AT<sub>2</sub> receptor antagonists, losartan (200 nM) and PD123, 319 (200 nM), or the ET<sub>A</sub> and ET<sub>B</sub> receptor antagonists, BQ123 (250 nM) or BQ3020 (10 nM) for 10 min prior to the addition of agonists. In some experiments, the BBs were superfused with the inositol triphosphate (IP<sub>3</sub>) receptor antagonist 2-aminoethoxydiphenyl borate (2 µM, which may also inhibit store-operated calcium channels at higher concentrations (Choi et al., 2010), or the PKC inhibitor GF109203x for 10 min prior to agonist addition. Pertussis toxin (1 µg mL<sup>-1</sup>) was added to the differentiation medium at least 3 h prior to the superfusion experiments. Images were captured as described above.

### Data analysis

The video captures were analyzed using Metamorph Imaging System (Molecular Devices Ltd, USA). An intensity threshold was imposed on each frame of a 10 s image capture. The Metamorph software was then used to track object movement through the 10 s image capture. The contraction amplitude (measured in pixels) was tracked at different time points plotted against time (Fig. 8A). The number of peaks within the 10 s capture was converted to beats per minute to represent the cardiomyocyte contraction frequency. The average contraction amplitude and frequency responses to agonist, in the absence or presence of antagonist(s), were reported as a percentage of the responses prior to agonist addition (i.e., under basal conditions). Figs. 8B and C show representative traces of LDS EBs responses prior to and following the addition of ET-1 (10 nM) or Ang II (100 nM), respectively.

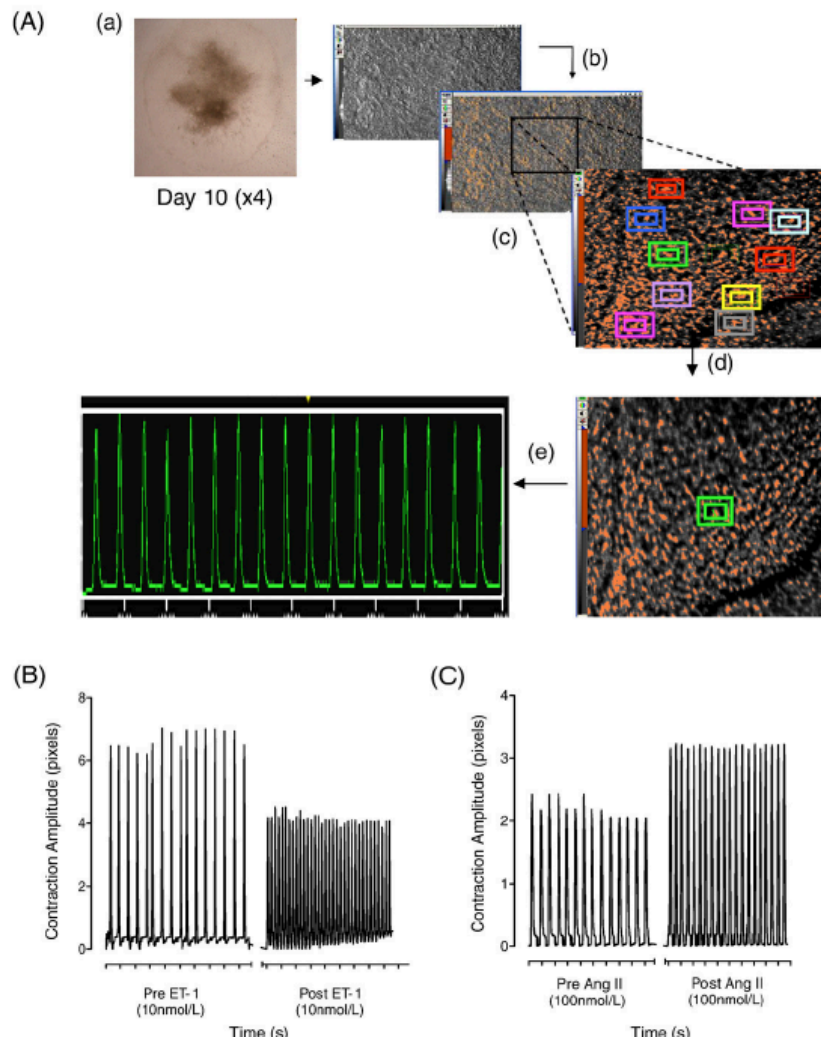


**Figure 8** (A) Capture analysis using Metamorph. (a) A beating region within the well was viewed through a camera coupled to a Nikon Eclipse TS100 inverted microscope with Hoffman modulation contrast optics. Ten-second captures of a beating cardiac region were recorded, and subsequently analyzed using the Metamorph program. (b) An intensity threshold is set using the phasecontrast image. (c) Several particles are selected and monitored within the area of interest. (d) The particle showing the greatest displacement from its point of origin is selected and tracked at the remaining time points. (e) A graph of displacement from origin (in pixels) is generated over the 10s capture period. Two representative 10s traces before and after the addition of (B) ET-1 (10 nM) showing an increase in the number of peaks within the 10s trace (i.e., rate) and a decrease in contraction amplitude. (C) In response to Ang II (100 nM), the number of peaks as well as contraction amplitude (in pixels) increases.

#### Statistical analysis

The maximum responses observed for contraction amplitude and frequency were reported. Curiously, only a proportion of the mESC-CMs responded to Ang II or ET-1

with a change in contraction frequency. Responding and nonresponding BBs were identified using a repeated-measures one-way ANOVA test of the time interval between beats at each 10s capture. Only responding BB effects were reported for analysis of peptide effects on contraction

frequency. None of the vehicles, Ang II or ET-1 receptor antagonists, or 2-APB, PTX, and GF109203x had any effect on the basal spontaneous activity of our cultures ( $n=4-7$ , data not shown). Differences between means were tested using Student's *t* test and one-way ANOVA (post hoc Dunnett's). Values of  $P<0.05$  were considered statistically significant ( $n=3-8$  responding bodies from 4 to 8 observations).

### Drugs and chemicals

Ang II, ET-1, BQ123, BQ 3020, carbachol, ryanodine, PD 123, 319, and losartan were reconstituted in PSS buffer. PDA, thapsigargin, and GF109203x were dissolved in DMSO. 2-APB was dissolved in methanol. The PTX vehicle contained 50% glycerol, 0.5 M NaCl, 50 mM tris, 10 mM glycine (pH 7.5). The final concentration of DMSO or methanol did not exceed 0.01% of the bath volume. PDA and ryanodine were purchased from Calbiochem-Novabiochem (Australia) and thapsigargin was purchased from LC laboratories (USA). All other drugs and chemicals were purchased from Sigma-Aldrich (Australia).

### Acknowledgments

This work was supported by the Australian Stem Cell Centre. We thank Dr. Sean Wu for the Nkx2.5-EGFP mESC line and the Monash University Core Flow Cytometry Facility Flowcore for their FACS work.

### References

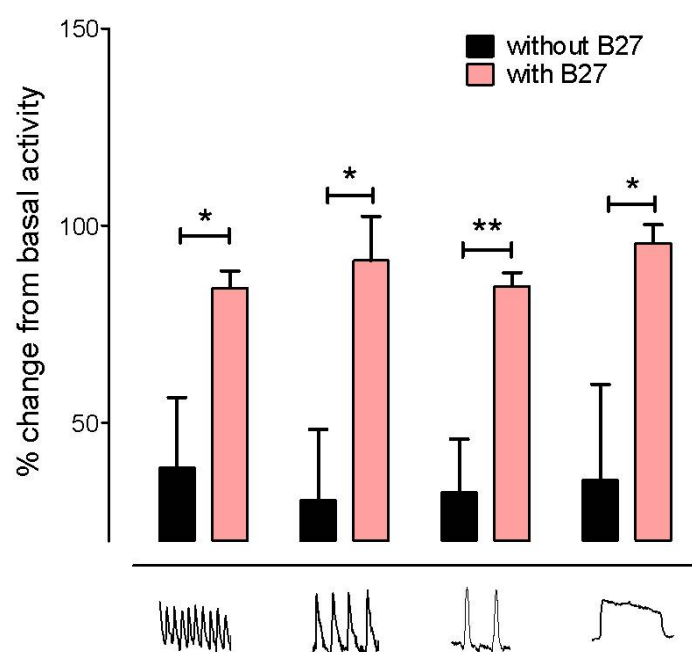
- Ali, N.N., et al., 2004. Beta-adrenoceptor subtype dependence of chronotropy in mouse embryonic stem cell-derived cardiomyocytes. *Basic Res. Cardiol.* 99, 382–391.
- Allen, I.S., et al., 1988. Angiotensin II increases spontaneous contractile frequency and stimulates calcium current in cultured neonatal rat heart myocytes: insights into the underlying biochemical mechanisms. *Circ. Res.* 62 (3), 524–534.
- Aramori, I., Nakanishi, S., 1992. Coupling of two endothelin receptor subtypes to differing signal transduction in transfected Chinese hamster ovary cells. *J. Biol. Chem.* 267 (18), 12468–12474.
- Banach, K., et al., 2003. Development of electrical activity in cardiac myocyte aggregates derived from mouse embryonic stem cells. *Am. J. Physiol. Heart Circ. Physiol.* 284 (6), H2114–H2123.
- Barbuti, A., et al., 2009. Molecular composition and functional properties of f-channels in murine embryonic stem cell-derived pacemaker cells. *J. Mol. Cell Cardiol.* 46 (3), 343–351.
- Boehler, K.R., et al., 2002. Differentiation of pluripotent embryonic stem cells into cardiomyocytes. *Circ. Res.* 91 (3), 189–201.
- Boehler, K.R., et al., 2005. Cardiomyocytes derived from embryonic stem cells. *Methods. Mol. Med.* 108, 417–435.
- Brunner, F., et al., 2006. Cardiovascular endothelins: essential regulators of cardiovascular homeostasis. *Pharmacol. Ther.* 111 (2), 508–531.
- Brutsaert, D.L., 2003. Cardiac endothelial-myocardial signaling: its role in cardiac growth, contractile performance, and rhythmicity. *Physiol. Rev.* 83 (1), 59–115.
- Choi, K., Kim, K., Kim, S., Kim, D., Park, H., 2010. Caffeine and 2-aminoethoxydiphenyl borate (2-APB) have different ability to inhibit intracellular calcium mobilization in pancreatic acinar cell. *Korean J. Physiol. Pharmacol.* 14 (2), 105–111.
- De Gasparo, M., et al., 2000. The angiotensin II receptors. *Pharmacol. Rev.* 52, 415–472.
- Del Ry, S., et al., 2001. Endothelin-1, endothelin-1 receptors and cardiac natriuretic peptides in failing human heart. *Life Sci.* 68, 2715–2730.
- Endoh, M., 2006. Signal transduction and  $\text{Ca}^{2+}$  signaling in intact myocardium. *J. Pharmacol. Sci.* 100, 525–537.
- Evans, M.J., Kaufman, M.H., 1981. Establishment in culture of pluripotential cells from mouse embryos. *Nature* 292 (5819), 154–156.
- Fareh, J., et al., 1996. Endothelin-1 and angiotensin II receptors in cells from rat hypertrophied heart: receptor regulation and intracellular  $\text{Ca}^{2+}$  modulation. *Circ. Res.* 78 (2), 302–311.
- Fijnvandstra, A.C., et al., 2003. Cardiomyocytes purified from differentiated embryonic stem cells exhibit characteristics of early chamber myocardium. *J. Mol. Cell. Cardiol.* 35 (12), 1461–1472.
- Fu, J.-D., et al., 2006. Crucial role of the sarcoplasmic reticulum in the developmental regulation of  $\text{Ca}^{2+}$  transients and contraction in cardiomyocytes derived from embryonic stem cells. *FASEB J.* 20 (1), 181–183.
- Grady, E.F., et al., 1991. Expression of AT2 receptors in the developing rat fetus. *J. Clin. Invest.* 921–933 (3), 921–933.
- He, J.-Q., et al., 2003. Human embryonic stem cells develop into multiple types of cardiac myocytes: action potential characterization. *Circ. Res.* 93 (1), 32–39.
- Hilal-Dandan, R., Urasawa, K., Brunton, L.L., 1992. Endothelin inhibits adenylate cyclase and stimulates phosphoinositide hydrolysis in adult cardiac myocytes. *J. Biol. Chem.* 267 (15), 10620–10624.
- Hilal-Dandan, R., Kanter, J.R., Brunton, L.L., 2000. Characterization of G-protein signaling in ventricular myocytes from the adult mouse heart: differences from the rat. *J. Mol. Cell. Cardiol.* 32 (7), 1211–1221.
- Hodgson, D.M., et al., 2004. Stable benefit of embryonic stem cell therapy in myocardial infarction. *Am. J. Physiol. Heart Circ. Physiol.* 287 (2), H471–H479.
- Izumi, M., et al., 2000. Negative inotropic effect of endothelin-1 in the mouse right ventricle. *Eur. J. Pharmacol.* 396 (2–3), 109–117.
- Jiang, T., et al., 1996. Endothelin-dependent actions in cultured AT1 cardiac myocytes: the role of the varepsilon isoform of protein kinase C. *Circ. Res.* 78 (4), 724–736.
- Kang, M., Chung, K.Y., Walker, J.W., 2007. G-Protein coupled receptor signaling in myocardium: not for the faint of heart. *Physiology* 22 (3), 174–184.
- Kapur, N., Banach, K., 2007. Inositol-1, 4, 5-trisphosphate-mediated spontaneous activity in mouse embryonic stem cell-derived cardiomyocytes. *J. Physiol.* 581 (3), 1113–1127.
- Kim, D., 1991. Endothelin activation of an inwardly rectifying  $\text{K}^{+}$  current in atrial cells. *Circ. Res.* 69 (1), 250–255.
- Kitazawa, T., Asakawa, K., Nakamura, T., Teraoka, H., Unno, T., Komori, S., Yamada, M., Wess, J., 2009. M3 muscarinic receptors mediate positive inotropic responses in mouse atria: a study with muscarinic receptor knockout mice. *J. Pharmacol. Exp. Ther.* 330 (2), 487–493.
- Klug, M., et al., 1996. Genetically selected cardiomyocytes from differentiating embryonic stem cells for stable intracardiac grafts. *J. Clin. Invest.* 98 (1), 216–224.
- Kohout, T.A., Rogers, T.B., 1995. Angiotensin II activates the  $\text{Na}^{+}/\text{HCO}_3^{-}$  symport through phosphoinositide-independent mechanism in cardiac cells. *J. Biol. Chem.* 270 (35), 20432–20438.
- Laflamme, M.A., et al., 2007. Cardiomyocytes derived from human embryonic stem cells in pro-survival factors enhance function of infarcted rat hearts. *Nat. Biotechnol.* 25 (9), 1015–1024.
- Lee, S., Schwinger, R.H., Brixius, K., 2008. Genetically changed mice with chronic deficiency or overexpression of the beta-adrenoceptors—what can we learn for the therapy of heart failure? *Pflugers Arch. Eur. J. Physiol.* 455 (5), 767–774.

## Subpopulation of mouse embryonic stem cell-derived cardiomyocyte-containing bodies

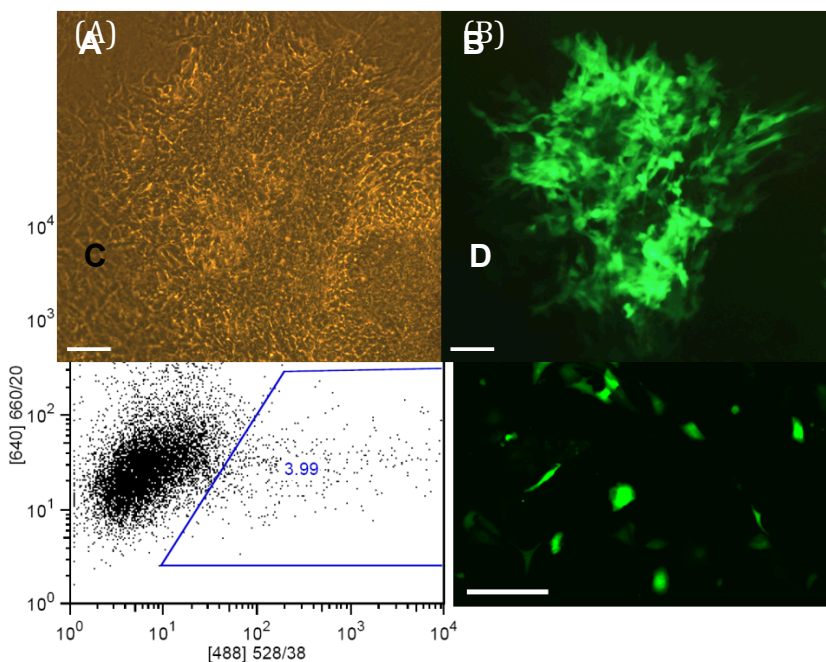
33

- Liu, S., et al., 2003. Endothelin-1 activates endothelial cell nitric-oxide synthase via heterotrimeric G-protein beta][gamma subunit signaling to protein kinase B/Akt. *J. Biol. Chem.* 278 (50), 49929–49935.
- Maltsev, V.A., et al., 1993. Embryonic stem cells differentiate in vitro into cardiomyocytes representing sinusnodal, atrial and ventricular cell types. *Mech. Dev.* 44 (1), 41–50.
- Mehta, P.K., Griendling, K.K., 2007. Angiotensin II cell signaling: physiological and pathological effects in the cardiovascular system. *Am. J. Physiol. Cell Physiol.* 292 (1), C82–C97.
- Molenaar, P., et al., 1993. Characterization and localization of endothelin receptor subtypes in the human atrioventricular conducting system and myocardium. *Circ. Res.* 72 (3), 526–538.
- Nagasaki, T., et al., 2003. Positive inotropic effect of endothelin-1 in the neonatal mouse right ventricle. *Eur. J. Pharmacol.* 472 (3), 197–204.
- Namekata, I., et al., 2008. Intracellular mechanisms and receptor types for endothelin-1-induced positive and negative inotropy in mouse ventricular myocardium. *Naunyn-Schmiedeberg's Arch. Pharmacol.* 376 (6), 385–395.
- Nishimaru, K., et al., 2003. Inhibition of agonist-induced positive inotropy by a selective Rho-associated kinase inhibitor, Y-27632. *J. Pharmacol. Sci.* 92 (4), 424–427.
- Ono, K., et al., 1998. Desensitization of ETA endothelin receptor-mediated negative chronotropic response in right atria-species difference and intracellular mechanisms. *Br. J. Pharmacol.* 125 (4), 787–797.
- Ophof, T., 2007. Embryological development of pacemaker hierarchy and membrane currents related to the function of the adult sinus node: implications for autonomic modulation of biopacemakers. *Med. Biol. Eng. Comput.* 45 (2), 119–132.
- Pieske, B., et al., 1999. Functional effects of endothelin and regulation of endothelin receptors in isolated human nonfailing and failing myocardium. *Circulation* 99, 1802–1809.
- Pönicke, K., et al., 1998. Endothelin receptors in the failing and nonfailing human heart. *Circulation* 97, 744–751.
- Pouton, C.W., Haynes, J.M., 2007. Embryonic stem cells as a source of models for drug discovery. *Nat. Rev. Drug Discov.* 6 (8), 605–616.
- Sakurai, K., et al., 2002. Negative inotropic effects of angiotensin II, endothelin-I and phenylephrine in indo-1 loaded adult mouse ventricular myocytes. *Life Sci.* 70, 1173–1184.
- Sedan, O., et al., 2008. 1,4,5-Inositol trisphosphate operated [Ca<sup>2+</sup>]i stores and angiotensin-II/endothelin-I signaling pathway are functional in human embryonic stem cell-derived cardiomyocytes. *Stem Cells* 3130–3138.
- Sekine, T., et al., 1999. Developmental conversion of inotropism by endothelin I and angiotensin II from positive to negative in mice. *Eur. J. Pharmacol.* 374, 411–415.
- Suzuki, T., Kumazaki, T., Mitsui, Y., 1993. Endothelin-1 is produced and secreted by neonatal rat cardiac myocytes in vitro. *Biochem. Biophys. Res. Commun.* 191 (3), 823–830.
- Wang, Z.-Q., et al., 1998. Immunolocalization of subtype 2 angiotensin II (AT2) receptor protein in rat heart. *Hypertension* 32 (1), 78–83.
- Wobus, A.M., et al., 2002. Embryonic stem cells as a model to study cardiac, skeletal muscle, and vascular smooth muscle cell differentiation. In: Turksen, K. (Ed.), *Embryonic Stem Cells*. Humana Press 185, 127–156.

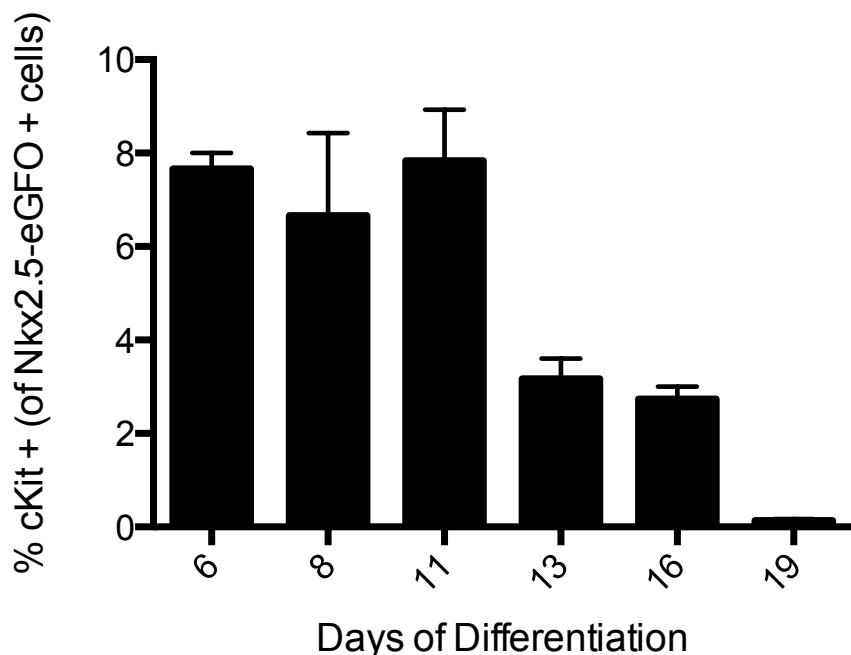
## Chapter 5 Supplemental Material



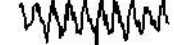
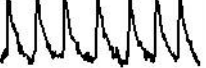
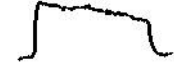
**Supplemental Figure S1: Rescue of Instability Following Addition of B-27®.** Use of anti-oxidant supplement B-27® during confocal  $\text{Ca}^{2+}$  imaging significantly maintains the functional integrity of spontaneous  $[\text{Ca}^{2+}]_i$  activity ( $^{**}P<0.01$ ,  $^{*}P<0.05$ , two-way ANOVA,  $n=3-19$  per waveform group), unveiling a range of kinetically distinct  $[\text{Ca}^{2+}]_i$  oscillation waveforms.



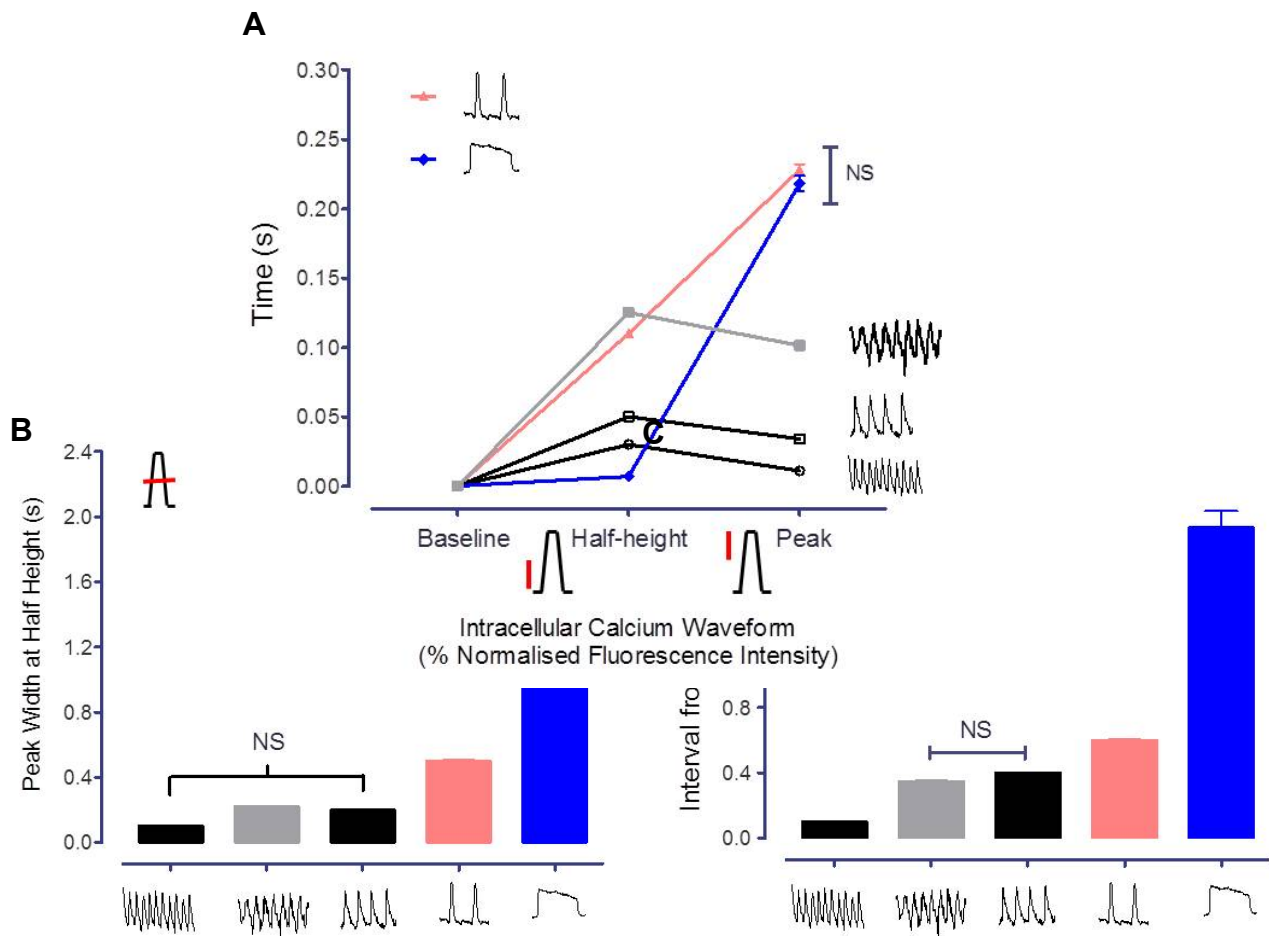
**Supplemental Figure S2:** Images of Nkx2.5-eGFP mESC-CMs. (A) White light phase contrast image of an (B) eGFP expressing mESC- derived cardiac body. (C) Representative FACS plot (population of sytox red negative, eGFP positive) of eGFP expressing cells. (D) Sorted cells were re-plated onto pre-collagen coated wells and maintained for at least 36 hours prior to imaging. Representative image of a field of view of Fluo-4 AM loaded cells. Scale bar= 150  $\mu$ m.



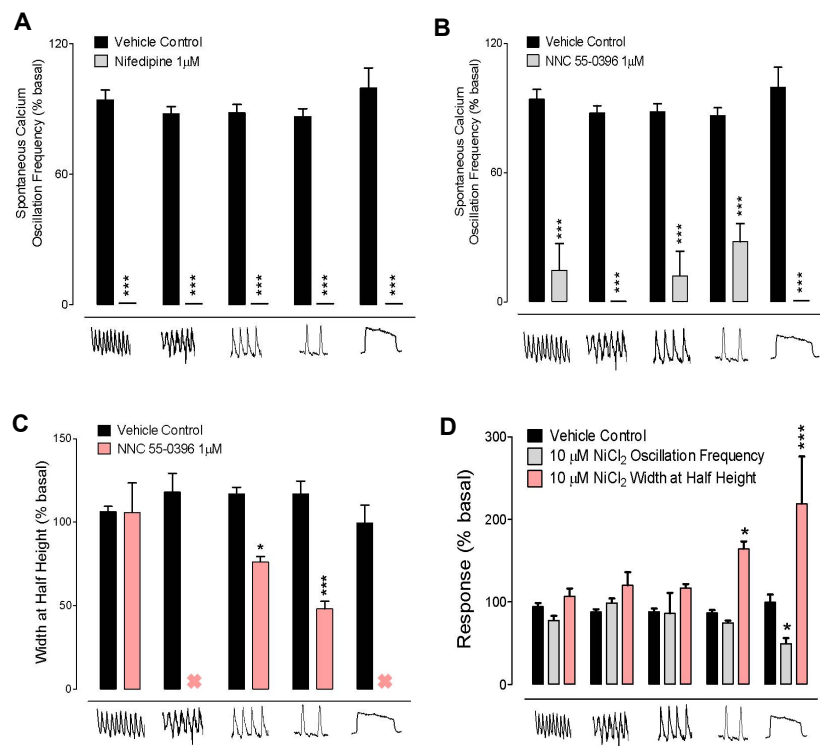
**Supplemental Figure S3:** c-Kit expression. C-Kit expression in the nKx2.5-egfp positive cells was measured using flow cytometry. The expression of c-kit markedly declined from day 13 of differentiation, disappearing from day 19.

Waveform	$\alpha$ MHC <sup>+</sup> / $\alpha$ SMA <sup>-</sup>	$\alpha$ MHC <sup>-</sup> / $\alpha$ SMA <sup>-</sup>	$\alpha$ MHC <sup>-</sup> / $\alpha$ SMA <sup>+</sup>	PGP9.5 <sup>+</sup>
	100%	-	-	-
	100%	-	-	-
	100%	-	-	-
	100%	-	-	-
	33%	-	67%	100%

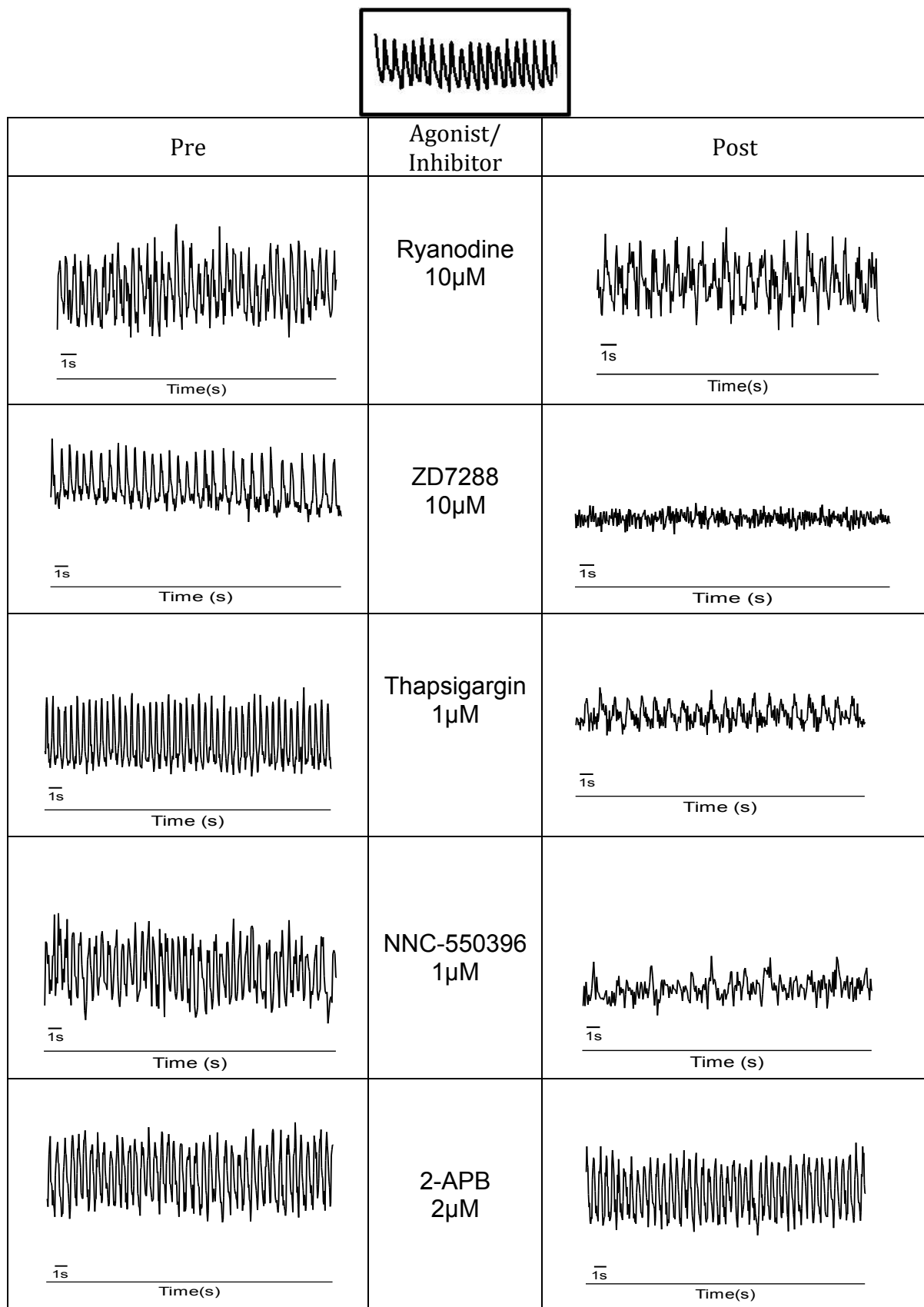
**Supplementary Table 1:** Immunocytochemical categorisation of the five most commonly occurring  $[Ca^{2+}]_i$  waveforms; n=3-10 cells per waveform group.

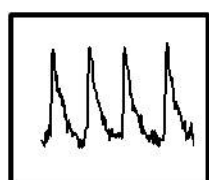
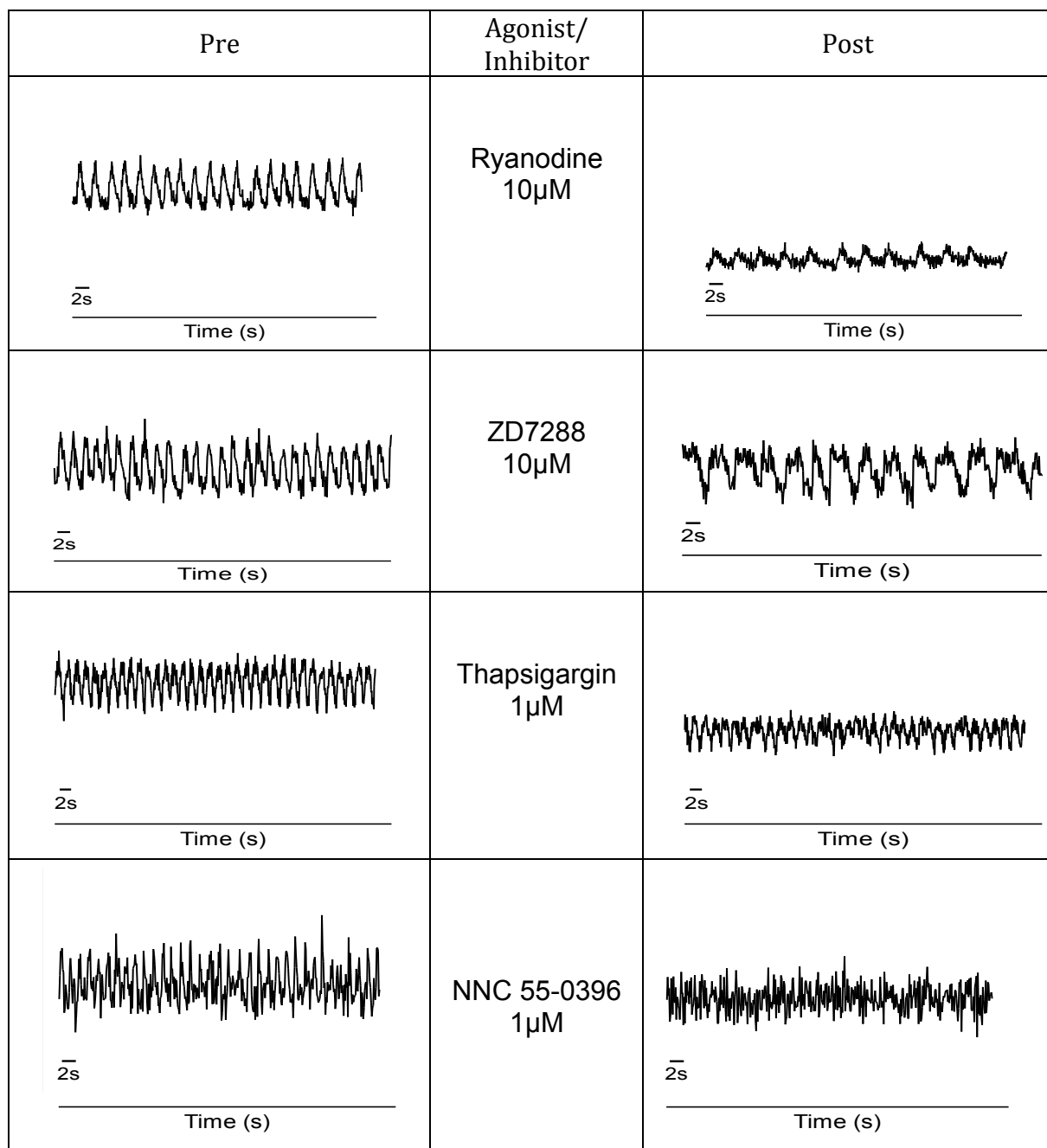


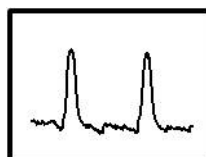
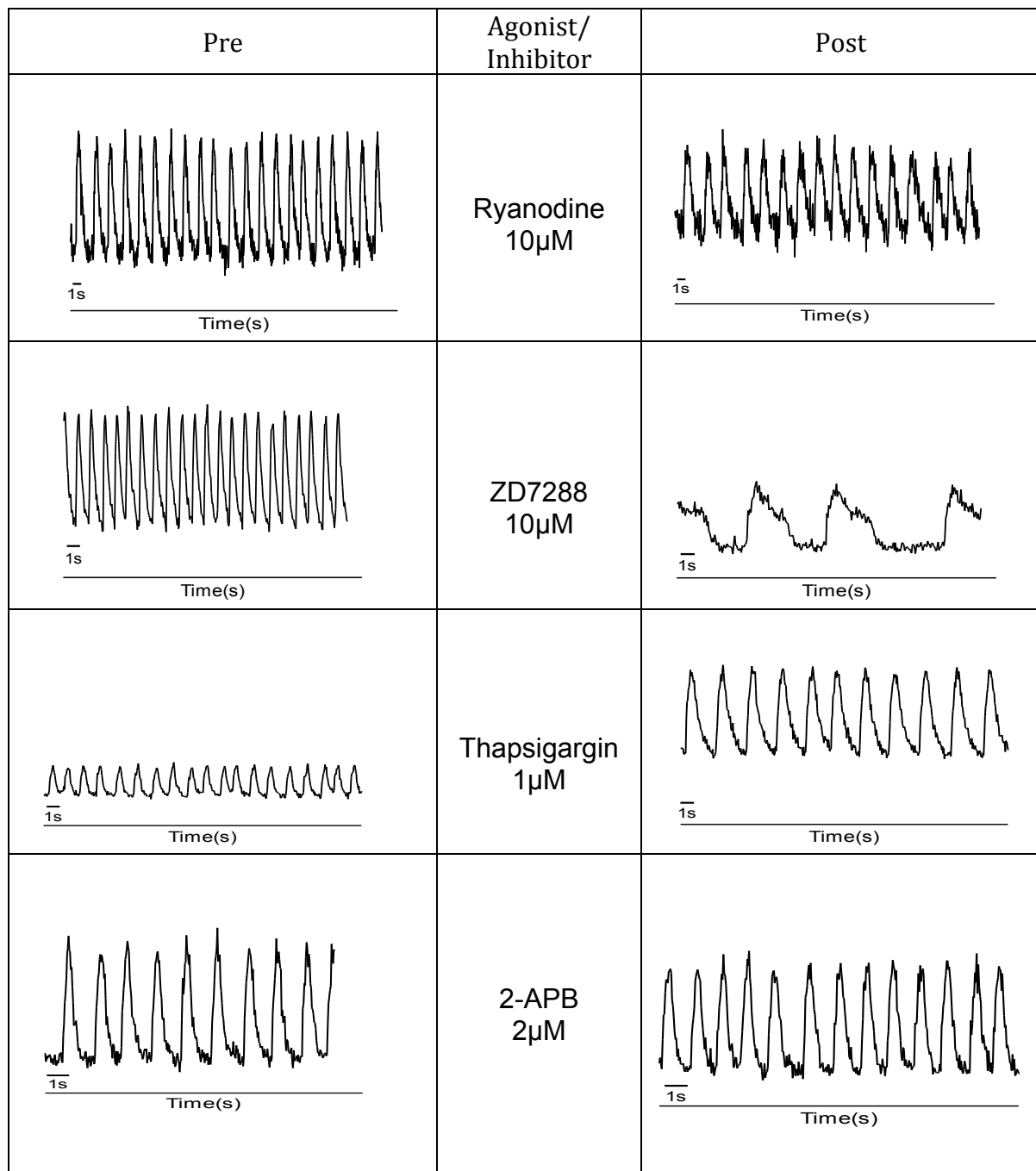
**Supplemental Figure S4:** Analysis of waveform kinetics. Once stabilised, the spontaneous  $[Ca^{2+}]_i$  waveforms could be divided into five distinct groups based on significant differences between the following analysis parameters: (A) the average interval of time (s) from 10% baseline to half the maximum peak value, and again from half the maximum peak value to peak (B) the average width at half peak height and (C) the average interval of time (s) from the peak value to 10% baseline of the descending slope. All columns within each parameter group were significantly different from one another, except where indicated (\*\*p<0.0001, one-way ANOVA, NS=not significant).  $[Ca^{2+}]_i$  oscillation peaks from at least 20 cells within each waveform group were analysed for each parameter.



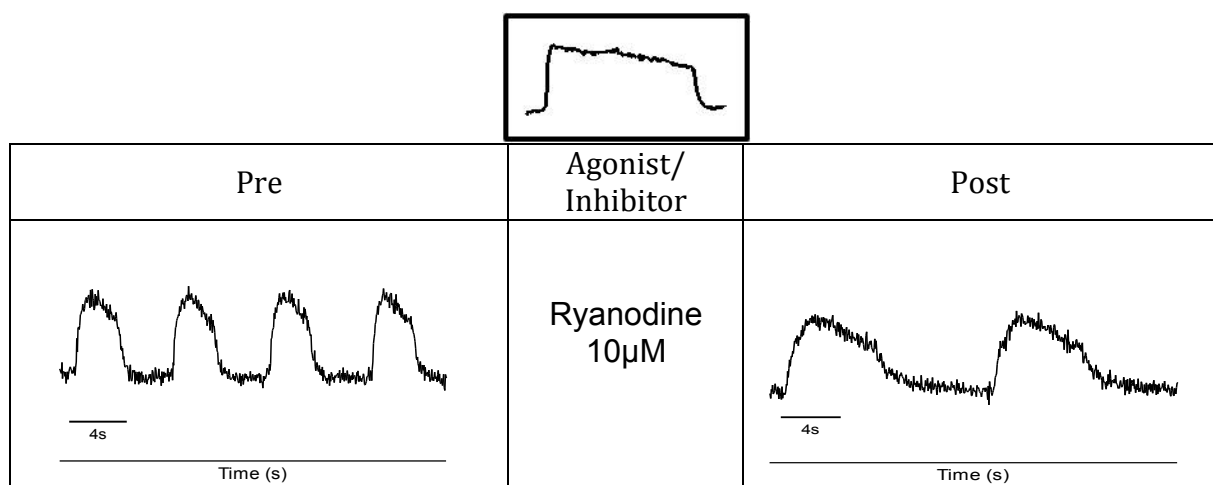
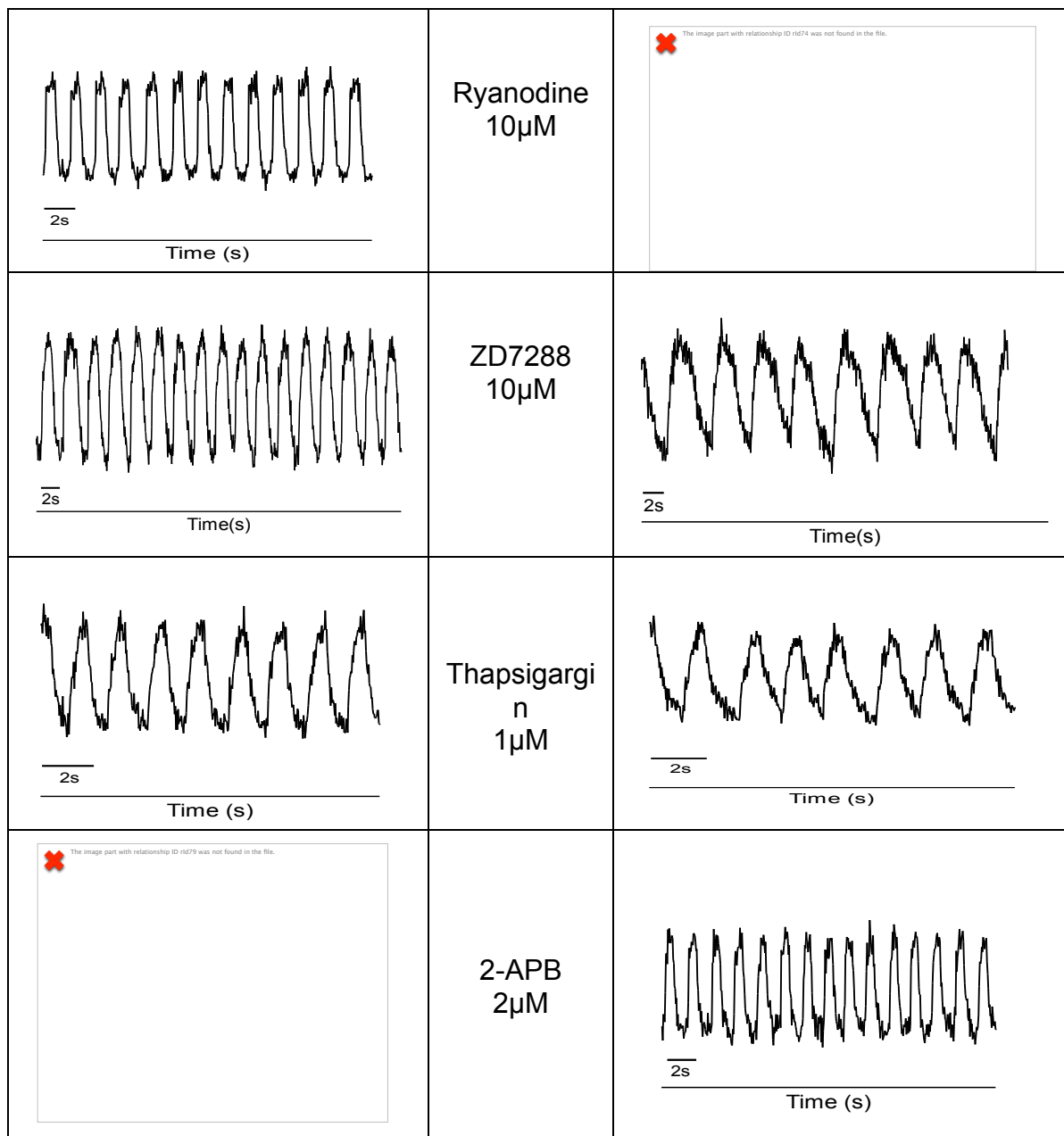
**Supplementary Figure S5:** (A) Addition of nifedipine (1  $\mu$ M) abolished spontaneous activity in all spontaneously active cells (\*\*P<0.001, one-way ANOVA, post-hoc Dunnett's, n=3-17 per waveform group). (B) The T-type channel blocker NNC 55-0396 significantly reduced the spontaneous activity and (C) the width at half-height in all pacemaker-like cells (\*\*P<0.001, one-way ANOVA, post-hoc Dunnett's, n=3-17 per waveform group). A red cross indicates the cessation of spontaneous activity. (D) NiCl<sub>2</sub> (10  $\mu$ M) significantly decreased the  $[Ca^{2+}]_i$  oscillation frequency of the slowest waveform group, as well as progressively prolonged the width at half height of each  $[Ca^{2+}]_i$  oscillation the slower the intrinsic pacemaker-like cell activity (\*\*P<0.001, \*P<0.05, one-way ANOVA, post-hoc Dunnett's, n=3-7 per waveform group).

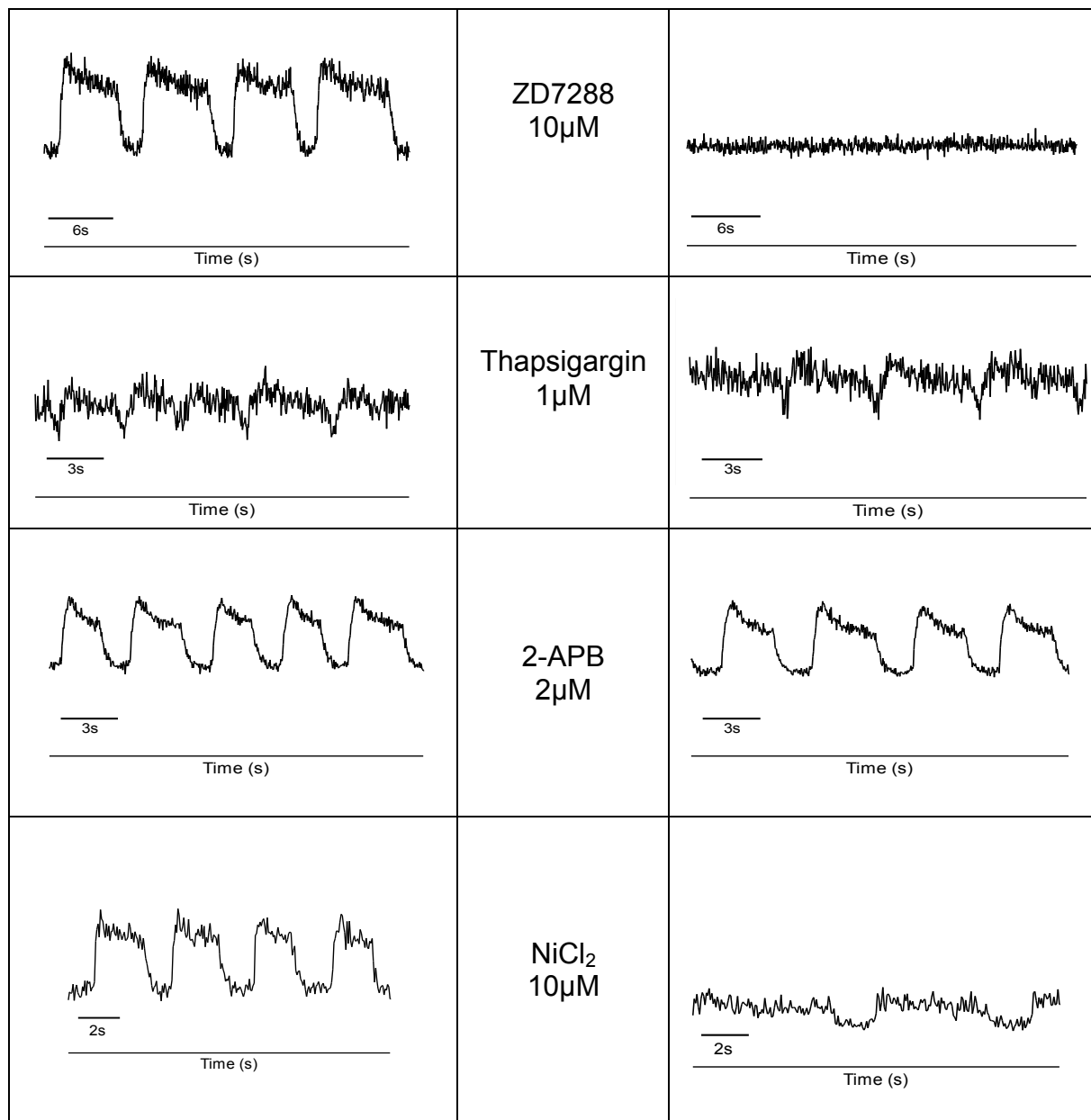






Pre	Agonist/ Inhibitor	Post
-----	-----------------------	------





**Supplementary Figure S6:** Representative traces of responses of each  $[Ca^{2+}]_i$  waveform group to Ryanodine (10  $\mu$ M), ZD7288 (10  $\mu$ M), Thapsigargin (1  $\mu$ M), 2-APB (2  $\mu$ M) and NiCl<sub>2</sub> (10  $\mu$ M)